A STUDY OF IONOSPHERIC IRREGULARITIES

by

A. W. Hooper, B.Sc. (Hons)

A Thesis presented for the Degree of

DOCTOR OF PHILOSOPHY

at the

UNIVERSITY OF ADELAIDE

(Physics Department)

December 1967

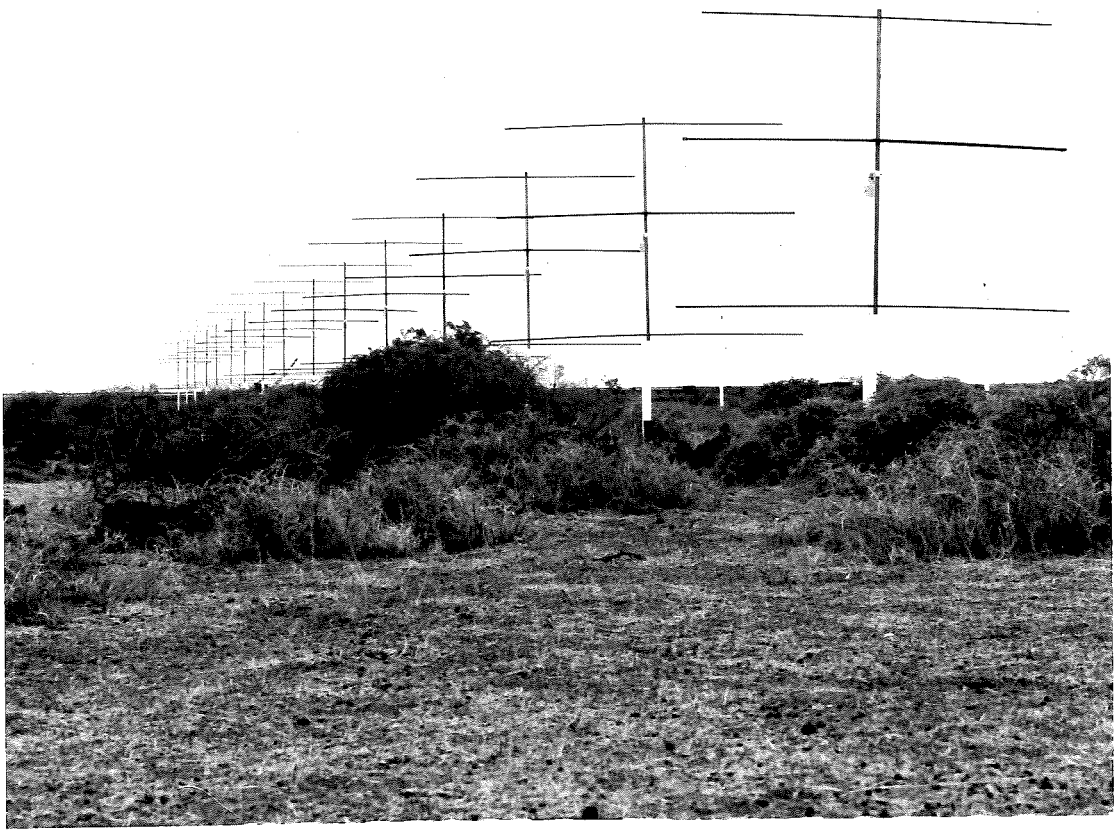

Frontispiece

The north-south fan beam phase-switched interferometer array used for the observation of radio star scintillations from St. Kilda, South Australia.

SUMMARY

The purpose of the work described in this thesis was to detect amplitude scintillations from discrete radio star sources, to associate the observed amplitude scintillations with sporadic-E and spread-F and to investigate the dependence of these scintillations on the zenith angle of observation of the source, and on the time of the day or year of the observation. The experimental work was carried out over the period December 1963 to July 1966, solar activity being appreciable only during the last six months of this period.

The necessary observations were taken from the records of two phase-switching interferometers operated at a frequency of 39.5 MHz.at St. Kilda, South Australia.

The smaller interferometer, consisting of two 4-element Yagi antennas spaced 4 wavelengths apart, supplied daily records of the scintillation of the Cygnus A source, and from the scintillation indices recorded over the two year period of observation, the temporal and zenith angle variation in scintillation activity are evaluated. A pronounced temporal variation is found but it is not possible to distinguish between a diurnal and seasonal variation using the results from a single source. The zenith angle variation expected from previous observations at other locations is not found

in the scintillations from the Cygnus source: rather, it is found that the scintillation amplitude decreases as the source nears the horizon. Several explanations are tentatively advanced which might explain this anomaly. Given that the thickness of the irregular ionospheric region increases towards the horizon, the intensity of the scintillation might decrease at large zenith angles due to the angular size of the source or due to the receiver bandwidth, but these are shown to be most unlikely explanations of the St. Kilda observations. Theoretical results for the zenith angle variation of radio star scintillation are evaluated for both isotropic and anisotropic irregularities.

Significant positive correlations are found between the scintillation indices and spread-F at night and between the scintillation indices and sporadic-E both at night and during the day. No correlation is found between the scintillation indices and $f_o F_2$ at night, even though at this time scintillation and spread-F are correlated and spread-F and $f_o F_2$ are anti-correlated. These correlation results are all expected from previous work and are interpreted and discussed with reference to the previous authors. An inconclusive result is found for the correlation of scintillation amplitude with planetary magnetic K_p indices.

A limited analysis of the associations of scintillation rate indicates that it is apparently more closely related

to the height of origin of the scintillations than to the planetary magnetic indices.

The possibility and probable magnitude of effects due to regular ionospheric spherical or wedge refraction on the timing and appearance of the Cygnus A records are discussed but such effects are not found. There are however several occasions when the records appear to be affected by irregular wedge refraction in the ionosphere.

The larger interferometer, consisting of sixteen 3-element Yagi antennas spaced 3/2 wavelengths apart with the centres of the interferometer halves separated by 12 wavelenths, was operated for a period of nine months, and regularly recorded the scintillation indices in the signals from eight sources. From the records of this interferometer, the temporal variation in the scintillation activity is resolved in favour of a diurnal variation and the expected zenith angle variation is found including a possible enhancement of scintillation detected in signals received from the magnetic zenith. Correlations between scintillation and other phenomena are evaluated - the results being similar to those found from analysis of the smaller interferometer, plus the additional result that the correlation between scintillation and sporadic-E decreases as the elevation angle of the source increases.

The possibilities of observing focussed scintillations

arising from single large irregularities and of observing radio source visibility fades are examined.

A lengthy introductory chapter particularly criticizes the explanations advanced by previous authors for their observations of the inversion of the usual relationship between the scintillation depth and observing frequency, and a brief final chapter discusses an investigation into the relationship between the F region critical frequency $f_o F_2$ at magnetically conjugate points.

Throughout the text, the use of correlation functions rather than correlation coefficients is emphasised since these enable spurious associations between parameters due to common or opposite seasonal variations to be recognized and also illustrate the independence (or otherwise) of data for one day compared with data from the next day.

To the best of the author's knowledge, this thesis contains no material previously published or written by another person, except where due reference is made. It contains no material which has been accepted for the award of any other degree or diploma in any University except where due reference is made.

(ANDREW W. HOOPER)

Adelaide University,
7/12/67.

ACKNOWLEDGEMENTS

The work described in this thesis was carried out in the Physics Department of the University of Adelaide under the supervision of Dr. B. H. Briggs. The author is grateful to Dr. Briggs for his help and encouragement throughout the course of the work.

The author would like to thank his colleagues in the Upper Atmosphere and Meteor groups of the Physics Department who from time to time assisted greatly in the carrying out of the experiment. In particular, he would like to mention Mr. Lindsay Hettner who was responsible for most of the mechanical work required for the successful erection of the interferometers, and Dr. Ian Parkin who supplied his correlation function and satellite orbit computer programs referred to in the thesis.

At various times throughout the experiment, the computing facilities of the Commonwealth Scientific and Industrial Research Organisation at Adelaide and Canberra, the Weapons Research Establishment at Salisbury, South Australia, and the University of Adelaide, were used. The Woomera ionograms were supplied by Mrs. Pat. McKenzie of W.R.E. and the other ionospheric data for Salisbury and Woomera were obtained from the bulletins published by W.R.E. The $f_o F_2$ data used in Chapter 10 were supplied by the World Data Center A, Washington, D.C., U.S.A.

The author is particularly grateful to Misses Janice Gordon and Elizabeth Henneker for their considerable assistance in the preparation of the diagrams and to Mr. and Mrs. Malcolm Golley for their helpful comments during the final preparation of the manuscript. Miss Elizabeth Doyle assisted greatly with the proof reading.

Finance for the project was provided by a grant from the United States Air Force (Grant AFOSR-298-63) and by the University of Adelaide Research Grant. The author was initially the holder of a Commonwealth Post Graduate Award and over the final months, of a University of Adelaide Research Grant.

C O N T E N T S

CHAPTER 1. HISTORIC REVIEW

1.1 Historic Outline of Scintillations and Theories of Development of Scintillation

The earliest realization that the ionosphere was capable of imposing variations on radio waves appears to have been by Ratcliffe and Pawsey (1933) who used a spaced receiver experiment to show that the amplitude and direction of arrival of broadcast signals varied after reflection from the ionosphere.

The first extraterrestial source of radio waves to be discovered was the sun, which in 1942, was recognized as being a source of interference in British army radars. Soon afterwards, Hey, Parsons and Phillips (1946) discovered the Cygnus A source and Ryle and Smith (1948) discovered the Cassiopeia A source. Both these sources were observed to be variable in strength, and until 1950 the variations were thought to originate from the sources themselves - as was in fact at least partially true in the case of the sun and which, for the sun, could be explained in terms of visible variations in solar activity.

In 1950, Smith, and Little and Lovell, in companion papers, established the terrestial origin of the signal fluctuations using in the first case a variable receiver

separation and in the second case a fixed large separation. They found that there was no detailed correlation between the records made for receiver separations greater than about 20 km. In the second experiment, which had a receiver separation of several hundred kilometres, it was observed that occurrence or non-occurrence of the fluctuations was generally common to both receivers but that there was no fine detail common to both records. This was taken to indicate that while the cause of the fluctuations was common to both stations, the scale of the disturbance was much smaller than the station separation. The authors realized that a diffraction process in the ionosphere could be responsible for the fluctuations and recognized the analogy with the twinkling of visible stars. They had used two wavelengths in the experiment, viz. 3.7 and 6.7 m, and were at the time puzzled that they should observe good correlation between them.

Following the discovery of the discrete radio sources, and the realization that the variations in signal strength were imposed during the passage of the signals through the ionosphere, the first attempt to use diffraction theory to describe the signal behaviour was by Booker, Ratcliffe and Shinn (1950). Hewish (1951)

introduced the concept of a phase screen. He considered that the fundamental effect of the ionosphere on radio signals was to introduce regions of varying electron density (and therefore varying refractive index). Although purely phase fluctuations were superimposed on the signal initially, diffraction theory showed that amplitude fluctuations developed as the signal was propagated beyond the screen. The screen was regarded as thin if no amplitude fluctuations developed until after the signal emerged from the screen. Hewish assumed a sinusoidal phase variation across the screen and was able to show that, provided the root-mean-square phase deviation (ϕ_0) was less than one radian, the scale of the observed diffraction pattern below the screen was the same as the scale of the screen. However, if ϕ_0 exceeded one radian, the observed scale below the screen contained fine structure ϕ_0 times smaller than the scale of the screen. Early theory and experiments soon produced data on the frequency dependence of the scintillation and gave values for the height and size of the irregularities causing the scintillation.

Fejer (1953) and then Bramley (1954) were the first to extend the theory to include the effects of a thick phase screen. Spencer (1955) showed, using a three

receiver experiment, that the irregularities were anisotropic with an axial ratio of about 5:1 and that they had their major axes aligned parallel with the earth's magnetic field.

Other effects related to the scintillations, such as the dependence of their visibility on source size, the inversion of the usual dependence of the scintillation depth on frequency, fadeouts - where the visibility of the source itself is reduced for a limited period, and the effects of the zenith angle on scintillation depth (not to be confused with a latitude variation which may be superimposed), have been explained satisfactorily using arguments based on diffraction theory. These effects are discussed in more detail in section 2 of this chapter.

Recently, theoretical work by Mercier (1962) and Bramley (1967) has been directed towards improving the theory for large values of ϕ_o, while Budden (1965 a and b) has considered the further properties of diffraction from thick phase screens and of the correlation between scintillations observed on different frequencies.

In contrast to the statistical diffraction approach, a ray optics treatment of scintillation has several advantages, notably when dealing with large scale individual irregularities with large values of ϕ_o. In particular,

Wild and Roberts (1956) and later Warwick (1964), using observations from swept frequency receivers, applied this type of theory to their results which, in some cases, showed scintillation (phase and amplitude) variation with frequency consistent with the passage of the radio waves through a single ionospheric lens rather than through a random diffracting screen. Gagnon (1964) showed how diffraction patterns on the ground could be computed using model (single and large) irregularities in the ionosphere. He was able to compute the changes in signal amplitude and the phase variations on the ground resulting from the passage of an irregularity overhead and, when he used a converging lens as a model, he showed that the radio energy could be focussed.

Hewish, Scott and Wills (1964) were the first to observe signal fluctuations due to irregularities outside the Earth's atmosphere. Initially, they suspected the existence of interplanetary scintillation after noticing that on some occasions the signals from newly discovered small diameter radio sources known as quasars were scintillating, whereas the signals from other larger sources were not. They justified their conclusions using diffraction theory arguments. Shortly afterwards, further evidence for the existence of interplanetary scintillation was

found as a result of correlation studies on records taken on receivers separated by several hundred kilometres and more, the experiment being similar in principle to that used to identify ionospheric scintillation in 1950.

Since the discovery of interplanetary scintillation in 1964, the development of the subject has been very rapid. Saltpeter (1967) summarizes the theory, and Cohen et al. (1967), the observations up to mid-1966. To date, observations have not been made in years of maximum solar activity: these will come over the next couple of years. Since the above review papers, Sharp and Harris (1967) have reported an association between an enhancement of interplanetary scintillation and a solar flare event, and Dennison and Hewish (1967) have pointed out that measurements of the solar wind (both speed and direction) using interplanetary scintillation are not confined to the ecliptic plane as is the case with measurements made from present spacecraft.

The way is now open for radio star scintillation observations to become as useful a tool in space research as they are in ionospheric research.

1.2 Some Special Effects Related to Scintillation

(i) Zenith Angle Effect. Although Hewish (1952) realized that the scintillation depth increased with

increasing zenith angle, his theory was incomplete, being derived from a flat earth approximation and confined to the near zone - where amplitude fluctuations are not fully developed. Booker (1958) extended the theory to include the far zone and took into account the fact that since the earth was not flat, the angle of incidence of the signal on the layer was smaller than the zenith angle measured in the ground. Briggs and Parkin (1963) formulated a much more complete theory which, as well as the above considerations, took into account the increased thickness at large zenith angles of the irregular regions along the line of sight, and the additional effects present due to the anisotropy of the irregularities. They were able to calculate the increase in scintillation depth expected when signals are received from the magnetic zenith, the enhancement being due to the elongation of the irregularities and superimposed on the effects present assuming the irregularities to be isotropic.

The theory of the zenith angle effect is outlined in more detail in section 5.3(i).

(ii) Variation of Scintillation Visibility due to Finite Source Size. Briggs (1966) indicated that if a source has a finite angular diameter θ, the scintillation visibility will be reduced if:

$$\theta \geq \frac{L}{Z} \quad \text{for } \phi_o < 1 \text{ radian}$$

$$\text{and if } \theta \geq \frac{L}{Z\,\phi_o} \quad \text{for } \phi_o > 1 \text{ radian}$$

where L is the scale size of the irregularities = $2\pi r_o$

r_o is the autocorrelation distance across a single irregularity

and Z is the distance to the diffracting screen.

Briggs (1961) suggested that this effect might explain the apparently anomalous reduction in the amplitude of scintillations from the source Cassiopeia A near lower transit at sunspot maximum. Under these conditions, the auroral zone, through which the line of sight to the source passed, was at its most active. This source had a diameter of 4' arc and a size effect was thought to be the most likely explanation when it was realized that Cygnus A, with half the angular diameter, did not show a similar anomalous reduction. Later, Aarons and Guidice (1966), at the Arecibo Observatory, used signals from sources of different angular diameter to view the same irregularity structure and, knowing the source size required to reduce the scintillation depth to half its point source value, were able to obtain a value for the size of the irregularities.

Bramley (1967) agrees with the above order of magni-

tude inequalities as part of his much more detailed theoretical investigation. He also describes the less readily observed effect on amplitude scintillation where, if the source has a finite angular diameter, there will be a distance from the screen (for any ϕ_0) for which the scintillation amplitude will be a maximum and beyond which it falls off to zero. This distance occurs further from the screen as the angular diameter of the source is reduced. This is in contrast to the scintillation amplitude arising from a point source which approaches a limit and never reaches a maximum for any distance from the screen. This effect has not so far been observed directly and an experiment to detect it would be difficult to arrange due to the varying distances from the screen at which measurements are required.

(iii) Inversion. The variation of scintillation depth with frequency usually observed agrees with the theoretical prediction that it should decrease as the observing frequency increases; however, under some circumstances, this usual variation with frequency is reversed. The first to observe this phenomenon were Kidd et al. (1962) who found that for the inversion to be observed, multiple scattering conditions should be present in the ionosphere and the line of sight to the source should be directed near

the magnetic zenith. Thus, the phase deviation ϕ_0 along the signal path was maximized, and in general, such conditions were most likely to arise during magnetically disturbed conditions (Kp $>$ 6). They observed both the Cygnus A and Cassiopeia A sources at frequencies of 62, 109 and 224 MHz. In a follow-up paper, Aarons et al. (1962) reported observations of Cygnus A on an extended range of frequencies (the previous frequencies plus 1300 and 3000 MHz) and were able, in several instances, to observe an inversion frequency above which the scintillation depth decreased as expected normally but below which, instead of increasing, the scintillation depth decreased again. The explanation advanced in both papers was in terms of the scale size of the diffraction pattern on the ground becoming less than the aperture of the antenna (an 84' parabola) thus causing a lack of correlation of the signal across the aperture which would bring about a reduction in the observed scintillation. They drew attention to the importance of considering other side effects as possible causes but did not evaluate their relative influences.

From Briggs (1966) it would appear that the effect of finite source size is more important than that of the aperture size as a cause of inversion.

Taking equations 4, 6 and 8 from Briggs paper and expressing the conditions in terms of the scale size L, the scintillation will be reduced if:

$L < \theta_o \, Z \, \phi_o$	source size condition
$L < \frac{\sqrt{BZC}}{f} \phi_o$	bandwidth condition
$L < D \, \phi_o$	aperture size condition

where the parameters for the source size condition have already been introduced in the previous section, B is the receiver bandwidth, c is the velocity of light, f is the frequency of the radio wave and D is the antenna aperture (or interferometer spacing).

Values may be assigned to the parameters as follows:

Z = 300 km	c = 300,000 km/sec
θ_o = 4' arc for Cassiopeia A	
2' arc for Cygnus A	
B = 1 MHz	f = 40 MHz

Substituting these values into the inequalities, the following results are obtained:

$L < 350 \, \phi_o$ metres	Size condition for Cassiopeia A
$< 175 \, \phi_o$ metres	Size condition for Cygnus A
$L < 250 \, \phi_o$ metres	Bandwidth condition
$L < D \, \phi_o$ metres	Aperture condition

These values of L are all frequency dependent due to the fact that ϕ_o is frequency dependent - i.e. it varies as the reciprocal of the frequency. Thus for appropriate values of ϕ_o, there will be a transition frequency below which the variation of scintillation amplitude with frequency will be inverted. With the exception of the L value depending on the receiver bandwidth, the above estimates of the critical value of L may be compared in magnitude directly from the above results. The exception arises because even if the ratio B/f is constant for all receivers (which it is not), the ratio $\sqrt{B}/f$ decreases as the frequency increases. It is probable that for the receivers and frequencies generally used for these experiments (Aaron's inversion frequency was near 200 MHz), the effect of receiver bandwidth will not be as important as the above figures suggest. The point to be made here is that the source size condition apparently dominates the aperture size condition (unless the aperture is large such that $D > \theta_o Z$, requiring $D > 175$ metres for Cygnus A), and should therefore be mainly responsible for the production of the inversion phenomenon. In particular, the source size condition should have the dominating influence in the experiments of Kidd et al. (1962)and Aarons et al. (1962) described here.

It is interesting to speculate whether the original Cassiopeia A experiment, which required the inclusion of the source size effect to explain anomalously low scintillation at certain times, and the experiment of Aarons and Guidice(1966), which determined the irregularity size from variations in scintillation depth of sources of different angular diameter, would have shown the inversion phenomenon had records been made on a sufficiently wide range of frequencies.

If the inversion phenomenon could be observed in the signals of the same source at the same receiving site using two different aperture antennas then the problem should be resolved experimentally. Provided ϕ_0 is greater than one radian over the frequency range used, the scale of the diffracting pattern will vary as $1/\phi_0$ over this same frequency range. Then, since the phase deviation ϕ_0 imposed on a wave travelling through the ionosphere varies inversely with the frequency, a 2:1 aperture ratio should give a 2:1 inversion frequency ratio if it is the antenna aperture size that is responsible for producing the phenomenon.

(iv) Fadeouts. A fadeout is an apparent reduction of source visibility in the output from an interferometer and is usually observed to persist for periods of from

5-100 minutes. Fadeouts have been observed by many authors over a range of frequencies from 45 to 223 MHz.

The first observations of fadeouts appear to have been by Koster (1958) in Ghana who showed that the effect was more severe when observed on a higher resolution interferometer and that it was highly correlated with the occurrence of intense equatorial Spread-F. At the time, he was not able to rule out absorption as a possible mechanism for the effect.

Fadeouts have also been observed in the northern auroral zone; in particular Benson (1960) noticed their association with line of sight aurora and later, Little et al. (1962) and Moorcroft (1963) established that they are not due to ionospheric absorption. Little et al. observed fadeouts on a phase-swept interferometer at the same time as on a phase-switched interferometer and at the time it was thought that this observation excluded their being observed in the signals from a point source.

The theoretical description of the phenomenon has recently been summarized by Bramley (1967) who points out that the effect may be observed with a point or extended source and that provided ϕ_0 is at least 1 radian, a fadeout may occur either due to a further increase in ϕ_0, or due to a reduction in the scale size of the irregularities. In either case, the result is that phase scintillations are

developed which are sufficiently large that the apparent position of the source is shifted rapidly over angles larger than the antenna lobe size. The interferometer is then viewing a source which is effectively larger than one antenna lobe and this has the effect of reducing the amplitude of the output of the receiver.

To date observations are limited to the equatorial zone and to the auroral zone where the degree of ionospheric disturbance (spread-F and/or aurora) is most intense. Fadeouts, if they occur, are unusual in mid-latitudes.

1.3 Methods of Detecting Ionospheric Irregularities

Irregularities in the electron density at various heights in the ionosphere have been the subject of intense experimental and theoretical investigations over the last fifteen years. A variety of techniques have been used in the experimental investigations.

(i) Ionosondes. These instruments may be operated from the ground or from satellites. They yield records which show the variation in the virtual height (or depth) of reflection with frequency and yield information on the electron content profile as far as, but not beyond, the

reflection point. Irregularities are recorded as sporadic-E or spread-F but little information can be obtained regarding the movements or size of the irregularities.

(ii) Fixed Frequency Sounders. These differ from an ionosonde in that only a single frequency is transmitted, the choice of frequency being determined by the ionospheric layer being investigated. A network of spaced aerials can be employed to detect the reflections and, using the ground pulse from the transmitter as a reference, the receivers can be suitably gated so that only the signals reflected from a limited height range are recorded. Either from a direct measurement of the time delays between prominent fades on the records from different receivers or from a full correlation analysis of a length of record, the speed and direction of drift, and the orientation and size of the irregularities, may be determined. This was the method used by McGee (1966) in his investigation of E region drifts from Adelaide.

(iii) Aspect Sensitive Echoes. In this technique, a radar transmitter is employed, the frequency being somewhat higher than the F region critical frequency. This means that the technique should be capable of detecting

irregularities above as well as below the F region electron density maximum. It is found that echoes are received only when the path followed by the signal is orthogonal to the magnetic field at the reflection point. If, at a given location, the transmitting aerial is slowly rotated at a fixed elevation angle, there will be a preferred azimuth from which the back-scattered signal is received. Knowing the range of the reflection point and the elevation of the transmitted signal, the height of the irregularities is readily evaluated. Goodwin (1965) sums up the Brisbane results which have included the recording of echoes in the E, F1 and F2 layers and incorporated appropriate correlations with sporadic-E and spread-F recorded on ground based ionosondes, and Unwin (1966) points out that at high latitudes aspect sensitive echoes have been associated with auroras.

(iv) Scintillations. These may be detected in the radio signals from radio stars or from satellites and, as in the case of aspect sensitive echoes, the detection of irregularities is not restricted to the near side of the F region maximum electron density.

In the case of radio star scintillations, because of the 4 minutes per day advance of sidereal time relative

to solar time, observations of a single source if continued for a full year can give information on the temporal and spacial variations in scintillation activity. However, to resolve the seasonal and diurnal variations it is necessary to utilize records from several sources taken over the same period and taken at the same site. In principle, the height of the origin of the scintillations may also be determined, but this is difficult. Spaced receiver experiments on radio star scintillations, since the source may be regarded as almost stationary, give values for the drift speed and direction of the irregularities. Their size, shape and orientation may also be determined. Since in many cases, a radio star may be detected from a given location for a period of several hours (as in the case of the Cygnus A experiment performed here, and also as in the case of the Cambridge, U.K. observations of the Cassiopeia A source, which is there circumpolar), records of radio star scintillation are better suited for comparison with other geophysical phenomena (such as magnetic field fluctuations) than are records of satellite scintillation.

In the case of satellite scintillation, spaced receiver experiments also lead to estimates for the size, shape and orientation of the irregularities but in contrast to the radio star case, the orbital velocity of the

satellite is so large that the irregularities rather than the source appear stationary to an observer on the ground. Thus, measurements of the drift speed of the diffraction shadow pattern over the ground give values for the height of the irregularities causing the scintillation rather than their drift velocity.

Due also to the rapid movement of the satellite, satellite scintillations should be better suited to investigations of the latitude and zenith angle variations of scintillations than are radio star scintillations - useful information being gained from a single pass of the satellite. However, to determine diurnal variations of scintillation, many satellite passes may have to be recorded before the required data is obtained in which case the advantage of using satellite data is reduced.

One line of investigation which is restricted to experimenters working with satellites is the recording of the Faraday rotation of the plane of polarization of a signal which occurs as it passes through an ionized region. This technique can be used to determine the total electron content of the ionosphere (and fluctuations in it) and cannot be applied to the signals from radio stars which in most cases emit broadband noisy signals which are unpolarized. In the case of a satellite, the polarization of

the emitted signal should be elliptical or linear and the satellite should be stabilized so that the variations in polarization of the downcoming signal are due solely to the influence of the ionosphere. The beacon satellites Be-B and Be-C are particularly suited to the investigation of the Faraday rotation.

1.4 Experimental Results of the Scintillation Observations

In the following sections, the observations of scintillation made up to the present time are discussed and the conclusions reached regarding the properties of the scintillations, the properties of the ionospheric irregularities giving rise to the scintillations, and the relationships between scintillations and other geophysical phenomena, are outlined. The different aspects of the scintillation behaviour are discussed under the headings of temporal variations in scintillation activity, height distribution of the electron density irregularities causing the scintillations, size, shape and orientation of these irregularities, special relationships between the scintillation and spread-F phenomena, and relationships with the earth's magnetic field parameters. Other aspects of scintillation behaviour such as the latitude distribution, and the possible connection with sporadic-E are included within the above categories where their discussion is relevant.

(i) Temporal Variations in Scintillation Activity.

Ryle and Hewish (1950) used a fan shaped aerial beam at Cambridge, England, to observe the radio sources Cygnus A, Cassiopeia A, Virgo A and Taurus A at their respective daily transits over a 15 month period. Since these sources had different right ascensions, the authors were able to plot the scintillation indices against the month of observation and the local time of observation separately, such a method of analysis being sufficient to distinguish between diurnal and seasonal variations in scintillation activity. They found a predominantly diurnal variation. There was little scintillation during the day and the maximum occurrence was observed about an hour after local midnight.

Bolton, Slee and Stanley (1953) observed scintillations of the signals from the sources Cygnus A, Taurus A and Virgo A from Sydney, Australia and, using plots similar to those of Ryle and Hewish concluded that the diurnal and seasonal variations were equally important. They, and also Wild and Roberts (1956) both observed a secondary maximum of scintillation activity around local noon which had not been observed in the northern hemisphere. At the time it was concluded that this discrepancy could have arisen from the fact that the northern hemisphere observations were in most instances made for sources near

the zenith whereas in the southern hemisphere the sources were all at zenith angles greater than 45°. Wild and Roberts, who observed only the Cygnus A source, did not attempt to distinguish between a diurnal and seasonal variation.

Briggs (1964) investigated the diurnal, seasonal and solar cycle variations in scintillation activity from Cambridge observations of the source Cassiopeia A for the years 1949-1960. He found that the scintillation activity, when it was averaged year by year, followed a similar pattern to the solar activity. He also found that the occurrence of scintillation was at its maximum near local midnight and that fluctuations in this time from month to month and from year to year were statistical rather than systematic in nature. There was little daytime scintillation recorded at Cambridge except during the years near sunspot maximum when it was sufficiently strong to remove much of the diurnal variation. Indirectly the results indicated the presence of a diurnal rather than a seasonal variation.

The overall predominance of the diurnal variation has been emphasised most recently by Smerd and Slee (1966). Using the east-west arm of the Mills Cross at Fleurs, near Sydney, they recorded scintillations in the signals of the eight strongest sources visible during the daily

transit of each source. Data was recorded over a four year period from 1955-1959. From these observations, they were able to exclude a strong seasonal variation in the occurrence of scintillations, and to conclude that the midday peak of occurrence, which from the southern hemisphere had been observed previously, was not confined to the signals from sources observed at low angles of elevation.

Parkin (1967) confirmed the existence of the subsidiary midday peak in scintillation activity from the observation of scintillations in the signals from the beacon satellites from St. Kilda, South Australia. This subsidiary peak of occurrence has been observed consistently from southern hemisphere mid-latitude regions and Mitra et al. (1964-65) observed it in the scintillations of the Be-B satellite signals from New Delhi, India at a geomagnetic latitude of ~ 20°N. It does not appear to have been reported from anywhere else.

Little et al. (1962) observed the Cygnus A and Cassiopiea A sources from College, Alaska - close to the auroral zone. They observed that scintillation activity was much stronger than would have been expected from the mid-latitude results, and that the diurnal variation, although present and in phase with the mid-latitude results, was much less marked.

To date, there do not appear to be any results from the equatorial regions which would suggest that the relative importance of seasonal and diurnal variations there should be different from that in the temperate and auroral regions.

Several aspects of the work of Smerd and Slee (1966) appear to warrant criticism: more specifically, part of their argument appears to rest on rather dubious foundations and their experimental technique for reputing the same argument does not appear to be sufficiently rigorous.

The co-authors state that the possibility exists that variations in scintillation occurrence generally interpreted as diurnal variations, could be due to variations in the angular distance between the scintillating source and the sun (with maximum scintillation being observed in the direction of the sun and in the direction of the anti solar point). The mechanism suggested has in fact been observed in the scintillations of very small diameter sources. While it is true that if such an effect were present, it would be difficult to distinguish from a diurnal effect, its presence would appear to be largely excluded (on purely theoretical grounds) from the scintillation of large diameter sources. Consideration of the solar wind velocity, the earth's orbital velocity, the

time scale of the scintillations observed on the ground, the finite diameter of the sources used (only Virgo A is less than 2' arc in diameter), and the scale sizes deduced on the ground should lead to the conclusion that interplanetary scintillations will not be observed in the types of experiment described here.

However, if these arguments are not considered sufficient to exclude a dependence on angular distance from the sun, then it is evident that a plot of scintillation occurrence against the angular distance between the scintillating source and the sun (incorporating the differences in right ascension and declination) will resolve any confusion present. Smerd and Slee attempted to do this by plotting the scintillation occurrence against right ascension and declination differences separately, combining observations from all the available sources. While it is true that the difference in right ascension between a source and the sun represents the angular distance between them quite well (but not exactly due to the $23\frac{1}{2}^{\circ}$ inclination of the ecliptic to the celestial equator), this distance is not well represented by the difference in declination. In particular, if the declination difference between a source and the sun is zero, the source can be at any angular distance from the sun depending on their respective right ascensions.

It is concluded here that if scintillation activity does depend on the angular distance between a source and the sun, then the analysis of Smerd and Slee would not necessarily have determined this. However, as they point out, if scintillation activity is plotted against the difference in right ascension between the scintillating source and the sun, the problem is not resolved because this particular plot would show the same behaviour if either (or both) variations were important.

Some further aspects of the temporal variations of scintillation activity are included in the following sections where their discussion becomes relevant to the interpretation of other observations.

(ii) The Height Distribution of Irregularities giving rise to Scintillation Activity. Three main techniques have given rise to estimates of the height of the irregularities. These estimates come from diffraction theory applied to the observation of radio star scintillation, from the correlation of scintillation occurrence and intensity with spread-F and sporadic-E, and from spaced receiver measurements or satellite scintillations. These are discussed here. Some estimates ofheight have also been made from satellite observations by noting the minimum height of the satellite for which scintillations

occur. The accuracy of these estimates is limited when it is realized that irregularities are more or less efficient at producing scintillations depending on their distance below the satellite, and that the weighting functions described by Briggs and Parkin (1963) must be taken into account in the interpretation of the observations. In any case, the method is not as direct as that using spaced receivers and is not described further here.

The diffraction theory of Hewish (1951, 1952) indicates that an irregularity height determination should be possible from the simultaneous observations of amplitude scintillations on spaced frequencies, or from the simultaneous observations of phase and amplitude scintillations on the same frequency. In the first case, the method is rather insensitive and the best estimate Hewish (1952) could make was that the irregularities were at a height not greater than 1500 km. From the second method, he was able to assign (in the same paper) a height of 400 km to the irregularities. His measurements referred to night time scintillation only.

As Chivers (1962) indicates, there has been a large amount of work done, over a wide range of northern and southern latitudes, on the day to day correlation of scintillation activity with spread-F and sporadic-E.

While positive correlations with spread-F, except perhaps in the polar regions, are wide spread, positive correlations with sporadic-E are generally restricted to the scintillations of sources at small elevations (where from spherical earth geometry, the E layer thickness increases relatively faster than the F layer thickness along the line of sight to the source), and to daytime scintillations. Wild and Roberts (1956), from their observations of radio star scintillations near Sydney, found that scintillations were associated with sporadic-E activity during the day, and with spread-F activity during the night. Briggs (1964) found a positive correlation between scintillation and spread-F at night, but during the day was unable to come to any conclusion regarding the correlation between scintillation and sporadic-E due to large gaps in the records of both phenomena. He realized that the occurrence of strong scintillation when spread-F was not detected could be explained if the irregularities were situated at heights above the level of maximum F region electron density.

Since the advent of the artificial earth satellite, some much more direct methods of height determination have become available. The most important of these depends on the fact that the velocity of a satellite is so large that the ionosphere may be regarded as frozen

during the satellite's passage. Using an array of spaced receivers (preferably at least three receivers not in the same line), the velocity of the diffraction shadow pattern across the ground may be measured and knowing the velocity and height of the satellite, the height of an irregularity may be determined.

Yeh and Swenson (1964) have published results of their investigations at Urbana, Illinois, which show that irregularities may be observed over all heights from 100 to 600 km. They are most likely to occur near 400 km (in the F region) and have a smaller peak of occurrence near 100 km (in the E region). McClure (1964) divided the same data into three-hourly time zones and showed that irregularities in the E region were dominant by day and that by night, they were dominant in the F region. This result agreed with the Australian correlation studies in so far as the different height associations by day and by night, but differed in the fact that the observations were not restricted to low altitudes. McClure did not correlate the scintillation occurrence with sporadic-E or spread-F. It should be pointed out that the predominantly E region heights of the irregularities by day and the predominantly F region heights of the irregularities by night do not necessarily indicate the existence of even a subsidiary maximum in scintillation activity during the day.

As indicated by Yeh and Swenson, other authors have observed irregularities by a similar method up to heights of 1000 km.

(iii) Measurements of Irregularity Size, Shape and Orientation. Booker (1958) summarized the early English observations and described how these first measurements of F region irregularity size appeared to be inconsistent until Spencer (1955) showed that the irregularities were anisotropic and were elongated along the magnetic field lines. The earliest conclusion was that at middle latitudes, the irregularities had axial ratios of about 5:1 and had a smaller dimension of about 1 km.

This result was further refined by Jones (1960) who, from night time observations, using three receivers, of the Cassiopeia A source to the north of Cambridge, U.K., verified Spencer's observations that the F region irregularities were field aligned and found that the axial ratio varied with elevation angle. The axial ratio was much larger when the source was observed at upper culmination than when it was observed at lower culmination and he interpreted this result as evidence of a variation in axial ratio with latitude. This result could be explained in terms of a varying ionospheric diffusion coefficient with height along and across the magnetic field lines if

the height of the irregularities decreased with increasing latitude.

In recent years, workers in this field have sought to establish the latitude variations in the irregularity size. Kent (1961), at Ibadan near the magnetic equator, from the observation of satellite signals on two spaced receivers, found values of $\frac{1}{2}$ km for the smaller dimension of the irregularities and variable axial ratios with a mean value of 6:1. He confirmed the magnetic field alignment.

Yeh and Swenson (1964) used satellite records to determine the smaller dimension over a range of latitudes but did not include equatorial regions in their experiment. They used the rather crude method of counting maxima in the scintillation records from single receivers over a restricted range of northern latitudes and as they pointed out, they were left with a possible error of 50%. Their results indicated a larger sized irregularity at Houghton and Adak (of similar magnetic latitude) than at their other stations at higher and lower magnetic latitudes. This rather surprising and unexpected result has not yet been confirmed or explained.

Most recently, Aarons and Guidice(1966) obtained values for the size of irregularities from the visibility

of scintillations of signals from radio sources of different angular diameters and compared their values of size with those of other workers spread over a range of latitudes. Although the other workers (Basu et al. (1964), Frihagen (1962), Jesperson and Kamas (1964), and Koster (1963)) all used different techniques, their results are compatible provided the difference between L, the peak to peak scale size of the diffracting screen, and $r_o = L/2\pi$, the size of a single irregularity, is realized. Also, correlation functions, if they are evaluated, must be interpreted in a consistent manner. The size estimations agreed with the earlier results of Kent (1961) and Jones (1960) already mentioned here and Aarons and Guidice were able to conclude that the shorter dimension of the irregularities appeared to increase with increasing latitude.

There is still a large amount of work to be done before the variation of F region irregularity size with latitude is known, and, as indicated by Jones, the possible presence and effect of a variation of irregularity height with latitude must also be taken into account.

In all the preceding experiments, care was taken to ensure that the measurements of irregularity size were made in quiet magnetic conditions and that single scattering

was taking place. It cannot be assumed that the irregularity size will be unchanged under other conditions. In particular, reductions in size, usually during periods of magnetic disturbance, have been shown to be a possible cause of radio star visibility fades.

Information regarding irregularity dimensions above the F region maximum has come from ionograms recorded on topside sounders carried in rockets and satellites. Calvert et al. (1962) observed ducts from a rocket borne sounder and measured values of about 1.4 km for their size transverse to the magnetic field. They may be hundreds of kilometers long in the direction of the field. Dyson (1967) showed from ray tracing techniques that ducts of these dimensions were capable of guiding the satellite or rocket transmissions along field lines down to and back from the signal reflection point in the F region whether the ducts contained an excess or deficiency of electron density compared to the ambient ionization.

(iv) Association between Scintillation and Spread-F. Soon after the terrestial origin of the signal fluctuations had been established, Ryle and Hewish (1950) and later Little and Maxwell (1951) showed that spread-F as observed on ground based ionosondes and the scintillation of radio

star signals tended to occur on the same nights.

Later, Dagg (1957 b) from observations at Jodrell Bank, England, found that although the diurnal behaviour of the two phenomena was very similar, showing a night time maximum and a day time minimum, the peak of scintillation occurrence preceded the peak of spread-F occurrence by up to four hours. He suggested that this might be explained in terms of blanketing by the F layer such that as the critical frequency of the F layer falls and the intensity of the irregularities remains the same, then because of the different frequencies used to observe the two phenomena, spread-F will be detected more strongly whereas the intensity of the scintillation will not change. Similarly, spread-F will be observed less strongly as the critical frequency increases. This effect would appear to operate successfully without the height of the irregularities changing with respect to the F region maximum.

Briggs (1964) confirmed that the result obtained by Dagg was valid over a whole solar cycle and Chivers (1963) showed that F region blanketing would be sufficient to explain the phase shift between the diurnal variations of the two phenomena.

Singleton (1962 a) obtained results at Brisbane, Australia showing that on a day to day basis, the correlation between spread-F occurrence and the F layer critical

frequency was significantly negative indicating that spread-F was more likely to occur when the critical frequency was low. This experimental result confirmed that the suggestion that blanketing was responsible for control of the spread-F diurnal variation could be a valid one.

It is also possible that the explanation lies in a difference in the diurnal behaviour of topside and bottomside spread-F. Recently, Krishnamurthy (1966) compared the diurnal behaviour of bottomside spread-F with that of the topside spread-F observed on the Alouette satellite ionograms, and he found that near the magnetic equator, the onset and peak of bottomside spread-F preceded the onset and peak of topside spread-F by about two hours. While this result can in itself be explained by an increasing height of the irregularities during the night, (or by the F layer height decreasing), it is not in the correct sense to explain Dagg's result. Unless there are marked changes in the phase of diurnal behaviour of topside spread-F with latitude, it seems that the phase difference between the diurnal variations of spread-F and scintillations must be explained solely in terms of blanketing. As yet there appear to be no diurnal plots of topside spread-F occurrence for high latitudes

which could alter the above discussion.

Chivers (1960) using four years of data from Jodrell Bank, and Briggs (1964) using twelve years of data from Cambridge, arrived independently at the conclusion that (at least at mid-latitudes) scintillation and spread-F activity showed opposite long term variations with solar cycle - the occurrence of scintillation increasing with solar activity and the occurrence of spread-F decreasing. In particular, Briggs found that in the years close to the sunspot maximum in 1957, there were many occasions when scintillation was visible but there was no spread-F. This situation did not occur near sunspot minimum. Dyson (1967) found, using data observed at several different Australian stations between October 1962 and March 1963, that irregularities were often observed on topside ionograms when the bottomside ionograms showed clear traces. However, further results are required from the coming period of sunspot maximum before the significance of his results can be fully realized.

Chivers (1960) concluded from his results that scintillation occurrence showed a seasonal variation, with maxima at the equinoxes, which became more apparent as solar activity increased. This variation contrasted with that of spread-F which showed a single maximum of occur-

rence in winter which became weaker as solar activity increased. Briggs (1964) preferred to interpret the variations in scintillation activity as solar and sidereal time variations rather than as seasonal variations although either conclusion is difficult to support using data from only one source.

Brigg's interpretation was given further support recently by the observations of Smerd and Slee (1966) from Fleurs, in Australia.

The positive correlation between the occurrence of spread-F and scintillation activity on a night to night basis (which excludes the similar diurnal variations from the correlation) appears to be well established. Ryle and Hewish (1950) and, in more detail, Briggs (1964) are among the many authors to obtain this result. Generally, a lack of complete correlation has been explained in terms of spread-F and scintillation not being observed at the same site, or in terms of the scintillating irregularities being above the height of the F region maximum for part of the time, in which case they are invisible to ground based sounders.

(v) Relationships Between Magnetic and Ionospheric Parameters. The influence of geomagnetic activity on ionospheric scintillations, spread-F, the

F region critical frequency $f_o F_2$, and the F-layer height, has in recent years been the subject of much investigation. Different authors have used various measures of geomagnetic activity including magnetograms recording the minute by minute changes in the vertical and horizontal components of the earth's magnetic field, the local K indices, or the planetary indices A_p and K_p. The relationships as they are currently understood and some of the background are summed up in the following paragraphs.

Soon after the discovery of scintillations in the signals from radio star sources, Hewish (1952) reported that he had found little correlation between scintillation amplitude and K index but that the F region drift velocity (which determined the scintillation rate) and K index were positively correlated. He noted further that although there was no detailed correlation between scintillation amplitude and K index, there was some tendency for the degree of irregularity to increase during periods of extended geomagnetic activity.

Dagg (1957 b) showed that both scintillation rate and amplitude had a diurnal variation similar to the magnetic K index but found no correlation between the K index and scintillation amplitude on an hour to hour basis. In a

companion paper (1957 a) he compared variations of scintillation rate and amplitude with records from a nearby magnetogram. In this case, he did find occasional detailed correlation between scintillation amplitude and geomagnetic activity. Generally, the correlation between the magnetic field changes and the scintillation amplitude was poor while the correlation between the magnetic field changes and the scintillation rate was good. In a few cases however, the scintillation amplitude showed good correlation (better than the scintillation rate sometimes) with the magnetic field changes. The correlation of scintillation rate with magnetic field changes was reduced when the changes were restricted to the horizontal component - a result supporting the theory that changes in the vertical component of the field correspond most closely to changes in the drift velocity of the irregularities. In some cases, Dagg observed time delays of up to one hour between the magnetic field changes and the scintillation amplitude and rate changes. He attributed these delays to the distance between the magnetic and ionospheric observing sites which could introduce a time delay if the disturbance mechanism was of a localized nature and was travelling in the appropriate direction.

Briggs (1961) summarized the results of correlating the scintillation amplitudes of the Cassiopeia A source recorded at Cambridge and Jodrell Bank with local K index. These results indicated that for the 38 MHz scintillation observations, the correlation was small and positive for all positions of the source at sunspot minimum but at sunspot maximum the correlation was positive when the source was near upper transit and negative when the source was near lower transit. The average correlation coefficient, for all positions of the source at sunspot maximum, was zero. He pointed out that, in view of the facts that a positive correlation between scintillation and spread-F was regarded as established for all latitudes (the same irregularities being supposed responsible for both phenomena), and that Shimazaki (1959 II), amongst others, had shown that spread-F and magnetic activity were also positively correlated - at least in middle latitudes, a positive correlation between scintillation amplitude and K index was expected and the 38 MHz results from Cambridge were therefore rather surprising. As discussed in section 1.2(ii), Briggs was able to resolve this anomalous result for sunspot maximum in terms of the finite size of the source which under certain conditions caused the scintillation amplitude to decrease even though the degree of

irregularity in the ionosphere had increased. He concluded that K index was in fact correlated positively with degree of irregularity of the ionosphere at all times, although the correlation was weaker at sunspot minimum than at sunspot maximum.

Slee (1962) supported Briggs' result for mid-latitudes with radio star scintillation observations from Fleurs, near Sydney, and emphasised Briggs' conclusion that confusion could arise if the inversion or source size effect was influencing the observations and their presence was not realized. He also pointed out that since the correlation between the phenomena, although significant, is only partial and since, in particular cases, scintillation may occur on magnetically quiet nights and may not occur on magnetically disturbed nights, that magnetic field fluctuations are not a direct cause of scintillation activity. They could however act to render a scintillation producing mechanism, already present, more effective.

Shimazaki (1959) showed that the correlation between spread-F and geomagnetic activity varied markedly with magnetic latitude, that it was strongly negative for latitudes less than 20 degrees, that it was positive in the range 20 - 60 degrees, and that for higher latitudes, it was again negative. He showed that the negative

correlation at high latitudes was partly influenced by the presence of polar blackout under disturbed conditions which rendered the spread-F, if present, invisible to ground based sounders. Rao and Mitra (1962) agreed with Shimazaki's calculation of negative correlation between spread-F and geomagnetic activity at the equator and indicated that part of the explanation of this might come from the observations showing that the height increase of the F layer, which normally preceded the onset of spread-F, was inhibited in the presence of disturbed magnetic conditions. They also stated that spread-F and geomagnetic activity are positively correlated at high latitudes but they did not justify this statement sufficiently and may not in fact have been referring to auroral latitudes. Calvert and Schmid (1964) gave support to Shimazaki's suggestion that polar blackouts were important in removing the correlation at high latitudes between spread-F and geomagnetic activity. Using the Alouette topside sounder satellite, they observed no reduction in topside spread-F occurrence near the magnetic pole. In data from a period of near minimum solar activity they observed no significant correlation between topside spread-F and geomagnetic activity in high latitudes.

Koster and Wright (1960) established that in

equatorial magnetic latitudes, the occurrence of both spread-F and scintillation activity is reduced during a magnetic disturbance. The effect is weak near sunspot minimum, but near sunspot maximum it is sufficiently marked so that it can often be taken as an indication that a magnetic storm is in progress.

King (1961) observed that in mid-latitudes the F region critical frequency $f_o F_2$ is, for the southern hemisphere summer months, negatively correlated with geomagnetic activity. In a later paper, King and Graham (1962) described a similar experiment with a longer length of data and showed that the negative correlation did not hold all the year round; it was positive in the winter months. Since in mid-latitudes, spread-F and geomagnetic activity are positively correlated, the negative correlation found by King for all but the winter months is consistent with Singleton's (1962a) result showing that in mid-latitudes, spread-F and $f_o F_2$ were negatively correlated.

King (1962) pointed out that in mid-latitudes, changes of F layer height (which can alter the amount of spread-F visible from the ground and which in equatorial latitudes may be partly responsible for the production of irregularities observed as spread-F), are very small during magnetic storms. Large fluctuations in height may occur during

individual storms, but as discussed by King and Scott (1962), the day to day changes in the F layer height are more closely associated with the solar flux than with magnetic activity.

King (1961) appears to have been the first to suggest that there might be real delay between a magnetic and an ionospheric disturbance and he showed that in making a selection of ionospherically quiet days in mid-latitudes, it was better to choose the day following a magnetically quiet day rather than the day itself. In earlier work, delays of the order of hours had been noted. In the case of the experiments investigating detailed comparisons between scintillation records and magnetograms the delay was explained in terms of the travel time of a disturbance from the magnetic to the ionospheric observatory and in the case of experiments involving the correlation of K indices with scintillation or spread-F occurrence indices, the delay could be explained if the onset of geomagnetic activity occurred during the day - in which case ionospheric effects (since scintillation and spread-F are basically nocturnal phenomena) would not be evident until after nightfall.

Briggs (1965) analysed spread-F indices from Slough, U.K., and magnetic indices from the nearby magnetic observatory at Hartland for the years 1949-1960. He

computed the auto and cross-correlation functions for these indices with the data broken up into yearly intervals. His results for the cross-correlation functions with no time shift confirmed those of earlier workers with regard to the variation in correlation through the solar cycle, but in addition, showed that the maximum correlations were obtained when the K indices were correlated with the spread-F indices corresponding to a later day. The time lag of the maximum correlation was generally 1 day but was as high as 2 days in the years preceding the 1957 maximum of solar activity. His value of 1 day for the time lag in 1960 agreed with King's result. Provided the time lag is included in an analysis, a significant positive correlation can be found between spread-F and geomagnetic activity for the whole solar cycle. This was not the case when the calculation was based on attempts to find a simultaneous correlation.

To date, a similar analysis does not appear to have been carried out at any latitudes using scintillation data, but the results of such an investigation are presented here in a later chapter.

It would be very interesting to extend the work of King (1961) and Briggs (1965) to auroral latitudes where the incoming charged particles responsible for magnetic field fluctuations are also regarded as a possible direct

agent in the production of irregularities in the ionosphere, so that in these regions a time delay between the onsets of geomagnetic activity and ionospheric activity would be rather surprising.

1.5 Theories of Irregularity Formation

To be completely successful, a theory of production of irregularities should explain satisfactorily all the physical properties of irregularities such as size, shape and intensity, all the temporal, geographic and height variation in the above, as well as in the occurrence frequency, and the correlation with magnetic activity. Although no single theory has as yet been found that satisfies all the above requirements, it appears that over the last decade, considerable progress has been made.

Dagg (1957c) critically reviewed the then current theories on the origin of ionospheric irregularities, among them being the Accretion and Evaporation theories which predicted unchanging behaviour from one day to the next, the particle influx theory which he criticized because its application was limited to high latitudes (it is now realized that this restricted validity is important), and the turbulence theories, later supported by Booker (1958) which then and later were shown to be inadequate because of the very high electromagnetic damping present in the F region,

and because of the doubtful validity of turbulence concepts, valid at lower altitudes, in the F region. Dagg (1957d), in a companion paper, suggested that turbulent motions in the dynamo region between 110 and 150km might be coupled into the F region via the magnetic lines of force - the electrical conductivity along the lines of force being large compared with that perpendicular to the lines of force.

Martyn (1959) proposed that an irregularity amplification mechanism would exist if there was a differential vertical velocity between an electron density irregularity and the background ionization. The mechanism would work for either an electron excess or deficiency in the irregularity which could be above or below the maximum electron density in the layer. If the relative vertical motion was in the appropriate sense, the irregularity would be amplified; with the relative motion in the opposite sense, it would be attenuated.

In a recent review paper, Herman (1966) stated that recent investigations point to the likelihood that no single theory can be expected to account for the existence and properties of irregularities in both equatorial and high latitude regions. He discusses critically the currently favoured theories and indicates their applicability in various geomagnetic regions. Some of these theories are briefly

recapitulated here under similar headings with some further comments.

(i) Amplification Theories of Irregularity Formation.

Since the conception of Martyn's theory, several difficulties have arisen with regard to its application. The main one is that the irregularity may not be stable over the time or vertical distance required either due to deformation as it moves relative to a background electron density gradient or due to the effects of diffusion. In addition, a driving force is required to move the irregularity relative to the background and while an east-west electrostatic field in the F region is sufficient to do this it is not clear how it gets there. Martyn points out that whenever electric fields exist in the dynamo region (100 - 130 km) they might be coupled into the F region by conduction along the lines of force of the earth's magnetic field. However, Calvert (1963) suggested that in equatorial regions where the field lines are almost horizontal, the coupling mechanism is not established but that a satisfactory electric field can be generated from the contraction of the neutral atmosphere as it cools after sunset. Calvert noted that the observed cooling appeared to provide the same degree of instability as that provided by the electric fields suggested

by Martyn.

The amplification theory does not in itself explain the origin of the irregularities but it has been invoked as part of several other theories for their origin. Possible mechanisms suggested for initiating instabilities in the F layer itself are the resistance of the ionization in the layer to gravitational forces due to the earth's magnetic field, and the gravity waves suggested by Hines (1960) which could be excited as a result of a sudden adjustment of the neutral atmosphere after sunset.

Some experimental support for the amplification theory and for Calvert's driving mechanism may be found from the work on F region field aligned echoes by Clemesha (1964) in Ghana. He measured differential vertical velocities (of up to 70 m/s) between the irregularities and the background ionization and stated that the echoes were rarely observed before the F layer started to fall after sunset. Schrader and Kan (1965) in a paper seeking an explanation for the peak occurrence of these field aligned echoes at sunset (reported over a wide range of equatorial and middle latitudes) found downward velocities of the F layer ionization had their maximum values at Puerto Rico at sunset (and sunrise), but their velocities were not as large as Clemesha's values. In evaluating the importance of the irregularity amplification mechanism, they considered that

the limiting factors were diffusion and the magnitude and persistence of the differential vertical drift velocity. They did not consider deformation of the irregularities in the presence of a background ionization gradient to have a limiting influence. In a series of calculations for different geomagnetic latitudes, they found when they neglected diffusion that the amplification factor had a maximum value of 5 at the geomagnetic equator and decreased with increasing latitude. They considered that in the presence of diffusion, the amplification would not be sufficient to explain the observed sunset peaks in F region field aligned echoes. In view of Clemesha's observations which indicated much larger velocities than were used in the above calculations, the topic must still be regarded as an open one.

(ii) Theories Depending on the Transfer of Irregularities into the F region. Many theories have been proposed which suggest that the irregularities originate in disturbances above or below the F region and are transferred or coupled into it.

Dagg (1957d) and later Piddington (1964) considered coupling from the E region (where turbulence is readily explained) as a possible cause of F region irregularities but for the equatorial regions, these theories have been criticized due to the weak nature of the coupling. Even if the amplification mechanism is invoked with Dagg's

theory, there remains a large gap between the irregularity sizes allowed in the theory and those actually observed. Coupling between the E and F regions has also been considered in high latitudes where the field lines are nearly vertical but when the theories are evaluated, they prove to be inconsistent with observations and at present the E region is not considered a major source of F region irregularities.

Dessler (1958) suggested that the interaction of the solar wind and the earth's magnetic field at the magnetospheric boundary could initiate large amplitude hydromagnetic waves which could then propagate downwards through the ionosphere. He interpreted the magnetic field fluctuations recorded at the earth's surface as being indicative of the existence of these waves and was able to suggest how they were attenuated (rather severely) when propagated below F region heights. Singleton (1962c) combined Dessler's hydromagnetic waves with Martyn's amplification mechanism to obtain a theory for production of equatorial spread-F.

Theories of formation of high latitude irregularities appear in many respects to be more satisfactory. In particular, the field lines being nearly vertical, charged particle influx may now be considered as a possible irregularity forming mechanism and disturbances from above or

below the F region can be coupled into the region much more effectively than is possible at lower latitudes. For instance, Axford and Hines (1961) proposed a single causative agency, responsible for a wide range of observed geophysical phenomena, which derives its energy from the interaction between the magnetosphere and solar wind. As yet, their theory is too general for detailed application.

(iii) Theories Involving the Protonospheric Heat Flux. Rothwell (1961, 1962) considered that many of the observed properties of the F_2 region could be explained in terms of heat transfer by protons travelling along magnetic field lines between conjugate hemispheres. It was put forward as a possible explanation for the anomalously large values of $f_o F_2$ in local winter compared with local summer. Apart from the transfer of heat energy from one side of the equator to the other as discussed by Rothwell, Bowhill (1964) considered that these geometrically trapped protons could absorb and store solar energy during the day and could release it into the conjugate F regions at each end of a magnetic field line at night. This could account for the maintenance of the F region ionization at night and the observed night time excess in electron temperature

relative to the temperature of the neutral background.

If inhomogeneties existed in this proton flux, they could give rise to weak, field aligned irregularities near the F region maximum and to stronger irregularities at higher altitudes. The theory predicts the observed coupling between F regions and F region irregularities at conjugate points, but not the day to day variations in irregularity occurrence or their correlation with magnetic activity.

Bowhill made quantitative calculations of the fluctuations in protonospheric flux required to produce the observed irregularities in electron density, found them to be feasible, and suggested experiments which should be capable of observing the fluctuations directly. As yet, no results appear to have been obtained to compare with the theory.

(iv) Charged Particle Theories of Irregularity Formation. The concept of irregularities arising due to the influx of energetic charged particles is not a new one and was first advanced as a possible cause of aurora in the last century. It was also suggested in the form of the Accretion theory as a possible cause of the irregularities giving rise to radio star scintillation but was shown in this form to be unacceptable. It is now

well known that under the control of the earth's magnetic field, charged particles of the energy required by the theories (1 - 100 KeV - a small energy by cosmic ray standards) cannot penetrate to ionospheric altitudes except in the polar regions. They are now accepted as the fundamental cause of auroral displays and Herman (1966) indicated that theories of F region irregularity based on particle influx in the polar regions are well able to predict the intensity and size of the electron density irregularities. Such a direct causative mechanism also readily explains the positive correlations between polar spread-F and magnetic activity and between polar spread-F and visual auroras.

Summing up the foregoing discussion, the current theories of formation of irregularities in the equatorial regions appear to favour generation in the F region (other than from turbulence) and the transfer of irregularities from outside the layer. Martyn's amplification mechanism, probably driven by electrostatic forces generated by vertical movements in the neutral atmosphere, can be invoked in these regions and can form part of the other theories.

In high latitudes, the favoured theories suggest that irregularities might be transferred into the F layer from above, or generated in the layer due to ionization from the downward heat flux lost by trapped protons or from the

influx of energetic charged particles.

CHAPTER 2. THE INSTRUMENTATION AND THE RADIO STAR SOURCES

2.1 The Receiving Site

The scintillation observations carried out in this experiment were all made from the University of Adelaide field station at St. Kilda, South Australia. This field station is situated some 17 miles north of Adelaide and was originally selected as it was surrounded by farmland with little traffic, few power lines and no radio transmitters in the vicinity. At present, there are two "permanent" buildings on the site and power is connected from the state electricity grid. The receiving equipment for the radio star scintillation experiment described here shares the site with several other experiments but none of these include radio transmitters so that any interference encountered in the experiment must come from a source other than the field station. The geographical co-ordinates of the site are:

latitude 34° 43' south, longitude 138° 35' east and the geomagnetic latitude is 44° 42' south.

2.2 The Antenna Arrays

The analysis described in this thesis was based on the records from two phase-switching interferometers, each tuned to a frequency of 39.5 MHz (wavelength

λ = 7.60 metres) and each having its halves on an east-west baseline so that the main lobe of the reception polar diagram was in the north-south vertical plane. Thus, the apparent diurnal motion of the various sources due to the earth's rotation was sufficient to generate interference fringe patterns which were recorded on the receiver output. The antenna arrays for the two interferometers (which were designed for different aspects of the experiment), are rather different and require separate descriptions. The technical data for the design and construction of the Yagi antennas used in each array was obtained from the R.S.G.B.Amateur Radio Handbook and the A.R.R.L. Antenna Book and the final design parameters of the Yagi antennas for both interferometers lie within the limits recommended by these handbooks.

A photograph of the first and smaller antenna array to be erected is shown in Figure 2.1 and the dimensions of the interferometer and of each Yagi antenna are shown in Figure 2.2. The interferometer was designed to detect the strong northern radio source Cygnus A which, at this latitude, reaches a maximum altitude of 15° above the northern horizon. The array was in use from December 1963 to December 1965 and consisted of two 4-element Yagi antennas (with the driven element folded) separated by a distance of

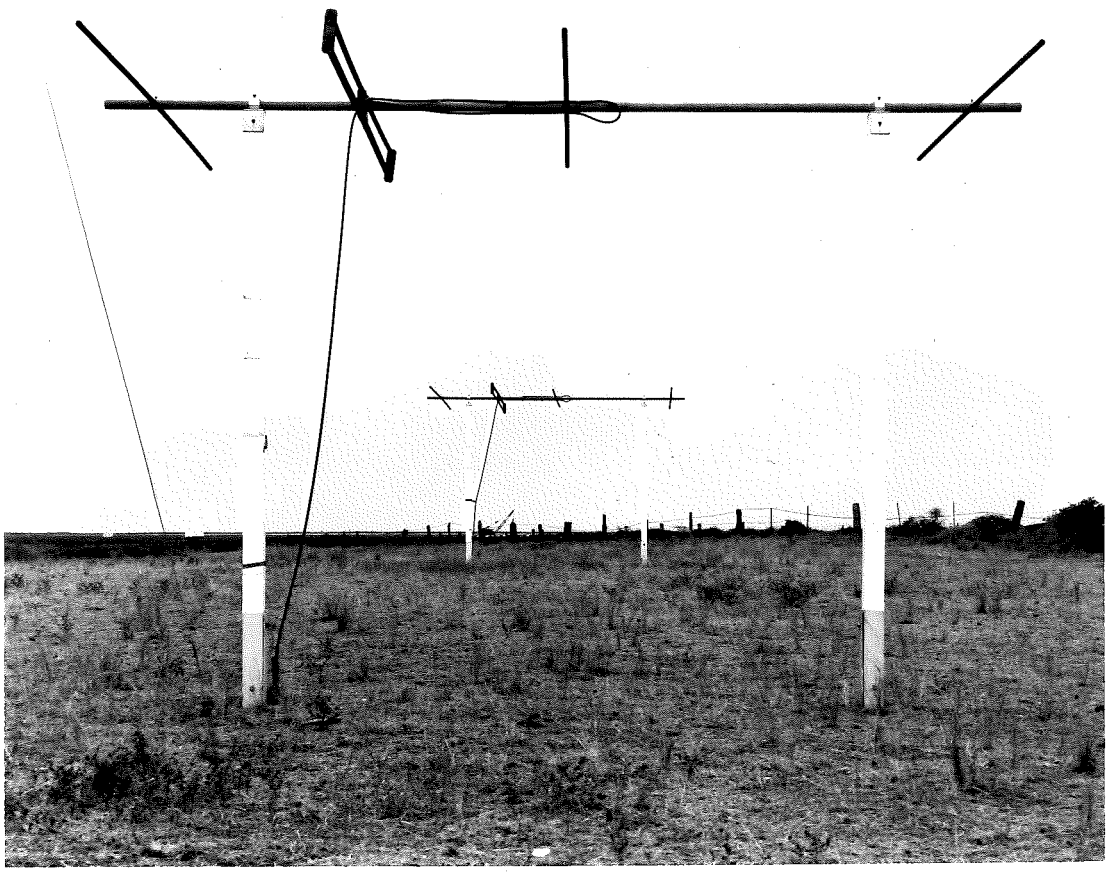

Figure 2.1 The Cygnus A interferometer array at St. Kilda, South Australia.

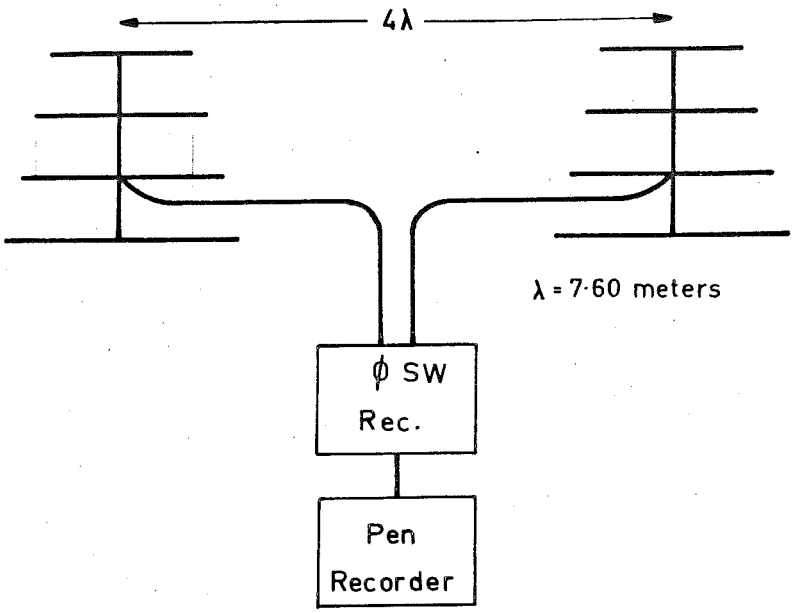

The dimensions of the interferometer.

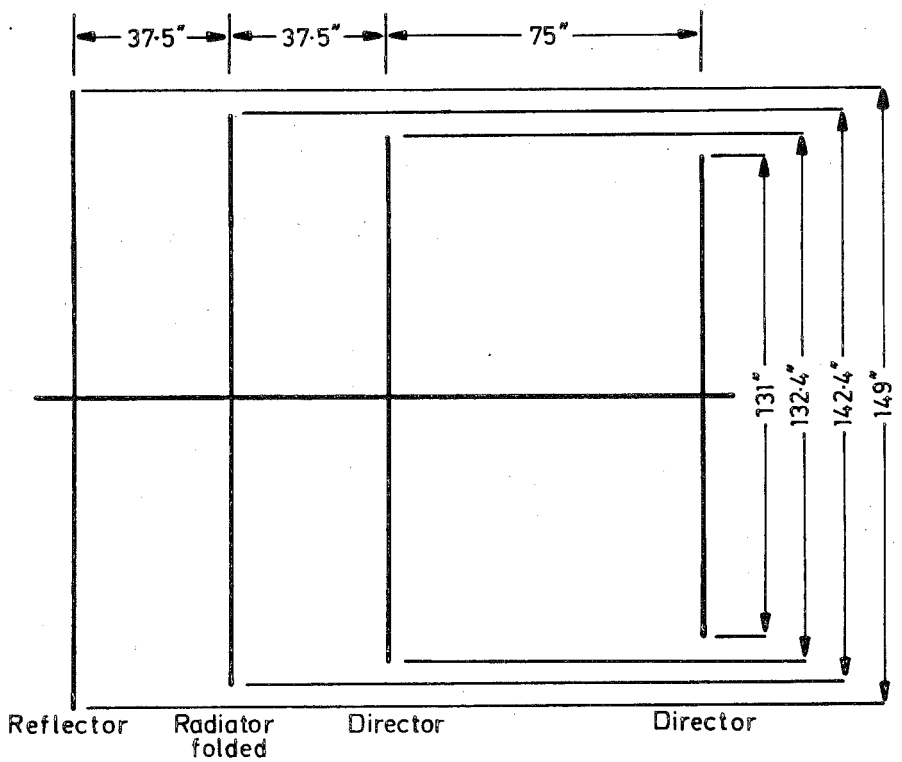

The lengths of the Yagi elements. Separation of folded element = 5"

Figure 2.2 The dimensions of the Cygnus A interferometer.

4 wavelengths and directed towards the northern horizon. With this arrangement, the polar diagram was not very directional, the range of azimuth angles over which the source could be detected being restricted by the polar diagrams of the Yagi antennas and a reduced response as the source neared the horizon. The height of the antennas above the ground was chosen to give a good response to signals from small elevation angles and, from Figures 2.26 to 2.43 of the A.R.R.L. antenna book calculated for horizontal and vertical antennas at various heights above the ground, a height of 3/8 wavelength was selected. It is to be noted that these figures may only be applied directly for an antenna with a polar diagram which is the same above and below the ground plane. This requirement is satisfied for a Yagi antenna if it is directed horizontally (as is the case here), but, due to the Yagi antenna's asymmetrical radiating properties, will not be satisfied for the same antenna directed elsewhere. The antenna mountings do not permit the array to be steered in any way, the only freedom allowed being a choice of the plane of polarization of the received signals. Although the figures from the A.R.R.L. antenna book indicate that signals from near the horizon should be received more strongly using vertical antennas, they are in fact received more strongly

with the antennas horizontal. This apparent discrepancy can be explained since the figures referred to are based on calculations assuming that the ground is a perfect electrical conductor. This assumption is not satisfied in practice and so, for all but a short trial period, the interferometer was operated with the antennas mounted horizontally.

The effects on the polar diagram of the array due to the directional radiation pattern of the Yagi antennas, and due to the proximity of the ground, are discussed in Appendix A, part 3.

The signals from the two antennas were transferred via co-axial cables to one of the permanent buildings where the phase-switching receiver and pen recorder were housed.

A photograph of the second and larger antenna array to be erected is shown as the frontispiece and the dimensions of the interferometer and of each Yagi antenna are shown in Figure 2.3. This interferometer, which was in operation from December 1965 until September 1966, was designed to detect many sources distributed over all values of right ascension and over a wide range of declinations. Since the Cygnus A source is stronger (by a factor of ten or more) than others detectable from the same site, and since it was desirable that the sources detected should interfere with each

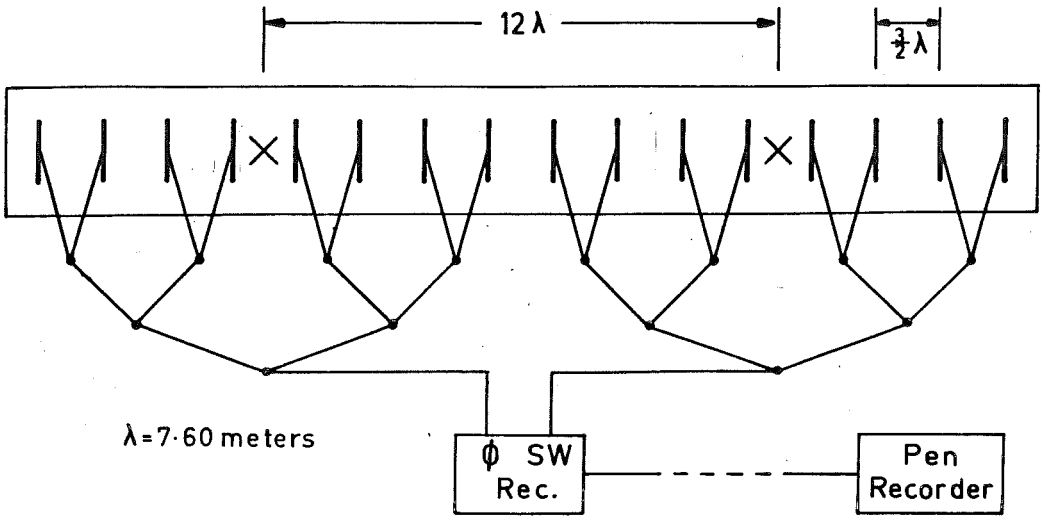

The dimensions of the interferometer.

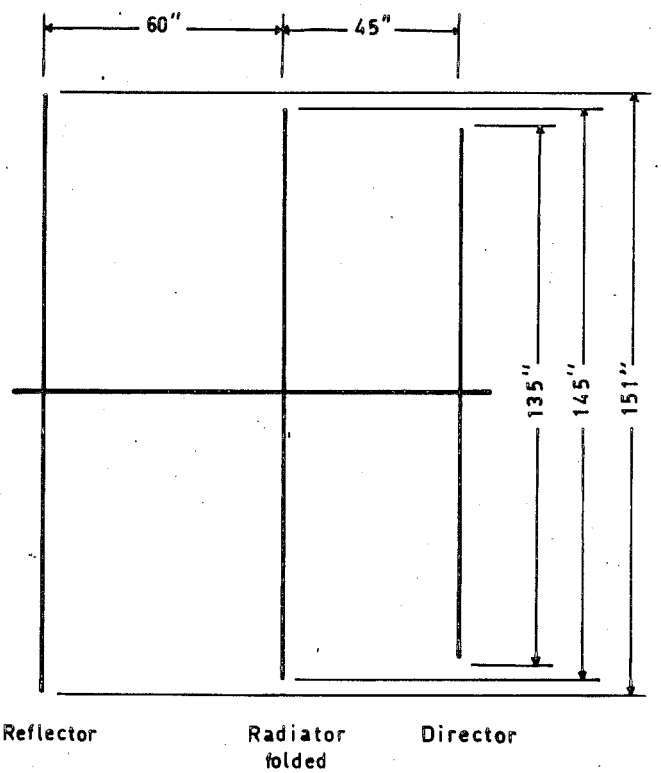

The lengths of the Yagi elements. Separation of folded element = 4"

Figure 2.3 The dimensions of the large interferometer.

other as little as possible, the collecting area of this interferometer array had to be larger than the Cygnus A instrument and the radiation polar diagram had to provide good resolution in right ascension and be relatively insensitive to declination. The array therefore consisted of sixteen 3-element Yagi antennas in a single line uniformly spaced 3/2 wavelengths apart. As in the case of the Cygnus antennas, the driven elements were folded.

Eight of the Yagi antennas constituted each half of the interferometer, the centres of the halves therefore being separated by 12 wavelengths. As is the case for any filled interferometer (where the antennas are uniformly spaced and there is no gap between the interferometer halves), the output of the phase-switching receiver consisted of a single maximum in the output for each source - each source remaining in the "field of view" for about twenty minutes.

The calculation of the reception polar diagram for each half of this interferometer array is described in Appendix A, part 1. Part 2 of the same Appendix outlines the effects of antenna directivity and proximity of the array to the ground on the envelope of the polar diagram. From this Appendix, it is to be noted that since the aerials are spaced more than one wavelength apart, there is a first order "diffraction grating" lobe present in the polar diagram

for $\theta = \arccos \lambda/d$, θ being the angle between the line joining the antennas and the direction of arrival of the signal.

The height above ground of the antennas making up this array is the same as that chosen for the Cygnus A array, although, since they were directed vertically in the normal course of running, the reasons, for the choice of this height (3/8 wavelengths) for the Cygnus A array, no longer apply here. The array is fully stearable, the necessary adjustments being made for each antenna in turn.

For the best overall results, the interferometer was operated with the antennas directed vertically and the antenna elements aligned east-west. When running was first commenced, the antennas were aligned north-south as shown in the frontispiece. This arrangement proved unsatisfactory with regard to the Cygnus A source which was then "viewed" almost end on to the antenna elements. Under these conditions, the deflection of the output signal on the pen recorder was not conducive to the easy reading of the transit time of Cygnus A or to the assignment of scintillation indices to the signals from the same source. Results for the Cygnus A source are not available for the first few weeks of running due to the antennas being aligned in this way. For a short time the interferometer was also

run with the antennas directed 45° above the northern horizon, the main advantage of this being to enhance the reception of sources for which the transit was north of the zenith at the expense of those for which the transit was to the south.

Although level ground was sought on which to erect the array, the western end of the array is in fact 2 feet 3 inches lower than the eastern end. In addition, there are irregular variations in the ground level rather smaller than this from one antenna to the next. In order that these small undulations should be averaged out, the array was erected so that the centres of the Yagi antennas were in a straight line parallel to the mean ground plane beneath the array. This small slope (gradient 1 in 250) was corrected for by incorporating a small delay (an additional 1.7 inches of cable) in to the signal arriving from the western half of the interferometer.

Since the centre of the array lies some 250 yards from the permanent buildings on the field station site, it was decided to terminate the cables from the interferometer halves in a weatherproof box some 50 feet north of the centre of the array. This box housed the phase-switching receiver and power supply for the array and the receiver output was taken to the pen recorder (housed in one of the

permanent buildings) via an overhead telephone line. Figure 2.3 illustrates the Christmas tree pattern adopted for the cable connections of the interferometer - the length of cable from the receiver to the antennas being uniform except for the groundslope correction indicated previously.

2.3 The Phase-Switching Receivers

Several phase-switching receivers similar to that described by Ryle (1952) have been used in conjunction with both interferometers for the detection of the radio sources. Ryle discussed the properties of these receivers in some detail and later Tiuri (1964) compared their efficiency with that of other types of correlation receivers used in radio astronomy.

The receivers and associated power supplies used throughout this experiment are similar to the standard phase-switching receivers and power supplies used at Cambridge, U.K. for some years for similar experiments there. The block circuit diagram of the receivers is shown in Figure 2.4.

The most important modifications made to the receivers for the present experiment were:

(a) The phase switch cables and the R.F. circuits were tuned to 39.5 MHz rather than 38 MHz - the latter frequency being that at which many of the Cambridge observations had

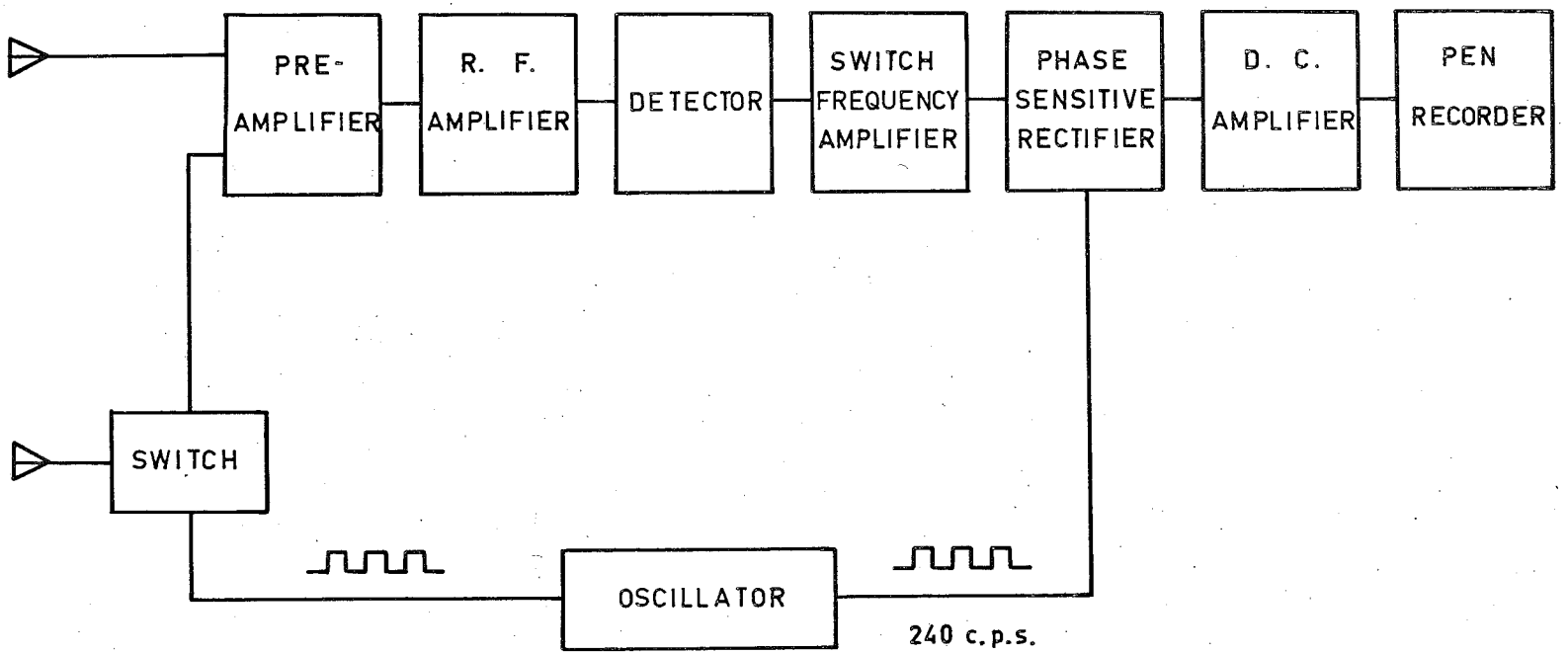

FIGURE 2.4 Block diagram of the phase switching receiver.

been made.

(b) A cascode circuit preamplifier was added to the input of each receiver and these improved the signal to noise ratio by a factor of 4 (6 db) and increased the overall gain of the system. These preamplifiers were not always connected for the Cygnus A experiment but were necessary for the recording of signals from the weaker sources detected with the larger array.

Other minor modifications were made - these were directed mainly towards prolonging the life of the series regulator valves in the power supplies and had no bearing on the experimental results.

The receivers had a radio frequency bandwidth of 1 MHz, they were operated with a time constant (determined in the D.C. amplifier stage) of 1 second, and the diodes in the phase-switching circuits were controlled by a 240 cycle per second square wave. An Evershed 3-track pen recorder (impedance 5000 ohm, time constant 1 second) was run generally at a chart speed of 3 inches per hour but on some occasions, a speed of 6 inches per hour was used. At the slower chart speed, the pen recorder could be left to run unattended for a period of 10 days although this was rather undesirable in practice. Alternative time constants in the receivers of less than 1 second were also available, but, as

the time constant was reduced, the receiver output became very noisy and the pen recorder was not sufficiently rapid to follow properly the faster fluctuations.

The application of several of the points made by Ryle (1952) (and others) concerning the properties of the phase-switching interferometer is now discussed for the present instruments.

2.4 The Output of the Phase-Switching Receivers

Following the original paper (but not the notation) of Ryle, the amplitude of the signal response of a phase-switching interferometer is given by:

$$A(\theta) = S_E(\theta) \cdot S_W(\theta) \cdot \cos\Phi(\theta)$$

where $\Phi = \frac{2\pi D}{\lambda} \cos\theta$ and is the phase difference between the signals arriving at the centres of the eastern and western halves of the interferometer array and D is the distance between the centres of the halves of the array.

The condition Φ(or θ) = constant generates a cone of semi angle θ and with its axis along the line joining the centres of the halves of the interferometer.

S_E and S_W are functions of this angle θ and describe the polar diagrams of the eastern and western halves of the interferometer array. Appendix A describes these functions for both the arrays used in this experiment and

indicates that in each case S_E and S_W are the same. Thus, the signal response of the interferometer is given by:

$$A(\theta) = S^2(\theta) \cdot \cos \Phi(\theta) \qquad (2.1)$$

Also in Appendix A, it is pointed out that the angle θ may be defined conveniently in terms of the celestial co-ordinate system:

$$\cos(\theta) = \cos(\text{declination}) \cdot \sin(\text{hour angle}) \qquad (2.2)$$

Taken together, expressions (2.1) and (2.2) are suitable for the calculation of the receiver output as a function of time for a particular source (cos (declination) is then constant), or for the calculation as a function of declination of the hour angle (period) of the interference fringes for either interferometer, or in the case of the large interferometer only, the hour angle of the first order diffraction grating lobe. The fringe periods are found by putting $\cos\theta = \frac{n}{4}$ for the Cygnus A interferometer, or $\cos\theta = \frac{n}{12}$ for the larger interferometer, and the hour angle of the first order diffraction grating lobe of the larger interferometer is found for $\cos\theta = 2/3$.

Representative results of these calculations are shown in Figures 2.5 to 2.8 which show the receiver outputs and the periods of the central maximum for each array and

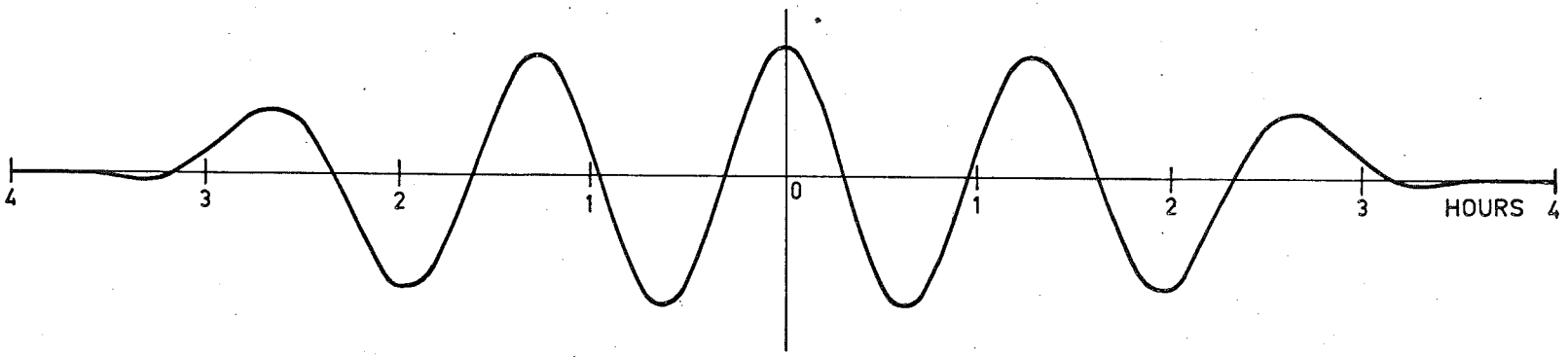

Figure 2.5 Response of the small interferometer to the Cygnus A source at declination 40·5°N

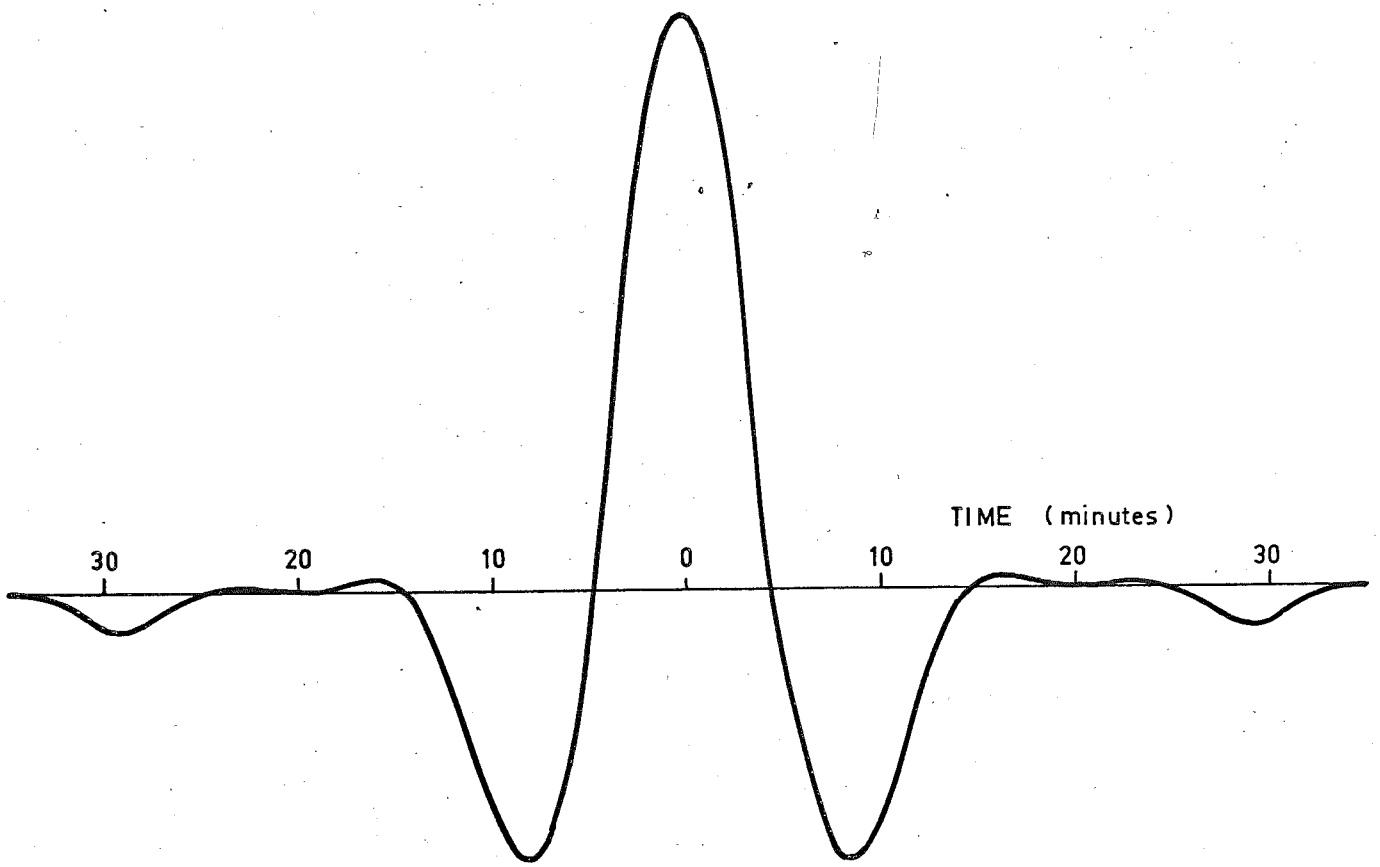

Figure 2.6 Calculated response of the larger interferometer to the Virgo A source at declination 12.5°N.

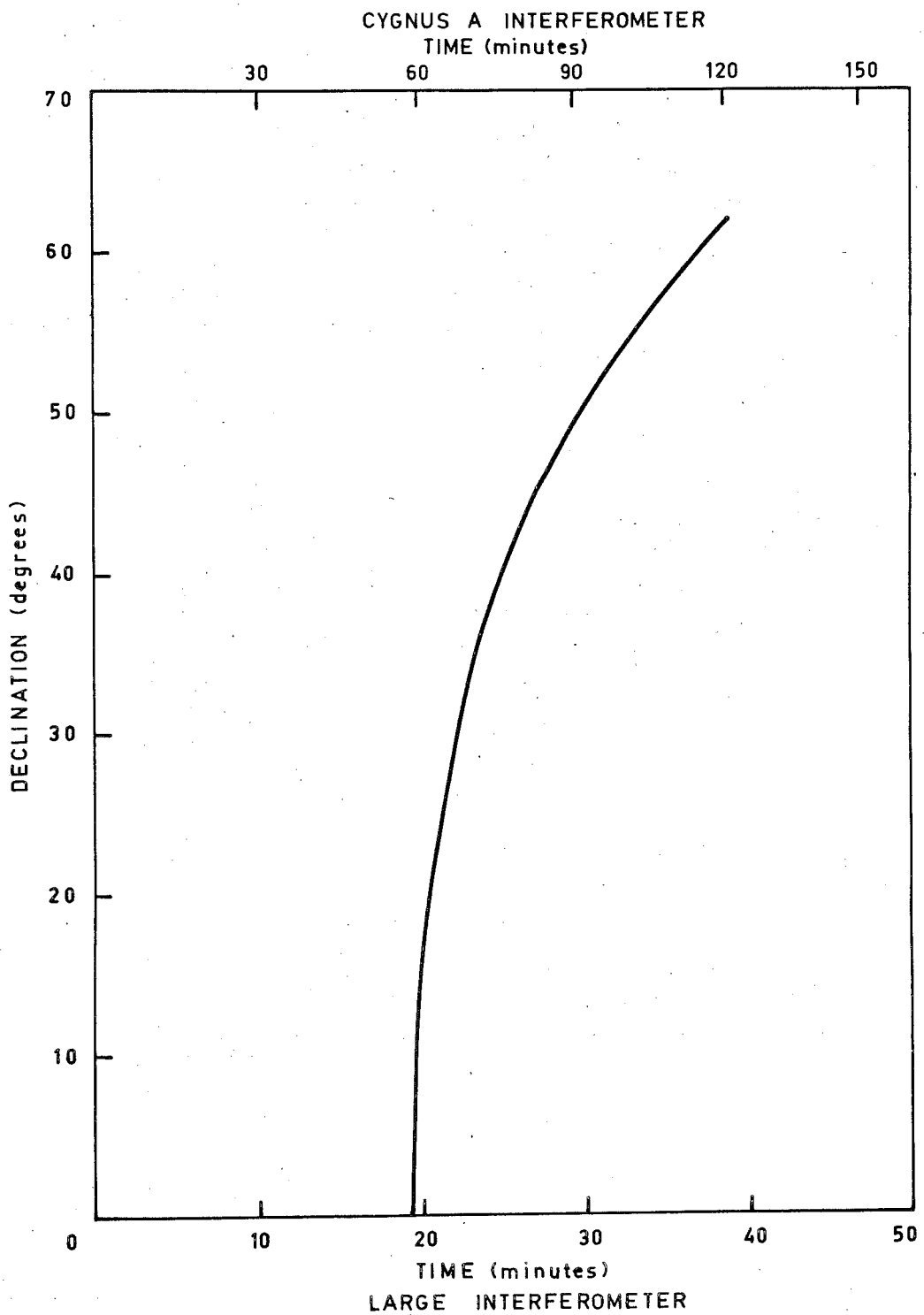

Figure 2.7 The variation is the period of the central maximum as a function of declination for both interferometers.

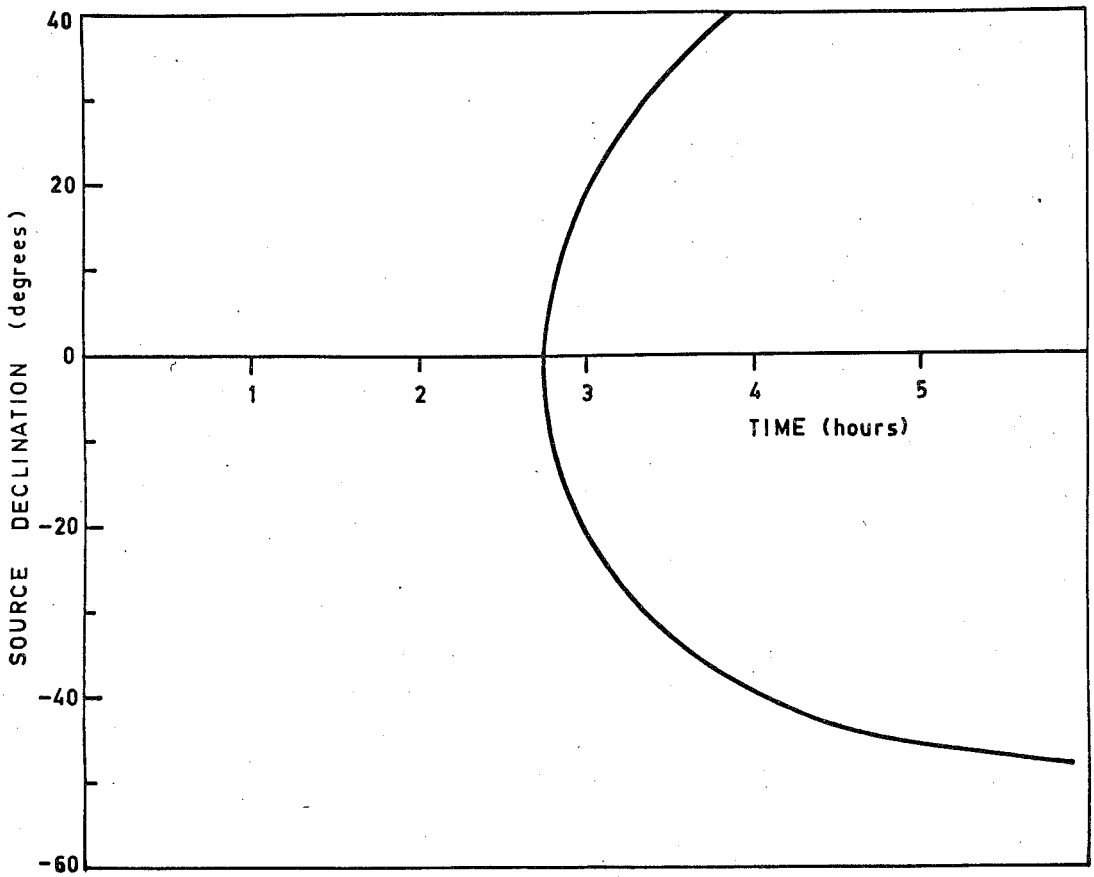

Figure 2.8 The hour angle of the first order diffraction grating lobe for the larger interferometer as a function of declination.

show the hour angle of the first order diffraction grating lobe for the larger array.

All the periods and hour angles calculated as indicated above are independent of the latitude of the observing site and this latitude need be included only when transformation is required from the celestial to a local altitude - azimuth co-ordinate system. The only bearing the latitude of the St. Kilda field station has on the present observations is that the northern source Cygnus A is not detected in the first order diffraction grating lobe of the larger array because it sets before reaching a sufficiently large hour angle. At St. Kilda, sources further north than 38 degrees declination will not be detected in the first order diffraction grating lobe for the above reason. The most southern declination (48 degrees) for which sources are detected in the first order diffraction grating lobe is determined by the 3/2 wavelength spacing of the antennas constituting the array and the northern declination limit would be similarly determined if the interferometer was erected at a sufficiently northern latitude.

Other results relating to the variation in sensitivity of the larger array in the main lobe, and in the diffraction grating lobe relative to the main lobe could be calculated for sources at various declinations. These results

are not reproduced here because of the rather arbitrary nature of the functions selected in Appendix A to describe the polar diagrams of the Yagi antennas and since these functions are required for these other results, the answers obtained would have doubtful physical significance.

In the case of the larger interferometer, the calculations of the celestial positions of the interferometer lobes have been verified from measurements of the apparent right ascensions of the sources detected. These lobe positions have also been verified from recordings made with a fast chart speed of passes of the beacon satellite Be - C which has an orbital inclination to the equator of 41 degrees and transmits a frequency of 40 MHz. The satellite observations were particularly useful in checking the positions of the diffraction grating lobes and are described in Appendix B.

2.5 Source Visibility Determined from the Interferometer Parameters

In section 1.2, it was shown that anomalous reductions of source visibility (fadeouts), lasting for short periods, could occur when angular scintillations from ionospheric irregularities were so severe that the apparent position of a source was shifted rapidly through angles larger than

the array lobe size. Fade outs were observed for point or extended sources. In the present problem, the source is considered to be extended and the size of the source is calculated for which the visibility will be reduced by a given amount in the absence of angular scintillation.

From Ryle (1952), the amplitude of the output of an interferometer due to an extended source will be reduced relative to the output from a point source by a factor sin x/x, where:

$$x = \frac{\pi d \Delta\theta}{\lambda}$$, d is the interferometer spacing,

and $\Delta\theta$ is the angular width of the source. (Notice that in Ryle's paper, $\Delta\theta$ represented half the angular width of the source and the value of x above does not contain his value of 2 in the numerator to allow for this).

For the larger of the St. Kilda interferometers, d = 12 wavelengths and the amplitude of the receiver output is reduced to one half for $\Delta\theta = 2.85^{\circ}$. It should be pointed out that in the case of an east-west baseline interferometer, the extension of a source is not important if it is restricted to the declination co-ordinate.

Neither of the Magellanic Clouds are detected with the larger St. Kilda interferometer because, although

they are both strong sources, the visibility of both is reduced due to their large angular extent.

In the case of the smaller interferometer which, firstly requires a more extended source to produce a similar visibility reduction and secondly, detects only Cygnus A (a small diameter source), there should, under the quiet ionospheric conditions assumed here, be no source visibility reduction effects observable due to any extended single source apart from the galactic background.

2.6 Scintillation Visibility and Receiver Bandwidth

In the discussion of inversion in section 1.2(iii), it was pointed out that the visibility of radio star scintillations could be influenced by the bandwidth of the receiver. In fact, the visibility of the scintillations will be reduced if the R.F. bandwidth of the receiver is larger than the bandwidth of the scintillations.

From Briggs (1966) the bandwidth of the radio star scintillations is given by:

$$\Delta f \sim \frac{f^2 L^2}{Zc} \quad \text{for} \quad \phi_0 < 1 \text{ radian}$$

$$\text{and} \quad \Delta f \sim \frac{f^2 L^2}{Zc\phi_0^2} \quad \text{for} \quad \phi_0 \geq 1 \text{ radian}$$

where, f is the frequency of the radio signal

L is the scale of the phase screen = $2\pi r_o$

r_o is the auto-correlation distance across a single irregularity

Z is the distance from the receiver to the irregularity layer

ϕ_o is the root-mean-square phase deviation of the signal in the layer

The relations are correct within an order of magnitude and the symbols the same as those used in section 1.2(iii). If the receiver bandwidth exceeds the above values of Δf then the scintillation visibility will be reduced.

If the values f = 40 MHz, L = 5 km, Z = 400 km, and $c = 3 \times 10^5$ km/sec are substituted into the above relations, then the following values for the scintillation bandwidth are obtained:

$$\Delta f \simeq 330 \text{ MHz} \quad \text{for} \quad \phi_o < 1 \text{ radian}$$

$$\text{and } \Delta f \simeq 330/\phi_o^2 \text{ MHz for } \phi_o \geq 1 \text{ radian}$$

The value of Δf for $\phi_o < 1$ radian is rather unrealistic for a frequency of 40 MHz but the calculation does indicate that even if Z is larger by a factor of 4 (as it

can be at low elevation angles), L must decrease to a value near 50 metres (which is unlikely, especially in the F region) before the bandwidth of the receiver (1 MHz here) becomes important. On the other hand, it does seem possible that the bandwidth of the receiver might become important under extremely disturbed conditions, especially at low angles of elevation where Z is large. Lawrence et al. (1964) chose to interpret some earlier results of Chivers and Davies (1962) who observed scintillations at low angles of elevation in terms of an effect present due to the bandwidth of their receiver.

The further discussion of the effect on scintillation visibility of the receiver bandwidth is postponed to later chapters where it is taken up again for particular aspects of the experiments.

2.7 Elimination of Man-Made Interference

Ryle (1952) pointed out that if the spacing of the arrays constituting the phase-switching interferometer was sufficiently large, then natural or man-made interference from nearby sources would not produce any output from the receiver because it was sensitive only to signals received in both halves of the interferometer. Unfortunately, these remarks do not apply to the equipment described here

because the spacings of the St. Kilda interferometers are only 4 and 12 wavelengths, and any interfering signals correlate in the receiver just as effectively as do signals from the distant radio star sources.

CHAPTER 3. SOURCE IDENTIFICATION AND THE INTERFEROMETER RECORDS

3.1 Methods of Source Identification

Initially, tentative source identifications were made for the output of both interferometers by examining the pen recorder charts, recording the transit time of a source, converting this to right ascension, and comparing the value observed with those published in radio source catalogues. The most general of these source catalogues is probably that of Howard and Maran (1965) which summarizes the results of over 250 radio star surveys and includes data on more than 1200 sources at northern and southern declinations. This catalogue contains information on the position, signal strength and spectral index for each source, and whenever possible includes notes on likely or established optical identifications and on the source size and fine structure. Although further source catalogues (in particular from Parkes, near Sydney, Australia) have been published since that of Howard and Maran, in the case of the relatively strong sources detected in this experiment, the Howard and Maran catalogue contains sufficient information.

In the case of a source at other than a small declination (where the period of the central fringe varies relat-

ively slowly), a good estimate of the source declination could be obtained from a measurement of the fringe period. However, it must be pointed out that this measurement on its own gives an ambiguous result since the declination so obtained can be either north or south and some other technique (such as redirecting the antenna to alter the array sensitivity for a given declination) must be employed to resolve this ambiguity.

A tentative identification was regarded as definite only if the observed signal strength (measured relative to other sources), right ascension, and declination (when it could be measured), corresponded to the catalogue data and if there were no other sources present either at a similar right ascension or at a right ascension such that they could be detected in the first order diffraction grating lobe at the same time.

3.2 Sources Identified and their Relevant Physical Properties.

From an inspection of the records from the smaller interferometer, it was concluded that only the Cygnus A source regularly produced a significant output from the receiver. The identification was supported by the time at which it was detected and its observed fringe period.

The sources Taurus A and Virgo A were also detected but not sufficiently strongly to make a scintillation analysis of their records possible. While it was straightforward to increase the gain of the receiver by connecting the cascode preamplifier so that these sources produced larger amplitude records, under these conditions, the amplitude of the output from the Cygnus A source was so large that the pen recorder was driven well off scale, and amplitude scintillation indices could no longer be assigned to the output of this source. This statement does not apply to records from the larger interferometer because, when the Yagi antennas of the array are directed upwards, the interferometer is less sensitive to sources at large zenith angles than it is to sources near the zenith and the outputs from the sources Taurus A and Virgo A are enhanced with respect to the output from Cygnus A.

The fringe periods were determined for all three sources using at least 15 passes of each source. The results of these measurements are compared with the predicted periods in Table 3.1.

Source	Cygnus A	Taurus A	Virgo A
Declination	+ 40.5°	+ 22.0°	+ 12.7°
Observed Period	75 ± 2 min	64 ± 2 min	61 ± 2 min
Predicted Period	75.7 min	62.0 min	58.9 min

TABLE 3.1

In the case of the larger interferometer, source identification was less straightforward due to the greater sensitivity of the array, and due to the limited resolution in right ascension and the large declination coverage of the fan shaped main lobe of the array.

As a result of a detailed examination of the records, it was evident that nine sources were observed strongly enough so that their output could be analysed for occurrence of amplitude scintillation. These sources and some of their properties are listed in Table 3.2 and for reference purposes, their numbers, from the Howard and Maran (1965) catalogue, and, where appropriate, from the revised 3C catalogue of Bennett (1962), are also included. The values of flux density listed in the table refer to a frequency of 38 MHz and are the best estimates available from the Howard and Maran catalogue.

From this catalogue, it is evident that all of the sources listed in the table show fine structure of some sort which can be resolved with a suitable instrument, and that, strictly, the size of none of them can be effectively described by a single parameter. For each source, the table lists the value of source size which will be most important in determining any effect that the source might have on the visibility of amplitude scintillations detected

Source Name	Catalogue Numbers: Howard and Maran	Catalogue Numbers: Bennett	Observed Right Ascension	Howard and Maran Catalogue Position Epoch 1950.0: Right Ascension	Declination	Zenith angle at Transit	Flux Density $\times 10^{-26}$ w.m^{-2}(c/s)$^{-1}$	Size	Fine Structure
Fornax A	119		0322	0320 36s	-37°23'	3°S	2000	29'	S
3C 123	155	3C 123	0431	0433 55s	+29°34'	63°N	600	12.5"	S
Pictor A	186		0521	0518 24s	-49°50'	16°S	3000	5'	S
Taurus A	194	3C 144	0529	0531 31s	+21°59'	57°N	2500	5'	E
Hydra A	302	3C 218	0915	0915 41s	-11°53'	23°N	1400	1'	CH
Virgo A	379	3C 274	1226	1228 17s	+12°40'	47°N	3200	5'	CH
Centaurus A	405		1325	1322 36s	-42°48'	8°S	20000	7'	
Hercules A	489	3C 348	1647	1648 40s	+5°5'	39°N	1400	2'	S
Cygnus A	591	3C 405	1953	1957 44s	+40°37'	75°N	24000	2'	M

TABLE 3.2

Properties of the Sources Identified in the output from the larger Interferometer.

in its radio emissions. As described in the following paragraph, various qualifying letters are entered for each source in the table and indicate the nature of the fine structure in each case.

Two of the sources (qualifying letters CH) consist of a central core plus a halo. In the case of the Hydra A source the angular diameter of the core is quoted since the halo is responsible for only 12% of the radio flux but, for the Virgo A source, the angular diameter of the halo is quoted since it is responsible for 80% of the radio flux. Four sources (qualifying letter S) are in fact twin sources, the size given for each being the separation between the two components, and the Cygnus A source (qualifying letter M) consists of three components where the value of 2' arc given for its angular size includes all three components. For all the above sources which consist of more than one component, the different components are comparable in strength. The Taurus A source (qualifying letter E) is elliptical in shape and the angular size of the major axis is given. As shown by Hewish and Okoye (1965), the fine structure of Taurus A also includes a source of quasi stellar dimensions, in the radio emissions of which interplanetary scintillations have been observed. However, this fact has no bearing on the present experiment.

In the case of the Centaurus A source, the radio emission comes from a very extended region covering 3^{o} in right ascension and 8^{o} in declination and also from a smaller source consisting of two components separated by 7' arc. The value of flux density for the Centaurus A source given in Table 3.2 refers to the integrated flux over the extended region. The flux from the small source is about 20% of the integrated flux from the whole region. Since it was shown in Section 2.5 that, if the angular size of a source in the right ascension co-ordinate was equal to 2.85^{o}, the output from the source would be reduced by half, then it is evident that the output of the receiver, from the extended regions of Centaurus A, is reduced by about this factor. However this output will still be greater than that from the small source so that the receiver output from the Centaurus A source as a whole is determined by the integrated flux over the whole region rather than the flux from the small source. Further, since Aarons and Guidice (1966) showed that in their observations the amplitude scintillation depth was reduced to half the point source value for a source of angular diameter 10' arc when ϕ_o was less than 1 radian, it is evident that no scintillations should be observed in the signals from the extended regions of the

Centaurus A source. In practice, scintillations are observed in the signals from Centaurus A but can only be due to the small two-component source.

The amplitude scintillation index for the Centaurus A source does not have the same meaning as that for the other sources because, for the purposes of analysis, the receiver output from the present interferometer for this source must be regarded as a superposition of the output from two sources - one giving rise to scintillations, and one (the stronger) not.

Not all of the sources are detected with the array antennas aligned in any one given direction. Table 3.2 represents the sum of the observations made with the antenna elements aligned east-west and directed either upwards or at an angle of 45° above the northern horizon.

Figure 3.1 shows the local time of transit at St. Kilda for the nine sources in Table 3.2, throughout the year.

During February, March and most of April 1966, the array was directed at an angle of 45° above the northern horizon. Under these conditions, the source Pictor A could no longer be detected at all and the visibility of the source Fornax A was considerably reduced. On the other hand, the source 3C 123 was not visible with the antennas directed vertically but produced a significant

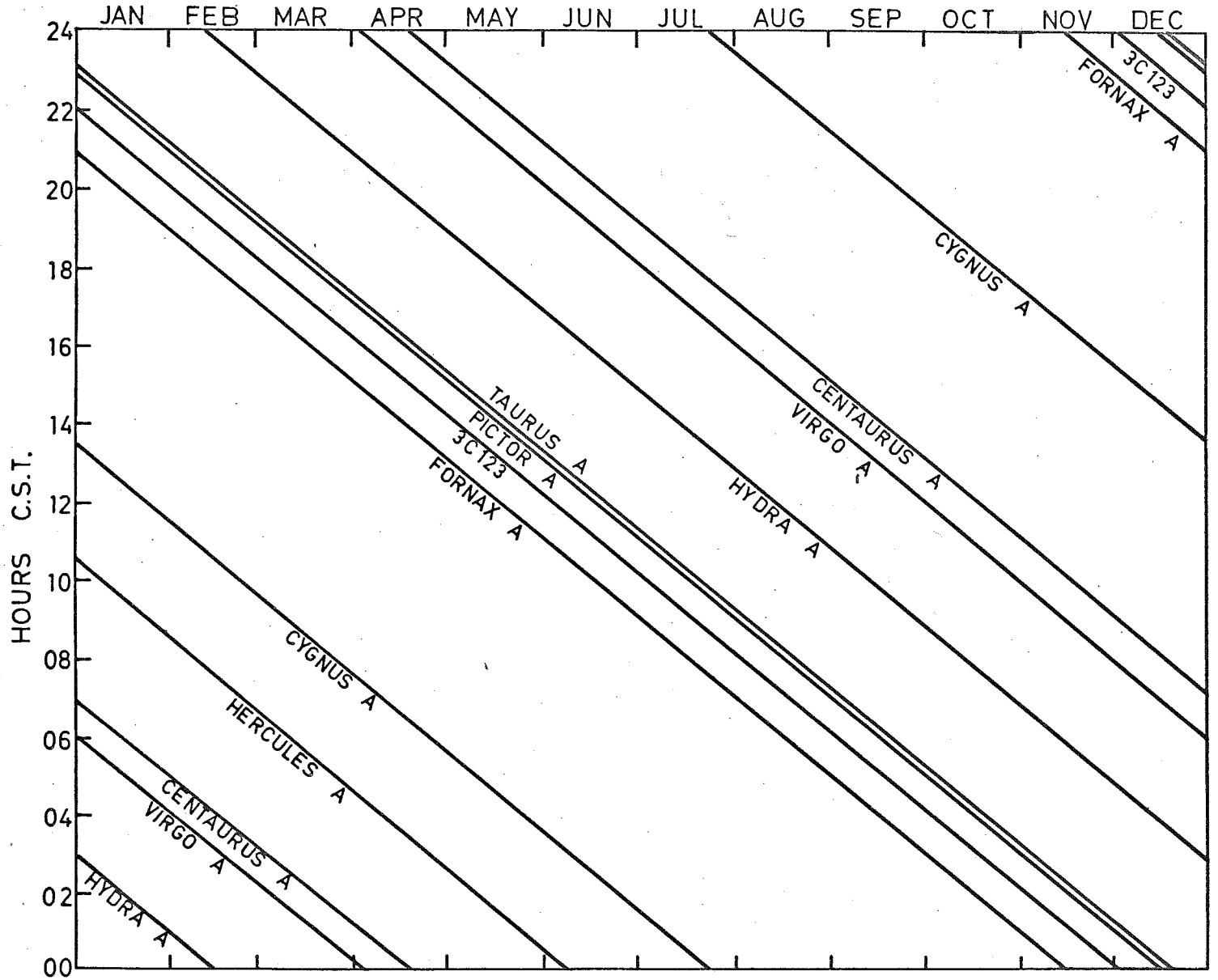

Figure 3.1 The transit times of the nine radio sources listed in Table 3.2

response from the receiver with the antennas directed to the north.

As was indicated in Section 2.2, the interferometer was operated initially with the array directed vertically and the antenna elements aligned north-south as shown in the frontispiece. It was also indicated there that this alignment was unsatisfactory. The main reason for this dissatisfaction is that when the antenna elements were aligned in this way, the interferometer was less sensitive to sources transiting at large zenith angles, the source Taurus A (zenith angle 57°) not being detected at all, and the source Cygnus A (zenith angle 75°) being detected in an anomalous manner. In fact, the Cygnus A source was detected 1 hour 7 minutes later than it should have been, was in the field of view for longer than it should have been, and produced an unexpectedly smooth trace on the pen recorder which on no occasion showed any amplitude scintillations. Figure 3.2 shows the normal and anomalous receiver outputs from the Cygnus A source. Unfortunately, records were not available for comparison which had the same chart speed as this speed was 6" per hour for all the time that the antennas were directed to the zenith with their elements aligned north-south and was 3" per hour for all other times. There were no records of Cygnus A transits showing no scintillation when the antennas and

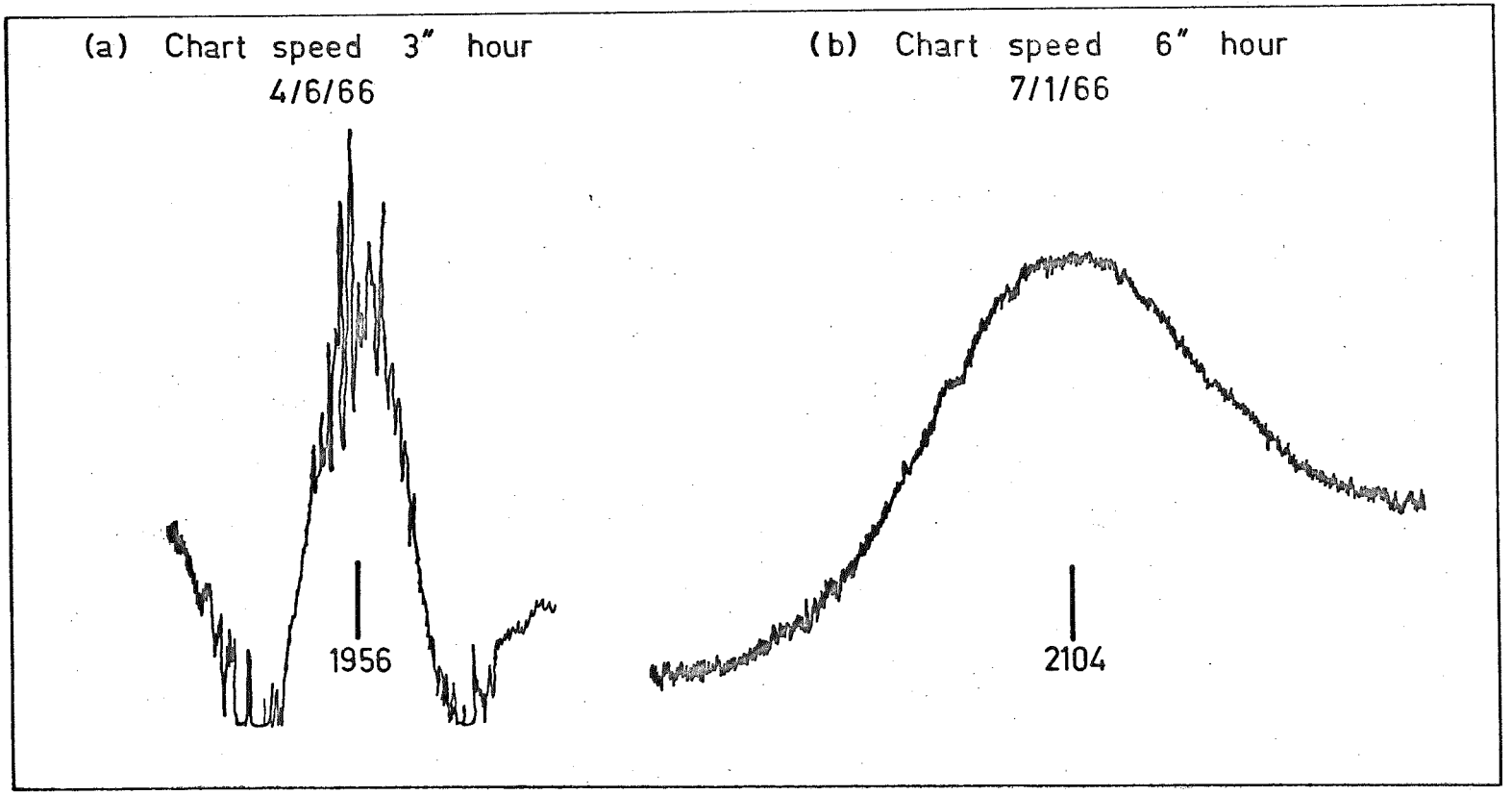

Figure 3.2 The expected (a) and anomalous (b) forms of the receiver output of the larger interferometer from the Cygnus A source with the Yagi antenna elements aligned east-west and north-south respectively - the antennas being directed to the zenith in both cases.
The apparent right ascension of the source is indicated for both records, the true value being 19 hours 57 minutes.

antenna elements were directed other than as above. The record shown for June 4th represents near minimum scintillation for the Cygnus A source.

These anomalies are rather difficult to explain because firstly, the satellite observations (made with the antenna elements aligned north-south) described in Appendix B show that at least out to zenith angles of 50°, the polar diagram of the array is as it should be, and secondly, appropriate calculations show that the small east-west slope of the array plus the maximum possible errors in the signal phases at the receiver due to the lengths of the leads being incorrect are not sufficient to explain the observed discrepancy in the apparent source right ascension.

The most likely explanation would appear to come from the fact that the anomalies were observed only in the observations of the Cygnus A source which was received from a direction almost end on to the antenna elements - the relative insensitivity of the antennas to signals received from this direction plus the presence of ground effects possibly being sufficient to explain the observations. It is still not easy to see how ground effects might contribute to the observed result as there are no differences in the terrain east or west of north from the receiving site, and therefore the presence of the

ground (if related to the anomalous observations) would be expected to affect the receiver output equally both before and after transit.

The Cygnus A source was observed at the expected time and in the expected manner when the antenna elements were aligned east-west - the source then being received from a direction side on to the antenna elements.

Radio sources other than the nine listed in Table 3.2 were detected by the interferometer but, either the receiver output from them was so weak that scintillation indices could not be assigned, or the catalogues showed that there were one or more other radio sources of comparable flux density with similar values of right ascension, in which case the receiver output could not be assumed to be due to any one particular source. In practice, most rejections of possible identifications were due to the concentration of many of the stronger sources in the Sagittarious region of the Milky Way between right ascensions of 16 and 20 hours. It was found that two radio sources could be resolved provided their positions differed in right ascension by 10 minutes or more.

With the Yagi antennas directed vertically, the interferometer is equally sensitive to signals from the sources Pictor A and Taurus A and the two sources are just resolved in right ascension. However, if detailed observations of

the Taurus A source are required, it is preferable to operate the interferometer with the antennas directed 45^{o} above the northern horizon as the output from Taurus A is then enhanced by a factor of 10 with respect to the output from the source Pictor A.

Only the strong sources Centaurus A, Virgo A, and Taurus A can be detected in the first order diffraction grating lobe of the interferometer. In each case the appropriate hour angle of the source before or after transit had been calculated and the output on the charts was readily identifiable. In no cases did the above sources interfere with a useful source due to their being detected in the diffraction grating lobe.

In addition to the galactic and extragalactic radio sources listed in Table 3.2, the sun was detected each day at a local time given by 1215 hours minus the equation of time, (or from the most recent editions of the Nautical Ephemeris, the local time of solar transit at Adelaide is 15 minutes later than the local time of transit at Greenwich for the same day). The receiver output from the sun varies from a single weak fringe (a smooth trace with no noisy spikes) under quiet conditions through to a trace which, under disturbed conditions could interfere seriously with the receiver output from other sources for a period of about 6 hours. On occasions, the pen of the recorder

was deflected off scale when the disturbed sun was detected in both the main lobe and the diffraction grating lobes of the interferometer and some records were lost due to these interfering signals. Figure 3.3 shows the observed variations in intensity of the signals received from the sun. Due to the noisy nature of the radio bursts from the disturbed sun (usually emitted from a small localized region), it was not possible to distinguish between ionospheric scintillations and variations in the emissions themselves. On the other hand, under quiet conditions, the solar radiation is uniformly emitted from the whole disc and the size of the source (30' arc) is too large to produce any ionospheric scintillations.

An index of solar activity on a scale 0 - 4 was assigned to each transit of the sun, an index of 0 indicating no enhancement of the solar emissions and an index of 4 indicating extreme enhancement of the emissions persisting for at least 6 hours.

3.3 Sources of Interference

Unfortunately, the records of the Cygnus A interferometer were subject to quite a lot of interference from both man-made and natural origins which resulted, over the 2 year period of operation, in the loss of 1

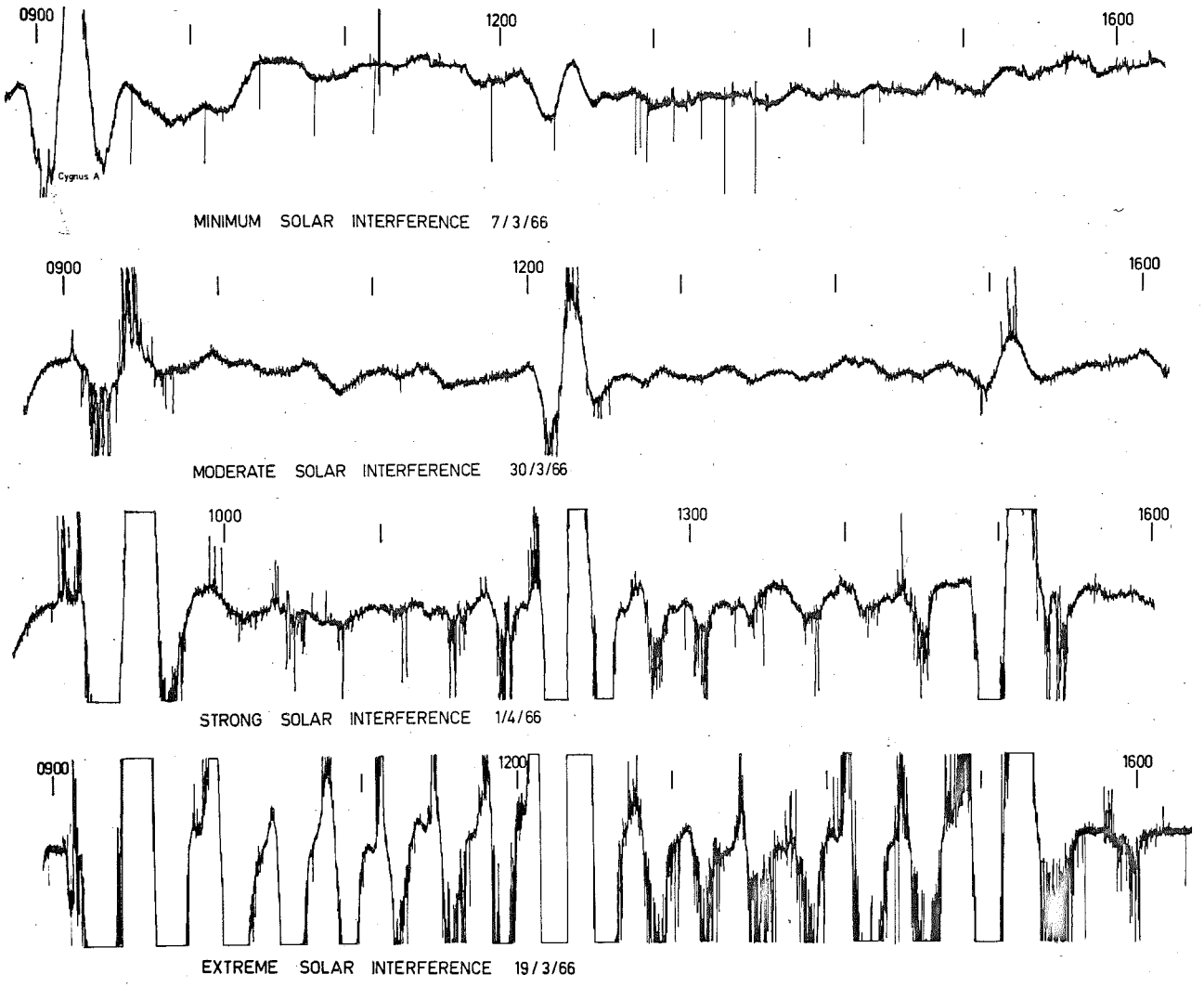

Figure 3.3 The observed variations in the intensity of signals received from the sun using the larger interferometer.

complete pass approximately every 10 days. The various types of interference which were observed to contribute to these losses are outlined briefly below.

For periods of several months early in both the years 1964 and 1965, short pulses of amplitude large enough to send the pen recorder trace off scale were recorded which, from their temporal characteristics, were obviously not of natural origin. Their presence also affected a meteor radar receiver in the same building causing its sequence unit to be triggered. Fortunately, during the months in which these pulses were detected, the Cygnus A transits took place between 0000 and 0800 hours local time when no pulses were received; otherwise the effect of their interference would have been more serious. Since there was little industrial activity to the north of the receiving site (where the Yagi antennas were directed), it was difficult to suggest an origin for the pulse emissions and their source was not identified.

A further series of pulses of much smaller amplitude, and which were recorded at 1 minute intervals, was detected over a 6 month period centred around February 1965, their origin being an electrical timer used to preset the recording intervals for the 2 beacon satellites. These satellites (Be-B as from October 10th, 1964; Be-C as from April 29th,

1965) were themselves detected regularly as illustrated in Figure 3.4(d) which shows several passes of the satellite Be-C superimposed on a Cygnus A transit. However, the passes of these satellites were sufficiently rapid and the amplitude of the pulses from the timer were sufficiently small, that the interference from these causes did not affect the accuracy with which scintillation indices could be assigned. It was thought possible that on a few occasions, signals were detected from the OGO-A satellite which had a much longer orbital period and thus remained visible from the receiving site for periods of several hours, but this possible source of interference was not established.

From time to time, faults developed in the radio receiver or associated power supplies which generally were due to component failure. Losses of records due to these faults were reduced due to the readiness of spare equipment but did occur on some occasions and several times were not noticed until several days had elapsed following the malfunction.

Thunderstorm activity (to which the array was particularly sensitive over a wide range of azimuth angles east and west of north), solar radio noise, and possibly noise bursts from the planet Jupiter were the most import-

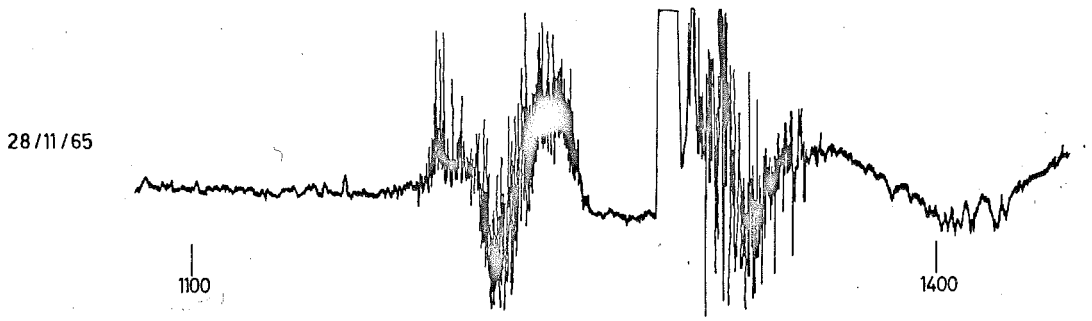

a) Intermittent output from the sun possibly associated with a solar noise storm

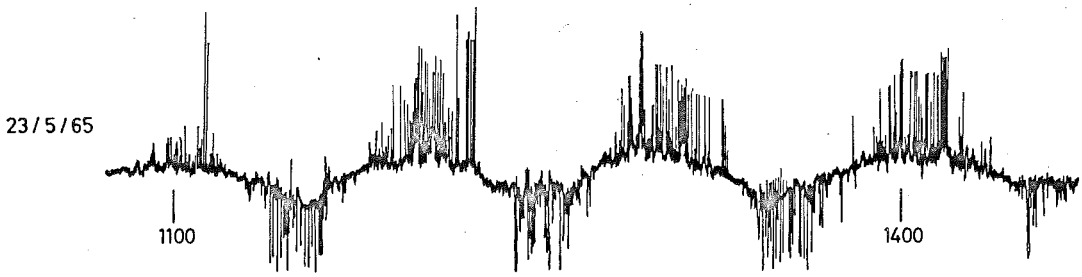

b) Steady background signals plus noise from the sun

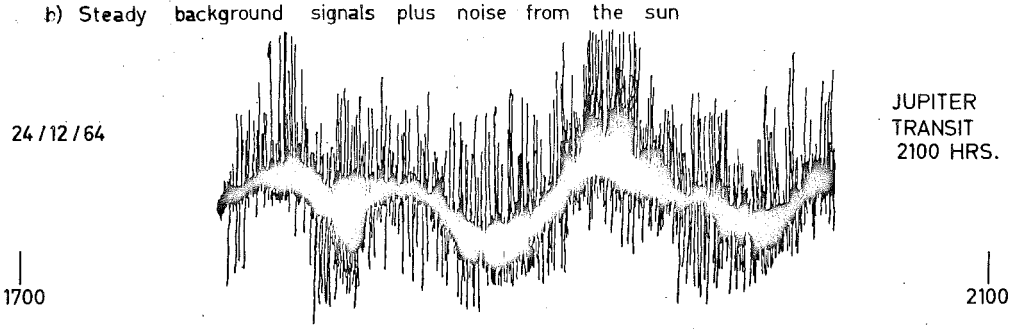

c) Possibly output from Jupiter superimposed on a very noisy background

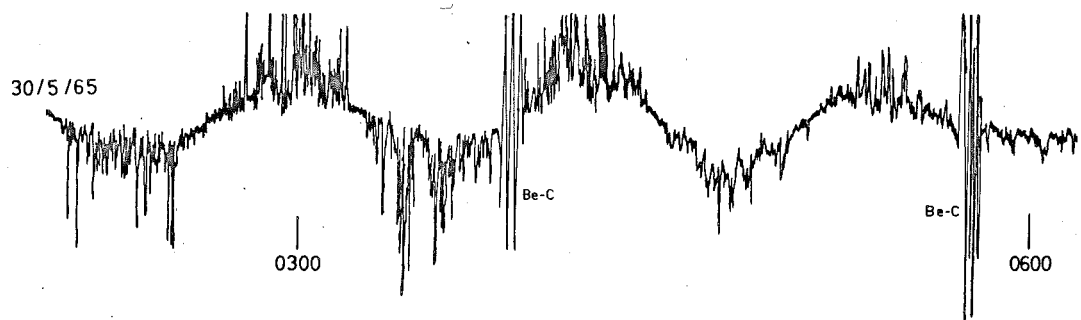

d) Passes of satellite Be-C superimposed on a Cygnus A record

Figure 3.4 Interference signals recorded with the Cygnus A interferometer

ant causes of natural interference. Steady background signals from the sun, sufficient to give a fringe output comparable in amplitude to the output from the Cygnus A source, were detected only on 5 days in May 1965 when solar activity had just begun to increase. Figure 3.4(b) shows the output from the sun on one of these occasions. It was observed that in 1966 when the interferometer was no longer operated on a routine basis, steady signals from the sun were detected quite often compared with the previous years. However, during the routine running period of the experiment, there were many occasions on which sporadic and noisy interference was observed and much of this was believed to originate from the sun. This belief was supported by the fact that many (but not all) of the bursts observed corresponded closely to the published times of solar flare events. Figure 3.4(a) shows this type of solar interference although in this case there was no simultaneous flare event recorded. The emission could however have been part of a flare eruption which took place some four hours earlier.

Since a future experiment to investigate radio emissions from the planet Jupiter was envisaged for the St. Kilda site, an attempt was made to identify output from this source on the interferometer records by noting the

local time of occurrence of all noisy bursts of interference, and comparing these times with the transit time of Jupiter. The occasions on which these noise bursts (which usually lasted only about 20 minutes) were superimposed on a fringe envelope were especially noted, and there were six of these events observed near Jupiter's transit time when the sun was below the horizon. Figure 3.4(c) shows the longest of these events: unfortunately the background was extremely noisy due to local thunderstorm activity which later increased, however the fringe pattern in the output is clearly visible and cannot be produced except by a moving source. The evidence found is not considered sufficient to prove that the few bursts seen, of the appropriate form and at the appropriate time, definitely originated from the planet.

As pointed out by Roberts (1963), steady thermal emissions from Jupiter at metre wavelengths are weak and although brief bursts of radiation (exceeded in intensity only by emissions from the disturbed sun), are well known at the same wavelengths, their peak occurrence occurs near a frequency of 18 MHz and they have been very rarely observed at frequencies near or above 39.5 MHz.

It is concluded that observations of radio emissions from the planet Jupiter with the Cygnus A interferometer are possible but rather unlikely and, from the evidence

presented here, they have not been established.

In the case of the larger interferometer the records are relatively free from interference, the detection of interfering signals being inhibited by the directional nature of the radiation polar diagram of the two 8-antenna Yagi arrays constituting the interferometer. Thus, although the gain of this interferometer is much higher than that of the Cygnus A instrument, thunderstorm and stray pulse activity were not as effective in producing interference on this interferometer output as they were for that of the smaller one.

As on the charts of the output from the Cygnus A interferometer transmissions from the beacon satellites were recorded but were so brief that the scintillation observations were not interrupted. The appearance and effects on the receiver output of the variable signals from the sun has already been described in the previous section, and illustrated in Figure 3.3

There were no occasions on which it was suspected that radio emissions from the planet Jupiter were being detected with the larger interferometer.

3.4 Analysis of the Records

Briefly, data was obtained from the records of both interferometers on the source transit times and scintilla-

tion amplitudes and from the records of the Cygnus A interferometer, data was also obtained on the scintillation rates and the changing appearance of the scintillation.

(i) Source Transit Times. Source transit times were read from the records of the smaller interferometer, initially from only a few transits, in order to identify the sources. Later, the transit times of most of the available Cygnus A passes were recorded, and used to investigate the possibility of the source transits being advanced or retarded due to wedge refraction occurring in the presence of east-west gradients in the total electron content, or to investigate the possibility of the fringe periods of the receiver output evaluated for daytime passes differing from the fringe periods evaluated for night time passes - the effects of spherical refraction, which would give rise to such a variation, being more important by day due to the larger amount of total ionization then present. The transit times for the sources detected by the larger interferometer were read from the records for a limited period of only a few weeks for the purpose of identifying the sources and no attempt was made to determine ionospheric refraction effects using the records from this instrument.

(ii) Amplitude Scintillation Indices. In the case of the records of the Cygnus A source from the smaller interferometer, an amplitude scintillation index in the range 0 - 5 was assigned to the 9 fringes each lasting about 20 minutes during the daily pass of the sourse - the indices assigned being modelled on those assigned by Briggs (1964) to the records of the source Cassiopeia A taken at Cambridge U.K. As pointed out by Briggs and Parkin (1963), Mercier (1962) has shown that this scintillation index is proportional to their index S_4, which is equal to the root-mean-square deviation of the signal power received from the source and is also the scintillation index most readily calculated from diffraction theory. Figure 3.5 shows selected passes of the Cygnus A source recorded at the St. Kilda site which illustrate the range of amplitude scintillation depths observed. It was only on very rare occasions that no amplitude scintillation at all was observed - especially on the larger amplitude central fringes.

It was evident from a detailed examination of records from the larger interferometer spanning several weeks of observation, that an amplitude scintillation index in the range 0 - 3 would be preferable to the larger range of indices described above. In this case an index of 0 indicated

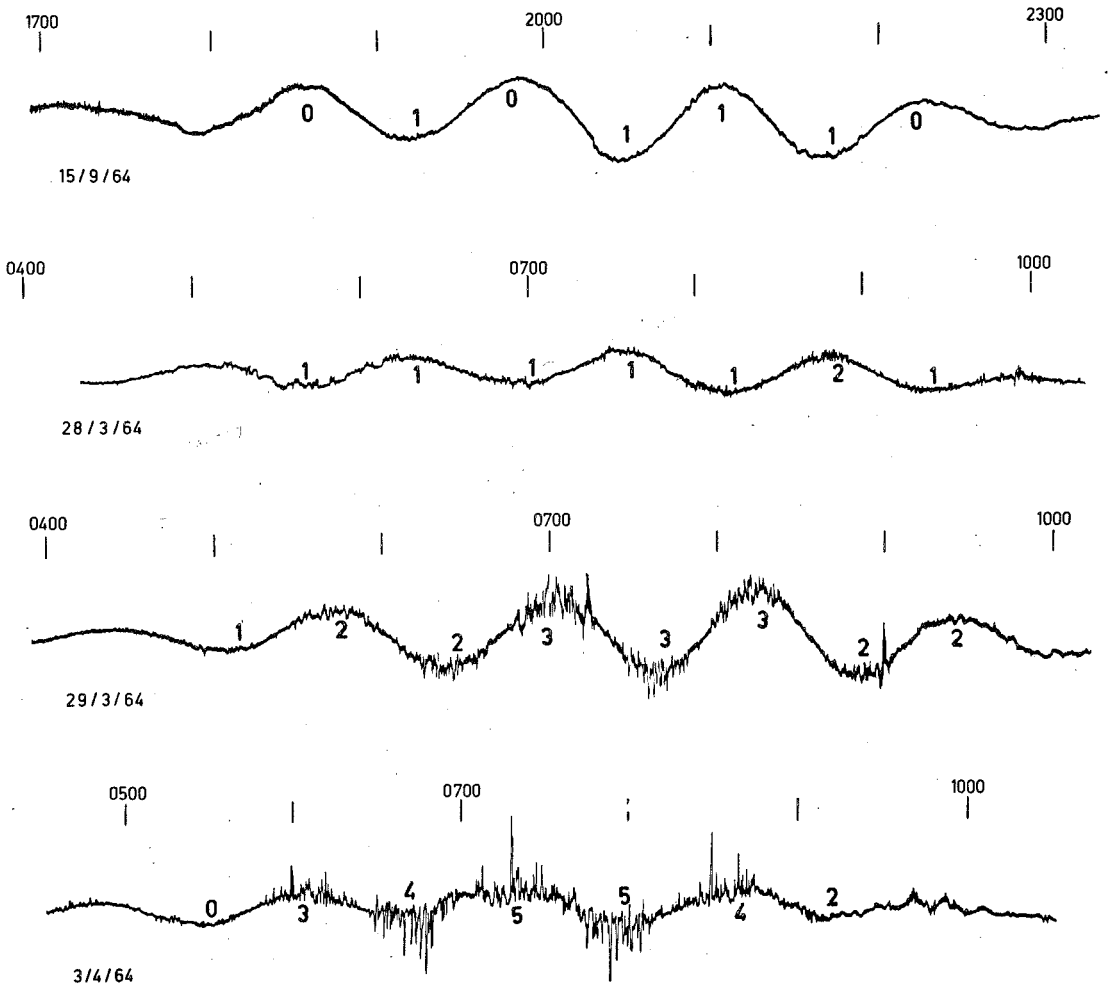

Figure 3.5 The variations in the intensity of the amplitude scintillations observed in the signals received from the Cygnus A source using the smaller interferometer.
The amplitude scintillation indices for each record are shown in the diagram.

no scintillation and an index of 3 indicated complete scintillation. The use of this alternative index (which should have statistical properties similar to those of the 0 - 5 index), seemed more appropriate because some of the useful sources were detected rather weakly and it was decided that an index in the range 0 - 5 could not be assigned with sufficient accuracy to the records of all the sources, and that an index in the range 0 - 3 represented the maximum accuracy attainable if the records of all the sources were to be analysed in a uniform manner. Figure 3.6 illustrates the range of scintillation depths observed for the source Virgo A.

In an attempt to maintain as much consistency as possible in the assignment of amplitude scintillation indices to the records, all the charts from both the interferometers were read by the author.

Due to the relative speeds of the chart (usually 3 inches per hour) and the scintillations (typical periods being 15 seconds up to 2 minutes), and in the case of the larger interferometer records due also to the short duration (typically about 6 minutes) of the output from each source, it was not possible to digitize the source output records and thus obtain a more accurate measure of the scintillation activity than that given by the scintillation indices described above. However, since the experiment is concerned

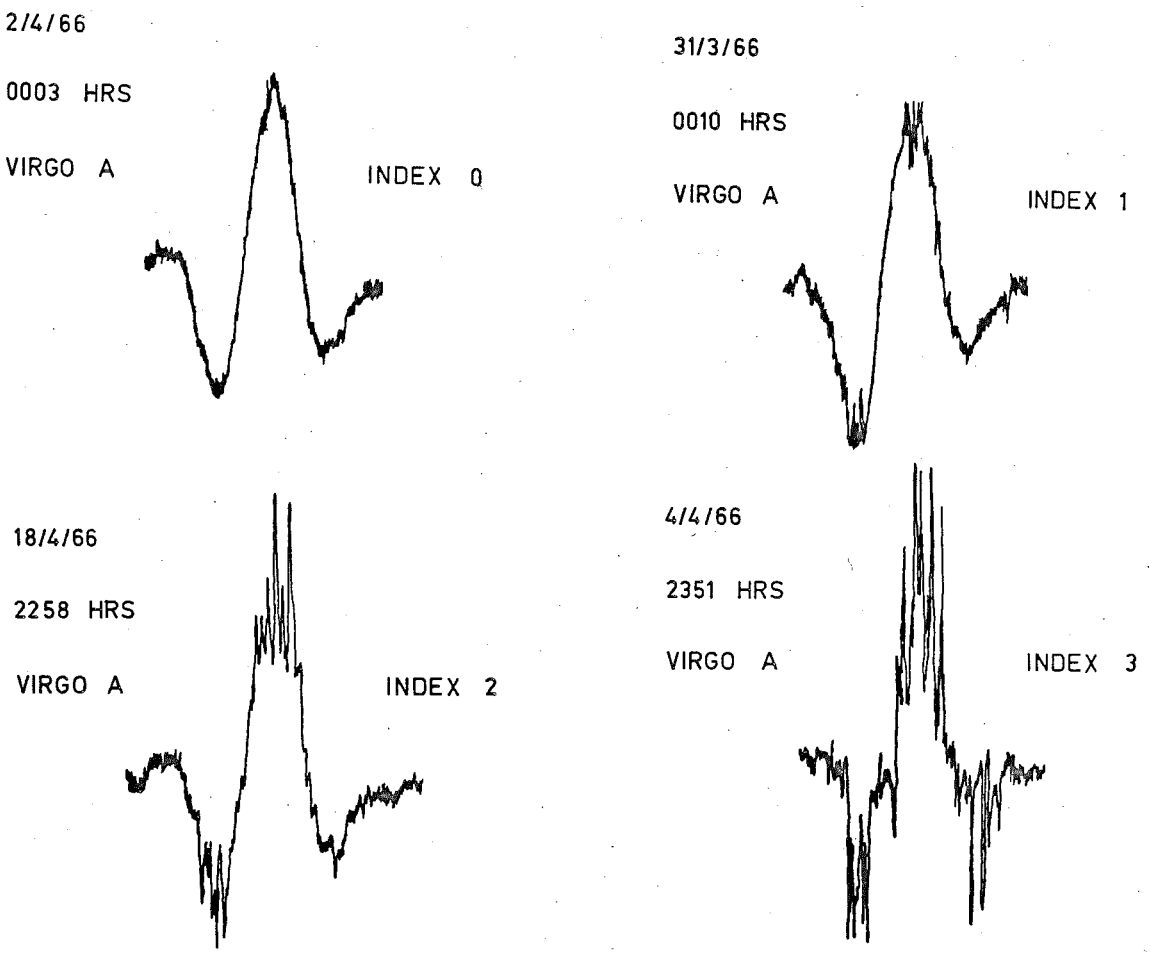

Figure 3.6 The variations in the intensity of the amplitude scintillations observed in the signals received from the Virgo A source using the larger interferometer.

with temporal variations in scintillation activity and the correlation of scintillation activity with the occurrence of other geophysical phenomena, and is not concerned with a detailed investigation into the statistical properties of the diffracting regions of the ionosphere, then the visually assigned amplitude scintillation indices described here should serve as an adequate measure of scintillation activity.

(iii) Estimate of Scintillation Rate. Estimates of scintillation rate were made only for the records of the Cygnus A source made with the smaller interferometer since it was felt that the output from each source detected with the larger interferometer was of too short duration for reliable estimates to be possible.

As indicated in the previous section, it was not feasible to make precise measurements of the amplitude scintillation indices and the same argument applies against the precise measurement of scintillation rate. However, even though the experiment was designed primarily for the routine assignment of amplitude scintillation indices, it was evident that from one source transit to another, the scintillation rate could vary quite considerably from as low as 1 fluctuation every 2 minutes (or longer) to as many as 10 or more in the same interval. The upper limit

for the number of scintillations observable in this interval was determined by the slow speed of the chart rather than by other factors. In practice, no index of scintillation rate was noted unless the rate was slower than 1 per minute or faster than 4 per minute, these rates being denoted by S or F (as distinct from M for moderate rate) and as shown in Figure 3.7, the different rates corresponding to these indices are readily distinguishable. In a later chapter, the relative occurrence of these indices, their associations with the scintillation origin and with the magnetic K_p index, are examined in some detail.

(iv) Other Data from the Records. Other data, concerned with possible variations in source visibility and further variations in the appearance of the scintillations are also discussed in the relevant later chapters.

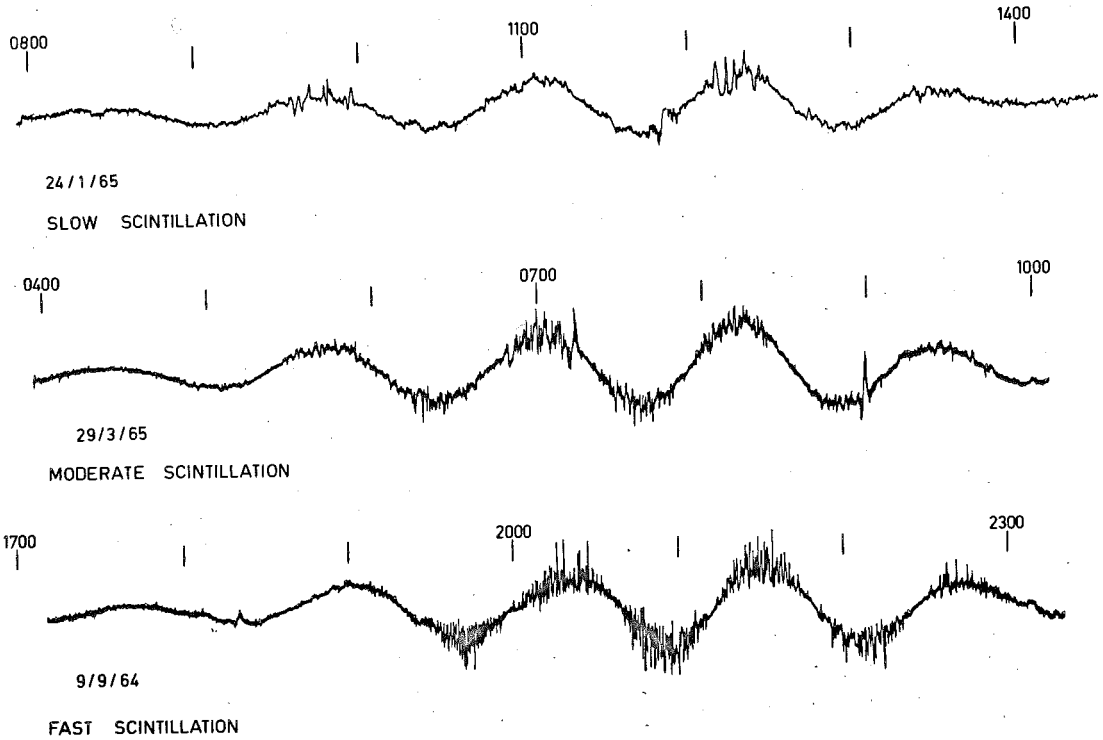

Figure 3.7 The variations in the rate of the amplitude scintillations observed in the signals received from the Cygnus A source using the smaller interferometer.

CHAPTER 4. IONOSPHERIC REFRACTION OF 40 MHz RADIO WAVES

4.1 Spherical Refraction in the Ionosphere

The effects of atmospheric refraction on 40 MHz radio waves are evaluated to determine how the apparent path of the radio source Cygnus A differs from the true path and whether the difference should be observable in the fringe period or amplitude of the St. Kilda records.

In the simple calculation performed here, the presence of the earth's magnetic field is neglected and the refractive index is considered to be a function only of height. As pointed out by Unwin (1966) this latter assumption requires the ionosphere to have a similar vertical electron density profile over distances in excess of 2000 km when the calculations are made for large zenith angles. Notice that when the magnitude of the east-west wedge refraction is estimated later, large east-west variations in total electron content are assumed to be present over a similar distance.

The refraction component calculated here is referred to generally as the spherical component as it arises purely due to the earth's curvature. In a flat earth approximation for a source at infinity, the true and apparent source directions would be the same.

To evaluate the bending angle due to refraction, Bouger's formula $\mu R \sin \theta$ = constant = $\mu_o R_o \sin$ (apparent zenith angle) is iterated from $R = R_o = 6371$ km to $R = R_o + h_{max}$ at height intervals Δh - a method similar to that used by Unwin (1966). The relation was iterated from the ground to 1000 km and it was found necessary to use height increments as small as 1 km.

It was necessary to assume some sort of model atmosphere in order to calculate the refractive index as a function of height. In this case analytic functions were used, each valid over a restricted height range, and these functions are now described.

4.2 Day and Night Model Ionospheres

In the case of the tropospheric refractive index, it was deemed unnecessary to tabulate the refractive index in detail as the water vapour content responsible for refraction at radio frquencies is highly variable and the table would have applied only to one particular set of atmospheric conditions. Figure 3 from Unwin's paper was adopted as being representative of average conditions and in order to estimate the order of magnitude of the tropospheric refraction, the further approximation was made such that

$$(\mu - 1) \times 10^6 = -17.7 \times H + 320.0 \qquad (4.1)$$

μ = refractive index, H = height in kilometres. From Smith and Weintraub (1953), this value of μ is independent of frequency in the range 0 -21,000 MHz.

For the ionospheric refraction, two ionization profiles were used, one each for day and night. In both cases, a parabola was fitted below H_{Fmax}(300 km) and an exponential curve was fitted from H_{Fmax} up to 1000 km. Previous authors, in particular Komesaroff (1960), appear to have chosen a parabolic fit above H_{Fmax} as well as below, probably because this form lends itself more readily to analytic approximations to the bending angle in restricted cases. However, here an exponential fit was preferred as there was no extra difficulty involved in the computation and such a curve seemed physically more reasonable. In a diffusion controlled region such as exists above H_{Fmax}, the height dependence would be exponential if the scale height were independent of height.

For both the day and night calculations, there was considered to be no ionospheric contribution to the refractive index for $H \leq 100$ km.

For the parabolic fits to the electron density below H_{Fmax}, we have:

$$N = N_{max} \left(1 - \frac{(H_{Fmax} - H)^2}{H_m^2} \right) \qquad (4.2)$$

where N_{max} = 1.0×10^6 electrons/c.c. by day
and 1.0×10^5 electrons/c.c. by night

The corresponding F region critical frequencies are 6.3 and 2.0 MHz.

H_m is a scale factor describing the thickness of the layer: H_m = 210 km by day (this value results from assuming $N = 10^5$ electrons/c.c. at 100 km as a boundary condition), and 120 km at night (from Komesaroff (1960)).

For the exponential fits to the electron density above H_{Fmax}, we have :

$$N = N_{max} \exp\left[- \frac{(H - H_{Fmax})}{H_m} \right] \qquad (4.3)$$

As boundary conditions, the following values are assumed for N at heights of 300 and 1000 km:

N_{max} = 1.0×10^6 e/c.c. day, 1.0×10^5 e/c.c. night
N_{1000} = 1.0×10^4 e/c.c. day, 1.0×10^4 e/c.c. night

and from these values for N,

H_m = 152 km day, 304 km night.

These values are in effect "scale heights".

The daytime value of H_m compares with the value of 200 - 250 km given by Hines et al. (1965) for the scale

height above the F region maximum at local noon. The refractive index obtained from the foregoing values of N will be a function of frequency given by:

$$\mu^2 = 1 - X$$

where $\mu \simeq 1 - \frac{1}{2}X$ for X small, (4.4)

and $X = \omega_N^2/\omega^2 = Ne^2/\varepsilon_o m \omega^2$. N is the plasma frequency.

For the calculation considered here, the largest value of X occurs at H_{Fmax} during the day:

$$X_{max} = 0.025$$

so that the approximation involved in making $\mu \simeq 1 - \frac{1}{2}X$ is a good one.

4.3 Calculation of the Spherical Refraction.

The relationship between the apparent and true zenith angles of a radio signal from a source at infinity is shown in Figure 4.1 in which the bending angle of the signal is highly exaggerated. The terminology used in the calculations is also given in the Figure.

The problem of calculating the apparent zenith angle of a signal from a radio source is complicated considerably if the source is at a finite distance because the calculations must be repeated several times if the ray path be-

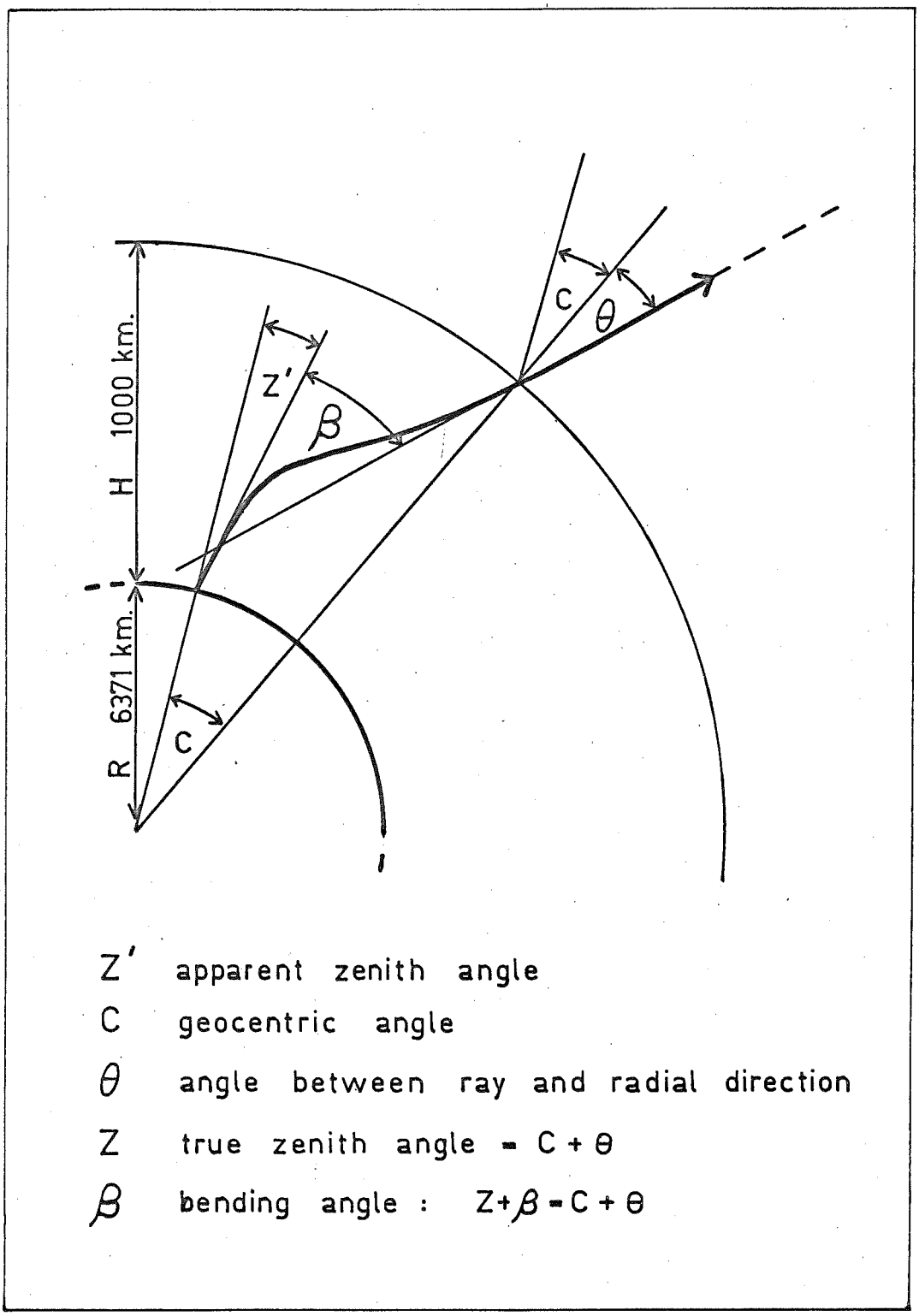

Figure 4.1 The relationship between the true and apparent zenith angles of a spherically refracted radio signal. The bending angle is highly exaggerated.

tween two fixed points in space is to be found. However, for a radio source at infinity where the incoming signals may be considered as a parallel beam, the problem is solved completely if the final direction of a signal emitted at a given zenith angle from the ground is determined.

Unfortunately, solutions to the problem using the true zenith angle as the independent variable cannot readily be found as foreknowledge is required of the geocentric angle C. Results can be found by initiating the calculation at the top of the atmosphere using the angle θ as the variable parameter but the angle C and therefore also Z and Z' are all not known until the bottom of the ionosphere is reached. The most convenient computation method appears to be to initiate the calculation on the ground and to use Z' as the independent variable.

The output from the computer program used for the calculations consisted of a table relating the true zenith angle to the apparent zenith angle together with the great circle range to the points over which the ray intersected heights of 300 km and 500 km.

The values appropriate to the day and night ionosphere profiles are listed for selected apparent zenith angles in Table 4.1

The results listed in Table 4.1 must be investigated in greater detail before the effect of spherical refraction

Apparent Z Deg	True Z Deg	Bending Angle (Deg)	R_{300} km	R_{500} km
a) $N_{max} = 10^6$ e/cm^3 - daytime profile.				
70	70.832	0.832	739.7	1124.8
75	76.371	1.371	952.0	1406.9
80	82.366	2.366	1277.1	1808.9
85	88.994	3.994	1772.7	2373.4
90	95.315	5.315	2385.4	3016.0
b) $N_{max} = 10^5$ e/cm^3 - night time profile.				
70	70.135	0.135	690.5	1051.3
75	75.184	0.184	863.3	1280.4
80	80.261	0.261	1107.7	1582.0
85	85.389	0.389	1460.8	1981.1
88	88.539	0.539	1745.7	2281.2
90	90.661	0.661	1968.9	2507.6
c) TROPOSPHERIC CONTRIBUTION				
70	70.054	0.054		
75	75.076	0.076		
80	80.124	0.124		
85	85.243	0.243		
88	88.402	0.402		
90	90.529	0.529		

TABLE 4.1

Values of Ionospheric Spherical Refraction

on the apparent position of the Cygnus A source can be ascertained.

The relative contributions to the total refraction from the troposphere and ionosphere are listed in Table 4.2 for both the day time and night time calculations.

Apparent Zenith Angle	Tropospheric Contribution	Ionospheric Contribution	
		Day Time	Night Time
Deg	Deg	Deg	Deg
80	0.099	2.267	0.162
82	0.122	2.826	0.181
84	0.156	3.475	0.200
86	0.213	4.141	0.216
88	0.312	4.675	0.227
89	0.382	4.831	0.230
90	0.430	4.885	0.231

TABLE 4.2

It has been pointed out by previous authors (for example Lawrence et al. (1964)) that tropospheric refraction becomes important only as the apparent zenith angle approaches 90°. This is borne out in the above table. Lawrence et al. also point out that since the ionosphere is situated at a greater height than the troposphere, the

rays will arrive at the ionosphere with reduced angles of incidence, and near the horizon the increase in refraction due to the ionosphere will not be as important as the increase in refraction due to the troposphere. The co-authors state that ionospheric refraction becomes relatively independent of zenith angle within 4 or 5 degrees of the horizon. The results above agree closely with this statement in the case of night time refraction and there is a lesser agreement evident in the case of day time refraction, where the ionospheric contribution still increases for the largest apparent zenith angles but not as rapidly as for smaller angles.

This situation is resolved when it is realized that in the case of the night time calculations, the values of electron density assumed are much smaller and refraction is significant only near 300 km, whereas in the case of the day time calculations, the electron density is assumed to be large enough to produce significant refraction down to the much lower height of 100 km. Thus, in the day time case, the importance of the effect described by Lawrence et al. (1964) is considerably reduced.

4.4 The Apparent Path of the Cygnus A Source.

In the absence of atmospheric refraction, the true path of the Cygnus A radio source is readily calculated

from the usual conversion relations between hour angle - declination co-ordinates and altitude-azimuth co-ordinates. In the ideal case of spherical refraction discussed here, where the bending angle is dependent on altitude only, the azimuth co-ordinate of the source will be unchanged and corrections need be made only to the altitude, which will be apparently increased. The overall effect will be to make the source visible for a longer period.

Unfortunately, as has already been pointed out, the true zenith angle cannot be used as the independent variable in the calculation of the bending angle. It is necessary to tabulate bending angles against the corresponding true zenith angles and interpolate between the angles in the table to find the bending angle corresponding to a particular true zenith angle. Knowing the azimuth and apparent altitude of the source, the output from the interferometer was then readily calculated. The day time ionospheric profile was used in the calculation as this represented conditions of maximum refraction and would have the greatest effect on the output of the interferometer.

The data used in the calculation is reproduced in Table 4.3.

True Altitude (Deg)	Bending Angle Correction (Deg)
-5.315	+5.315
-4.213	5.213
-2.987	4.987
+5.052	2.948
7.364	2.366
10.104	1.896
13.629	1.371
16.990	1.010

TABLE 4.3

If true altitude and bending angle are plotted against each other, the interdependence is not linear. However, the curvature is not large and if the values in Table 4.3 are used, good accuracy is obtained using a linear method of interpolation.

It was at first thought that the output from a source would be described by the output curves characteristic of its apparent declination. From this argument, in the case of Cygnus A observed through a refracting atmosphere, the altitude is apparently increased, the declination apparently reduced, and thus the fringe period would be expected to be reduced. However, the argument is not a valid one. The

source movement is decided by its true declination and any effect the presence of refraction will have on the output of the receiver will be determined by the radiation polar diagram of the interferometer.

The results from the path calculation computer program consist of:

(1) A graph of receiver output against hour angle. The outputs corresponding to the presence and absence of refraction are superposed on the same set of axes. The hour angle scale is three inches to one hour which is the same as used for most of the actual records.

(2) A table showing azimuth and true and apparent altitude as a function of hour angle.

(3) Times in minutes at which the output crosses the zero line correct to 3 decimal places.

Figure 4.2 shows the phase switching receiver outputs from the Cygnus A source calculated in the presence and absence of spherical refraction. That part of the Figure illustrating the output in the absence of spherical refraction effects is the same as Figure 2.5. Figure 4.3 shows how the true and apparent altitudes vary with the hour angle (or azimuth) of the source.

The theoretical results showing the predicted fringe periods with and without the effects of refraction are shown in Table 4.4

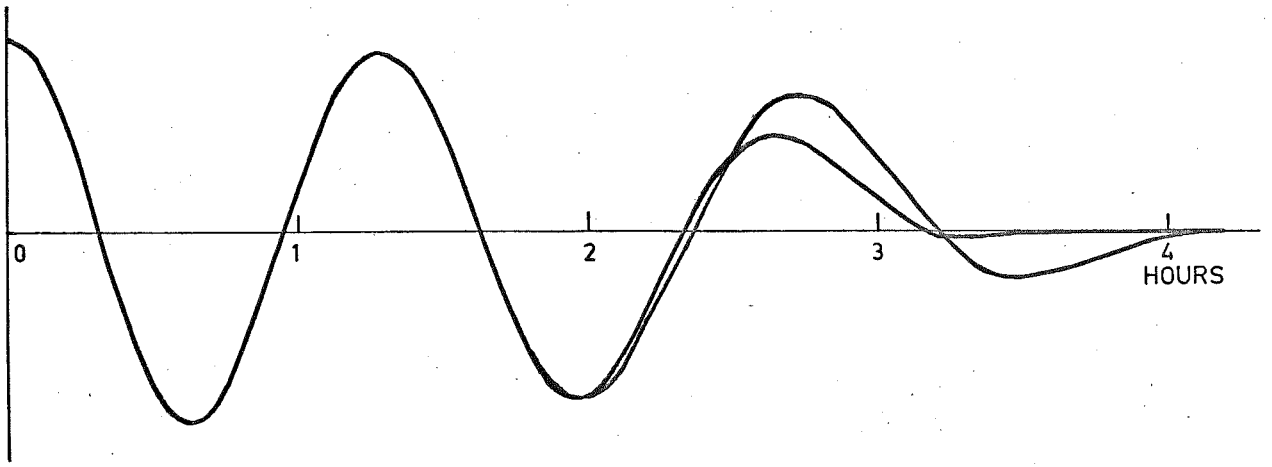

Figure 4.2 The output from the phase-switching interferometer calculated with and without the influence of spherical refraction. At large hour angles, the output in the presence of refraction is of greater amplitude and the oscillations slightly longer in period.

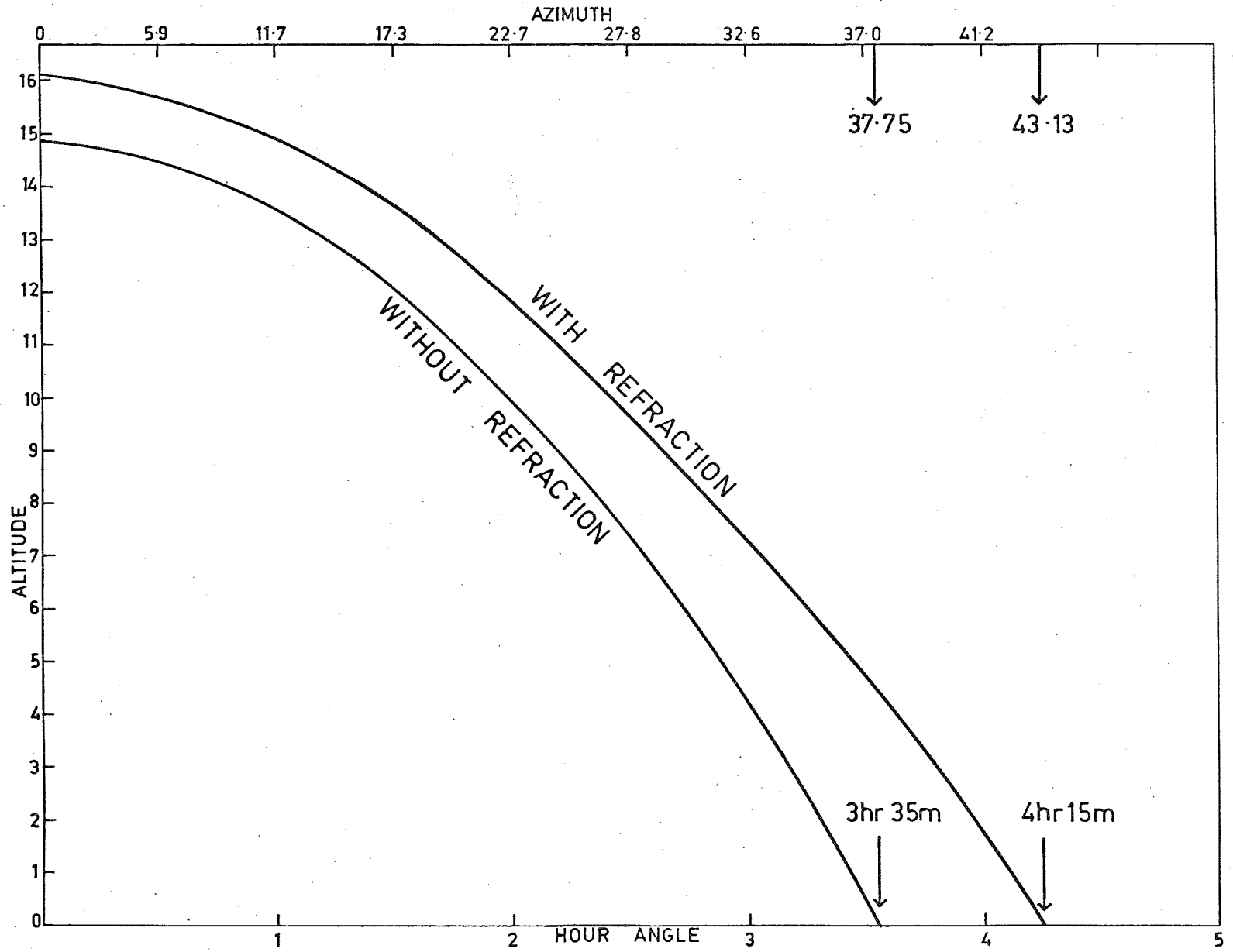

Figure 4.3 The apparent altitude of the Cygnus A radio source

Fringe	1	2	3	4	5	6	7	8
Without Refraction (times in minutes)	47.00	41.78	39.16	38.04	38.04	39.16	41.78	47.00
With Refraction (time in minutes)	47.28	42.12	39.44	38.27	38.27	39.44	42.12	47.28

TABLE 4.4

The periods tabled above are the time intervals from one maximum or minimum to the next, as it was this interval which was measured on the records. The results show that the effect of refraction is very small, being not greater than 1% for any of the fringe periods.

To try and observe the effect, the fringe period was determined separately for day time and night time Cygnus A passes. The criterion for distinguishing between day time and night time passes is that $f_o F_2$ should be near its diurnal maximum during day time passes and near its diurnal minimum during night time passes, the times involved being centred around 1400 hours and 0200 hours rather than around midday and midnight to satisfy the above conditions. For the source Cygnus A, the dates appropriate for day time passes were from November 1st to January 31st, and for night time passes from May 1st to July 31st. For the day time

passes, the mean $f_o F_2$ was always greater than 6.5 MHz and for the night time passes, always less than 4.0 MHz. Approximately 50 passes were analysed during each period.

Inspection of the Woomera ionograms showed that if any effect due to refraction is present it will be at a maximum for a source such as Cygnus A, which, in the southern hemisphere, has its day time transits in local summer and its night time transits in local winter.

The times of maxima and minima of the output records were recorded rather than the zero crossing times, although, due to the presence of scintillation (it was rather uncommon for scintillation not to occur), it was found that the most accurate way to obtain the times of maxima and minima was by first recording the zero crossing times (which were well defined even in the presence of scintillation), and then defining the maximum or minimum as occurring midway between them. In the case of the measurements made on the first and last fringes, the time of the maximum had to be obtained by direct inspection as there were no preceding or following zero crossings to use as references. In practice, each fringe period was read and assigned to the nearest minute. Due to the somewhat variable values of period from day to day (several minutes variation), this accuracy seemed to be sufficient.

The results obtained for the fringe periods for day time and night time passes are shown in Table 4.5 together with the respective standard deviations of each average period.

Fringe	1	2	3	4	5	6	7	8
Night time	39.3 (3.0)	39.1 (2.5)	38.8 (1.7)	36.6 (1.8)	36.5 (1.6)	36.9 (1.7)	39.4 (2.3)	39.1 (3.4)
Day time	39.4 (3.0)	40.1 (3.0)	38.4 (2.9)	36.9 (2.4)	36.0 (1.9)	36.6 (2.4)	36.6 (2.6)	37.3 (4.4)

TABLE 4.5

Taking fringe 8 as the fringe for which the greatest discrepancy exists between the day and night values, the standard error of the difference is 0.9 and the difference is 1.8. Taken alone, this result might be regarded as being significant but since none of the other fringes show a significant difference between day and night, the overall conclusion is that no significant difference between the period of day time and night time passes has been detected. The day to day fluctuations within each period seem to be large enough to swamp the much smaller effect sought here. It is noticeable that the standard deviations of the fringe periods increase as the fringes referred to are further

from the centre of the pass, due especially in the case of the outside fringes, to increased difficulty in reading the records.

The difference between the observed and predicted periods appears to be a real one for reasons not well understood at the present. In the case of the outside fringes only, the problem is partly resolved when it is remembered that the time corresponding to the maximum excursion is recorded for these fringes rather than the time corresponding to the mid point between two zero crossovers. These two times can be different if the "effective strength" of the source varies with hour angle as indeed it does due to both the effect of the Yagi polar diagrams and the "ground effect" as it approaches the horizon. An estimate of the period of the first and last fringes was made assuming that the Yagi polar diagram varied as $\cos^2$(azimuth) and that the ground losses had the effect of reducing the output by the factor $\sin^2(9 \times \text{Alt})$ for an altitude less than 10°. This corresponds to the output being reduced by a factor of 2 at an altitude of 5°. Under these conditions, the predicted period of the first and last fringes is now 43.96 minutes with refraction and 40.21 without refraction which agrees much better with the observed result.

If records of Cygnus A day time and night time passes are traced and superimposed, it is evident that there is

no noticeable difference in the fringe periods for day and night.

4.5 The Effect of Spherical Refraction on the Horizontal Distance from the Receiving Site to the Sub-Sporadic-E Layer Point.

In the absence of refraction, the ray from the Cygnus A source to the interferometer intersects the sporadic-E layer (height assumed to be 105 km) over Woomera, two hours after transit, and arrives at the interferometer with an altitude of 10°. If refraction is taking place, according to the results obtained from the calculations made using the day time ionospheric profile, the apparent altitude of the ray from the source at the same time is increased by 1°, and, since except for the small tropospheric contribution, all of the bending is taking place above 100 km, the distance to the point under the sporadic-E layer intersection of the ray may be calculated assuming the ray to be undeviated between the ground and the layer and with altitude equal to the apparent altitude of the ray at the ground.

The result of this calculation is that the point on the ground underneath the sporadic-E layer intersection is about 30 km nearer to the interferometer when refraction is taking place. This distance is not great enough to be

considered in Chapter 6 where the results of the correlation analysis of sporadic-E at Woomera with the low angle St. Kilda scintillations are presented.

4.6 Signal Cut off due to Complete Reflection

The possibility of a radio wave from Cygnus A at a frequency of 40.0 MHz being completely reflected and thus preventing the penetration of signals to the ground was investigated as a function of the parameter $f_o F_2$. The bending angle program already described was suitable for this calculation with $f_o F_2$ included as an additional variable.

The values of electron density at 100 km (10^5 electrons/c.c.) and at 1000 km (10^4 electrons c.c.) remained the same for all $f_o F_2$, and for each value of $f_o F_2$ the corresponding values of maximum electron density, layer thickness below 300 km, and scale height above 300 km, were evaluated from the usual relations.

It was found that for $f_o F_2$ less than 7.5 MHz, no reflection of a transmitted ray from the ground could occur and the angles for which complete reflection occurred were evaluated for selected frequencies in the range 8.0 MHz to 12.0 MHz.

Selected results, which are typical of all those evaluated are presented in Table 4.6.

Critical Frequency $f_o F_2$ MHz	Apparent Zenith Angle (Deg)	Critical Zenith Angle (Deg. Min)	Bending Angle (Deg)
8.0	86.0	101° 42'	15.70
	87.0	109 49	22.81
	87.20	112 56	25.73
	87.40	118 29	31.03
	87.450	121 8	33.68
	87.470	122 54	35.44
	87.4750	123 39	36.17
	87.4760	Complete Reflection	
12.0	71.0	79 12	8.20
	71.50	82 36	11.10
	71.80	88 54	17.10
	71.840	91 58	20.13
	71.860	95 57	24.09
	71.8610	96 25	24.55
	71.8620	Complete Reflection	

TABLE 4.6

The apparent zenith angles for which complete reflection occurs are shown for the remaining frequencies in Table 4.7.

Critical Frequency $f_o F_2$ MHz	Apparent Zenith Angle	Critical Zenith Angle	Bending Angle
8.0	87.475°	123° 39'	36.17°
8.5	83.935	118 17	34.35
9.0	81.616	114 19	32.69
9.5	79.670	110 53	31.22
10.0	77.920	107 17	29.36
10.5	76.296	104 37	28.33
11.0	74.758	101 36	26.85
11.5	73.285	99 6	25.82
12.0	71.861	96 25	24.55

TABLE 4.7

In each case, an increase of 0.001° in the apparent zenith angle results in complete reflection taking place.

The calculations may be iterated further to more accurate apparent zenith angles but the above table probably represents the best data available since the accuracy is limited by the height increment used (i.e. 1 km). Since the condition $f > f_o F_2$ is well satisfied for all cases, the errors introduced by neglecting the earth's magnetic field are still acceptable.

The results show that as the signals become nearly reflected, the total bending angle becomes large and the true and apparent zenith angles differ considerably. However, even though signals transmitted from the ground will be internally reflected below a critical altitude, the table shows that the true position of the source, for the above range of frequencies, is always below the horizon for the ray which just penetrates the ionosphere. Although the apparent path of the source is modified considerably, the source is never rendered undetectable on the ground while its true position is above the horizon.

It is also evident that as the true position of the source nears the horizon, a small change in the apparent zenith angle corresponds to a very large range of true zenith angles.

This critical zenith angle was discussed by Titheridge (1964 a and b) in connection with the refraction of 20 MHz satellite transmissions and he used measurements of the critical angle to determine the electron density scale height near the F layer maximum.

From the Woomera ionogram records, it is evident that during 1964 and 1965, summer day time values of $f_o F_2$ rarely exceeded 9.0 MHz, while winter night time values dropped to as low as 2.5 MHz. Thus the calculations made cover adequately the range of conditions likely to be met in practice.

It has been shown that the presence of refraction should make the source visible for longer on each pass and that a complete reflection condition cannot prevent the source being detected at a frequency of 40 MHz. The computed output curves show that if the assumed output dependence on azimuth and altitude is correct, then the visibility of the first and last fringes will be enhanced in the presence of refraction. Since such an enhancement is not noticeable on the records, it is likely that the effects of ground losses at low altitudes, plus the increased absorption due to the increasing signal path length through the ionosphere D region (which has been referred to before), are sufficient to overcome the possible enhancement due to spherical refraction.

It appears that of all the effects considered it is not spherical refractions which determine the visibility of the Cygnus A source as it nears the horizon.

4.7 Wedge Refraction in the Ionosphere

As well as the spherical refraction effects present in a smooth ionosphere, an additional component of refraction, generally referred to as wedge refraction, will be present if horizontal gradients exist in the total electron content. Such gradients are present due to the regular

diurnal changes in total electron content and also due to irregular variations.

The regular wedge refraction of signals from the Cygnus A source was investigated qualitatively by Smith (1952) at Cambridge, U.K. at a frequency of 81.5 MHz. From his results, he derived information on the electron content above the F region maximum. Lawrence and Jesperson (1961), receiving signals from the same source at Boulder, Colorado at a frequency of 108 MHz, investigated the occurrence of irregular refraction and obtained estimates of the percentage fluctuations in total electron content consistent with their observations. Amongst others, Rao (1967) investigated directly the fluctuations in total electron content over short distances using the Faraday rotation of the 40 and 41 MHz transmissions of the beacon satellite Be-C and he associated the observed irregularities with the large scale travelling ionospheric disturbances detected on ground based sounders. The topic is further discussed in the review paper of Lawrence et al. (1964).

Although gradients in the total electron content can exist in any direction, in the present experiment the output of either interferometer is sensitive only to the effects of an east-west gradient which causes the observed transit time of the source to be either advanced or retarded.

From Lawrence et al. (1964), the angular deviation of a wavefront incident from near the zenith, produced by a horizontal gradient in electron density is given by:

$$\tau = \frac{d}{dx} \text{ (phase path length)}$$

$$= \frac{e^2}{2\epsilon_0 m \omega^2} \frac{d}{dx} \int N \, dh \text{ radians} \qquad (4.5)$$

The symbols used have their usual meaning and x represents a horizontal distance. Some estimate of $\frac{d}{dx} \int N \, dh$ must be made before τ can be evaluated.

4.8 The Regular Component of Wedge Refraction

For the present calculation, the order of magnitude of the regular component of wedge refraction is estimated using the diurnal variation of $f_o F_2$ at Woomera as a measure of the daily electron content variation and a value for the effective thickness of the layer is assumed.

It appears that the fastest rate of change of $f_o F_2$ at Woomera is about 1 MHz/hr. and persists for about 3 hours at dawn and dusk - the parameter increasing at dawn and decreasing at dusk. At latitude 35^oS this "electron content wedge" moves about 1000 km in 1 hour due to the earth's rotation. Thus the model used assumes that in 1000 km, $f_o F_2$ changes by 1 MHz and if $f_o F_2$ changes from 4 to 5 MHz

in this distance, the electron density changes by 2.5x10" electrons/metre^3 at the height of the F layer maximum.

If the effective thickness of the F layer is assumed to be 100 km, then from expression 4.5, τ = 2.16' arc = 9 seconds of time.

When corrected for the $1/(\text{frequency})^2$ dependence of τ, this result agrees with that found by Smith (1952) who observed a maximum angular deviation due to wedge refraction of 0.75' arc.

If the effect were as small as calculated above, it would not be detectable on the records of the Cygnus A interferometer used here as the interferometer has a baseline of 4 wavelengths and when the signal amplitude is adjusted correctly for the detection of amplitude scintillations and the chart run at a slow speed, then the zero crossing times cannot be read with sufficient accuracy. Smith was able to obtain the required accuracy since the baseline of his interferometer was 105 wavelengths. However, from Lawrence et al. (1964), provided that the thickness of the layer dominating the wedge refraction is not too large, the effect will be enhanced away from the zenith by a factor approximately equal to the secant of the zenith angle. Thus, for the Cygnus A source at an angle of elevation of 10°, the signals from the source could be refracted

by as much as 15' arc (1 minute of time), and this shift in position should be detectable by averaging the transit times from a large number of records.

The sense of the effect is that the apparent right ascension of a source should be increased in the morning (causing the source to be observed later) and should be decreased in the evening (causing the source to be observed earlier).

4.9 Comparison with Cygnus A Observations

Each Cygnus A pass lasts approximately 4 hours and occurs 4 minutes earlier each day. Consequently, certain dates correspond to particular pass times. Figure 4.4 shows for Adelaide during 1965:

(1) The time of the Cygnus A transit and the times of the beginning and end of each pass.

(2) The times of sunrise and sunset.

(3) The classification into time zones describing the behaviour of $f_o F_2$ values at Woomera. During the day and night zones, $f_o F_2$ has steady maximum and minimum values; it increases at a maximum rate through the morning zone and decreases at a maximum rate through the evening zone. It is evident from the figure that the morning and

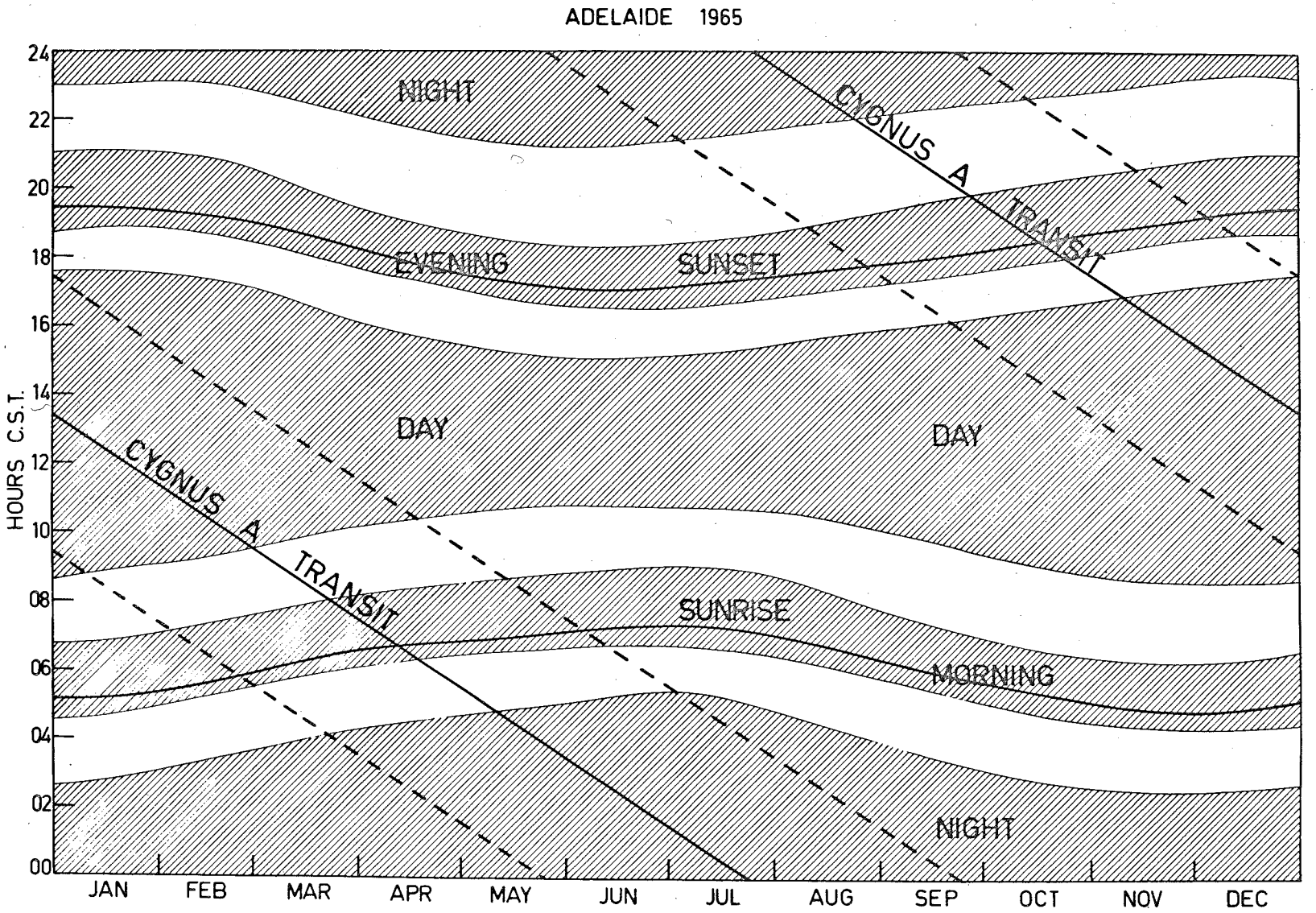

Figure 4.4 $f_o F_2$ behaviour and the transit time of the Cygnus A source.

evening zones are retarded by about 1 hour with respect to the sunrise and sunset times and that the day and night zones are similarly retarded with respect to midday and midnight. These are well known F region phenomena.

The calendar dates appropriate for each type of F region behaviour can be read from Figure 4.4.

To obtain the best possible values of the sidereal time of the maximum of each fringe, as many Cygnus A passes as possible were read for the morning and evening time zones. (This covered both years for which the interferometer was in operation). However, the day and night zones were found to be longer and data from one year of the records proved sufficient. Local times were converted to sidereal times using the appropriate data from the Astronomical Ephemeris.

Having discarded those passes which were obviously incorrectly timed (generally due to a power failure or other interruption to the record), the average sidereal time for each fringe maximum was then evaluated for every time zone. This showed that as expected, the day and night zone sidereal times were similar and so data from these zones was combined to give a reference for comparison with the morning and evening transits.

Table 4.8 shows the sidereal times of each fringe maximum for day and night passes respectively, includes

the difference and standard error of the difference between the sidereal times and justifies the lumping together of this data. The initial results also justified lumping together the morning data from the 2 years but unfortunately, less data was available for the evening passes due to equipment difficulties in the evening period in 1965.

The results of the calculations comparing the lumped day and night sidereal times with the morning and evening pass times are shown in some detail in Table 4.9. These results show that fringe maxima observed in the morning time zone are observed about 1 minute early - a rather surprising result since the discussion in Section 4.8 indicated that the source should be observed later when the total electron content was increasing. The time differences found are about three times their respective standard errors which indicates that they are unlikely to have arisen by chance. In the case of the evening passes, the results are distributed between an advance and a retardation of the pass time, and this is in particular true of the only two sidereal time differences which greatly exceed their standard error.

The conclusion is that no consistent sidereal time difference is observed for the evening passes but that an anomalous result has been found for the morning passes.

Fringe	1	2	3	4	5	6	7	8	9
1964/5 Day	1714.8	1754.3	1834.6	1912.5	1949.6	2025.7	2102.4	2138.9	2216.3
Standard Devn. of Mean	0.67	0.50	0.61	0.42	0.36	0.38	0.50	0.60	0.80
N	33	36	38	40	41	40	36	32	29
1965 Night	1715.0	1754.4	1833.5	1912.4	1949.0	2025.5	2102.3	2139.7	2218.5
Standard Devn. of Mean	0.48	0.46	0.38	0.39	0.35	0.33	0.39	0.50	0.53
N	48	54	56	58	58	57	55	50	47
Difference (night - day) minutes	+0.2	+0.1	-1.1	-0.1	-0.6	-0.2	+0.1	+0.8	+2.2
Standard Error of Difference	0.82	0.68	0.72	0.57	0.50	0.50	0.63	0.78	0.95
Combined Data	1714.9	1754.4	1834.0	1912.4	1949.2	2025.6	2102.4	2139.4	2217.7
Standard Devn. of Mean	0.40	0.36	0.34	0.29	0.25	0.25	0.29	0.38	0.45
N	81	90	94	98	99	97	91	82	76

TABLE 4.8 Sidereal times of the 1964/5 Day and 1965 Night fringe maxima together with their relevant statistics.

Fringe	1	2	3	4	5	6	7	8
Day and Night	1714.9	1754.4	1834.0	1912.4	1949.2	2025.6	2102.4	2139.4
Standard Devn. of Mean	0.40	0.36	0.34	0.29	0.25	0.25	0.29	0.38
N	81	90	94	98	99	97	91	82
Morning	1715.3	1752.6	1832.2	1910.9	1947.5	2024.8	2102.1	2139.4
Standard Devn. of Mean	0.46	0.42	0.39	0.38	0.38	0.37	0.43	0.49
N	35	44	58	63	51	43	34	18
Difference (morning, D and N) minutes	0.4	-1.8	-1.8	-1.5	-1.7	-0.8	-0.3	0.0
Standard Error	0.60	0.54	0.51	0.47	0.46	0.44	0.53	0.63
Evening	1715.9	1755.8	1834.2	1913.0	1947.8	2025.4	2102.0	2141.1
Standard Devn. of Mean	0.81	0.53	0.60	0.61	0.41	0.44	0.35	0.72
N	19	24	26	21	17	18	18	14
Difference (evening, D and N)	1.0	1.4	0.2	0.6	-1.4	-0.2	-0.4	0.7
Standard Error	0.90	0.62	0.69	0.68	0.48	0.50	0.48	0.82

TABLE 4.9 Sidereal times of the combined 1964/5 Day and 1965 Night fringe maxima compared with the same fringe maxima observed in the morning or evening together with the relevant statistics.

The diurnal variation sought in the sidereal times of the fringe maxima has not been found although it is evident that the accuracy is sufficient to observe the variation if it is present with the strength predicted in Section 4.8.

It is probable that the model used here has greatly over emphasised the importance of the zenith angle variation which is known to decrease in importance as a thicker region becomes responsible for the wedge refraction. In fact the diurnal increase and decrease of total electron content occurs through the whole ionosphere although most of the contribution to the wedge refraction will come from within 50 km or less of the electron density maximum. It is doubtful whether this region can be considered sufficiently thin for the zenith angle effect to be as important as is supposed here.

The zenith angle effect seems to have more direct application in the investigation of the irregular component of wedge refraction, which is now discussed.

4.10 The Irregular Component of Wedge Refraction

The most recent observations of the total electron content by Rao (1967) and the observations of Lawrence and Jesperson (1961) on the variations in apparent position

of the Cygnus A source show that changes in the total electron content similar to the regular diurnal changes can be observed over horizontal distances of the order of 100 km. The gradients due to these variations are therefore about 10 times as large as the regular gradients and, from a fixed observation point on the ground, are typically observed to persist for about 20 minutes and occasionally up to 1 hour. Consequently, the angular deviations to be expected from the irregular gradients are about 10 times as large as those expected from the diurnal gradients. They have been associated with the passage of travelling ionospheric disturbances which have been extensively investigated by Munro (1958) and others.

Large east-west and north-south gradients of the total electron content have also been observed recently from Adelaide in records taken from passes of the beacon satellites Be-B and Be-C. The results of this work by A. Beresford are not yet published.

A small proportion of the Cygnus A records showed effects thought to be due to irregular ionospheric refraction and some of these are shown in Figure 4.5.

Since apparent changes in radio source position can also be caused by phase scintillations (in some respects a similar phenomenon on a much faster time scale), the choice

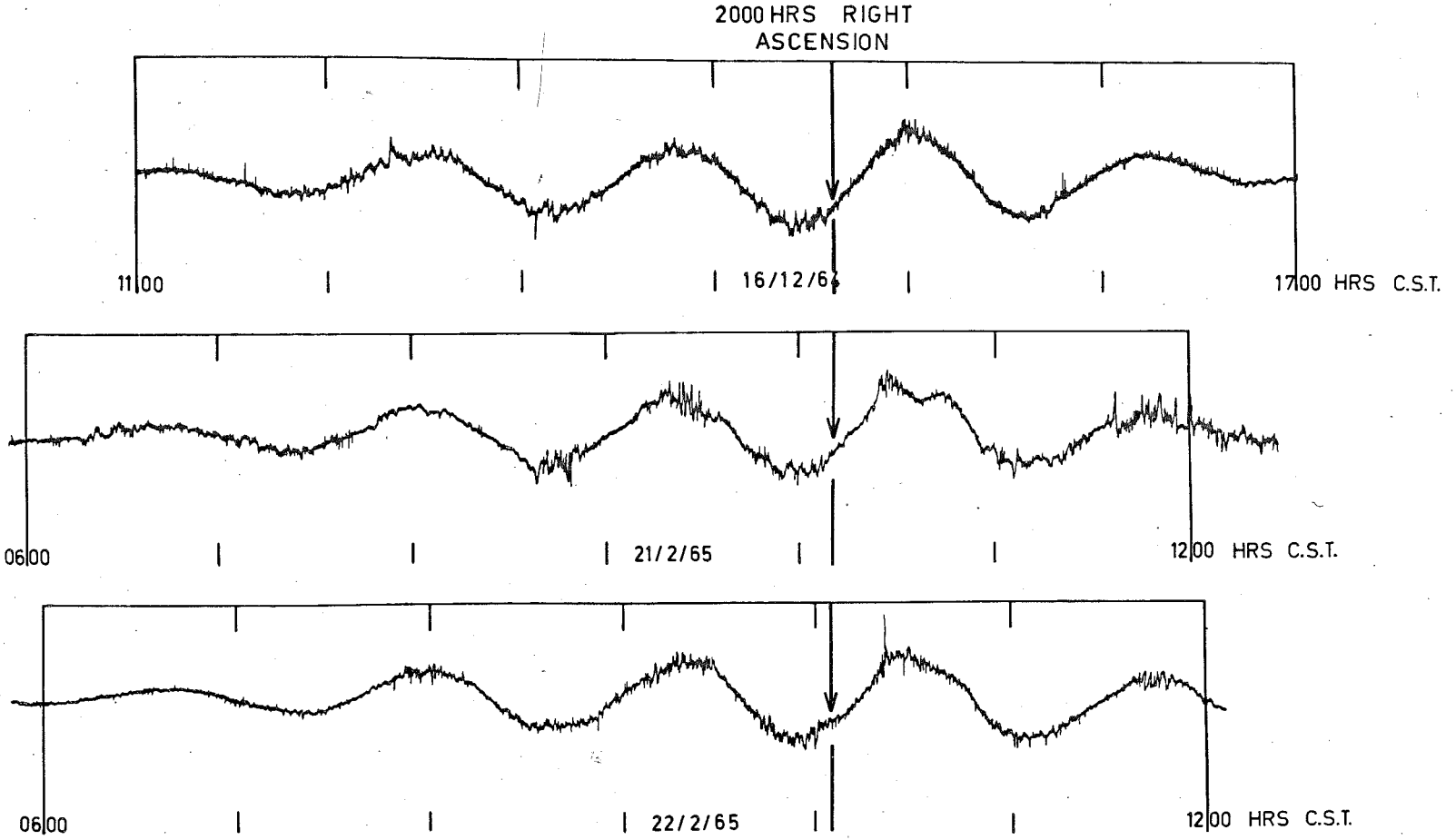

Figure 4.5 Two records of Cygnus A showing irregularly spaced zero crossings.

of records chosen for detailed inspection was restricted to those which showed weak, or at the most, moderate amplitude scintillation over the interesting section of the pass. To enlarge on the statement in brackets above, Warwick (1964) interpreted broad band scintillations in terms of a refraction effect but on a much faster time scale than for the effect sought here.

In Figure 4.5, the record of the Cygnus A pass of 16/12/64 is shown as an example of a pass showing little scintillation and having a smoothly varying fringe amplitude. The passes of 21/2/65 and 22/2/65 both show marked deviations from a smoothly varying fringe amplitude - notably around the zero crossing following the reference arrow and in the subsequent fringe. Although other records were taken on which the deviations from normal behaviour compared with the two shown, none appeared to show the effect more strongly. If the records shown are superimposed, the zero crossings referred to above are seen to be displaced by a maximum of 1 minute indicating an apparent movement of the source of 0.25 degrees. As this irregular effect was estimated here (with support from the results of previous authors) to be about 10 times as large as the regular effect, in the light of the above result, the search for the effects of the regular component of wedge refraction seems rather ambitious.

Also in Figure 4.5, the local time of each pass is shown and a reference point common to all passes at 2000 hours right ascension is included.

The fact that the records shown here all refer to daylight hours should not be taken as an indication that the effect is more likely to occur by day. Rather, it is the selection condition imposed by the small amplitude scintillation requirements which is masking the observation of refraction effects at night - when scintillation is strongest and most frequent. In fact, Lawrence and Jesperson (1961) did observe a maximum occurrence of irregularities in the total electron content during the day but they were using equipment designed especially for these measurements whereas this was not the case here.

CHAPTER 5. OCCURRENCE OF SCINTILLATION AND OBSERVED VARIATIONS IN ITS ACTIVITY

5.1 Scintillation Occurrence

(i) Smaller Interferometer Records. As indicated in section 2.2, the smaller interferometer was operated for a period of two years during which signals from the source Cygnus A were recorded daily for six hours centred about the source transit time and, as indicated in section 4.6, the length of time for which the source was visible each day was not affected at all by the occurrence of spherical refraction in the ionosphere, but rather was governed by the effects of ground losses and increased D region absorption in the signals when the source was near the horizon. As was discussed in section 3.4(ii) and illustrated in Figure 3.5, nine maxima on minima (referred to as fringes) were regularly observable in the receiver output for each transit of the source, and an amplitude scintillation index in the range 0 - 5 was assigned to each fringe of each transit.

Figure 5.1 shows the probability of occurrence of each amplitude scintillation index for the central fringe only calculated (a) for the year 1964, (b) for the year 1965, and (c) for the two years combined.

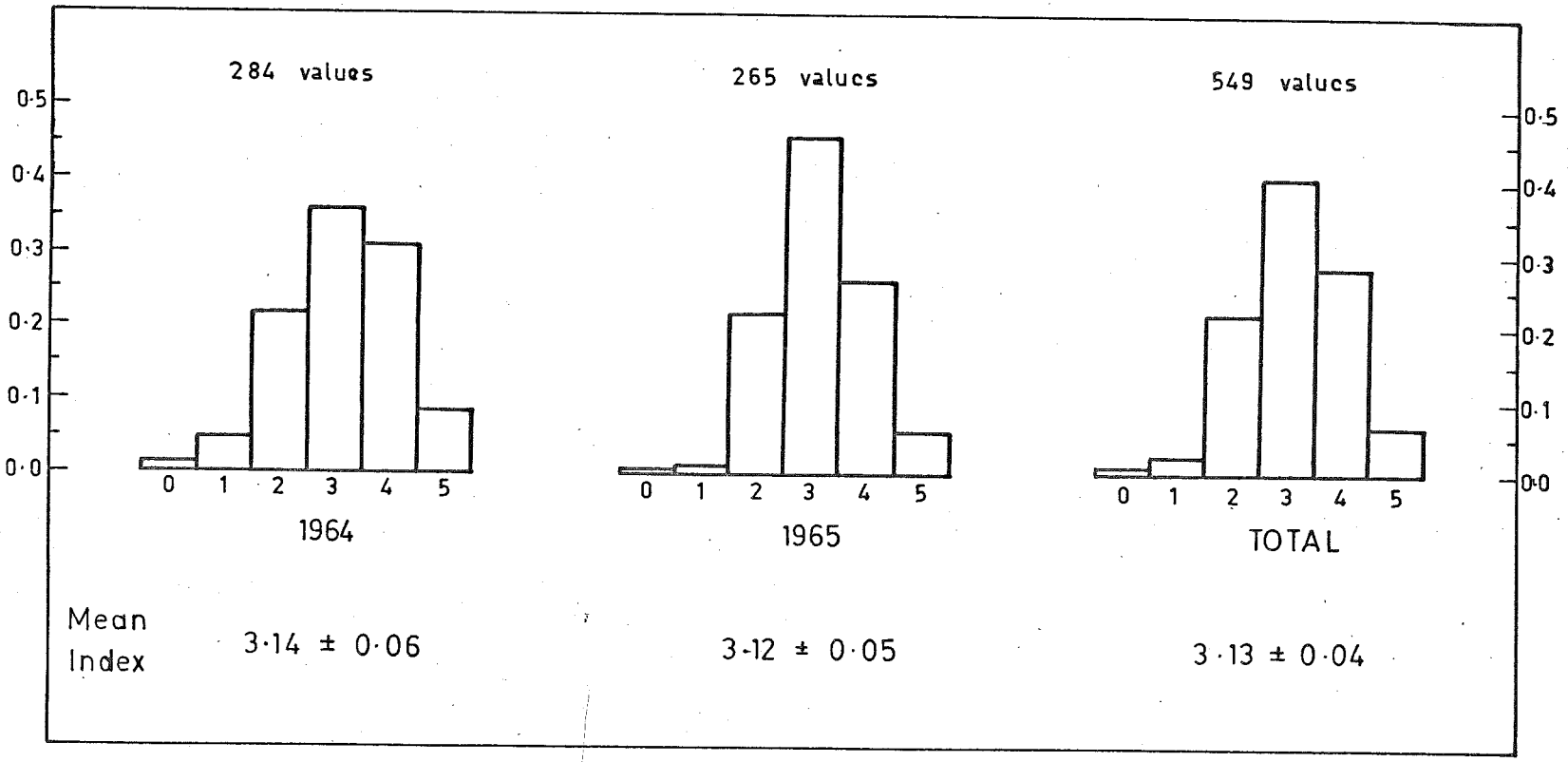

Figure 5.1 The probability of occurrence of each amplitude scintillation index in the output from the Cygnus A source from the small interferometer.

The most obvious conclusion to be made from the data presented in Figure 5.1 is that there is no change in the mean amplitude scintillation index over the period of running of the experiment. This result is an expected one since (as was discussed in section 1.4(iv)), scintillation activity is correlated positively with solar activity and the two years 1964 and 1965 were both years of minimum solar activity. (The daily Zurich sunspot numbers averaged 10 and 15 for the two years respectively, compared with a value of several hundred for a year of maximum solar activity).

It is also evident from the figure that an amplitude scintillation index of 3 was the most likely index for both years and that there were very few occasions on which no scintillation was observed. In fact over the two year period, there were three occasions when an index of 0 was observed and fourteen occasions when an index of 1 was observed in the central fringe. The only difference between the histograms for the years 1964 and 1965 is in the different occurrence probability of indices 3 and 4 in the two years. It appears that the other indices occur with similar probabilities for both years and that the increase of index 3 in 1965 is almost entirely at the expense of index 4. Since indices 3 and 4 both represent

at least moderate scintillation, and since all the scintillation indices were assigned using an approximate method relying only on visual inspection, it is probable that the assignment of the indices 3 and 4 (in particular) is not sufficiently reliable that the observed differences in occurrence probabilities between 1964 and 1965 can be regarded as significant.

(ii) Larger Interferometer Records. As indicated in section 2.2, the larger interferometer was operated from December 1965 to August 1966 during which time signals were recorded from up to 9 radio sources as identified in table 3.2. As was discussed in section 3.4(ii) and illustrated in Figure 3.6, a single maximum in the receiver output was observed for each transit of each source and an amplitude scintillation index in the range 0 - 3 was assigned to every recorded source transit.

Figure 5.2 shows the probability of occurrence of each amplitude scintillation index from each source, the number of observations made for each source and the mean amplitude scintillation index for each source. It is evident from the various histograms making up the figure that all the sources except Cygnus A and Taurus A are more likely to produce a scintillation index of 0 than any higher index.

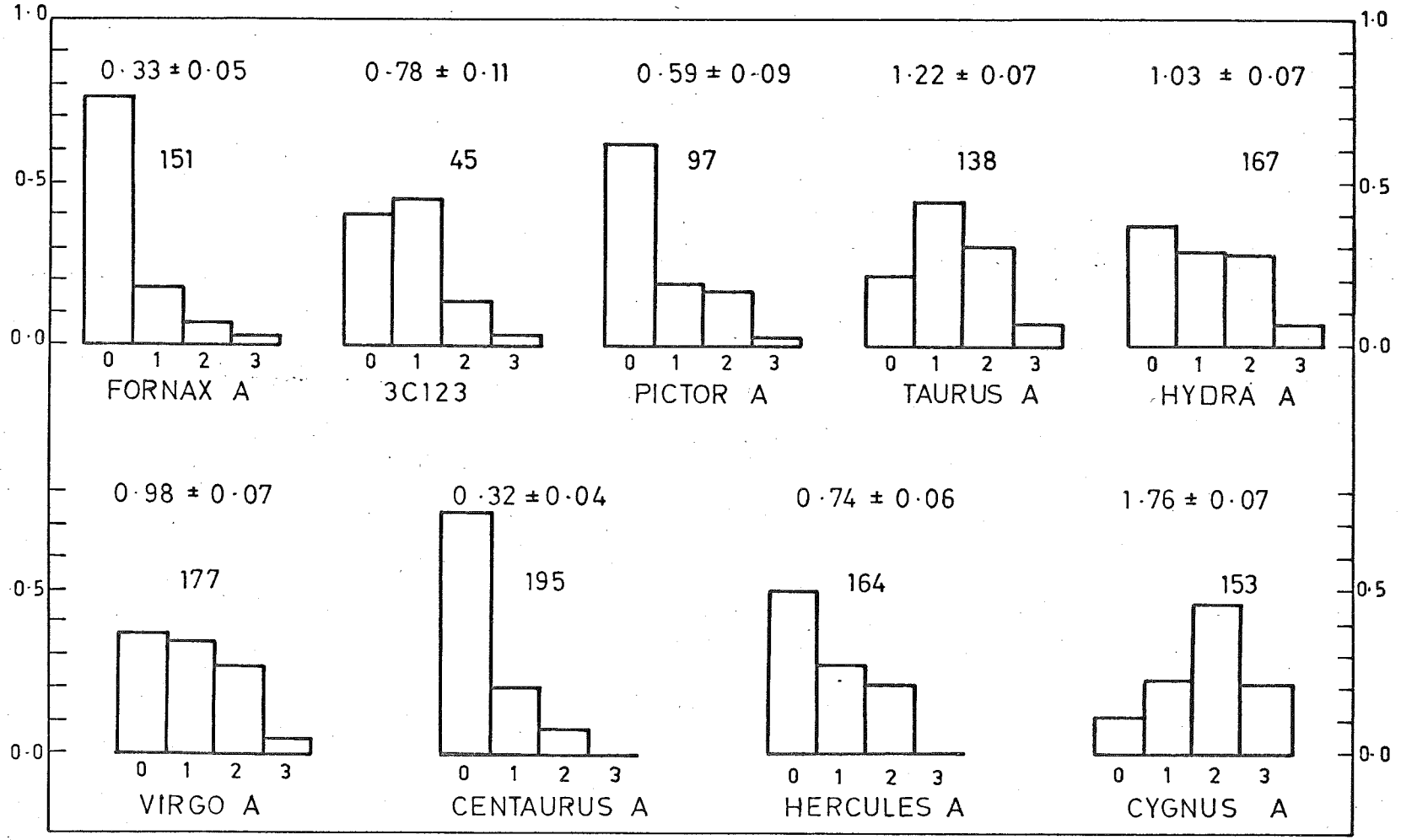

Figure 5.2 The probability of occurrence of each scintillation index in the output of all the sources detected for the larger interferometer.

Taurus A has a most probable index of 1 and Cygnus A of 2 - the latter result in agreement with the observations in the preceding years with the smaller interferometer. In fact, taken over all the sources, there is here a much larger variability in the intensity of amplitude scintillation than there was was for the observations of the Cygnus A source with the smaller interferometer. The reasons for this increased variability are discussed in later sections in terms of the variable sizes of the sources and the different zenith angle at which each source transits. If it is desired to compare scintillation occurrence between these sources then a normalizing procedure must be used, such as Smerd and Slee (1966) used in their work, which takes these effects into account.

Apart from the previous comment that signals from the Cygnus A source had a maximum probability of showing moderate to strong scintillation in the records of both interferometers, it was not possible to combine data from both experiments and come to any conclusion regarding the long term trend in the scintillation activity. As well as the difficulties due to the variable source parameters pointed out in the preceding paragraph, the different fringe shapes and the different ranges of scintillation indices used also made any direct comparison difficult.

The histograms of Figure 5.2 cannot be taken as truly representing the probability of occurrence of the various scintillation indices for each source because the observing period did not last for a full year and therefore each source was not observed at all possible transit times. If there is a pronounced diurnal or seasonal variation of scintillation activity, then the missing transit times (different for each source) or months (September to November) could well represent periods of different scintillation activity - sufficient to modify the mean scintillation activity and the shapes of the histograms. However, as is shown later in this chapter, meaningful average scintillation indices can be evaluated for most of the sources and useful estimates made of the dependence of scintillation activity on the zenith angle of the source transit.

5.2 Temporal Variations in Scintillation Activity

Figure 5.3 shows the mean amplitude scintillation indices observed with the smaller interferometer for the Cygnus A source. Each point is calculated from data recorded over a six week period which is equivalent to a variation of three hours in the source transit time. The months and local times of the observations are indicated in

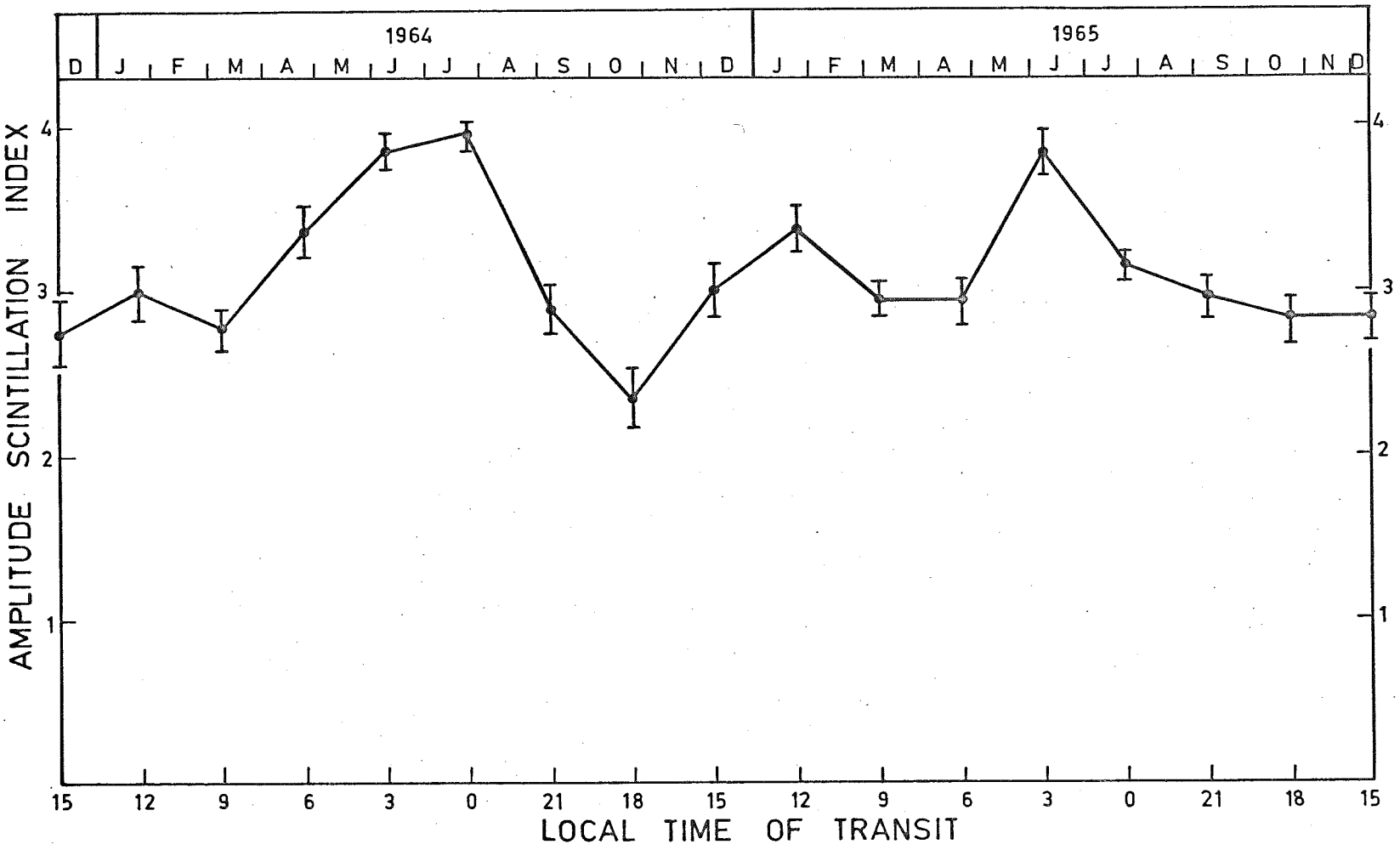

Figure 5.3 The mean amplitude scintillation indices of the source Cygnus A plotted against the month and local time of the observation.

the graph and the error bars represent the standard error of each mean value. Significant maxima are consistently observed for both years of observation for midnight (or winter) and midday (or summer). Anticipating the results of the larger interferometer observations and assuming the maxima to be the result of a diurnal variation, the major night time peak in activity is seen to occur nearer to 0300 hours than to midnight while the day time peak occurs nearest noon.

The results shown in Figure 5.3 are discussed further following the presentation of the results for the larger interferometer.

Figures 5.4 and 5.5 show the mean amplitude scintillation indices observed for the various sources detected by the larger interferometer. The indices are plotted against the local time of source transit and the middle of the month of observation in the two diagrams respectively. Each point on the curves represents one month of observation or (which is equivalent) a two hour range of transit time. The relationships between the calendar date and the transit times of each source may be seen in Figure 3.1.

From Figure 5.5, it is evident that the mean scintillation index is unusually high for most sources in February and from figure 5.4, it is evident that most sources show

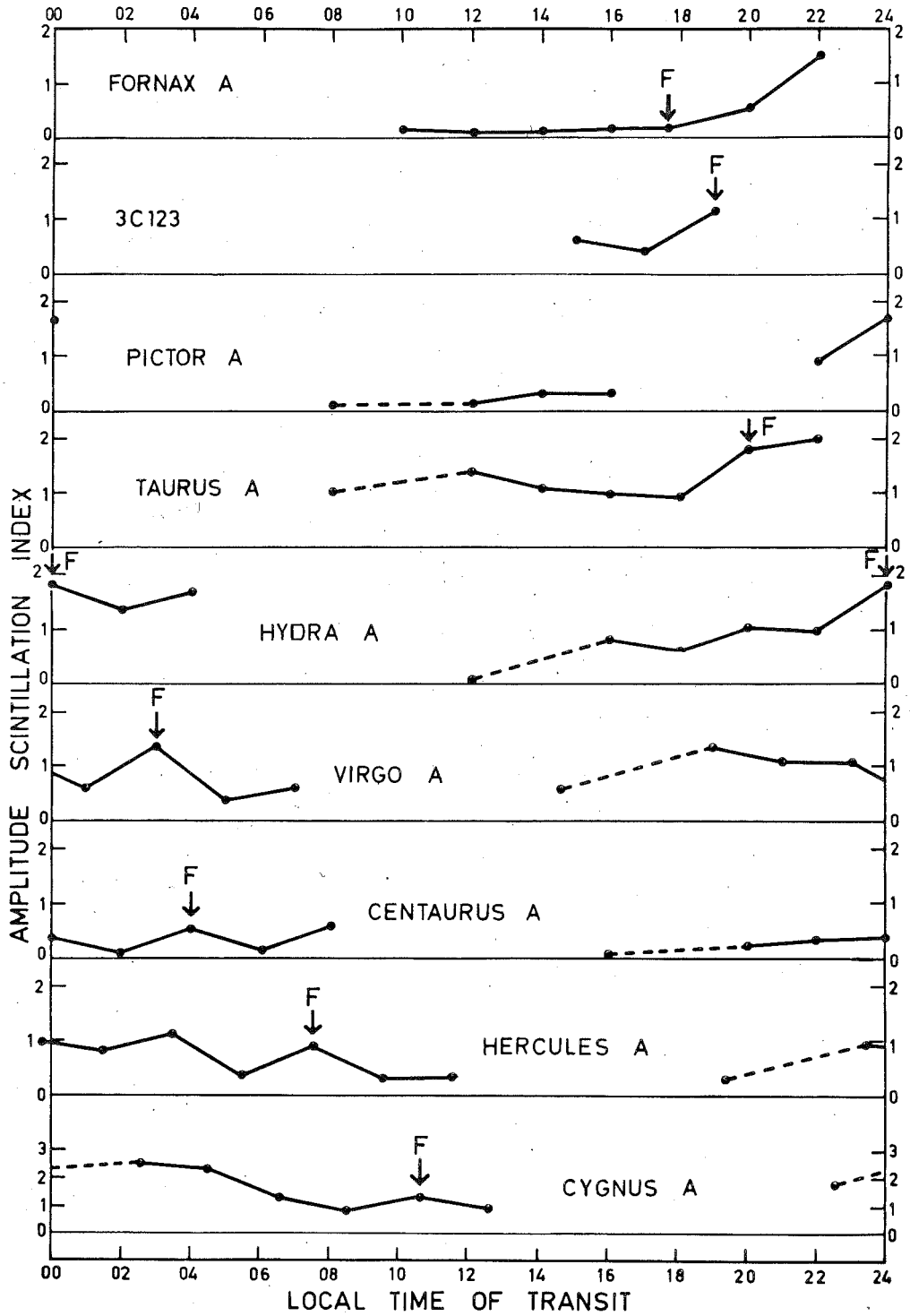

Figure 5.4 The mean amplitude scintillation indices observed for the various sources detected by the larger interferometer plotted against the local time of the source transit.

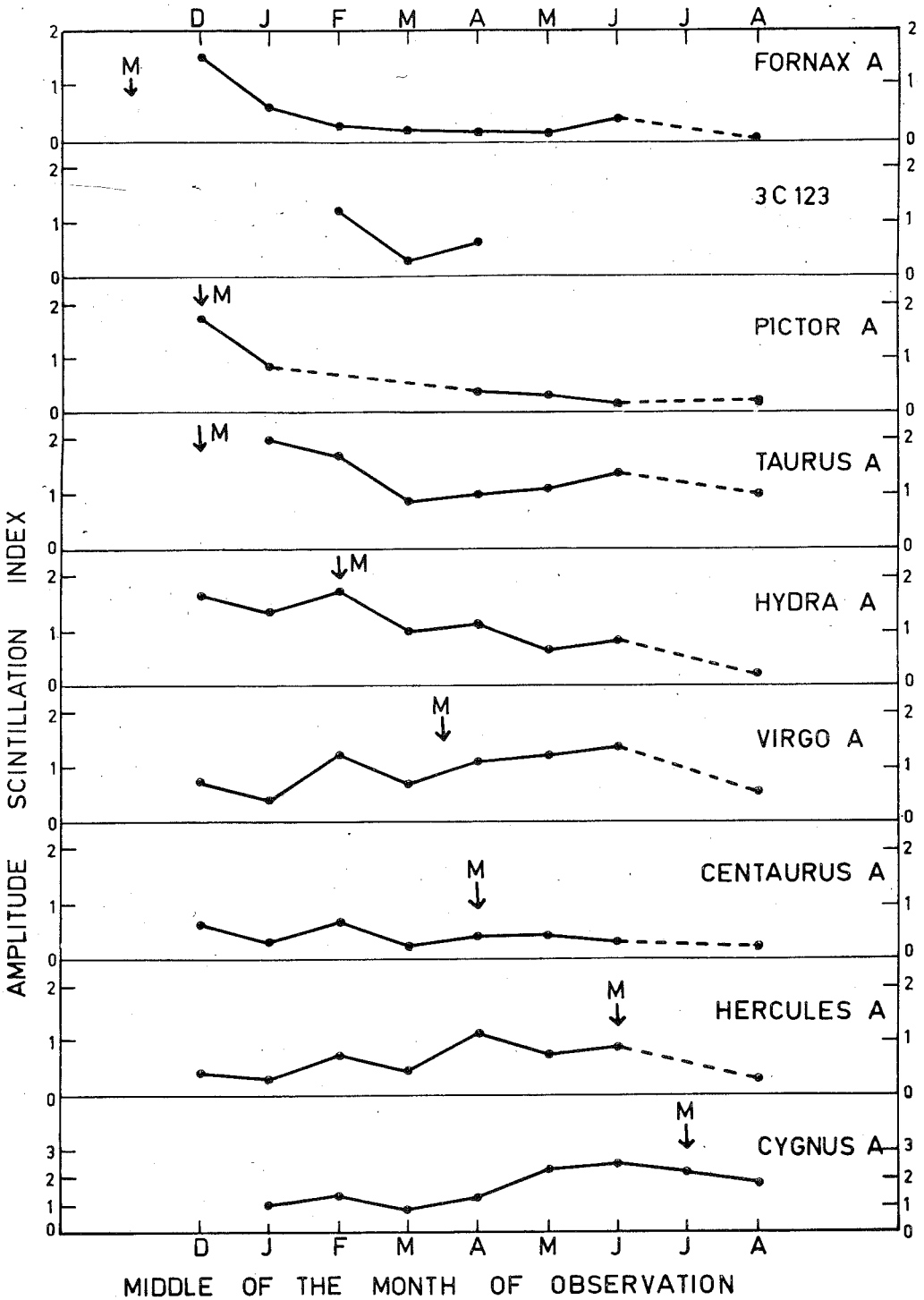

Figure 5.5 The mean amplitude scintillation indices observed for the various sources detected by the larger interferometer plotted against the month of observation.

a maximum of scintillation activity near or after midnight. The transit time corresponding to the month of February is marked F for each source in Figure 5.4 and the month corresponding to a transit time of midnight is marked M for each source in Figure 5.5.

Due to the observation that signals from the Cygnus A source show more intense scintillation than signals from other sources, the vertical scintillation index scale for Cygnus A is half that of any other source.

Apart from the consistently high values of the scintillation indices in February, the results appear to favour a predominantly diurnal rather than a seasonal variation, although the conclusion cannot be as decisive as that of Smerd and Slee (1966) who combined the scintillation data from eight sources into single curves plotted against a monthly and local solar time scale using normalized scintillation indices from many years of observations.

From the present results, a dominant seasonal variation of the scintillation indices would appear to be discounted, since if the following pairs of sources are considered; a) Fornax A (right ascension 0321) and Virgo A (1228), b) Taurus A (0532) and Hercules A (1649) and c), Hydra A (0915) and Cygnus A (1958) - each pair consisting of two sources separated in right ascension by at least 9 hours, then,

excluding the high values of scintillation index observed in February, Figure 5.5 shows that the members of each pair of sources show opposite long term trends in scintillation activity with respect to each other. Members of these pairs of sources of nearly opposite values of right ascension would have shown similar long term trends in the curves of Figure 5.5 if a seasonal effect had dominated the temporal variation in scintillation activity.

The conclusion that a diurnal effect dominates the temporal variation in scintillation activity comes from the curves of Figure 5.4 which indicate that all the sources observed except 3C123 (for which appropriate scintillation indices are not available), and Centaurus A (which shows little scintillation activity at any time), show a tendency for the maximum scintillation indices to occur at night - in most cases between midnight and 0300 hours local time.

Although scintillation indices observed near midday were available for all the sources except Virgo A and Centaurus A, only Cygnus A and Taurus A showed a maximum (albeit a subsidiary maximum) in scintillation activity at this time. In particular, the strong midday maximum of scintillation activity observed by Smerd and Slee (1966) for the source Pictor A was not found in the results of

this experiment, possibly because the signal strengths recorded from this and the Taurus A source were similar and the difference in their right ascension co-ordinates was small, thus causing difficulties in the interpretation.

The maximum values of scintillation activity observed in February are evident for all radio sources except Fornax A for which results are available for this month, and only in the cases of the sources Hydra A and Cygnus A does this maximum occur at a time when it could be interpreted as part of a diurnal variation. The observation of this February maximum is rather unexpected and from the observations of Smerd and Slee (1966) who, from scintillation observations from 1955 to 1959, did not detect it, it is hardly likely to be an effect reproducible in several years data. If it is to be regarded as a short term effect, it is still difficult to explain because solar activity in February 1966 as defined by the 2800 MHz daily flux measurements or by the indices assigned to the interferometer charts (discussed in section 3.2), which are correlated with the 2800 MHz daily flux, is less than that observed in the preceding or following months.

The conclusion is that the scintillation activity observed with the present two interferometers is controlled by a diurnal rather than a seasonal variation, and this

conclusion will be made use of in the following section where the zenith angle variation is determined for the scintillation activity of the radio sources observed by the larger interferometer.

5.3 Zenith Angle Variations in Scintillation Activity Measured with the Larger Interferometer

Figure 5.6 shows the average scintillation indices evaluated for all sources observed with the larger interferometer(except 3C123) plotted against the zenith angle of transit of each source. Since the interferometer was not in operation for a full year, the total observations for each source could not be used in calculating these averages as sufficient of the diurnal variation in scintillation activity was not recorded to eliminate this variation. If this variation is to be allowed for in any way, it is necessary to compare the scintillation activity of the different sources at a fixed transit time. Accordingly, the indices plotted in Figure 5.6 were averaged from source transits recorded between 1900 and 2300 hours local time. Each point in the figure was calculated from about 60 observations and the standard error of about $\pm$ 0.15 in the mean values of the scintillation indices is shown in the figure.

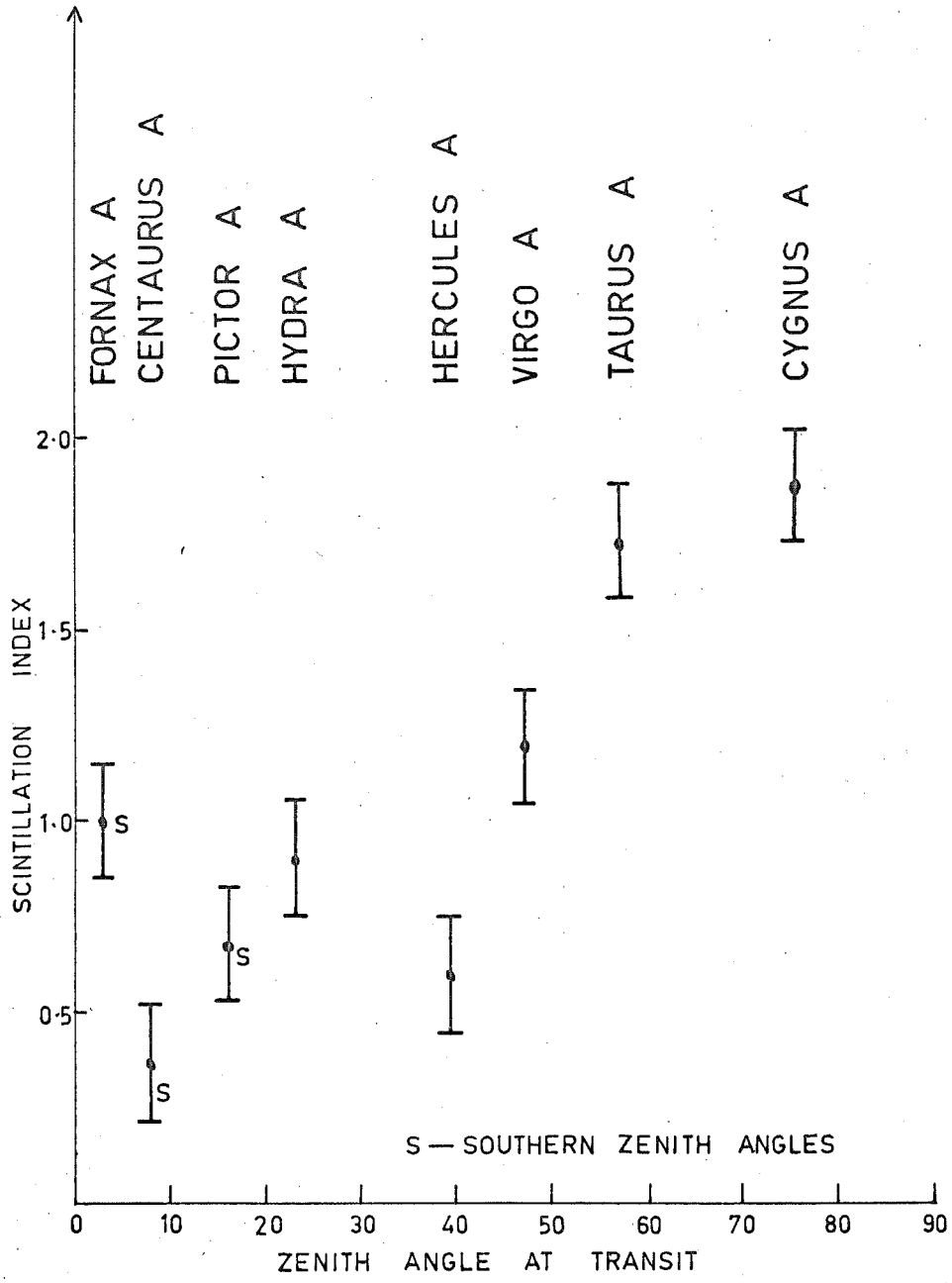

Figure 5.6 The zenith angle dependence of the mean scintillation indices.

The most obvious result to be seen from Figure 5.6 is that the average scintillation indices for the three sources furthest from the zenith are significantly higher than the indices for the other sources. The increase is largest for the indices observed in signals from the Cygnus A source, these indices being increased by a factor of 3.

As was anticipated in section 3.2, the amplitude scintillation indices of the Centaurus A source are less than those of any other source, this being due to the superposition of background emission from a large angular region. Transits of this source were observed each day 1 hour after transits of the Virgo A source and it was obvious from inspection of the records that signals from Virgo A showed much more intense scintillation than did signals from Centaurus A. Figure 5.7 shows transits of these two sources detected 1 hour apart and includes one of only 4 occasions on which the Centaurus A source showed the more intense scintillation, this particular pass of the Centaurus A source being one of the few to show such strong scintillation. These isolated instances would arise if the extent of the irregular regions near the receiving site was patchy or very localized. It should be noted that the smaller amplitude of the output from the Virgo A source in

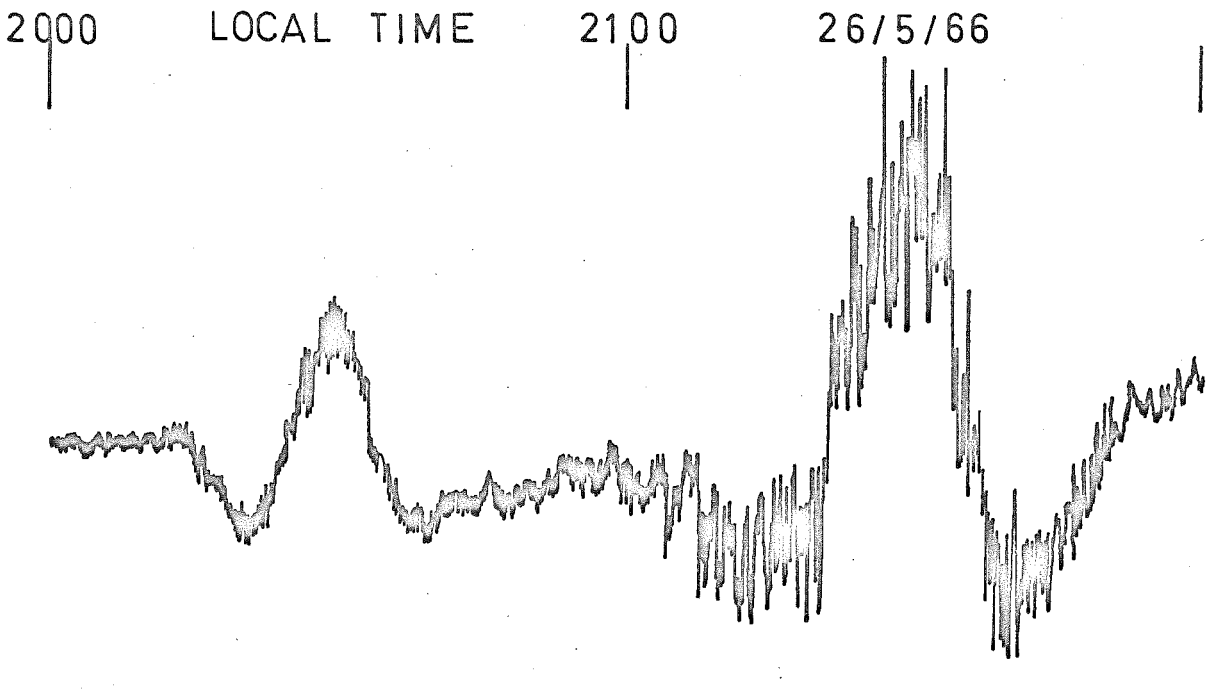

(a) A most unusual observation showing the more intense scintillations of the Centaurus A source.

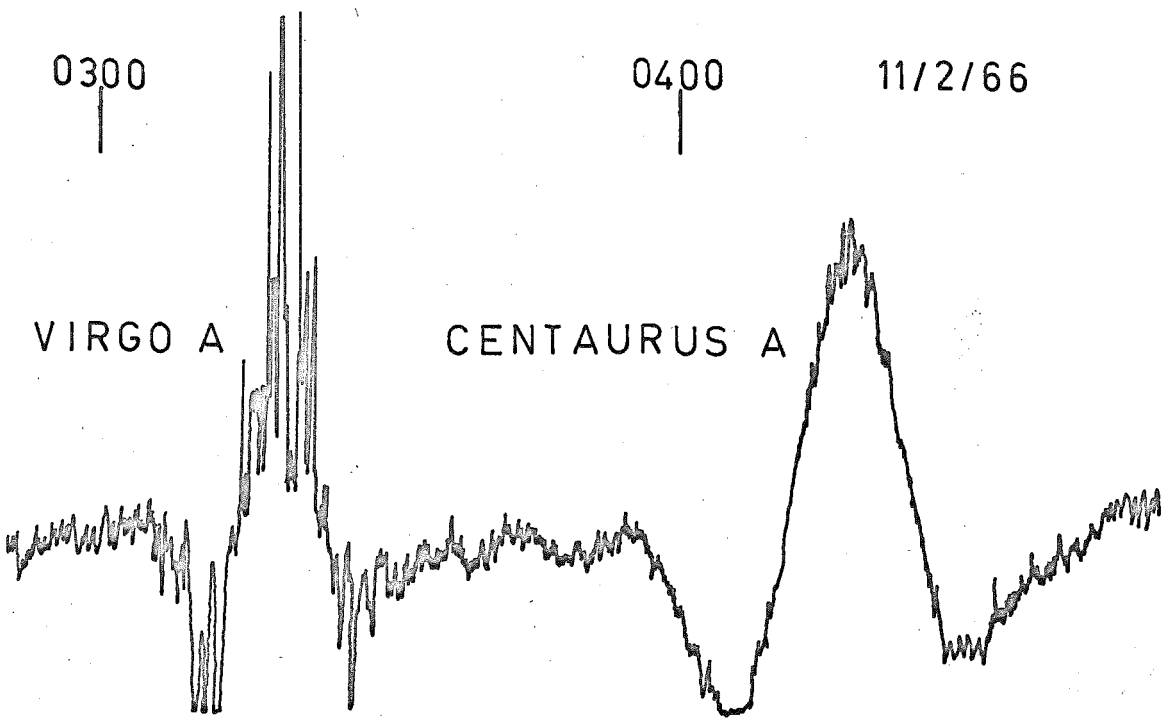

(a) The usual and expected observation showing the more intense scintillations of the Virgo A source.

Figure 5.7 Comparison of the scintillations in the signals from the sources Virgo A and Centaurus A.

the May record compared with the February record is due to the array being directed to the zenith in May while in February it was directed 45 degrees north of the zenith.

If the average scintillation indices are to be corrected for the effect of source size, consideration of the result of Aarons and Guidice (1966) and of the source parameters listed in Table 2.2 shows that only the sources Fornax A and Centaurus A are large enough in angular extent for their observed scintillation indices to be reduced. Since the Fornax A source consists of two components each of angular diameter 18' arc and separated by 29' arc, its scintillation indices would be expected to be reduced by a factor of at least 2 but as this effect was not observed, it was considered pointless to apply the correction. In the observations of Smerd and Slee (1966) the Fornax A scintillation indices were slightly less than those of other sources but not as much less as suggested here. In the case of the Centaurus A source, the correction factor is very uncertain and no attempt was made to normalize the scintillation indices from this source by taking its size into account. Smerd and Slee did not include observations on the Centaurus A source in their paper, probably for the above reason.

Another feature of Figure 5.6 is the increased average scintillation index for the Hydra A source compared with

the sources Hercules A and Pictor A at slightly larger and smaller zenith angles respectively - this observation agreeing with that of Smerd and Slee. This enhancement which, in the present case, has only limited significance is possibly due to the fact that, assuming the irregularities responsible for the scintillations lie in the F region, they are field aligned and the daily transit of the Hydra A source is observed at the same elevation angle as the magnetic zenith (zenith angle 23°) and the irregularities are being observed end on. This point is enlarged in the following section.

5.4 Theory of the Zenith Angle Effect on Scintillation Activity

The diffraction theory of Briggs and Parkin (1963) shows that for isotropic irregularities, a general increase in the depth of amplitude scintillations with increasing zenith angle is expected due to the lengthening of the signal path through the diffracting region and also (under some conditions) due to the increasing distance from the observing site to the layer. Figure 5.8 shows the variation of the scintillation depth S with the dimensionless parameter $P = \lambda z/r_o^2$ for an isotropic phase screen where λ is the wavelength of the radiation, z is the distance to

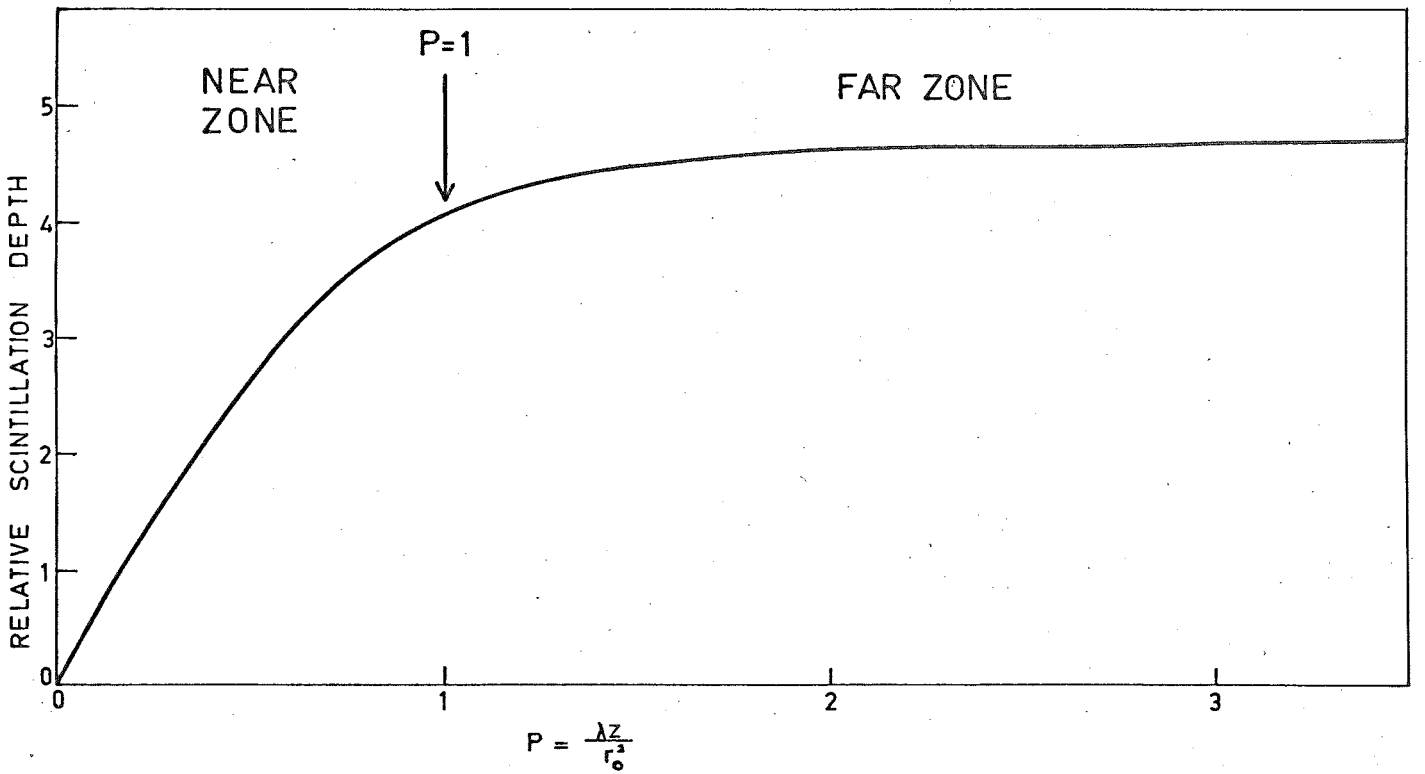

Figure 5.8 The scintillation depth as a function of the parameter P for an isotropic phase screen ϕ_o = 1 radian.

the layer and r_o the irregularity size. The curve applies for ϕ_o, the root-mean-square phase deviation of the irregularity structure, equal to 1 radian and is taken directly from Figure 3 of the Briggs and Parkin paper. For $P < 1$, $S \propto z$, and for $P > 1$, S becomes relatively independent of Z; the two regions are referred to as the near and far zones respectively, and amplitude scintillations may be regarded as completely developed when observed from the far zone.

In the observation of scintillations arising in the F region with the present equipment, $\lambda = 8$ metres, $r_o = 1$ km and $P > 1$ for $z > 125$ km. Since the F layer height is greater than this, scintillations originating in F region irregularities may be regarded as being observed from the far zone for all zenith angles and for isotropic irregularities, the scintillation depth observed from the ground increases only because of the lengthening of the signal path through the diffracting region. However for irregularities in the E region with the same value of r_o, observations at zenith angles of up to 40^o will be made in the near zone.

In the case of isotropic irregularities, Briggs and Parkin have already calculated curves showing the dependence of scintillation depth on zenith angle. They used the appropriate formula,

$$S \propto \lambda (\sec i)^{\frac{1}{2}} \left(1 + \frac{\pi^2 r_o^4}{4\lambda^2 Z^2}\right)^{-\frac{1}{2}} \qquad (5.1)$$

where i is the angle of incidence of radio waves on the layer and the other variables have already been defined. The approximation is valid for small ϕ_o and the contribution from the term $\pi^2 r_o^4/4\lambda^2 Z^2$ is not important if all observations are made sufficiently into the far zone.

Figure 5.9 shows curves similar to those of Briggs and Parkin calculated for the E and F region for isotropic irregularities of scale size 1.0 km in the F-region and 1.0 and 0.1 km in the E region. These two values, probably representing the extremes, for the E region scale size are included because experimentally, the sizes in this region (E_S rather than E) are not as well known as the F-region sizes and also, it is not always certain that scintillation activity originates in this region. Briggs and Parkin (1963) arrived at one estimate for the size of irregularities in the E region using the scintillation observations of Chivers and Davies (1962). From various arguments, they accepted Chives and Davies height estimate of 100 km for the irregularities and from the theoretical curves of the zenith angle variation for different values of r_o, they concluded that in the E region, r_o was not less

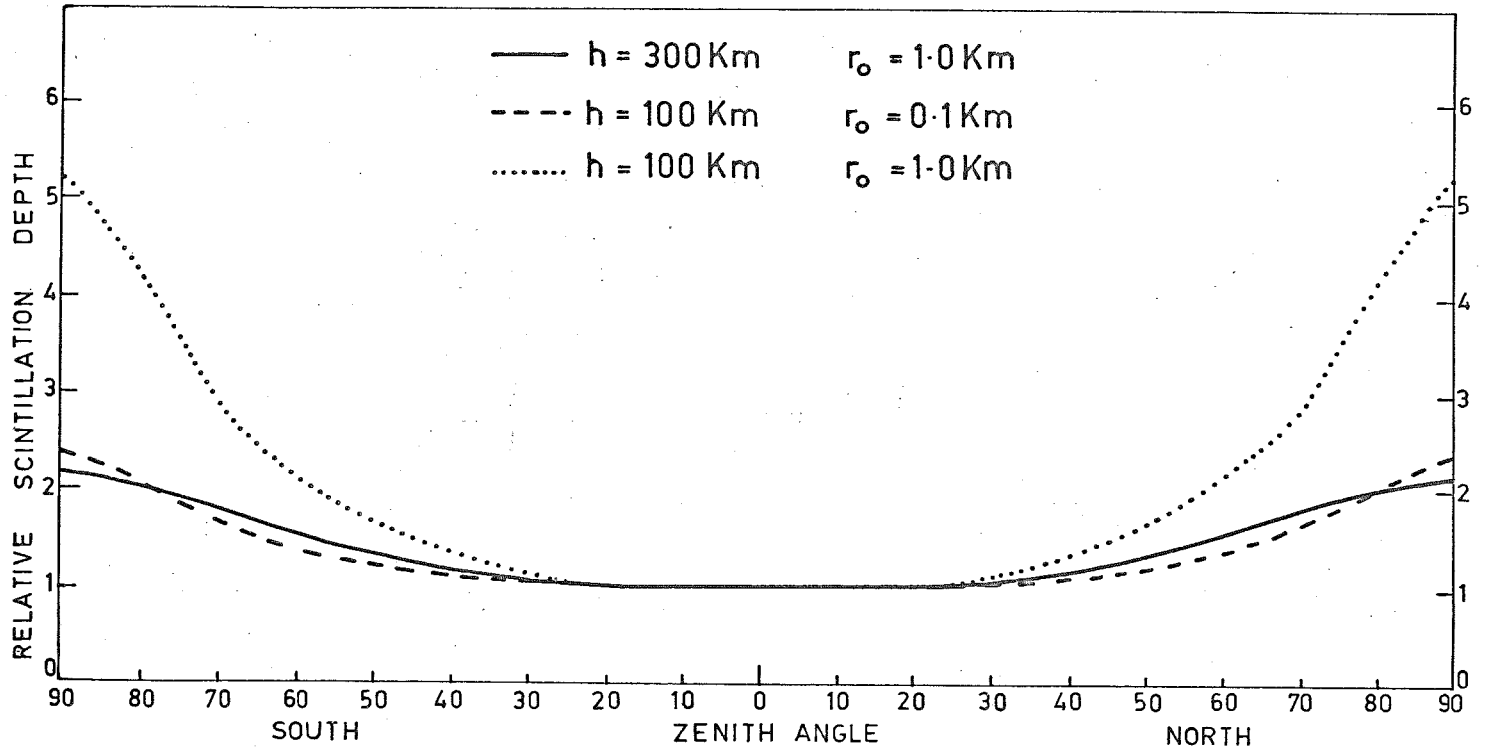

Figure 5.9 The scintillation depth, normalized to unity at the zenith, as a function of zenith angle for radio star scintillations originating from isotropic irregularities of various sizes in the E and F regions.

than 0.3km.

It should be noted that, everything else being equal, zenith angle effects should be more noticeable in E region scintillations because the layer being lower means that the angle of incidence of the radio waves on the layer will be larger for a given zenith angle, and the sec i factor in equation 5.1 will undergo a larger variation.

While it is probably true that the calculation of the zenith angle effect, assuming isotropic irregularities, is acceptable for the E layer, this is not the case for the F layer.

Briggs and Parkin calculated the zenith angle effect on scintillation depth for some special cases - none of which are applicable to the present observations. However, the required calculation is readily performed using the following equations from their paper:

$$\beta = (\alpha^2 \sin^2 \psi)^{\frac{1}{2}} \qquad (5.2)$$

where, ψ is the angle between the earth's magnetic field vector and the direction of travel of the radio wave,

α is the axial ratio of the irregularity

β is the axial ratio projected onto a plane perpendicular to the direction of travel of the radio wave,

$$\phi_0 \propto \lambda \, (\sec i)^{\frac{1}{2}} / \beta^2 \qquad (5.3)$$

where the variables have their previous meanings

$$\text{and } S = \sqrt{2}\,\phi_0 \left[1 - (\cos u_1 \cdot \cos u_2)^{\frac{1}{2}} \cdot \cos \tfrac{1}{2} (u_1 + u_2) \right]^{\frac{1}{2}} \qquad (5.4)$$

$$\text{where } u_1 = \operatorname{atan} \frac{2\lambda Z}{\pi r_0^2} \quad \text{and} \quad u_2 = \operatorname{atan} \frac{2\lambda Z}{\pi r_0^2}$$

this final expression (5.4) being an approximation valid for small ϕ_0.

Curves showing the zenith angle variation of the scintillation depth of radio star scintillations have been evaluated from equations (5.2), (5.3) and (5.4) assuming a scale size of 1 km, an axial ratio of 5:1, and a local magnetic dip angle of 67°. The angle of intersection of the signal with the diffracting layer, and the distance to the layer, are readily calculated as functions of the zenith angle using the appropriate formulas based on spherical earth geometry, but for the present case the calculations at all zenith angles were based on the same value of the magnetic dip angle - ignoring the changes in this angle as the latitude of the intersection point between the signal and the ionospheric layer varied.

Figure 5.10 shows curves drawn for a layer height of 300 km. for both isotropic and anisotropic irregularities. The isotropic curve is normalized to equal 1 at the origin and the anisotropic curve is superimposed on this in such a way that the two curves fit best where the effect of the anisotropy of the irregularities is least. The curves show that the enhancement of the scintillation index in the direction of the magnetic zenith (zenith angle = 23 degrees) is comparable with the enhancement at large zenith angles compared with the values for overhead.

Experimentally, the enhancement of the scintillation index in signals received from near the magnetic zenith is very evident in the observations of Parkin (1967) and later of Beresford (unpublished) of satellite scintillations from the same site. They found that the amplitude scintillation indices in signals from the beacon satellites are noticeably larger for signals received from a direction within 10 degrees of the magnetic zenith and, on at least some occasions, the scintillation rate also increases. As was indicated in section 5.3, in the present experiment, the Hydra A source was detected from the direction of the magnetic zenith and the observed increase in the scintillation indices of this source could be due to the presence

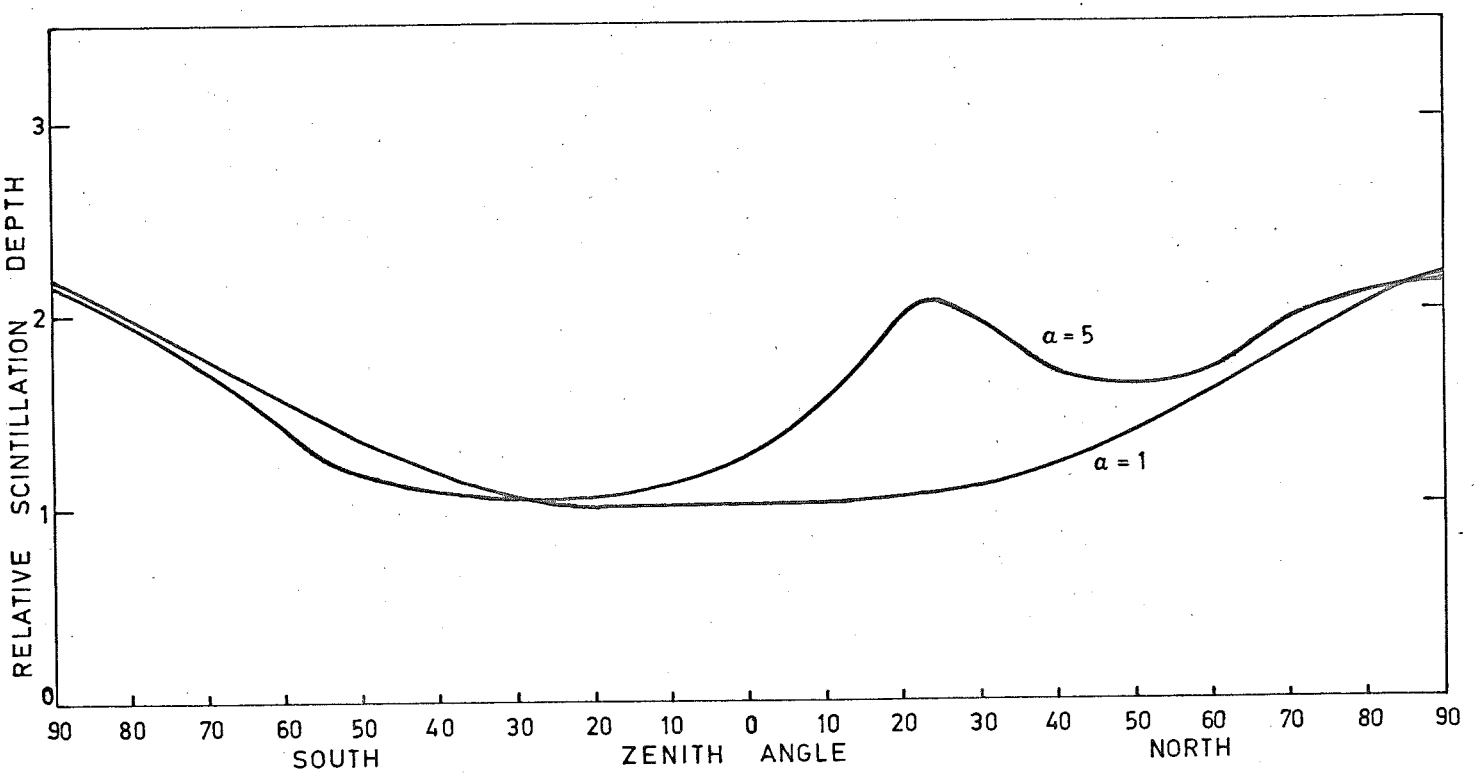

Figure 5.10 The variation of the scintillation depth of radio star scintillations with zenith angle for both isotropic and anisotropic irregularities at a height of 300 km and with scale size r_o = 1 km.

of anisotropic irregularities seen end on by the signals from this source.

The theory shows that for an irregularity layer height of 300 km and scale size of 1 km, the amplitude scintillation depth of radio star scintillations should increase by a factor of about 2 from the zenith to the horizon. The increase observed here is in fact a little larger than this (Cygnus A signals showing scintillation indices a factor of 3 larger than the sources near the zenith), but this can be explained either by the existence of irregularities of larger scale size in the same diffracting layer or due to scintillations being partly introduced to the signals in the E region, the increase in r_o or the decrease in layer height both tending to increase the importance of the zenith angle variation. It is also possible that there could be a latitude variation in the occurrence and intensity of the ionospheric irregularities but there is no evidence for this at the latitude of the St. Kilda field station (45°S geomagnetic), this latitude being well away from the transitional latitudes at the edges of the auroral and equatorial zones.

Since, from the preceding discussion, it appeared likely that the scintillation of all the radio sources could not be described in terms of the same origin (either

in the same ionospheric layer or with the same parameters applying to the one layer), no attempt was made to fit any particular theoretical curve to the zenith angle variation observations.

5.5 Zenith Angle Variations in Scintillation Activity Observed with the Smaller Interferometer

To ascertain the zenith angle variation in amplitude scintillation depth from the Cygnus A data recorded by the smaller interferometer, it is sufficient to average the scintillation indices for each maximum in the pen recorder fringes separately. Then each maximum or minimum in the output can be regarded as originating from the same source but from a different range of hour angles (each hour angle corresponding to a given zenith angle).

Since, if the Cygnus A passes containing readable amplitude scintillating indices for some, but not all, fringes were included in the analysis, the results might be influenced by random day to day fluctuations (one fringe being interfered with on a day of strong scintillation - another being interfered with on a day of weak scintillation), only those passes for which all nine fringes were observable were considered. Also, since there was a delay of 5 hours between the recording of the first and last

fringes, the diurnal variation of the scintillation indices corresponding to each fringe would (if determined) be out of phase - the phase difference between the first and last fringes being near 1/4 cycle. Therefore it was necessary to analyse data covering a full year (or multiples of a full year) and it was only because the running period of the interferometer was almost exactly 2 years that all the available complete Cygnus A passes could be included in the analysis.

Table 5.1 shows the hour angle of each fringe maximum with respect to the centre of the pass and the corresponding values of right ascension and zenith angle. The data on which the values of source zenith angles, with and without the effect of sperical refraction, are based is taken directly from Figure 4.3. The values of the right ascension of each fringe are included to emphasize the fact that each source pass was observed 7 minutes early due to a small difference in the lengths of the leads from the two antennas - this difference, once found, was left to ensure consistency in the results throughout the whole running period of the experiment.

In the table, the hour angles are quoted in hours, minutes, and decimals of a minute, the apparent right ascension in hours and minutes, and the zenith angles in degrees and decimals of a degree.

Fringe Number	1	2	3	4	5	6	7	8	9
	Before Transit				Pass Central Fringe		After Transit		
Hour Angle	2.31.3	1.52.5	1.14.2	36.5	0	36.5	1.14.2	1.52.5	2.31.3
Apparent Right Ascension	1719	1758	1836	1914	1950	2026	2104	2142	2221
Zenith Angle no Refraction	83.5	80.1	77.5	75.9	75.2	75.6	76.7	79.0	82.2
Zenith Angle with Refraction	81.0	78.1	76.0	74.6	74.0	74.2	75.3	77.2	79.9

TABLE 5.1

Since with and without the influence of spherical refraction, the change in zenith angle throughout the whole pass is small and the actual angles involved are very similar, the discussion of the zenith angle effects observed with the smaller interferometer will be restricted to considering the effects using the values of zenith angle appropriate to the source positions calculated without any modifications due to the presence of refraction.

Figure 5.11 shows the mean amplitude scintillation data plotted against a linear time scale (this figure showing the variation in scintillation depth through the pass), and Figure 5.12 shows the same data plotted against a linear zenith angle scale. It should be noted that the small asymmetry in the values of the zenith angles before and after transit has little effect on the values near the centre of the pass but at the extremes of the pass, the values are altered by up to 1^{o}; (this makes a total difference of twice this since the zenith angles of two fringes are altered - one increasing and one decreasing).

The two figures show that for scintillation of the signals from the Cygnus A source at low angles of elevation, the average scintillation depth decreases with

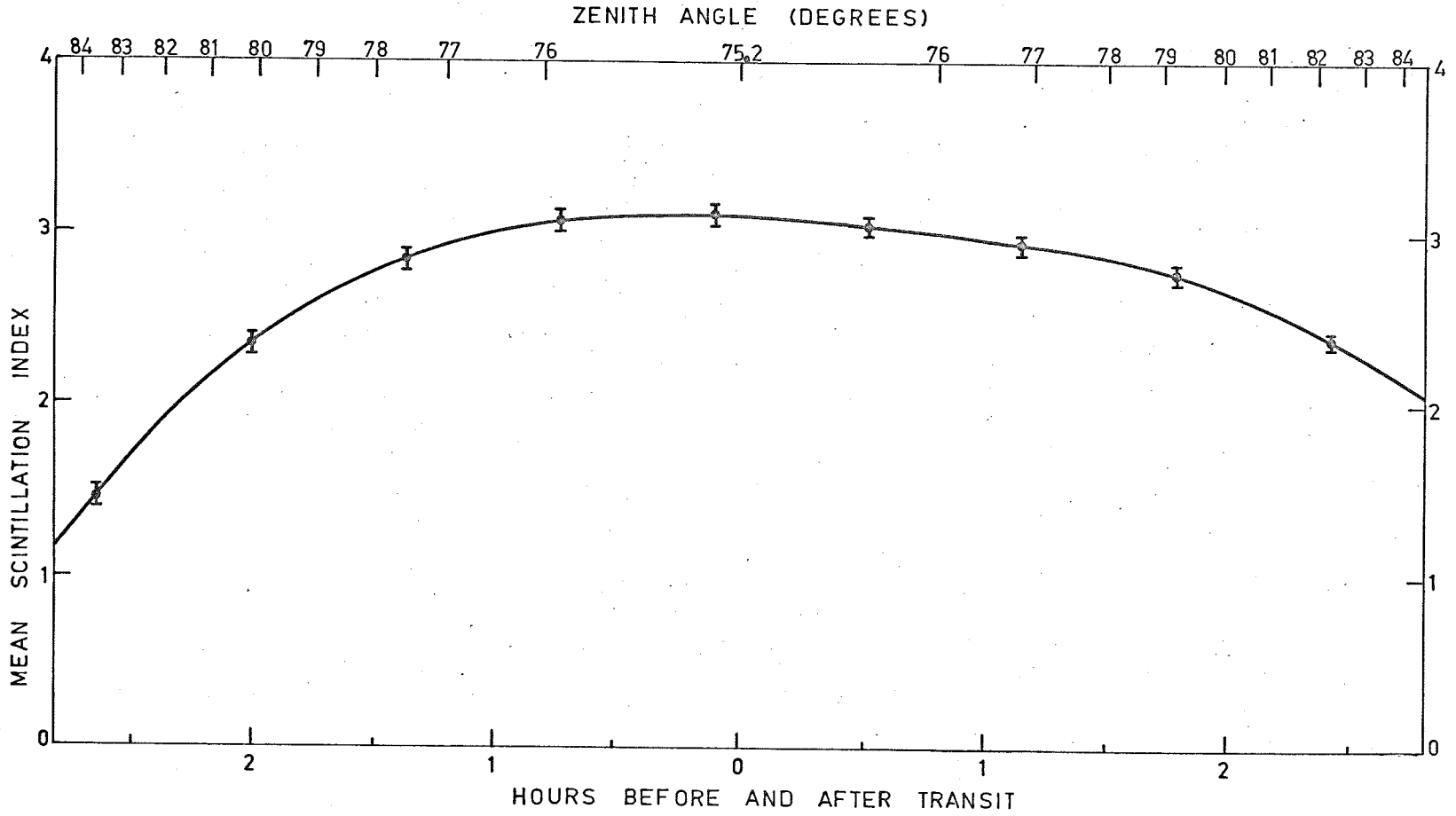

Figure 5.11 The mean amplitude scintillation indices of each fringe in the output of the smaller interferometer from the Cygnus A source plotted against a linear time scale.

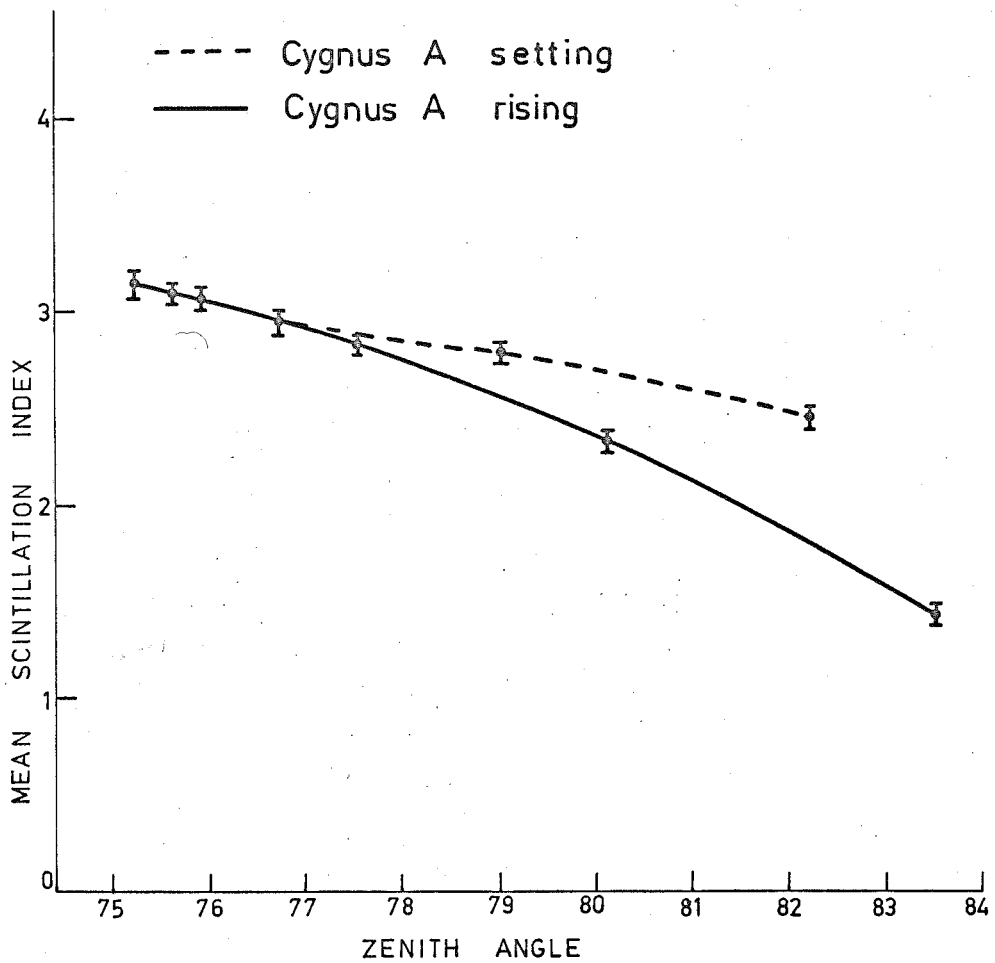

Figure 5.12 The dependence on zenith angle of the mean amplitude scintillation indices of the Cygnus A source.

increasing zenith angle. They also show that for the outer two fringes in the output from the receiver, the average amplitude scintillation indices are not the same when the source is rising as they are when it is setting. This discrepancy between the rise and set of the source would appear greater if the corrections for the whole pass being 7 minutes early were not applied.

The significance of the zenith angle curves is indicated by the error bars attached to each of the nine experimental points. Each point is calculated from 410 observations and the error bars represent the standard deviation of the mean scintillation indices. The maximum error in the nine values is $\pm$ 0.05.

5.6 Discussion of the Zenith Angle Variation Results from the Smaller Interferometer Observations

(i) The Reduction in Scintillation Index with Increasing Zenith Angle. The observed reduction of the mean amplitude scintillation depth with increasing zenith angle is not the result expected from the theory outlined in section 5.4, the expected result being that the scintillation depth should increase with increasing zenith angle probably only a little if the scintillations originate in the F region but more markedly if they originate in

the E region. Two possible explanations for the observed discrepancies that can rapidly be discarded are firstly that the reduction could be due to increased steady absorption in the D region at low angles of elevation and secondly that there could be a latitude effect in the intensity of the irregularities responsible for the scintillation. As pointed out by Castelli et al. (1964), any absorption of the signal (from an ionospheric or other origin) would affect both the total power and scintillating component, would not affect the measured scintillation index, and as pointed out in section 5.4, the presence of a latitude variation in the observation of scintillations north of the St. Kilda field station is most unlikely, the range of geomagnetic latitudes involved being 39^{o}S to 41^{o}S if the scintillations originate in the F layer.

Several authors have already reported results relevant to the present discussion, among them being Briggs (1961 and 1964), Castelli et al. (1964) and Chivers and Davies (1962). Castelli et al. observed the Cygnus A source from the Sagamore Hill Radio Observatory in Massachusetts, U.S.A. at frequencies of 63, 112, 225 MHz and found that at all these frequencies, the scintillation depth increased as the elevation of the source decreased,

and they observed the source between elevation angles of 5° and the horizon. Chivers and Davies found a similar result from observations of the same source at angles down to its lower culmination at an elevation of 4°. They observed the source from Jodrell Bank, U.K. at a frequency of 1390 MHz and were able to separate scintillations of ionospheric origin (probably E region) from those of tropospheric origin which are often observed at the same and higher frequencies. Briggs (1964) presented the Cambridge, U.K. observations of the Cassiopeia A source, made at a frequency of 38 MHz, the observations being restricted to zenith angles between 0° and 70°. He found that although there was a general increase in the observed scintillation depth with increasing zenith angle, in the years 1956-1959 (around the sun-spot maximum) there was a decrease in scintillation depth for zenith angles greater than 60°, and he explained this as a secondary effect due to the finite angular size of the source (this effect has already been referred to in the introductary section 1.2(ii) and in section 5.3). Although the angular size of the Cygnus A source (2' arc) is only half that of the Cassiopein A source and although the present observations do not involve scintillations originating in the auroral zone, the zenith angles in the present case are

larger and may compensate sufficiently for the other parameter changes which tend to reduce the effect. Further, if the mechanism is found to be feasible, it can also explain why the reduction of scintillation depth near the horizon has not been observed at higher frequencies.

From section 1.2(iii), the scintillation depth will be reduced due to the finite size of a source if:

$$2\theta > 2\pi r_0 / \phi_0 \qquad (5.5)$$

and from equation (5.3)

$$\phi_0 \propto \lambda \cdot (\sec i)^{\frac{1}{2}} / \beta^2$$

where the symbols have already been introduced except that it is worth noting again that the parameter β includes the effect of anisotropy in the observations. Calculations are readily performed for both the E and F regions of the ionosphere but for the E region the parameter β is put equal to 1. For the F region, α is assumed equal 5 in the evaluation of β.

Table 5.2 shows the parameters appropriate to the maximum elevation of the Cygnus A source (15°) and for zero elevation for both the E and F layers.

In terms of the variable parameters, the condition for which the scintillation depth should be reduced is that:

$$Z\phi_0 > \frac{2\pi r_0}{\theta_0} \qquad (5.6)$$

Zenith Angle	E Layer 100km		F Layer 300km		
	$(\sec i)^{\frac{1}{2}}$	Z km	$(\sec i)^{\frac{1}{2}}$	Z km	$\beta^2(\alpha=5)$
75°	1.71	371	1.46	929	15.9
90°	2.36	1130	1.83	1979	21.3

TABLE 5.2

From the values in the table, it is evident that the ratio,

$$(Z\phi_o)_{90^\circ} \Big/ (Z\phi_o)_{75^\circ} = 2.0 \text{ for the F region}$$

and = 4.2 for an E region with isotropic irregularities.

The difference in the values of Z appropriate to the two layers at the different elevation angles is mainly responsible for the difference in the ratios for the two regions.

From equation (5.6) for the case of irregularities in the F region with scale size r_o = 1 km, ϕ_o must be at least 10 radians at an angle of elevation of 15° and at least half this at 0° elevation before the observed scintillation depth of signals from Cygnus A will be reduced due to the

angular size of the source. Such large values are possible under disturbed magnetic conditions but would not normally be expected. For irregularities in the E region with the same scale size, ϕ_o must be at least 25 radians at an angle of elevation of 15^o and at least 6 radians at zero degrees of elevation. If the lower limit to the scale size of irregularities of 0.3 km (assigned by Briggs and Parkin (1963) to the results of Chivers and Davies (1962)) is used, the values of ϕ_o for this region are reduced to 7 and 2 radians respectively. The likely intensities of irregularities at a height of 100 km (in the E_s rather than E region) are not as well known as those at F region heights: however, as Lawrence et al. (1964) indicate, the observation by Chivers and Davies (1962) of scintillation indices 5% of the total power from the Cygnus A source indicates a root-mean-square phase deviation of 3 radians at their observing frequency of 1390 MHz, which implies a value of 53 radians at 79 MHz (106 radians at 39.5 MHz). It should be noted that, although such large values of the scintillation index were often observed, the experiment was performed in February 1959 when solar activity was still high enough for Briggs' (1964) zenith angle observations of Cassiopeia A to be affected by source size; the scintillations originated in or near the auroral zone where

the irregularities are expected to be more intense, and also, the high scintillation indices were only observed during periods of strong magnetic activity - such as did not occur during the running of the present experiment.

One point that is clear from the preceding discussion is that since from equation (5.3), ϕ_0 is directly proportional to λ, the phase deviation is reduced in a signal of a higher frequency f by a factor $^1/f$. Thus, at a higher frequency, a given degree of irregularity in the electron density will produce a smaller value of ϕ_0 and scintillations in the signals from a source of finite angular size are less likely to be reduced due to the finite angular size. This seems to be a possible explanation of why observers using higher frequencies have not detected the fall off in scintillation near the horizon detected in the present experiment.

It is also evident from section 1.2(iii) that the correlation bandwidth of the scintillations is reduced as the zenith angle increases due to both the root-mean-square phase deviation ϕ_0 and the distance to the layer Z increasing with zenith angle. The condition is that if:

$$\phi_0 > \frac{2\pi r_0 f}{\sqrt{BZC}}$$

the visibility of the scintillations will be reduced. The

variables were defined in the earlier section.

If values appropriate to the present experiment ($f = 39.5$ MHz, $B = 1.0$ MHz) are substituted into this relation, compared with the critical phase deviations required for scintillation depth reduction due to the finite angular size of the source, the values of phase deviation required here to satisfy the inequality are about 50 per cent larger for E and F layer irregularities of scale size 1 km, and about the same for the E layer irregularities of scale size 0.3 km. In a general way, the effects of scintillation bandwidth become less important at higher frequencies in the same manner as the effects due to source size from the linear dependence of ϕ_0 on λ: however, receiver parameters for the different experiments also affect the above statement and must be taken into account.

It is noted that in the present experiment, the scintillation depth has an approximately equal chance of being reduced with increasing zenith angle due to the bandwidth of the scintillations or due to the finite size of the source. The aperture of the interferometer array is also capable of causing a reduction in scintillation depth with increasing zenith angle and, if present, the effect would also be dependent on zenith angle but as

evident from section 1.2(iii), the effect depends in this case on $(\sec i)^{\frac{1}{2}}$ only (not on Z) indicating only a slight variation and is in any case expected to be overshadowed by the other criteria.

Unfortunately, there is at least one argument quite strongly against the uniform application of the inversion phenomena being invoked as an explanation for the decrease in scintillation depth with increasing zenith angle and that is that as Figures 3.5 and 3.7 show, the scintillation depth is reduced for the early and late fringes in each pass even when the maximum scintillation depth observed in the centre of the pass is very small. That these small scintillation depths in the centre of a pass do in fact indicate the presence of weak ionospheric irregularities and are not themselves the result of modification due to inversion is indicated in the following chapters dealing with the correlation of the scintillation indices with observations of sporadic-E and spread-F. However, it is probably true to say that in the case of the passes showing strong scintillation, if the root-mean-square phase deviations in the ionosphere are sufficient to cause 100 per cent scintillation at an angle of elevation of 15°, then the scintillation index should be reduced at lower angles of elevation where the root-mean-square

phase deviations are larger.

If the zenith angle observations are analysed in more detail by grouping them according to the three hour time zone in which the observation of the central fringe was made, then the statistics of the results are not as good because only an average of 25 values are used for each experimental point, but the analysis does show that for some time zones the maximum scintillation depth is not observed in the centre of the pass. However, there are still no occasions for which the scintillation depths of the first and last fringes are greater than the values for the centre fringes and the results found for a given time of observation in 1964 are generally not reproduced in the results for the same time of observation in 1965. Figure 5.13 and 5.14 show the zenith angle observations of the Cygnus A source grouped according to the three hour local time zone in which the observation was made for the years 1964 and 1965 respectively. The standard error of each mean is too small to plot on the graphs (maximum standard error $\pm$ 0.20), but in most cases the occurrence of a maximum elsewhere but in the centre of the pass cannot be regarded as statistically significant. Some differences in the observed zenith angle behaviour of scintillation depths observed at night time and day time might have been expected from the difference in the

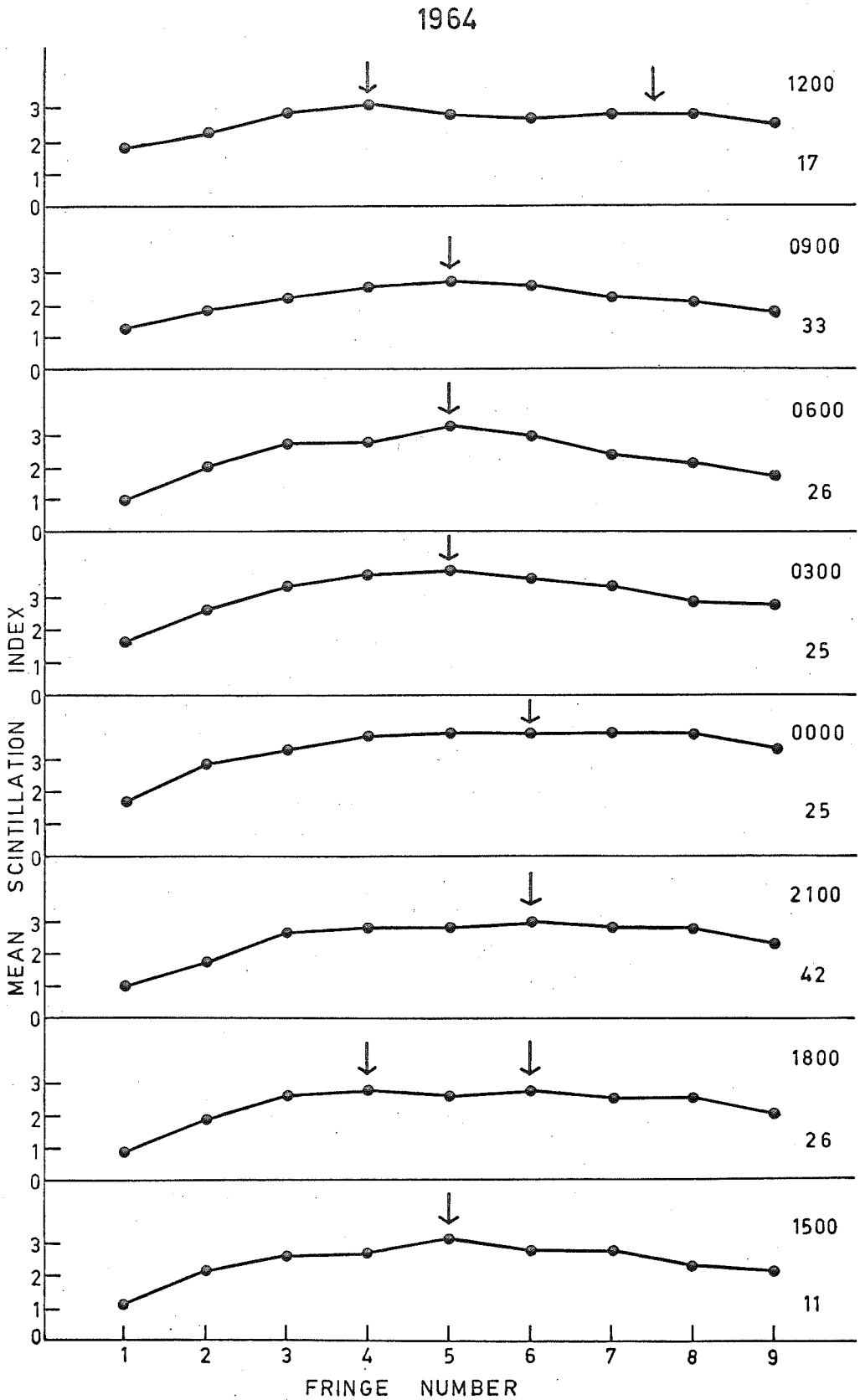

Figure 5.13 Zenith angle variations 1964.
The local time and number of values used for each graph are indicated and the maxima marked with arrows.

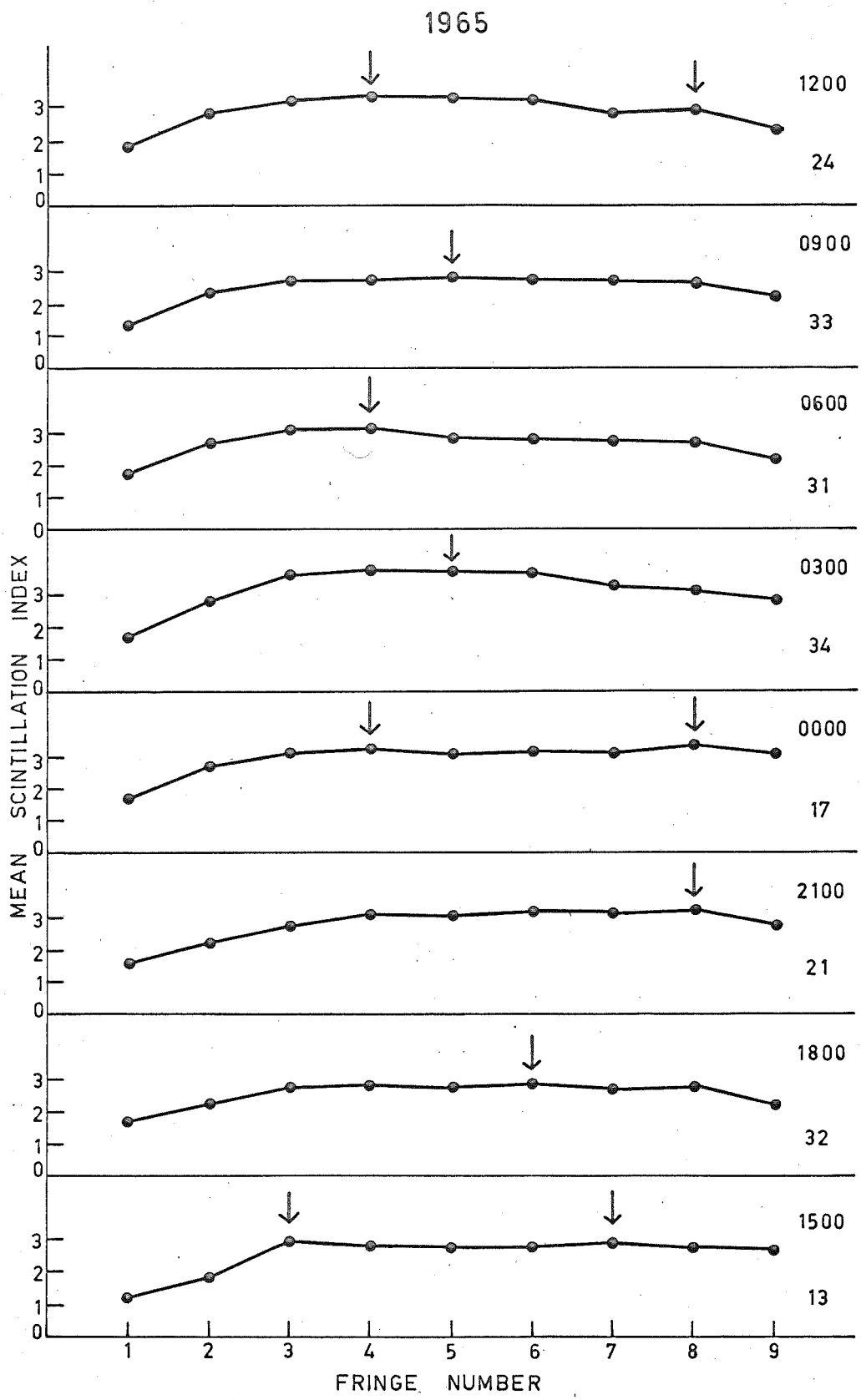

Figure 5.14 Zenith angle variations 1965.
The local time and number of values used for each graph are indicated and the maxima marked with arrows.

relative importance of the E and F region irregularities at these times and from the different behaviour of the parameters of the two layers determining the increase in scintillation depth with zenith angle or the possible decrease with zenith angle if inversion is important. No difference between the day time and night time behaviour was found.

The conclusion is that a significant reduction in the scintillation depth observed at very low angles of elevation is found from analysis of the records of the smaller interferometer. An inversion effect, dependent on the finite angular size of the source or on the scintillation bandwidth, is suggested as a possible explanation but does not explain the presence of this observed reduction in the case of records showing only weak scintillation.

(ii) The Asymmetric Values of Scintillation Index for the Rising and Setting of the Cygnus A Source. From Figure 5.12 it is evident that, as well as the unexpected reduction in scintillation depth with increasing zenith angle, for zenith angles greater than 77° (i.e. half each transit on a linear time scale), the average scintillation indices at a given zenith

angle while the source is rising are significantly smaller than the average scintillation indices at the same zenith angle while the source is setting. This asymmetry in the scintillation indices before and after transit is noticeable on the record dated 3/4/64 in Figure 3.5 and on the record dated 9/9/64 in Figure 3.7.

Differences in the scintillations observed during the rising and setting of the Cygnus A source have previously been observed by Castelli et al. (1964) who found that they could explain their observations in terms of the larger dip angle of the region of the ionosphere traversed by the radio signals as the source rose, causing these signals to show stronger and faster scintillations than did the signals from the setting source. As the source rose, its signals passed through the centre of the auroral zone; this was not the case when the source set. Little et al. (1962), observing from Alaska, also noticed differences in the degree of scintillation activity for the Cygnus A source before and after lower culmination - the increased scintillation depths observed after lower culmination being explained in terms of the higher geomagnetic latitude of the intersection with the F layer of the line of sight to the source. They observed the source Cygnus A down to elevation angles of 10^{o} at frequencies of

223 and 456 MHz. The zenith angle behaviour of the scintillation indices of the Cassiopeia A source was opposite in sense to that of the Cygnus A source and they suggested that this occurred as a result of the larger angular size of the Cassiopeia A source.

In the present experiment, the Cygnus A source is detected at low angles of elevation north of Adelaide and table 5.3 gives the geomagnetic latitudes of the intersection points of the signals from the source with the E and F layer heights. The terms "rise" and "set" actually refer to the source positions $2\frac{1}{2}$ hours before and after transit, the source zenith angle then being 83° and corresponds to the largest zenith angle for which results have been obtained.

Layer	Rise	Transit	Set
E(100 km)	$-39^{\circ}\ 10'$	$-41^{\circ}\ 22'$	$-39^{\circ}\ 56'$
F(300 km)	$-32^{\circ}\ 50'$	$-36^{\circ}\ 21'$	$-34^{\circ}\ 20'$

Table 5.3

The different values for rise and set of the source arise because at Adelaide, geomagnetic north is 7° east of the geographic north.

It is evident from the table that the signals from the setting source intersect the E or F region at a more southern geomagnetic latitude than do the signals from the rising source. However the difference is so small (46' arc in the E region, 1° 30' arc in the F region), and the general ionospheric region so far from the auroral or equatorial zones that (as has been stated before) what amounts to a geomagnetic latitude effect is most unlikely to be the required explanation.

Another possible mechanism which can give rise to the observed asymmetry in the scintillation indices before and after transit, arising from the fact that the direction of magnetic north is not the same as the direction of geographic north, is that if the ionospheric irregularities are anisotropic, as indeed they are in the F region (but probably not in the E region), then the signals from the radio source will see the irregularities in a different aspect before and after transit. However, if this mechanism was important, the signals would see the irregularities more nearly "end on" before rather than after transit and the scintillation indices would be greater before the transit of the source. As Figure 5.12 shows that the opposite is observed here, the mechanism can only be regarded as a possibility if the very disturbed conditions required for

inversion to be important are considered a regular occurrence. In this case, the observed result can be explained from the above arguments, but in most cases they cannot be effective as in the next chapter it is shown that weak scintillations really do indicate weak irregularities.

Apart from considerations of the earth's magnetic field, there do not appear to be any other factors present which could produce the asymmetry in the scintillation depth observed between the source rising and setting.

CHAPTER 6. CORRELATIONS BETWEEN THE AMPLITUDE SCINTILLATION INDICES AND OTHER GEOPHYSICAL PHENOMENA

6.1 The Woomera Ionosonde and its Position Relative to the St. Kilda Based Scintillation Observations

Correlation analyses were performed to investigate the possible relationships between the amplitude scintillation indices recorded at St. Kilda using both interferometers and the various indices describing the behaviour of spread-F, sporadic-E, critical frequency $f_o F_2$, and the planetary magnetic indices Kp. Only instantaneous associations were sought between the scintillation and ionospheric indices but it was still considered desirable to evaluate the appropriate correlation functions for a small number of time shifts to demonstrate that any instantaneous correlations observed were in fact genuine. In the case of the Kp indices, correlation functions were evaluated for several days shift in the data to investigate the possibility of a magnetic disturbance preceding an ionospheric disturbance. This point has already been discussed in Section 1.4(v).

The ionospheric data for comparison with the amplitude scintillation indices of the Cygnus A source observed with the smaller interferometer were all obtained from the

records of the Woomera ionosonde situated at latitude 30.8°S, longitude 136.3°E - some 491 kilometres from the St. Kilda field station and at a bearing of 26° 26' west of north.

Figure 6.1 shows the geographic locus of the point of intersection of the line of sight from the receiving antennas at St. Kilda to the Cygnus A source with the 100 km E layer height and with the 300 kmF layer height. The individual points on the graphs represent one hour intervals before and after source transit and the Cygnus A source is at an altitude of 10° when the E layer intersection point of the line of sight to the source is nearest to the Woomera ionosonde. The Figure is based on a zenithal equiangle projection with the pole situated at latitude 36°S, longitude 135°E. The position of the pole is indicated in the Figure. This projection has the properties that azimuth angles around the pole are preserved as are radial distances from the pole. Although the St. Kilda receiving site is 330 km (3°) from the pole of the projection, the points on the Figure are plotted relative to St. Kilda assuming that the special properties of the pole are still satisfied about this point. Since none of the following results depend on the accuracy of the points plotted, any errors introduced due to the St. Kilda

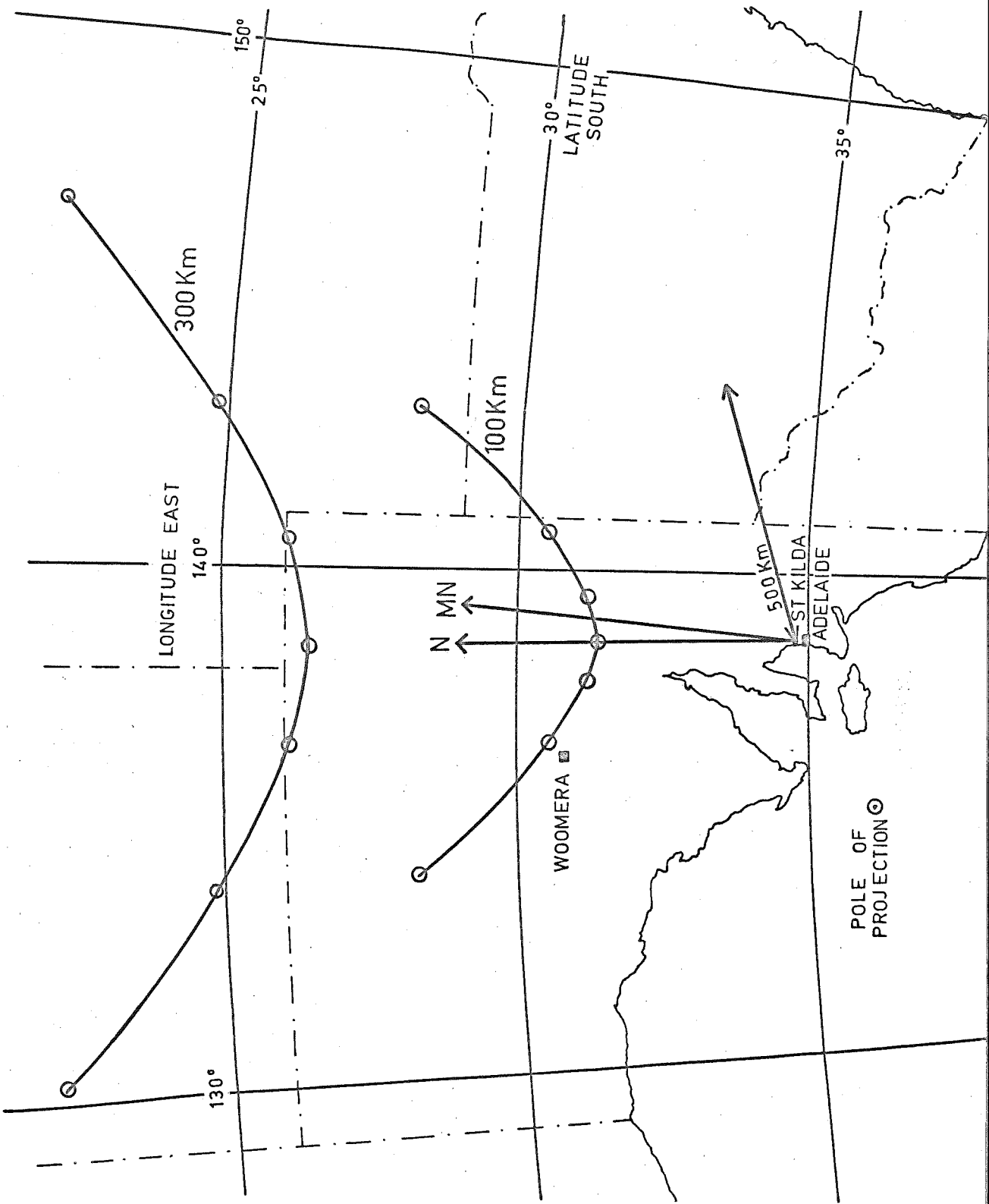

Figure 6.1 A map showing the relative positions of the St. Kilda observing site and the Woomera ionosonde. The loci of the intersection points in the ionosphere of the signals from Cygnus A to the observing point are shown for layer heights of 100 and 300 km.
The directions of geographic and magnetic north are indicated.

receiving site not coinciding with the pole of the projection will not be important.

Table 6.1 shows the great circle distances between the Woomera ionosonde and the points on the ground beneath the intersections with the E and F layers of the line of sight from St. Kilda to the Cygnus A source. The distances are calculated for the source position as it transits the St. Kilda meridian and for the source position 2 hours after transit.

Distance km	Source Position At Transit	Source Position At Transit + 2 Hours
E Layer Intersection	189	56
F Layer Intersection	769	738

TABLE 6.1

It is evident that 2 hours after the Cygnus A source transit, the amplitude scintillation indices of this source are particularly well suited to a correlation analysis with the Woomera sporadic-E observations. In the case of the F layer intersection point, the distance from the Woomera ionosonde is similar for the two positions of the source and from Figure 6.1 it is seen that for both positions, the difference in latitude is about twice the difference in longitude. This distance from the

Woomera ionosonde to the F layer intersection is in fact rather larger than is desirable for the correlation analysis; to quote one example, Lawrence, Jesperson and Lamb (1961) who summarized the results of several authors, suggested that patches of irregularities responsible for spread-F occur over regions of about 500 km in lateral extent. In more detail Briggs (1958), in a study of spread-F occurrence and correlation at widely spaced observing sites in the northern mid-latitude region, found that the irregularities occurred in patches of extent 500 km north-south and of a larger extent east-west. Koster (1958), from a correlation analysis between radio star scintillation and spread-F in the equatorial zone, confirmed the above result with his observation of a positive correlation between the two phenomena with an east-west distance of 450 km between the two regions of the ionosphere observed by the radio star receiver and the ionosonde. Although the large distance involved in the present experiment is undoubtedly sufficient to reduce the correlation between scintillation and spread-F, the correlation should not be completely removed if the results found by the previous authors are valid for the mid-latitude region north of the St. Kilda observing site.

The ionospheric data for comparison with the amplitude scintillation indices of the various sources observed with

the larger interferometer were obtained partly from the records of the Woomera ionosonde (spread-F and $f_o F_2$) and partly from the records of the Salisbury ionosonde (sporadic-E). The Salisbury ionosonde is situated at latitude 34.7°S, longitude 138.6°E and these co-ordinates are the same as those for the two interferometers within the accuracy of the above figures.

Table 6.2 shows, for all the sources, the great circle distances between the appropriate ionosonde and the points on the ground beneath the intersections with the E and F layers of the line of sight from St. Kilda to the sources. The distances are calculated for the source position as it transits the St. Kilda meridian.

Source	E Layer Intersection (km) Salisbury Ionosonde	F Layer Intersection (km) Woomera Ionosonde
Fornax A	6	558
Centaurus A	13	515
Pictor A	28	500
Hydra A	43	380
Hercules A	82	294
Virgo A	107	248
Taurus A	145	222
3C 123	196	245
Cygnus A	371	769

TABLE 6.2

Remarks similar to those already made for the distances involved in the correlations of the smaller interferometer data also apply to the correlations of the larger interferometer data. From Table 6.2, it should be noted that the distances involved with the spread-F correlations are now all smaller than in Table 6.1: which ionosonde is better suited to the sporadic-E correlation depends on the source which is being observed.

6.2 The Suitability of the Woomera Ionograms

On most occasions, the Woomera ionograms are recorded at 1 hour intervals although there have been some periods when recording has been more frequent. Since each scintillation index refers to a 30 minute period of observation of the Cygnus A source, the hourly ionogram nearest in time to a scintillation observation will not refer to a time differing by more than 15 minutes from the time of the scintillation observation and in many cases, especially with regard to F region phenomena, this is an acceptable time difference. However, it was evident that the appearance and intensity of sporadic-E often changed considerably with a time scale of much less than an hour and on fewer occasions, changes in spread-F from one ionogram to the next were observed - the changes not being consistent with

the diurnal behaviour of the phenomenon. In particular, on June 7th 1964, the 6 ionograms covering the period of the Cygnus A pass from 00 to 05 hours (local time) alternately showed complete spread-F and no spread-F. This was an extreme case but there were others showing behaviour a little less anomalous which suggested that there might be some occasions when spread-F was present and not detected on the ionograms and perhaps other occasions when it was detected but did not persist in the time interval between the recording times of the ionograms. However, either possibility is unlikely to affect the period covered by more than two ionograms and when the spread-F and sporadic-E indices were being assigned, the above considerations were borne in mind and it was always evident from the series of ionograms during the whole Cygnus A pass whether or not the readings from the ionogram used for the correlation analysis were reliable.

Thus, although it is still probable that, due to time differences of up to 15 minutes between the scintillation and ionogram observations, any correlations observed might be less than those actually present, such reductions in correlation coefficients should not be serious.

6.3 The Ionospheric and Magnetic Indices

As stated very briefly in Section 6.1, the amplitude

scintillation intensity was correlated with the intensity of spread-F, the critical frequency of the sporadic-E layer, the critical frequency $f_o F_2$ of the F layer and the planetary magnetic indices Kp.

In the case of the critical frequency $f_o F_2$, it was considered unnecessary to read the ionograms themselves and the values (correct to the nearest 0.1 MHz) were taken from the appropriate data bulletins for Woomera published by the Weapons Research Establishment, Salisbury, South Australia. However, it was necessary to read the ionograms to obtain the required details of the occurrence of sporadic-E and spread-F. The index used to describe the intensity of sporadic-E was the maximum frequency (also correct to the nearest 0.1 MHz) at which a reflection from the layer was observed - this corresponding to the critical frequency of the extraordinary ray. An index in the range 0 - 3 was visually assigned to each ionogram to describe spread-F activity of increasing intensity, this being the scale originally described by Briggs (1958).

For the correlation analysis of the scintillation indices taken from the records of the larger interferometer with sporadic-E, hourly values of $f_o E_s$ were read directly from the data bulletins for Salisbury, also published by the Weapons Research Establishment, Salisbury, South Australia.

In the initial stages of the analysis, an attempt was made to obtain spread-F indices directly from the Woomera data bulletins by utilizing the qualifying letters F, UF and occasionally UUF which were applied to the tabled values of $f_o F_2$ according to the difficulty of reading these values from an ionogram in the presence of spread-F. However, comparison of these qualifying letters (or their absence if there was no difficulty in reading $f_o F_2$) showed that their application was most inconsistent and that they were very unreliable as parameters describing the intensity (or even simply the occurrence or non-occurrence) of spread-F.

An examination of the ionograms recorded over the 2 year period of the experiment showed that some care is required in the interpretation of the correlation coefficients found between scintillation and spread-F or sporadic-E due to the temporal behaviour of these phenomena. In the case of sporadic-E, the combined annual and diurnal variations in its occurrence (in any form) are such that the phenomenon occurs most strongly during the daytime in summer and least strongly at night time in winter, and in the case of spread-F, its temporal variation is predominantly diurnal and it occurs most strongly at night and rarely during the day. Thus sporadic-E is the more common phenomenon during the day time passes of the Cygnus A source and spread-F the

more common during the night time passes. Special care must be taken in the interpretation of the correlation coefficients involving sporadic-E occurrence at night and involving spread-F during the day as these phenomena may never occur at these times throughout the period referred to by the correlation coefficient and this could lead to a spurious or incalculable correlation. A related difficulty was encountered by Koster (1958) when he found that the occurrence of both spread-F and radio star scintillations at the equator near the maximum of the solar activity cycle "became so nearly continuous as to make the correlation coefficient virtually meaningless."

Details of the effects of complete occurrence or non-occurrence of sporadic-E or spread-F on the present results are given in Section 6.7 following the presentation of the results.

The spread-F observed from Woomera over the period 1964 - 1965 was invariably of the frequency spreading type which has been distinguished from the range spreading type by Singleton (1957). The observed sporadic-E took many forms; some of these separate forms are discussed in Chapter 7 but are not distinguished between in the present analysis.

The indices used in the correlation analysis to describe magnetic activity were taken from the Journal of

Geophysical Research - the two 3 hour planetary Kp indices recorded nearest in time each day to the Cygnus A transit being averaged to provide the required index. The 9½ hour time difference between Universal Time and local time was taken into account. The 2 year period of the experiment was not a magnetically active one and the highest value of Kp observed during a Cygnus A pass was 5 - this index being observed on not more than 10 occasions.

6.4 Calculation of the Correlation Coefficients

As in the case of the investigation (described in Section 5.2) of the diurnal and seasonal variations of the Cygnus A source scintillation recorded by the smaller interferometer, the available data from the two years of observation were divided into periods of 6 weeks, each period representing a 3 hour span in local time. For the purpose of the present analysis, this was a length of data which represented a compromise between a length short enough to give a good resolution in local time, and a length long enough to enable significant correlation coefficients to be obtained. Since each set of data represented only 6 weeks or 3 hours - a small fraction of the year or day, it was considered unlikely that common diurnal or seasonal trends should be present in the data used for each coefficient strongly enough to give rise to a spurious value of

the correlation coefficient. It was possible to ascertain that there was no such influence present in the instantaneous coefficients from a comparison with the values of the coefficients calculated for a 1 day advance or retardation of one of the sets of data being correlated - these coefficients having values similar to the instantaneous coefficients if variations were present in the data with periods comparable with the total length of the data.

Various longer and shorter lengths of data were used in the correlation analysis of the larger interferometer scintillation indices with the ionospheric and magnetic indices and in the correlation analysis of the smaller interferometer scintillation indices with the magnetic indices. The above precautions were taken to ensure the correct interpretation of the results.

The subject of the use of correlation coefficients and the application of statistical significance tests to them has been well covered inthe literature, therefore the following discussion on the calculation of the correlation coefficient and that in the next sections on the application of statistical tests is limited to those points which have particular application to the present analysis.

The correlation coefficients are readily calculated on a computer using the equation:

$$\rho = \frac{\sum_i x_i y_i - \sum_i x_i \sum_i y_i / N}{\sqrt{\left\{ \left(\sum_i x_i^2 - \frac{\sum_i x_i \sum_i x_i}{N} \right) \cdot \left(\sum_i y_i^2 - \frac{\sum_i y_i \sum_i y_i}{N} \right) \right\}}} \qquad (6.1)$$

where x and y are the two variables being correlated and N is the total number of members in each variable array. The coefficient may take extreme values of ± 1 indicating perfect correlation or perfect anticorrelation and may take any other value intermediate between these extremes.

The value of the coefficient is not dependent on the choice of origin of either variable but it is evident that in equation 6.1, the denominator becomes zero if either variable has the same value for all i (i.e. has zero variance) and the coefficient is then meaningless.

The computer program used to calculate the correlation coefficients was originally written by I. A. Parkin and it calculates correlation functions using a corrected sums technique such that for each shift of one set of data with respect to the other, only the cross product term of the correlation coefficient has to be completely evaluated - minor modifications to the other terms being sufficient to evaluate them exactly once their values for zero shift have been computed. The method is very rapid

and involves no approximations. A particular feature of the program (and in this respect it appears to differ from the library programs available locally), is its ability to take into account any missing values in the sets of data used in the analysis. Since the original version of the program was written, many modifications have been made both with regard to streamlining the calculation and with regard to the addition of new facilities such as a variable input data format, an optional plotting of the output, and a large range of non-fatal diagnostics which assist in the location of otherwise fatal errors in the data, and allow computation to proceed on subsequent correct sets of data.

At various times, the program has been run on a wide range of I.B.M. and C.D.C. computers - the choice of machine depending largely on its availability at the time. The maximum rate of calculation attainable is of the order of 30 coefficients per second when the data is of intermediate length (about 100 points in each set of data), and is attained when the program is run on the University of Adelaide's C.D.C. 6400.

6.5 Statistical Significance Tests on the Correlation Coefficients

It was indicated in the previous section that the

correlation coefficient was restricted to the finite range of values between -1 and +1 and from this it is obvious that it cannot have a Normal Distribution and any "standard error" in the coefficient cannot be interpreted in the usual way. However, if the value of N is sufficiently large and the value of ρ sufficiently small, the distribution of ρ is approximately Normal and its standard error may be estimated from the equation:

$$\text{Standard Error of } \rho = \frac{1 - \rho^2}{\sqrt{N}} \qquad (6.2)$$

Since the value of N should be at least 100 before this estimate of the standard error should be applied, it was not used in the present analysis.

It was decided that Fisher's test supplied the most reliable estimate of the statistical significance of the present results. A new variable Z is defined in terms of the correlation coefficient ρ by the equation:

$$Z = \frac{1}{2} \log_e \left(\frac{1 + \rho}{1 - \rho} \right) \qquad (6.3)$$

The variable Z may take any value between plus and minus infinity and is distributed with a standard error given by the equation:

$$\text{Standard Error of } Z = \frac{1}{\sqrt{N - 3}} \qquad (6.4)$$

The procedure followed to establish the confidence limits of a given value of ρ is to take the appropriate values of ρ and N, and from them calculate the equivalent values of Z and its standard deviation. Equation (6.3) may be transposed such that ρ is expressed in terms of Z.

$$\text{Thus } \rho = \frac{\exp(2Z) - 1}{\exp(2Z) + 1} \qquad (6.5)$$

and the values of ρ are then calculated which are equivalent to the initial Z value plus or minus the desired multiple of its standard deviation.

In the estimates of statistical significance outlined in the appropriate sections later in this chapter, the values of ρ are calculated which differ from zero by 1, 2, or 3 standard deviations, using the method outlined above. These significance levels correspond to probabilities of 32%, 4.5% and 0.3% respectively that the given correlation coefficient should be observed by chance.

A further important point which has not yet been emphasised here and which must be considered is that the values of N used in the calculation of the standard errors of ρ and Z refer to the number of <u>independent</u> data points

used in the evaluation of the cross-correlation coefficients. In the case of most geophysical parameters, each daily value (such as used here) may not be independent of the values of the same parameter on the preceding or following day. To give an example, if it is found that only half the indices used to calculate a correlation function are independent, then the effective value of N as far as the statistics are concerned is only half the actual N. In the present analysis, an estimate of the ionosphere memory in relation to scintillation, spread-F, sporadic-E and $f_o F_2$ can be obtained from the width of the peak of the appropriate auto-correlation function. It should be noted that the cross-correlation functions can also indicate that ionospheric memory is important but do not in themselves indicate whether it is significant in only one or in both parameters used to evaluate the function. Physically, broad peaks in the correlation functions (indicating an ionospheric memory) will arise if any of the parameters tend to occur in groups of days and then tend not to occur in similar groups of days.

The correlation program described in Section 6.4 indicated when the correlation coefficients exceeded the significance levels determined from the addition of 1, 2 and 3 standard deviations in Z, but this result from the

program could not necessarily be taken at face value due to the uncertainty, for the reason outlined above, in deciding the correct value of N to be used.

6.6 The Correlation of Scintillation with Sporadic-E, Spread-F and $f_o F_2$- Smaller Interferometer Results

As discussed in Section 6.4, values of scintillation indices were correlated with hourly values of the ionospheric parameters - each length of data used in the analysis representing 6 weeks of elapsed time or a 3 hour period of local time. The hourly values used all referred to a local time 2 hours after the transit time of the Cygnus A source since, as stated in Section 6.2, this meant that the distance was least between the regions of the ionosphere responsible for the recording of the sporadic-E and scintillation data. Correlation functions were evaluated between all pairs of parameters for all local times, the number of shifts in the functions (4) being sufficient to distinguish between correlations due to simultaneous occurrence of the parameters and correlations due to the presence of long term variations common to two or more of the parameters.

Table 6.3 shows the instantaneous correlation coefficients between the scintillation indices, the sporadic-E maximum frequencies and the spread-F indices, and Figures 6.2, 6.3 and 6.4 show some of the correlation functions for which

Local Time (Hrs)	Scintillation Sporadic-E		Scintillation Spread-F		Spread-F Sporadic-E	
	1964	1965	1964	1965	1964	1965
0000	0.44	0.03	0.50	0.40	0.21	0.05
0300	0.20	0.30	0.48	0.23	0.22	0.07
0600	0.26	-0.05	0.06	0.26	-0.23	0.00
0900	0.08	0.22	0.44	0.34	-0.05	0.26
1200	0.28	0.42	0.06	0.28	-0.15	0.07
1500	0.51	X	0.08	X	0.20	X
1800	0.12	0.24	-	0.28	-	-0.05
2100	0.42	0.23	0.63	0.40	0.20	0.07

TABLE 6.3

The correlation coefficients between the Cygnus A scintillation indices, the spread-F indices and the sporadic-E maximum frequency.

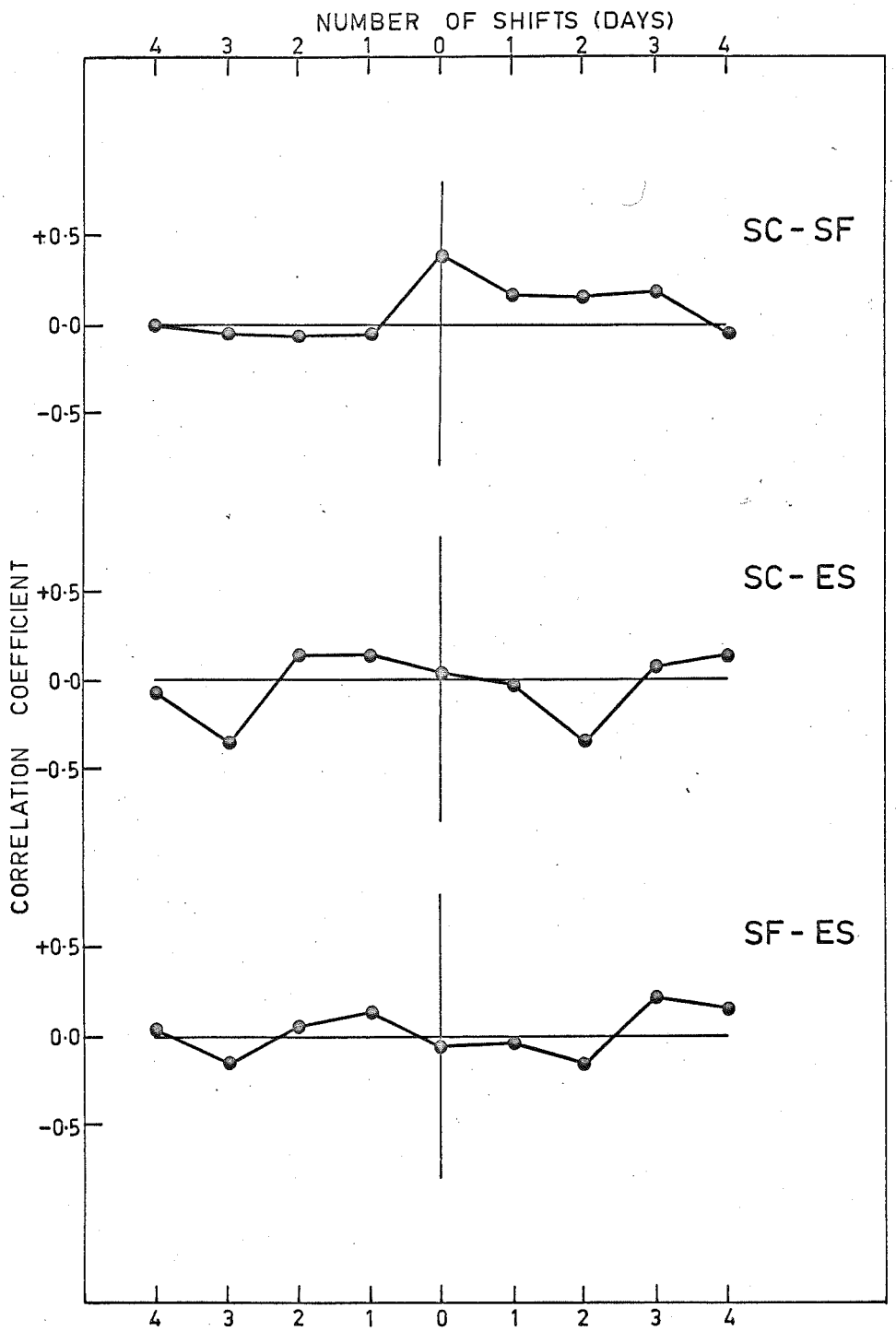

Figure 6.2 Correlation functions for 0000 hours 1965 between scintillation, sporadic-E and spread-F. They show a positive correlation between scintillation and spread-F but otherwise no correlation between the parameters.

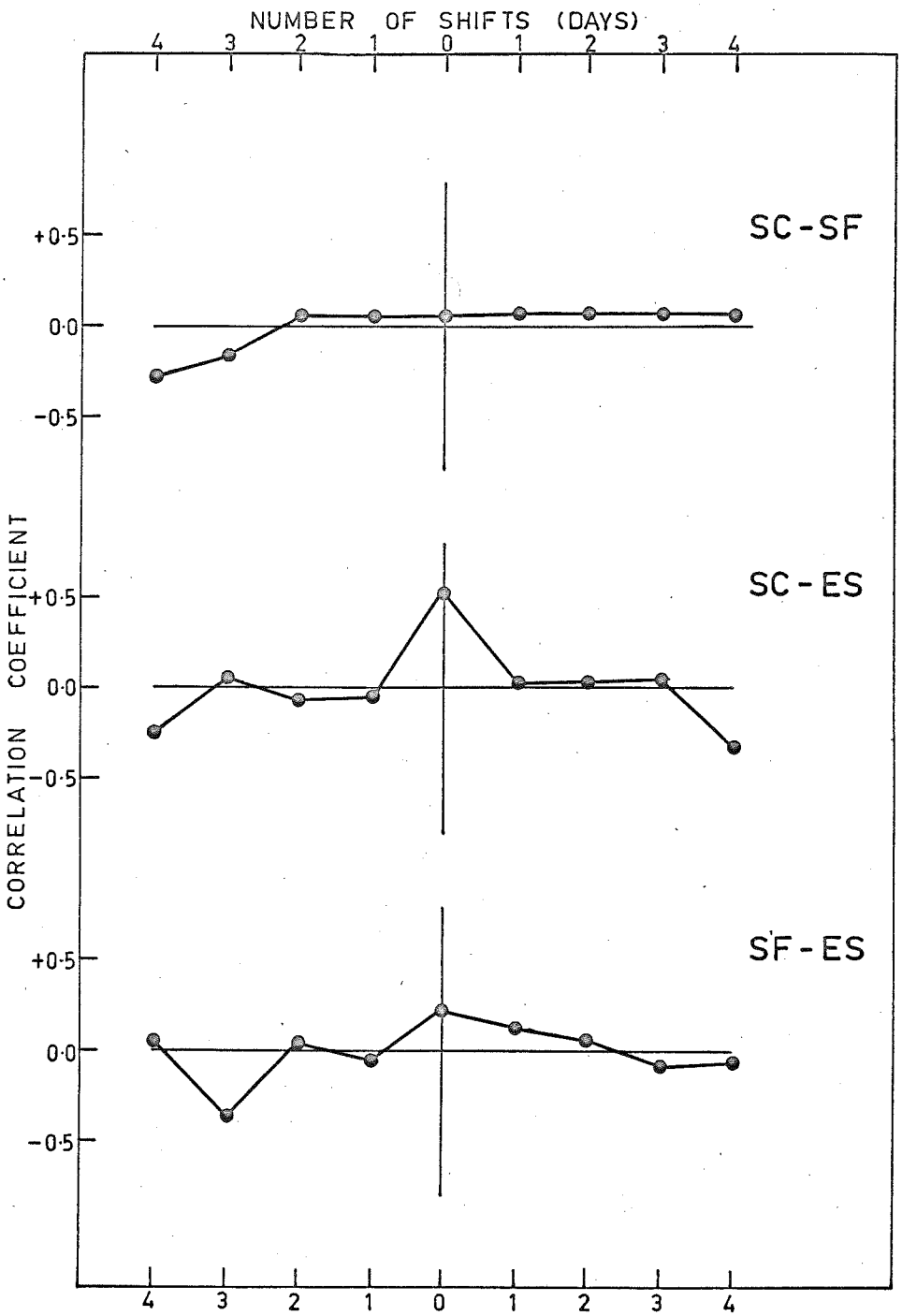

Figure 6.3 Correlation functions for 1500 hours 1964 between scintillation, sporadic-E, and spread-F.
They show a positive correlation between scintillation and sporadic E but otherwise no correlation between the parameters.

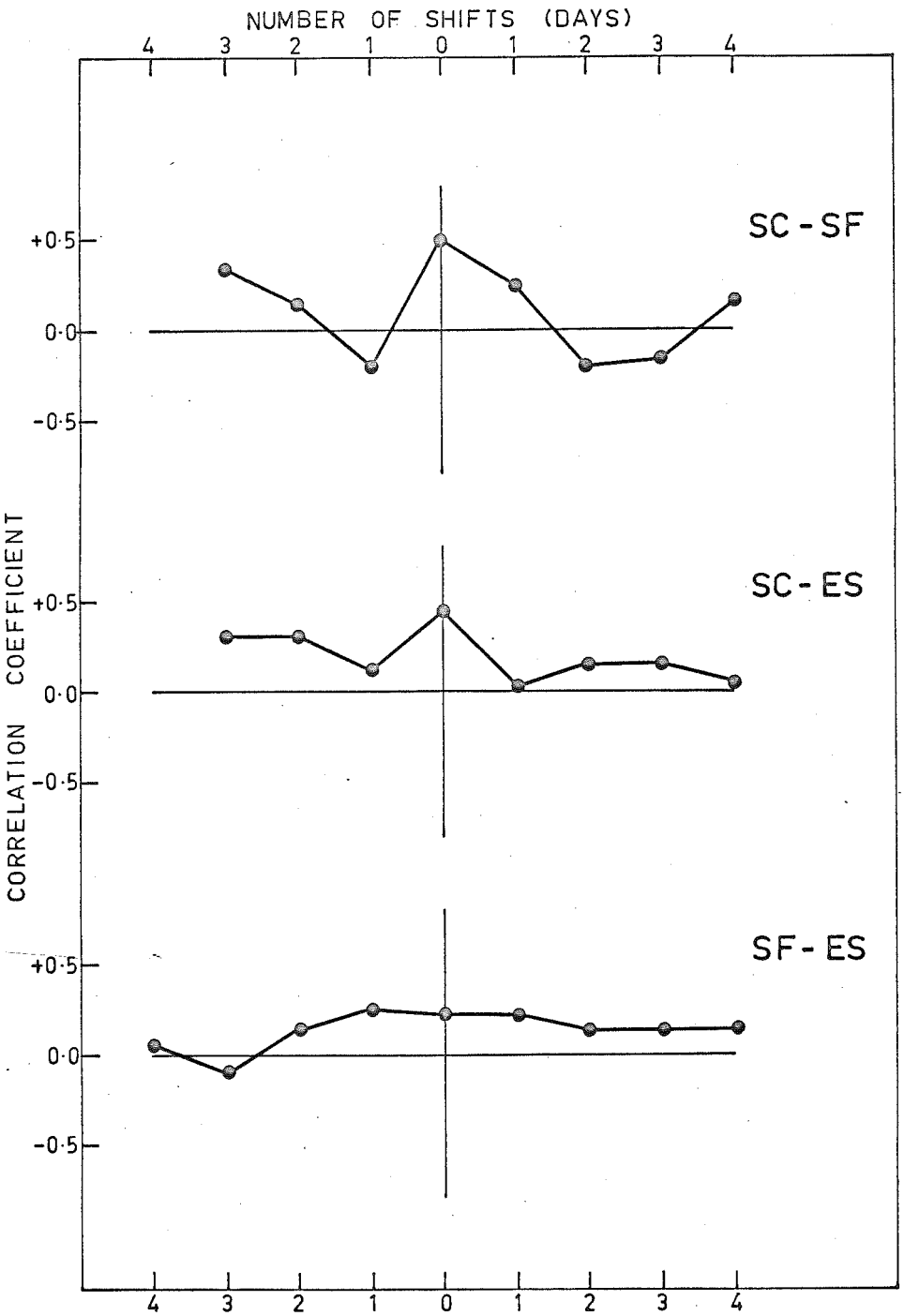

Figure 6.4 Correlation functions for 0000 hours between scintillation sporadic-E and spread-F showing strong positive correlation between scintillation and both sporadic-E and spread-F and a small "long term" correlation between sporadic-E and spread-F.

only the coefficient for zero shift is included in Table 6.3. The Figures show examples of significant correlation of scintillation with spread-F and not with sporadic-E and vice-versa. An example is also shown of a significant correlation of scintillation with both spread-F and sporadic-E.

Table 6.4 shows the instantaneous correlation coefficients between the scintillation indices, the spread-F indices, and $f_o F_2$ and Figures 6.5 and 6.6 show some of the associated correlation functions which illustrate the positive correlation observed between scintillation and spread-F, the negative correlation between spread-F and $f_o F_2$, and the absence of correlation between scintillation and $f_o F_2$.

Although it is unimportant in the present analysis, where correlations other than instantaneous ones are not being considered, it should be pointed out that in Figures 6.2 - 6.6, the correlation functions are drawn such that the first named parameter in each function identifier is correlated with an earlier value of the second named parameter on the right hand side of the diagram and vice-versa on the left hand side of the diagram. This convention will be adhered to in all the diagrams illustrating correlation functions.

Local Time (Hrs)	Scintillation Spread-F		Scintillation f_oF_2		Spread-f f_oF_2	
	1964	1965	1964	1965	1964	1965
0000	0.50	0.40	-0.08	0.06	-0.40	-0.22
0300	0.48	0.23	-0.08	0.62	-0.47	0.01
0600	0.06	0.26	-0.10	-0.14	-0.44	-0.46
0900	0.44	0.34	-0.19	-0.19	-0.37	-0.08
1200	0.07	0.28	-0.03	-0.26	-0.02	-0.12
1500	0.08	X	0.16	X	-0.02	X
1800	-	0.28	-0.13	-0.22	-	-0.60
2100	0.63	0.40	0.20	0.12	-0.21	-0.15

TABLE 6.4

The correlation coefficients between the Cygnus A scintillation indices, the spread-F indices and $f_o F_2$ for 1964 and 1965.

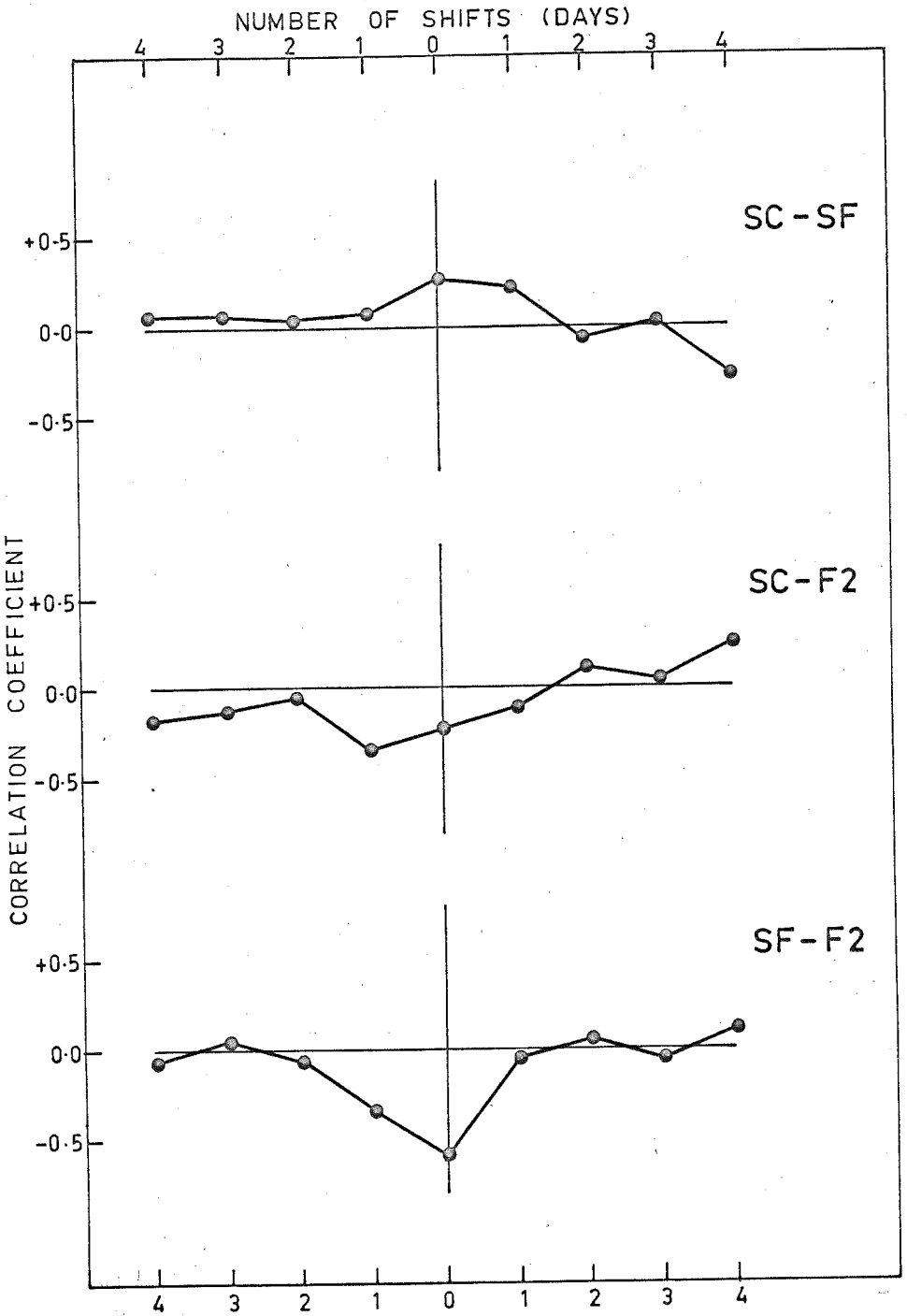

Figure 6.5 Correlation functions for 1800 hours 1965 between scintillation, spread-F and f_oF_2 showing a large negative correlation between spread-F and f_oF_2 compared with the lesser correlations between other pairs of parameters.

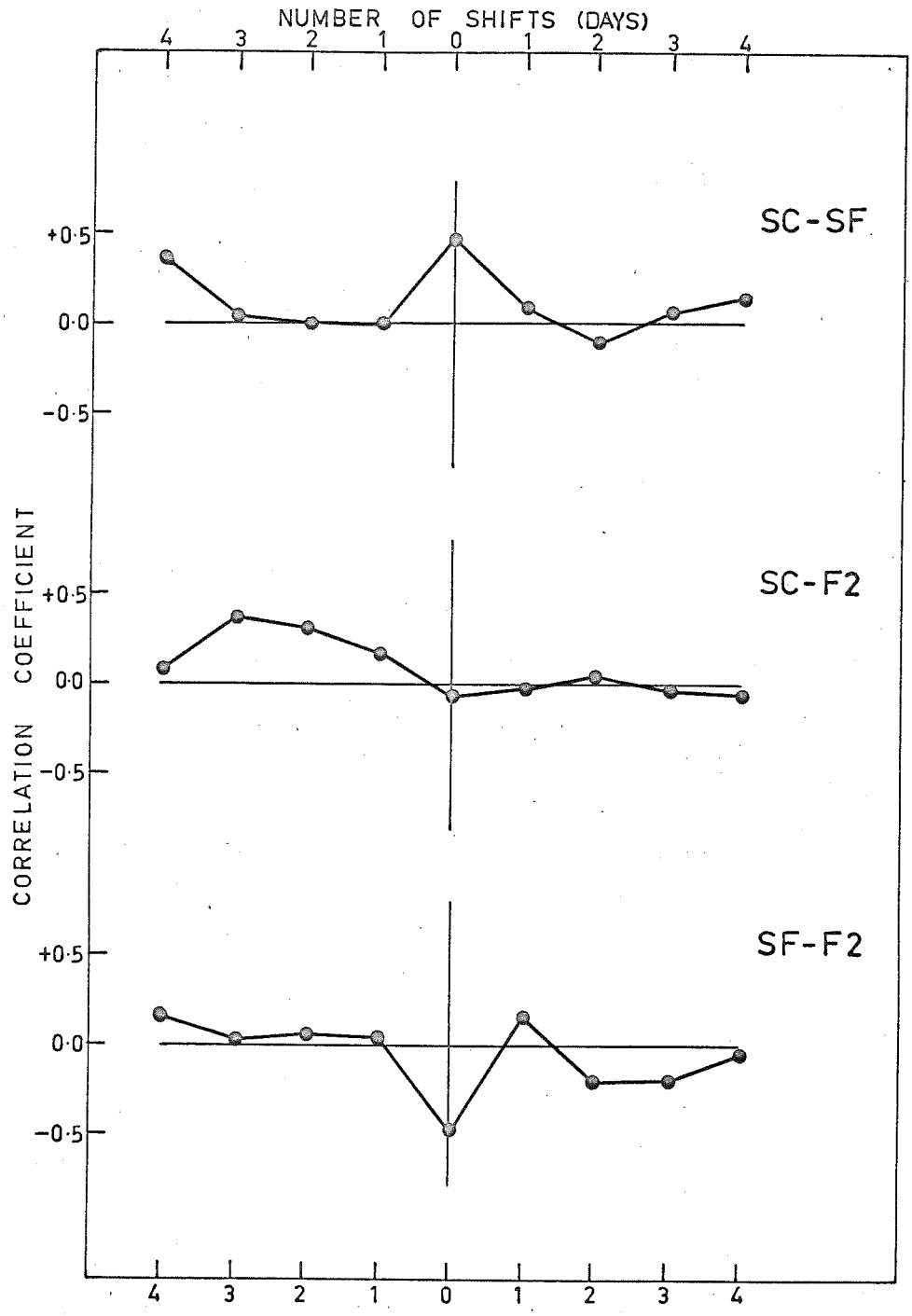

Figure 6.6 Correlation functions for 0300 hours 1964 between scintillation, spread-F and f_oF_2 showing a strong positive correlation between scintillation and spread-F, a strong negative correlation between spread-F and f_oF_2 and no correlation between scintillation and f_oF_2.

The correlation coefficients for 1500 hrs 1965 are not included in the Tables since the months corresponding to this time were December 1965 and January 1966 when scintillations were no longer being recorded. The coefficients involving spread-F for 1800 hrs 1964 were not available due to the complete absence of spread-F from the relevant ionograms which meant that the set of indices representing spread-F had zero variance and the resulting correlation coefficient was undefined.

6.7 Discussion and Interpretation of the Results

The various significance levels for the correlation coefficients presented in Tables 6.3 and 6.4 are readily calculated using Fisher's Z transformation as described in Section 6.5.

For the 6-weeks-long sets of data used to obtain the coefficients, each set would have contained 45 data points had there been no values missing. However, since in fact there were a number of values missing from the data sets, the average value of N used in the calculations was reduced to 35. It is evident in Figure 6.2 - 6.6 that those cross correlation functions which contain a significant positive or negative peak at zero shift, show this peak in a single coefficient only: thus the value of N used in the correlation calculations may also be regarded as the number of

independent points inthe data and can be used in the estimate of the statistical significance of the coefficients.

The calculations based on Fisher's Z transformation show that relative to a correlation coefficient of zero, the values $\pm$ 0.17, $\pm$ 0.34 and $\pm$ 0.47 have respective probabilities of occurring by chance of 32%, 4.5% and 0.3%.

Basically, the coefficients in Table 6.3 indicate that the correlation between scintillation and sporadic-E is predominantly positive; several day time and night time coefficients exceed the 95% significance level and one (at 0500 hrs 1964, ρ = 0.51) exceeds the 99% significance level. The Table also shows that the correlation between scintillation and spread-F is strongly positive - especially at night where most of the coefficients approach or exceed the 99% significance level. The correlation coefficients between spread-F and sporadic-E are included in the Table since if these show a positive correlation, and if one of the corresponding coefficients between scintillation and spread-F or sporadic-E shows positive correlation, then the other of these corresponding coefficients must also be expected to show positive correlation since spread-F and sporadic-E and hence the correlations of these with scintillation cannot be regarded as independent. The importance of these "partial correlations" is discussed later in this section.

The coefficients in Table 6.4 also show the positive correlation between scintillation and spread-F and in addition show a predominantly negative correlation between spread-F and $f_o F_2$, and (with the notable exception of the coefficient for 0300 hrs 1965, $\rho = 0.62$) show a general lack of correlation between scintillation and $f_o F_2$.

These results are interpreted in terms of the phenomena they represent and compared with previous results of other authors following the detailed discussion of some apparently anomalous coefficients in the two Tables.

Some discussion is required concerning the positive correlation coefficients found between scintillation and spread-F during the day. As previously indicated, the coefficients involving spread-F indices at a local time of 1800 hours 1965 were incalculable due to the complete non-occurrence of spread-F in this period and it was further evident that this was almost the case for all the sets of spread-F indices read from day time ionograms - the local times concerned being from 0600 to 1800 hrs. Specifically, the set of spread-F indices for 0900 hrs 1965 included only 6 occurrences of spread-F (maximum index 1) and the other sets within the above time zone all included 3 or less occurrences (also with a maximum index of 1). Since at least moderate strength scintillation is still present more often than not at these times, it is somewhat surpris-

ing that some of the coefficients, involving spread-F, evaluated for the day time hours have values which, from the previous statistical calculations, should have a probability of less than 5% of occurring by chance.

A closer inspection of the correlation functions appropriate to these day time correlation coefficients shows that some of the positive correlations between day time scintillation and spread-F are not quite so strongly positive as indicated. In particular, the coefficient (ρ = 0.44) for 0900 hrs 1964 is actually part of a very broad peak, its value only 0.1 greater than the neighbouring coefficients, and the coefficient (ρ = 0.26) for 0600 hrs 1965 actually represents a negative peak of correlation, its value 0.1 less than the neighbouring coefficients. The coefficients for 0900 hrs 1965 (ρ = 0.34) and for 1200 hrs 1965 (ρ = 0.28) are in fact genuine positive peaks of correlation of the magnitude indicated in Table 6.3. Figure 6.7 illustrates these examples of spurious and genuine positive correlation between day time scintillation and spread-F.

From the above discussion, only the correlation coefficients for 0900 hrs 1965 and for 1200 hrs 1965 indicate a real positive day time correlation and neither of these reaches the maximum level of significance.

For the same reasons as outlined above based on the almost complete non-occurrence of spread-F during the day,

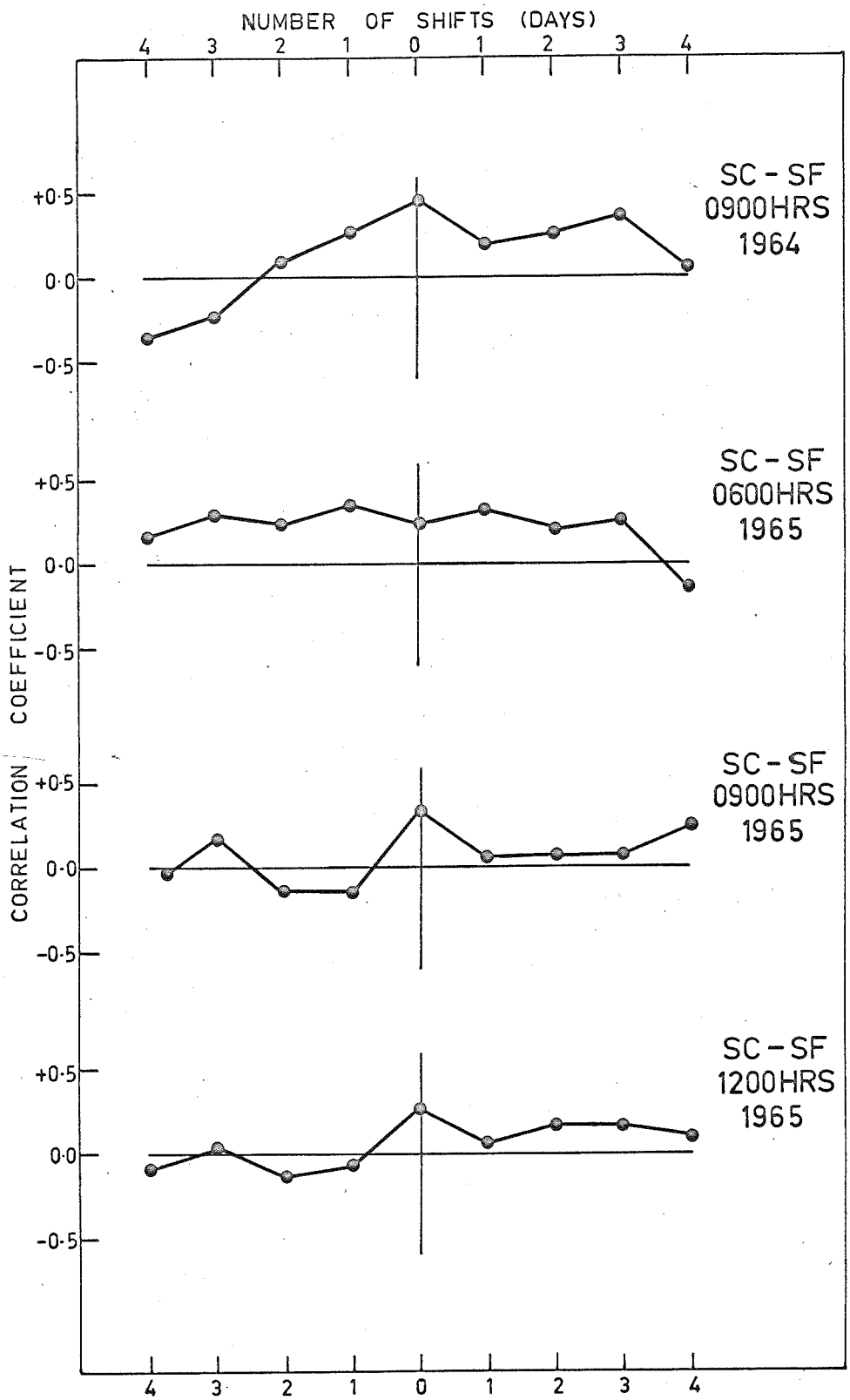

Figure 6.7 Some spurious and genuine positive correlations between daytime scintillation and spread-F.

it is surprising to find significant negative correlations between spread-F and $f_o F_2$ during day time hours. A closer inspection of the results, similar to that carried out for the day time coefficients between spread-F and scintillation, shows that most of these day time coefficients are spurious. Specifically, the coefficient ($\rho = -0.44$) for 0600 hrs 1964 is part of a broad negative peak, its value no lower than the neighbouring coefficients; the coefficient ($\rho = -0.37$) for 0900 hrs 1964 is also part of a broad negative peak, its value only 0.1 lower than the neighbouring coefficients, and the coefficient ($\rho = -0.46$) for 0600 hrs 1965 is similarly part of a broad negative peak, its value being only 0.1 lower than the neighbouring coefficients. The coefficient ($\rho = -0.60$) for 1800 hrs 1965 is in fact a genuine negative peak of correlation; it has already been illustrated in Figure 6.5 and is the only coefficient to show significant negative correlation between spread-F and $f_o F_2$ during the day.

Figure 6.8 illustrates the above three examples of spurious negative correlation between day time spread-F and $f_o F_2$.

Just as surprising as the apparently significantly negative correlation between spread-F and $f_o F_2$ by day, is the presence of a single correlation coefficient between the same parameters by night which does not show a signifi-

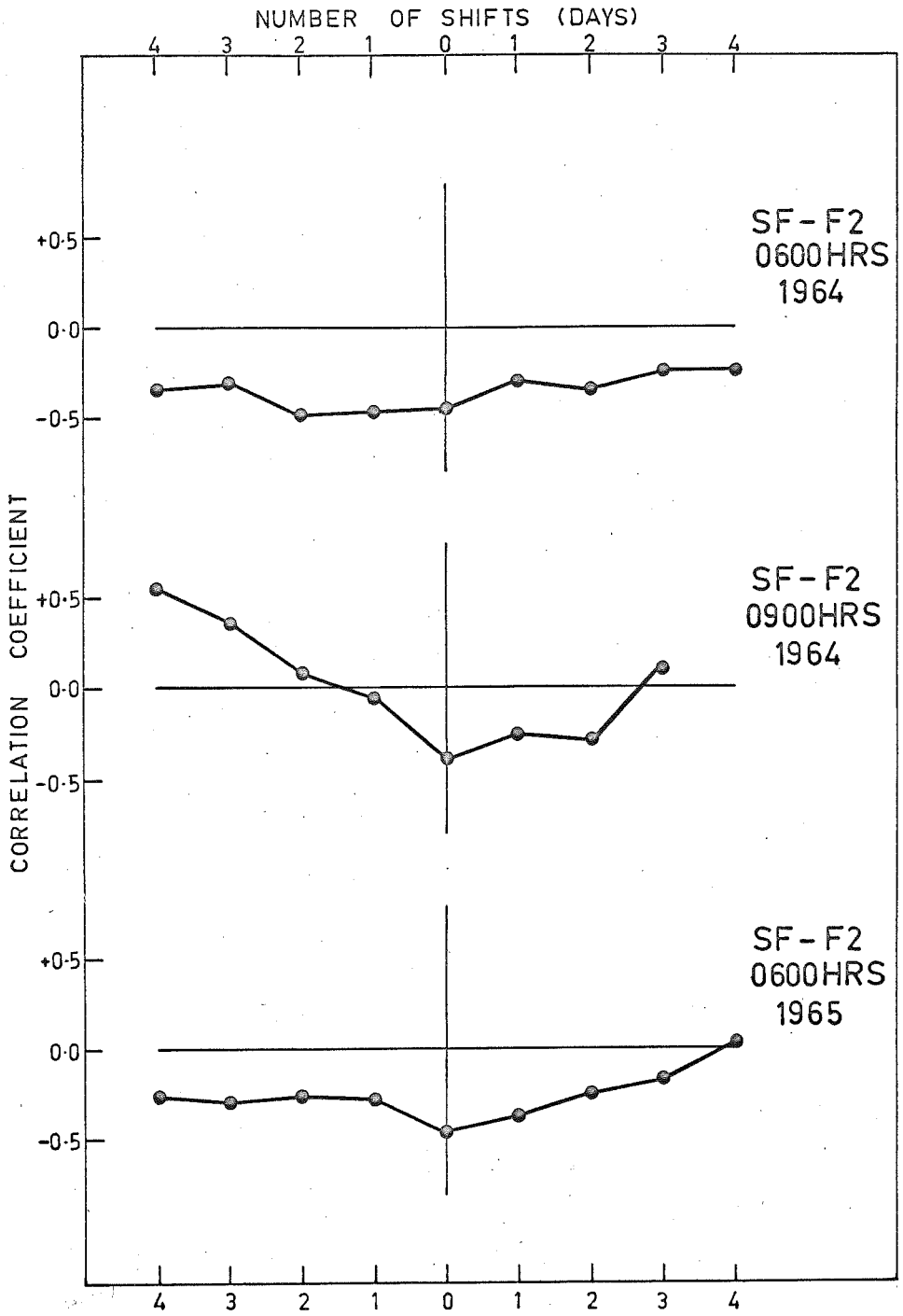

Figure 6.8 Three examples of spurious negative correlation between daytime spread-F and f_oF_2.

cant negative correlation. This coefficient (ρ = 0.01) at 0300 hrs 1965 does in fact represent nothing other than a zero correlation, the neighbouring correlation coefficients not being significantly different. This correlation coefficient and also the large (ρ = 0.62) coefficient found for the correlation between scintillation and $f_o F_2$ at the same time are both anomalous with respect to the other coefficients at different local times between the same pairs of parameters and cannot readily be explained. The large positive correlation coefficient above is in fact slightly reduced in significance due to the background correlation of 0.2 shown by the neighbouring coefficients and was also calculated from less than the average number of data points (30), but these considerations do not alter its meaning appreciably. Both of the above anomalous correlation functions are illustrated in Figure 6.9.

Although there were present in the spread-F data several sets showing near complete occurrence of the phenomenon (particularly 0300 hrs 1964 and 1965), there was no difficulty in the calculation of the relevant correlation coefficients arising from this situation, since in each data set indicating near total occurrence of spread-F, the indices were well distributed among the values 1- 3 which represented different intensities of the phenomenon. Thus the points in these sets of spread-F data still had a large variance.

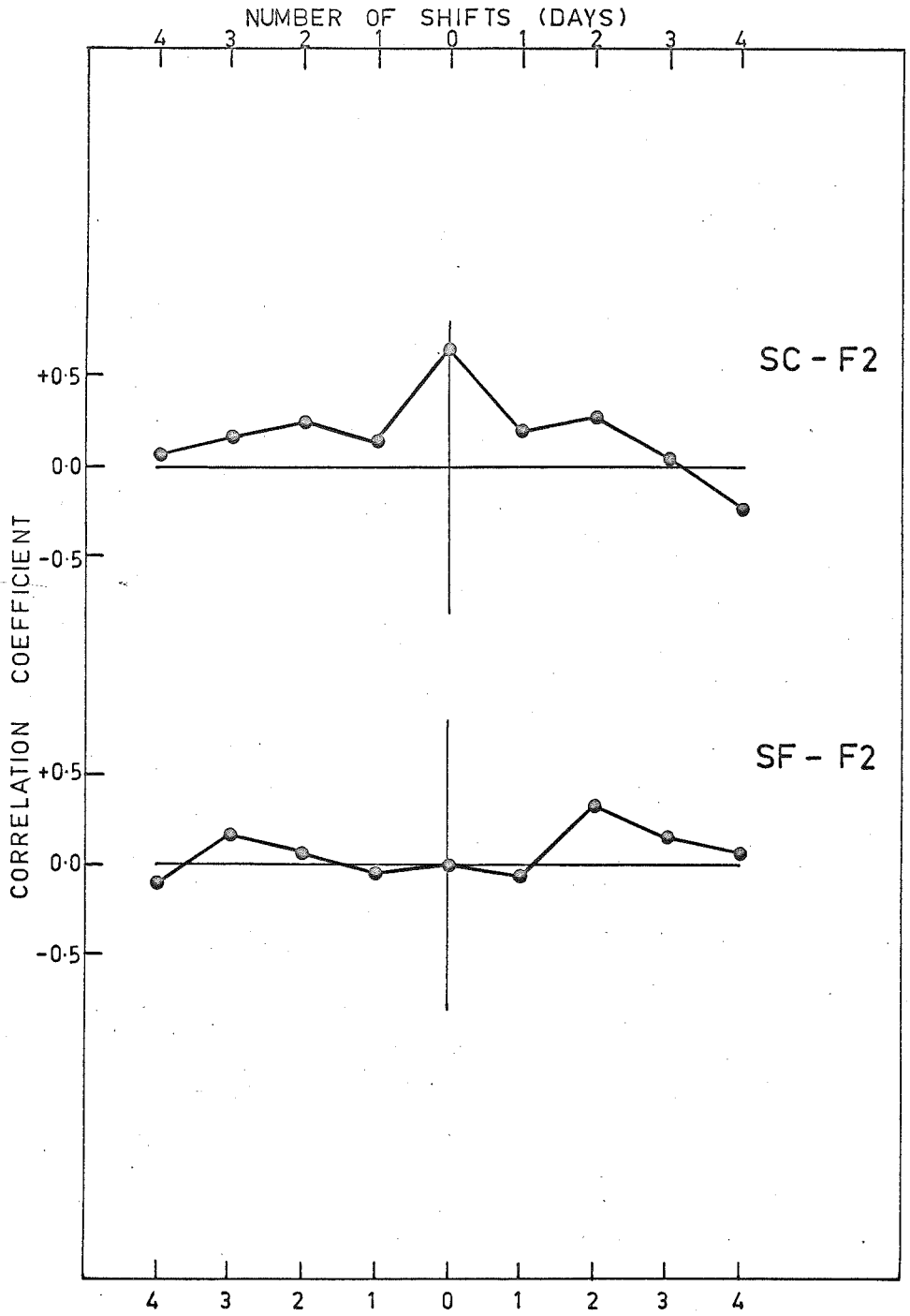

Figure 6.9 The anomalous correlation coefficients between scintillation and f_oF_2 and between spread-F and f_oF_2 at 0300 hours 1965.

An inspection of the remaining correlation functions, some of which have been shown in Figures 6.2 - 6.6, showed that all the positive correlations between scintillation and sporadic-E, all the night time positive correlations between scintillation and spread-F, and all the night time negative correlations between spread-F and $f_o F_2$, are in fact genuine: for all these cases, the correlation coefficients evaluated for zero shift between the respective pairs of parameters are significantly different from the neighbouring correlation coefficients evaluated with one parameter of the respective pair being shifted in time relative to the other.

As pointed out earlier in the discussion, if three parameters are interdependent, then the correlation of any two of the parameters cannot be regarded as being independent of the correlations of each with the third.

From Yule and Kendall (1949)

$$\rho_{12\cdot3} = \frac{\rho_{12} - \rho_{13}\cdot\rho_{23}}{(1 - \rho_{13}^2)^{\frac{1}{2}}\cdot(1 - \rho_{23}^2)^{\frac{1}{2}}} \qquad (6.6)$$

where $\rho_{12\cdot3}$ is the intrinsic correlation coefficient between parameters 1 and 2 with the influence of parameter 3 removed, and ρ_{12}, ρ_{13}, and ρ_{23} are the apparent correllation coefficients between the indicated two parameters

with the influence of the third still present.

An example can be considered from Table 6.3 where, for certain local times, there is a significant instantaneous positive correlation between scintillation and both spread-F and sporadic-E and there is a smaller positive correlation coefficient between spread-F and sporadic-E. Table 6.5 lists the intrinsic (partial) and apparent correlation coefficient between scintillation, spread-F and sporadic-E for 2100 hrs 1964 calculated from equation (6.6).

	SC-ES	SC-SF	ES-SF
Apparent Correlation	0.42	0.63	0.20
Intrinsic Correlation	0.39	0.62	

TABLE 6.5

The statistical significance of the intrinsic correlation coefficients is determined from a value of N one less than the value used to determine the significance of the apparent correlations.

In the case of the results for 0000 hrs 1964 which, from Table 6.3, would appear to require similar treatment in order to obtain the intrinsic correlation coefficients, the small positive correlation between sporadic-E and spread-F arises in fact from a long term rather than instantaneous effect, and as such has no influence on the simultaneous intrinsic coefficients between scintillation and

spread-F or sporadic-E. This long term correlation is illustrated in Figure 6.4. Although not illustrated, the correlation coefficient (ρ = 0.20) between sporadic-E and spread-F at 2100 hrs 1964 is in fact a real instantaneous correlation of the magnitude indicated.

Table 6.5 shows that the intrinsic correlation coefficients between scintillation and both sporadic-E and spread-F are a little smaller than the respective apparent correlation coefficients, but the relative magnitudes of the two intrinsic coefficients are similar to the relative magnitudes of the two apparent coefficients. The small apparent positive correlation between sporadic-E and spread-F is not large enough to make the statistical interpretation of the intrinsic correlations any different from what it was for the apparent correlations.

The conclusions arising from the foregoing results and discussion are that the scintillations of the signals of the Cygnus A source are associated with spread-F during the night and with sporadic-E during the day and night. The night time associations with sporadic-E are not as strong as those with spread-F and there then appears to be no association between spread-F and sporadic-E.

As Briggs (1964) has already indicated, even if the irregularities responsible for spread-F are directly responsible for radio star scintillation a correlation coefficient

$\rho = 1$ cannot be expected between scintillation and spread-F since the observation of scintillation is not dependent on the height of the irregularities in the same way as is the observation of spread-F. In the present experiment, further reasons for expecting at best a strong partial correlation are the association between scintillations and sporadic-E and the large distance (~ 750 km) between the regions of the ionosphere responsible for spread-F and scintillation.

The results of the analysis do suggest that irregularities capable of producing scintillations are present at both E(100 km) and F (300 km) heights but do not exclude intermediate or greater heights for the origin of the scintillations. Specific examples of associations of scintillations with spread-F and sporadic-E are examined in the next chapter in an attempt to resolve them in more detail. The present results are in general agreement with those of previous authors: the relevant previous results have already been discussed in Section 1.4(ii).

The analysis also shows that during the night, spread-F then being common, spread-F and $f_o F_2$ are consistently anti-correlated but there is no association either positive or negative between scintillation and $f_o F_2$. The anti-correlation between spread-F and $f_o F_2$ has already been

observed by Singleton (1962a) and its interpretation in terms of the blanketing of spread-F by high values of the critical frequency has already been discussed in Section 1.4(iv). It was also pointed out there that the observation of scintillation should not be similarly dependent on the critical frequency.

The anti-correlation of spread-F and $f_o F_2$ and the lack of correlation of scintillation and $f_o F_2$ could also arise from a decrease in the height of the F region maximum being associated with increasing critical frequency but this is not necessarily implied by the present observations. The experimental results of Singleton (1962b) do not support this explanation as he found that the association between spread-F and the height of the F region maximum appeared to be independent of the association between spread-F and the critical frequency.

6.8 The Correlation of Scintillation with Sporadic-E and Spread-F - Larger Interferometer Results

As was the case for the scintillation indices assigned to the Cygnus A records of the smaller interferometer, those recorded for the various sources detected by the larger interferometer were correlated with the appropriate hourly values of ionospheric parameters.

The correlation of the larger interferometer scintillation indices was carried out for each source separately but, since the instrument was operated for a period of only 9 months each source was observed over a range of only 18 hours in the local time of transit and the desirable situation that records be available for both day time and night time transits of the one source was not achieved for all sources. Figure 5.4 shows the range of transit times for which each source was observed.

For the purposes of the correlation analysis, the scintillation indices for each source were grouped together under the headings of day (1000 - 1400 hrs local time of transit) and night (1900 - 0500 hrs local time of transit) the night time hours being defined as those for which severe spread-F was often observed and the day time hours being defined as those for which severe spread-F was rarely observed. The analysis was carried out only between scintillation indices, spread-F and sporadic-E, the ionospheric indices being as described in Section 6.3 and the purpose of the analysis being to differentiate if possible between the relative associations of spread-F and sporadic-E on scintillations for sources at different zenith angles. The correlation coefficients between f_oF_2 and the above parameters were not required for this purpose.

Scintillation indices for the Centaurus A source were not included in the analysis due to the reduced occurrence

of scintillations in the signals from this source compared with the signals from other sources. This reduction in occurrence is evident in Figure 5.2 and the reduced mean scintillation index compared with that of other sources (at the same transit time) is evident in Figure 5.6.

Table 6.6 shows the correlation coefficients evaluated between the three parameters for the night time hours together with the average number of data points used in the calculations for each source and the corresponding values of the coefficients which have probabilities of 4.5% and 0.3% of differing from zero by chance. As previously, these values are derived using Fisher's Z transformation calculated on the assumption that all the data points are independent of those for the preceeding or following day.

Many of the correlation coefficients in the Table can be rejected immediately on the grounds that they are not statistically significant, however, some of those between scintillation and sporadic-E and between sporadic-E and spread-F, and most of those between scintillation and spread-F, appear to exceed the 95% significance level.

Correlation functions were again evaluated for a small number of shifts to distinguish between long term and instantaneous correlations and are illustrated for those coefficients in Table 6.6 which apparently exceed the 95%

Source	Zenith Angle	Correlation Coefficient			Average N	Correlation Coefficient Significant to	
		SC-ES	SC-SF	ES-SF		95.5%	99.7%
Fornax A	3°S	0.26	-0.29	0.15	25	0.40	0.55
Pictor A	16°S	0.48	0.18	0.12	24	0.41	0.57
Hydra A	23°N	0.27	0.43	0.33	83	0.22	0.32
Hercules A	39°N	-0.05	0.39	0.07	86	0.22	0.32
Virgo A	47°N	0.29	0.55	0.27	93	0.20	0.30
Taurus A	57°N	0.35	0.45	0.53	40	0.32	0.46
3C 123	63°N	0.27	0.42	0.00	28	0.39	0.54
Cygnus A	75°N	-0.10	0.27	0.07	70	0.24	0.35

TABLE 6.6

Night time Correlation Coefficients

significance level. Figures 6.10, 6.11 and 6.12 respectively show the correlation functions between scintillation and sporadic-E, scintillation and spread-F, and sporadic-E and spread-F, and it is evident from these illustrations that only for some of the scintillation - spread-F correlation functions and for that between scintillation and sporadic-E for the Hydra A source is there a peak of correlation for zero time shift significantly different from the values of the adjacent coefficients.

The most notable feature of the remaining correlation functions is that a peak of correlation still exists for zero time shift but that it is markedly broadened. These broad peaks are interpreted as being caused by a lack of independence between the parameters of successive days and this interpretation should be contrasted with that for the correlation functions in Figure 6.4 (SF-ES) and Figure 6.7 (0600 hrs 1965) which was in terms of a common long term variation in the parameters.

Following an examination of the auto-correlation functions of the parameters for the different sources, it was found that for many of the sources, the auto-correlation coefficients for one day shifts in the scintillation and spread-F both were still large (> 0.40) and that they

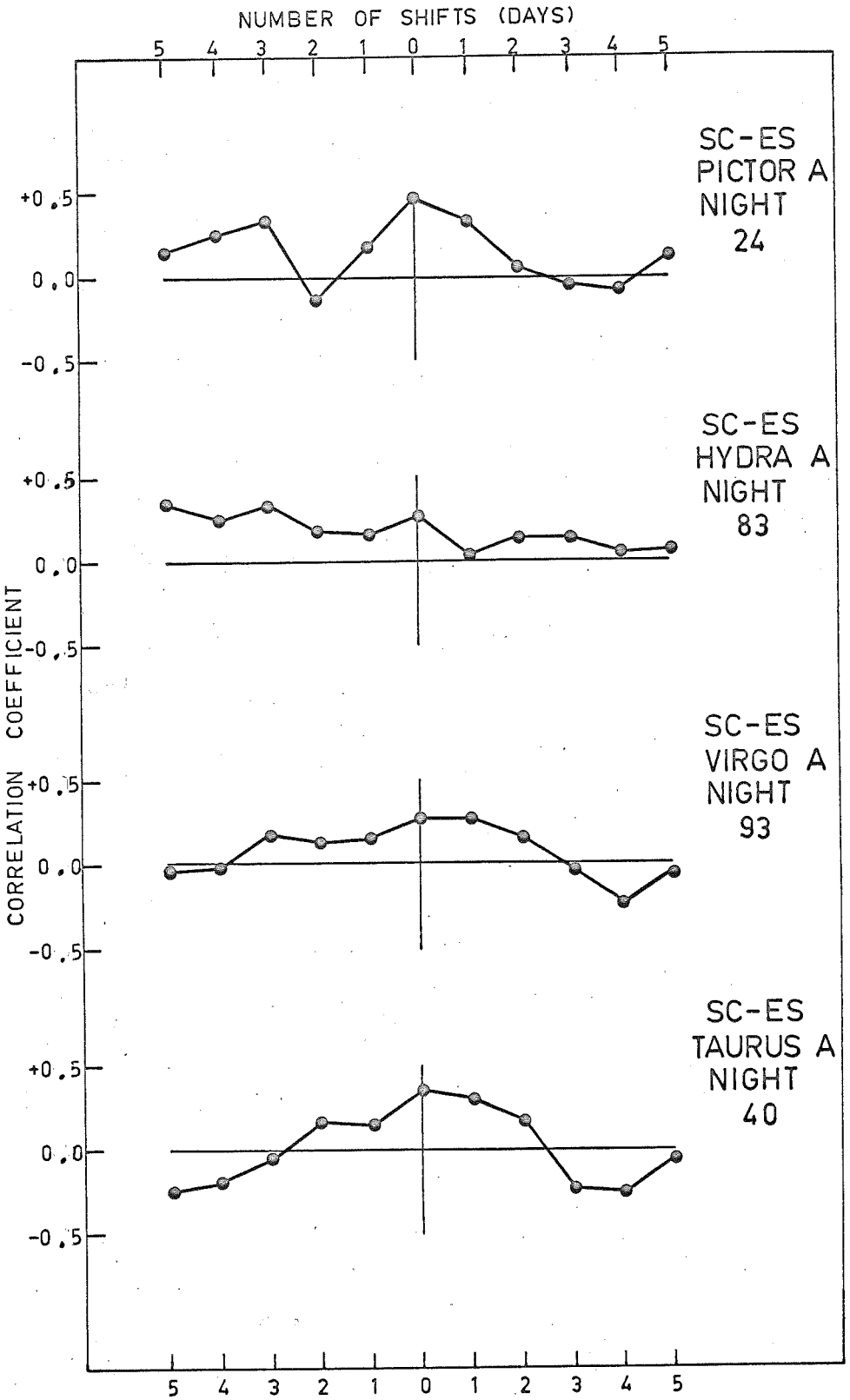

Figure 6.10 Night time correlation functions between scintillation and sporadic-E. The average number of data points used for each correlation function is indicated.

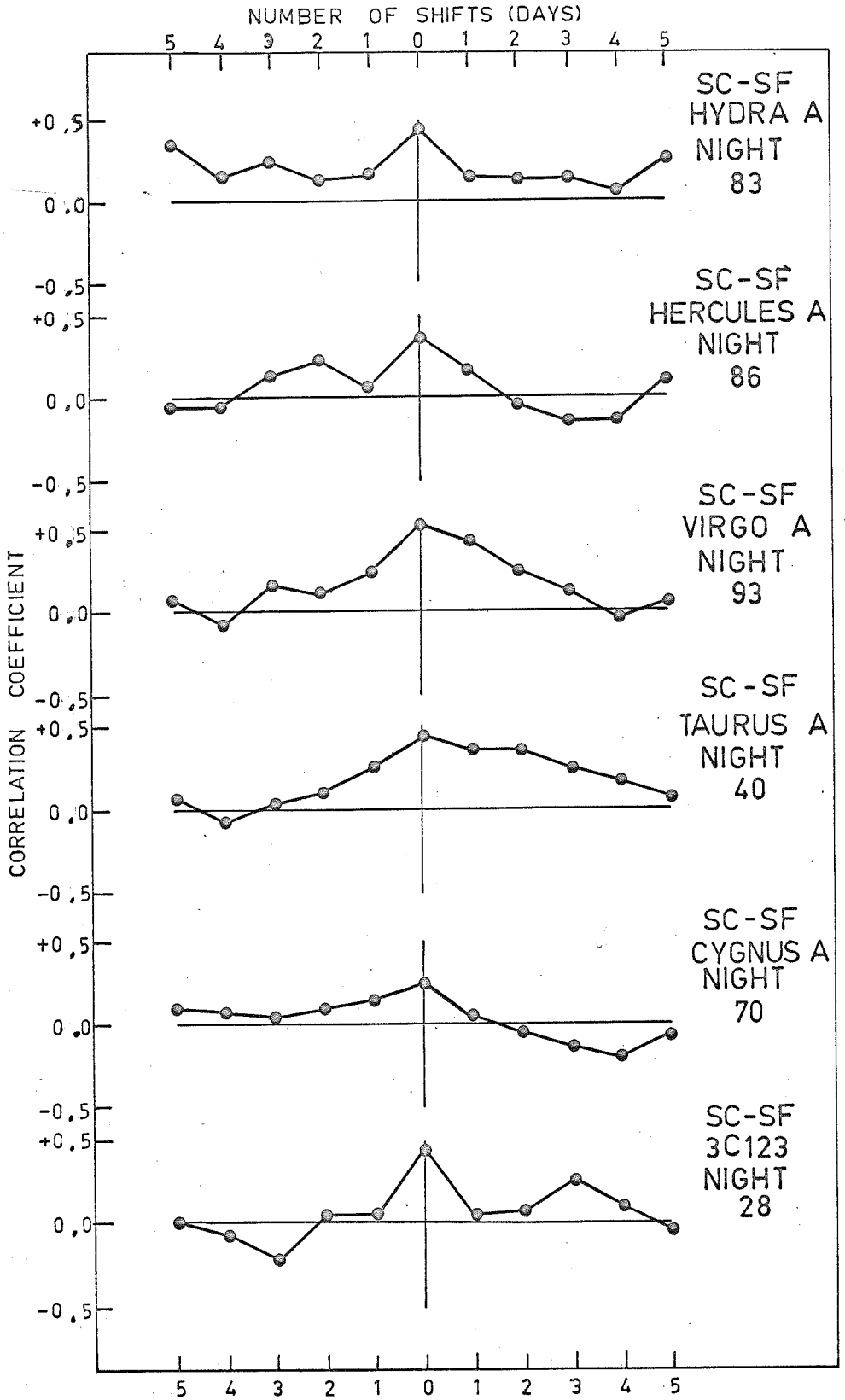

Figure 6.11 Night time correlation functions between scintillation and spread-F. The average number of data points used for each correlation function is indicated.

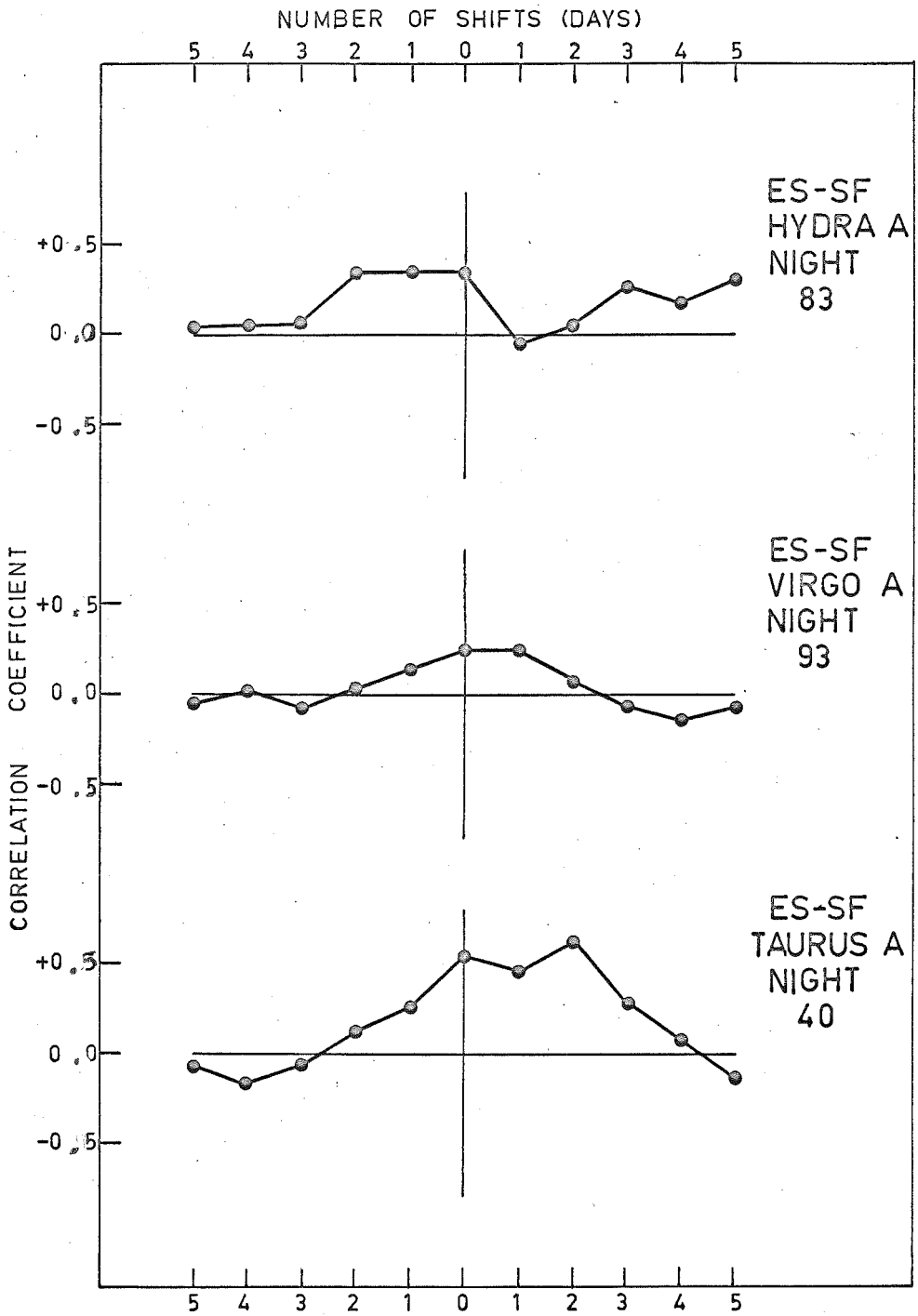

Figure 6.12 Night time correlation functions between sporadic-E and spread-F. The average number of data points used for each correlation function is indicated.

were largest for the data relating to the Taurus A and Virgo A sources for which the peaks in Figure 6.10 - 6.12 are broadest. The value of N used to determine the statistical significance of the correlation coefficients should probably be reduced by a factor of 2 for these sources.

From the above discussion and from Figures 6.10 - 6.12, it is evident that the associations between the parameters are not so strong as indicated from Table 6.6 above. However the general results obtained from the Cygnus A night time records of the smaller interferometer are verified with regard to the existence of association between scintillation and sporadic-E for some sources and spread-F for most sources and to the relative importance of these associations. Possible variations with zenith angle of the associations are discussed following the presentation of the day time results.

Table 6.7 shows the available day time correlation coefficients evaluated for the 3 parameters plus the same information for each source as that given in Table 6.6, the correlation coefficients including spread-F for the Cygnus A source being undefined due to the complete non-occurrence of this parameter at the appropriate times.

Source	Zenith Angle	Correlation Coefficient			Average N	Correlation Coefficient Significant to	
		SC-ES	SC-SF	ES-SF		95.5%	99.7%
Fornax A	3°S	-0.12	0.08	0.05	52	0.28	0.40
Pictor A	16°S	-0.31	0.46	-0.26	38	0.32	0.46
Taurus A	57°N	0.21	0.22	0.09	40	0.32	0.46
Cygnus A	75°N	0.42	-	-	24	0.41	0.57

TABLE 6.7

Day Time Correlation Coefficients.

The Table indicates that significant associations appear to exist only between the Cygnus A scintillation indices and sporadic-E and between Pictor A scintillation indices and spread-F but, as in the analysis of the night time data, the coefficients cannot be interpreted correctly without the additional aid of the correlation functions. Figures 6.13, 6.14 and 6.15 respectively show the correlation functions between scintillation and sporadic-E, scintillation and spread-F, and sporadic-E and spread-F which confirm the observations based on the coefficients in Table 6.7 and in addition, suggest possible associations between the Taurus A scintillation indices and both sporadic-E and spread-F - the possible association with spread-F being

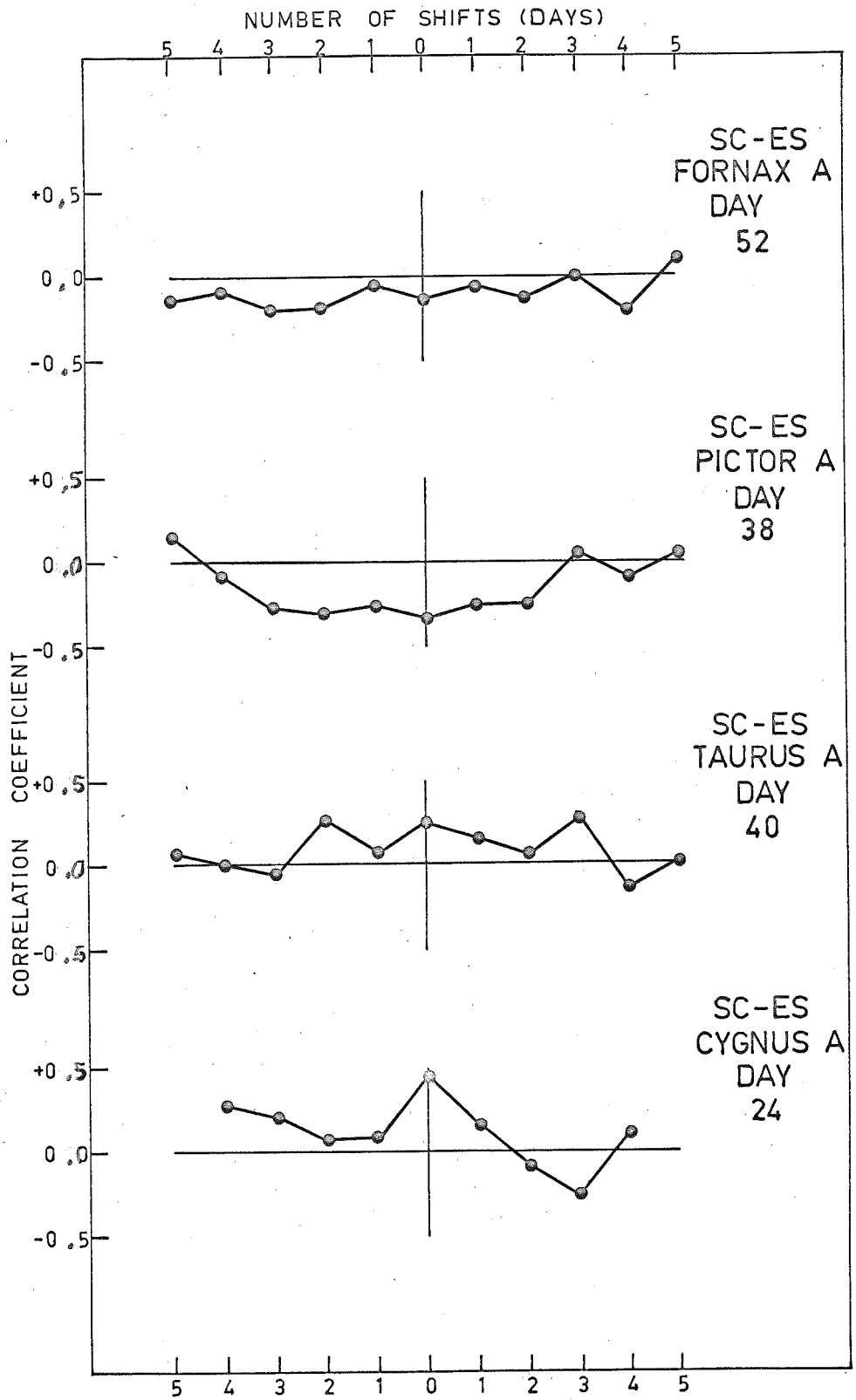

Figure 6.13 Daytime correlation functions between scintillation and sporadic-E. The average number of data points used for each correlation function is indicated.

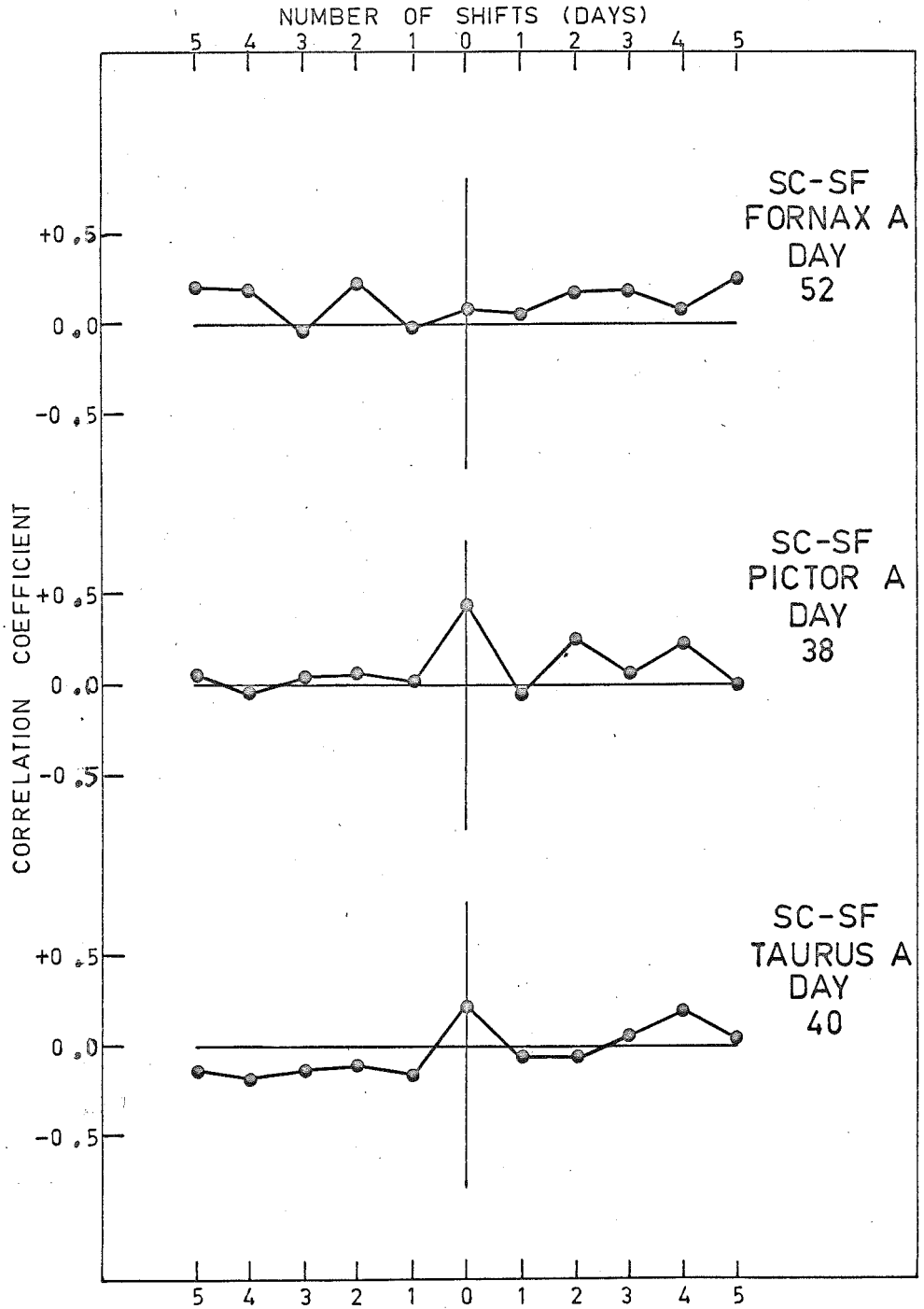

Figure 6.14 Daytime correlation functions between scintillation and spread-F. The average number of data points used for each correlation function is indicated.

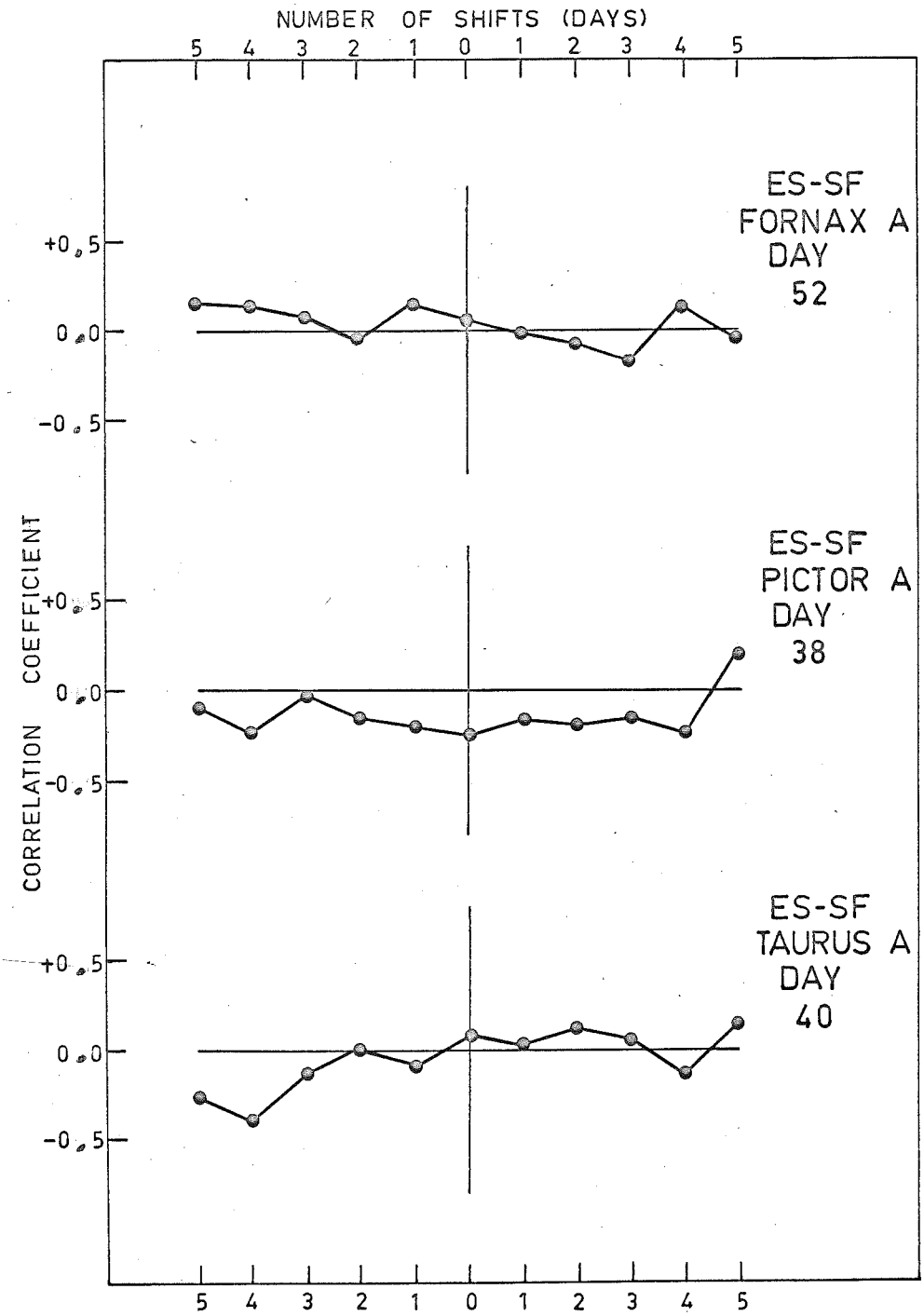

Figure 6.15 Daytime correlation functions between sporadic-E and spread-F. The average number of data points used for each correlation function is indicated.

stronger than that with sporadic-E.

The accuracy of the results of the analysis of the day time scintillation data as presented here is somewhat limited since, in the signals from most of the sources, scintillation is not a common day time event. Figure 5.4 shows that only the signals from the sources Cygnus A, Taurus A, and to a lesser extent Hercules A (for which insufficient day time data is available for a correlation analysis to be meaningfull), exhibit a significant amount of day time scintillation. Since there are no observations in the same figure to contradict the rather tentative conclusion that in the present experiment, day time scintillations are restricted to the signals from sources which transit at the larger zenith angles, it may be true that correlations of ionospheric parameters with scintillation can not be satisfactorily investigated during the day for those sources which transit at the smaller zenith angles.

As was discussed in Section 6.7 with regard to the Cygnus A source scintillation indices recorded by the smaller interferometer, spread-F is also likely to occur rather rarely during the day. However, it was ascertained from the appropriate ionograms that the occurrence of spread-F when transits of the Pictor A and Taurus A sources took place during the day was sufficient, (although the spread-F

was never very intense), so that the associations of spread-F with the scintillation indices of the above sources could be regarded as genuine in the absence of other accuracy limitations. The occurrence of spread-F during the day time transits of the Pictor A and Taurus A sources does not necessarily conflict with the fact that some of the Cygnus A source correlation coefficients are undefined due to the complete non-occurrence of spread-F, since the Cygnus A source day time transits occur in the summer, six months before the Pictor A and Taurus A source transits **at the same local time.**

Due to the various accuracy limitations which had to be considered in the interpretation of the correlation functions from the larger interferometer observations, it was not thought desirable to attempt to distinguish between the apparent and intrinsic correlation coefficients using a partial correlation analysis for either the day time or night time analysis.

6.9 Review and Discussion of the Larger Interferometer Correlation Results

The night time correlation analysis showed that the scintillations in signals from all the sources except Fornax A and Pictor A, (for which the least amounts of

data were available), were associated with spread-F as was illustrated in Figure 6.11, but that only the scintillations in signals from the sources Pictor A, Hydra A, and to a lesser extent Virgo A and Taurus A, exhibited any association with sporadic-E. These sporadic-E associations were not as significant as the spread-F associations and could not be regarded as being established beyond doubt. They have been illustrated in Figure 6.10.

If these results are compared with the distances listed in Table 6.2, it is evident that the strongest associations between scintillation and spread-F are obtained from analysis of signals from the sources for which the distance between the origins in the ionosphere of scintillation and spread-F (recorded by the Woomera ionosonde), is least. The correlation coefficients appear to be reduced if this distance exceeds 400 km. A similar interpretation, although statistically less certain, applies to the associations between scintillation and sporadic-E. Bearing in mind that the sporadic-E indices originated from the Salisbury ionosonde, the critical distance between the origins in the ionosphere of scintillation and sporadic-E, beyond which the associations are reduced, is about 150 km.

Specifically, there can be no suggestion from the results of the night time analysis that associations between

scintillation and sporadic-E are dominant in the signals from sources which transit at large zenith angles, or that associations between scintillation and spread-F are dominant in the signals from sources which transit at small zenith angles.

The day time correlation analysis showed that only the scintillations in signals from the sources Taurus A and Pictor A were associated with spread-F and this was illustrated in Figure 6.14. The day time correlation analysis also showed that the scintillation in signals from the sources Cygnus A (where the association was based on a minimal amount of data), and possibly Taurus A, (but not Fornax A or Pictor A - the two sources for which the distance between the origins of scintillation and sporadic-E is least), were associated with sporadic-E. This was illustrated in Figure 6.13.

The occurrence of day time scintillation for the various sources and of day time spread-F generally was discussed, and it was noted that the correlation analysis to investigate associations during the day between scintillation and sporadic-E and spread-F might be limited to the records of sources which transit at large zenith angles. The association between the scintillation of signals from the Cygnus A source and sporadic-E during the day should be

contrasted with the lack of association between the same parameters at night; the suggestion being that locally, the extent of sporadic-E patches might be somewhat larger during the day than during the night.

In Section 5.4, it was noted that the mean night time scintillation indices of the various sources observed with the larger interferometer increased with increasing zenith angle more rapidly than was expected from the theoretical estimates based on an F region origin for the scintillations and a scale size r_o = 1 km for the small dimension of the irregularities. Further, it was pointed out that the observations would be resolved if it could be shown that irregularities of similar scale size were present at a lower height (i.e. in the sporadic-E layer) or if irregularities of larger scale size were present at the same height.

The results from Section 6.7 showing that the Cygnus A source scintillation indices recorded by the smaller interferometer were influenced by sporadic-E by day and night, and the present results from the records of the larger interferometer showing by day a similar sporadic-E influence on the scintillation indices of the same source, suggest that the presence of irregularities in the E region has an effect on the observed zenith angle variation of the mean scintillation indices which was illustrated in Figure 5.6.

The fact that the present results from the Cygnus A records of the larger interferometer at night do not show an association between scintillation and sporadic-E does not contradict the above conclusion provided it is true that the observed lack of correlation is due to the large distance between the origins of the scintillation and sporadic-E.

Even if it is true that irregularities in the E region have an important influence on the observed zenith angle variations of the mean scintillation indices, the possibility of a similar influence arising from the existence of irregularities of larger scale size in the F region cannot be excluded.

6.10 The Correlation of Scintillation with Planetary Magnetic Kp Indices

The amplitude scintillation indices assigned to the central fringe of the Cygnus A records of the smaller interferometer were correlated with planetary magnetic Kp indices. As described in Section 6.3, the Kp indices used in the analysis represented the average world wide magnetic activity over a period 3 hours before and after the Cygnus A source transit. The data available from the 2 years of observation was subdivided into day time (source transit 0900 - 1500 hours), and night time (source transit

2100 - 0300 hours) records for the 2 years 1964 and 1965, and correlation functions, were evaluated from the data for time shifts of up to 15 days.

Figures 6.16 and 6.17 respectively show the day time and night time correlation functions and the sense of the time shift (already defined in Section 6.6) is indicated in the Figures. The number of data points used in the evaluation of each correlation function is also indicated and refers to the coefficient evaluated for zero time shift.

Table 6.8 shows the values of the correlation coefficients appropriate to each correlation function which, from Fisher's Z transformation, have probabilities of 4.5% and 0.3% of differing from zero by chance.

		N	Correlation Coefficient Significant to:	
			95.5%	99.7%
Day	1964	60	0.26	0.38
	1965	108	0.19	0.28
Night	1964	115	0.19	0.27
	1965	88	0.21	0.31

TABLE 6.8

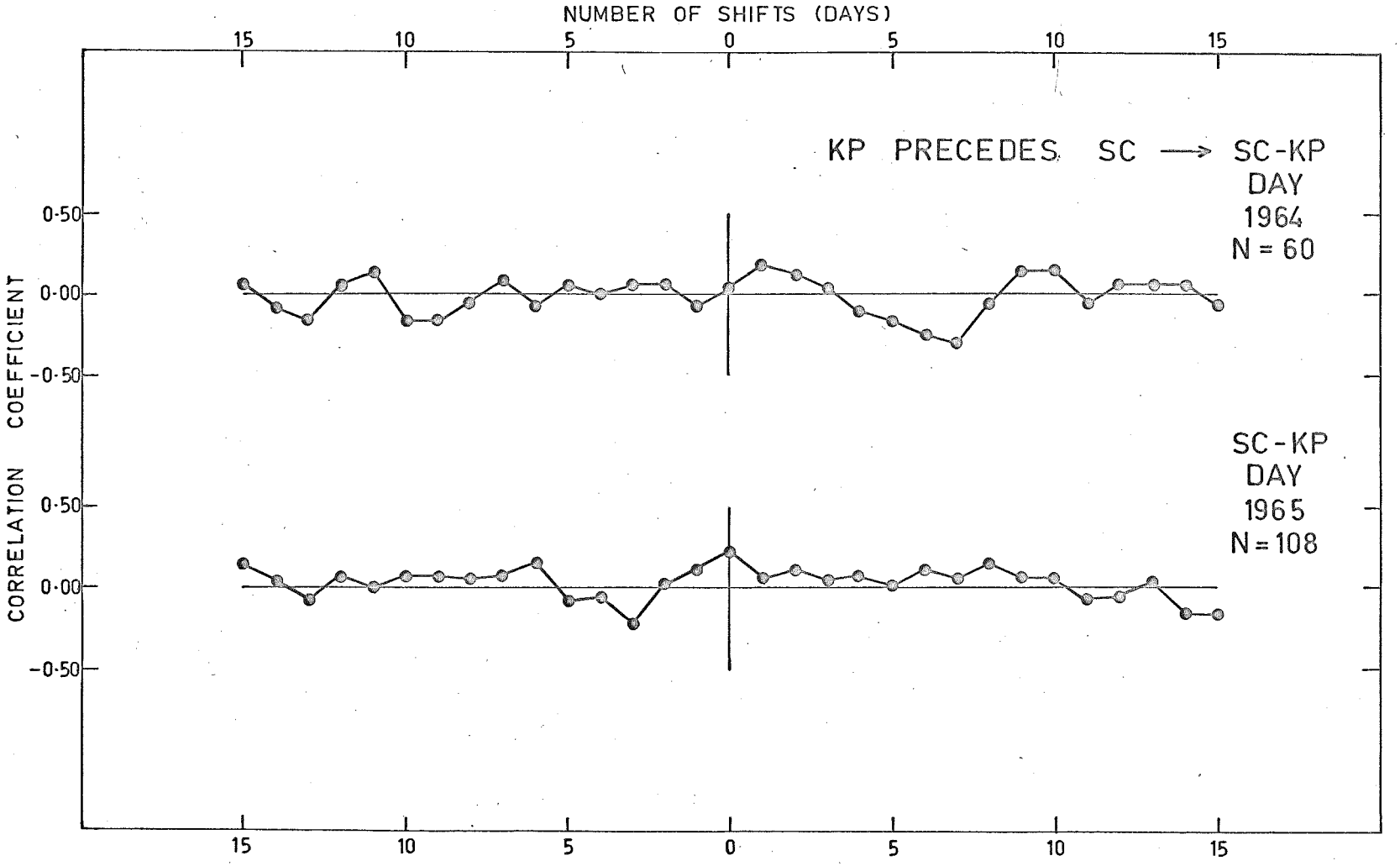

Figure 6.16 Correlation functions between scintillation and planetary K_p indices by day.

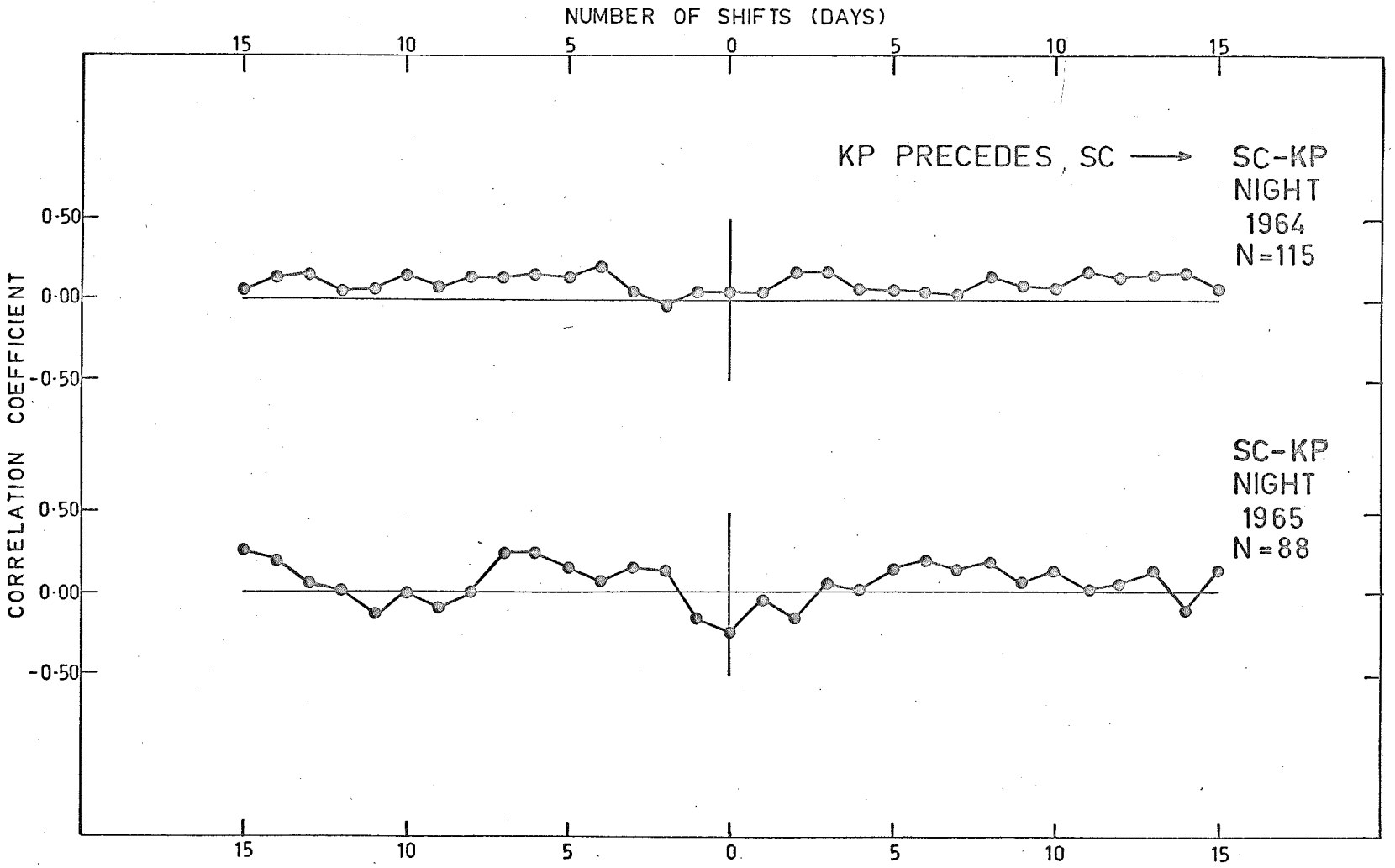

Figure 6.17 Correlation functions between scintillation and planetary K_p indices by night.

From Figures 6.16 and 6.17 it is evident that the correlation functions for both day time and night time in 1964 show no association between amplitude scintillation and magnetic activity for zero time shifts. Further, those for day time and night time 1965 respectively show positive and negative associations for zero time shift, both the respective correlation coefficients exceeding the 95% significance level, and both of the correlation functions of the 1964 data show a positive peak of correlation corresponding to a time lag of from 1 to 3 days in the scintillation activity with respect to the magnetic activity, although statistically, only the night time peak is significant.

The above results are far from conclusive but, with the exception of those from the night time 1965 analysis, possibly indicate a very weak association between scintillation amplitude and magnetic activity, the effect of magnetic activity on scintillation possibly being delayed by several days.

Previous inconclusive results for the association between the same parameters have already been discussed in Section 1.4(v). In particular, Hewish (1952) reported that scintillation amplitude appeared to be influenced by magnetic activity only if the duration of the activity was rather extended, and Briggs (1961) was able to show that a

small positive correlation existed at all times between magnetic activity and the presence of ionospheric irregularities but that a coresponding increase in scintillation amplitude was not always observed because of the finite angular size of the source. For the present experiment, the possible effects of the finite angular size of the Cygnus A source on the zenith angle variation of the scintillation depth of signals from the source, have already been discussed in Section 5.6. It was there concluded that it was possible, but rather unlikely, that on some occasions the root-mean-square phase deviations in the irregularities responsible for the scintillation could become large enough so that the scintillation amplitude observed on the ground was less than it would have been had the root-mean-square phase deviation not been so large.

If this inversion of the usual relationship between scintillation depth and the intensity of the ionospheric irregularities responsible for scintillations did occur, then an otherwise positive association between scintillation amplitude and magnetic activity in the present experiment would be observed as a zero or negative association.

To check on the possibility of inversion occurring, correlation functions between scintillation amplitude and magnetic activity were examined for those times (the times

are evident from Figure 5.3) when scintillation activity was least. There was no evidence for an enhanced positive correlation at these times and it is virtually certain that the reduced scintillation was then not due to inversion.

The suggestion that ionospheric disturbances might be delayed with respect to magnetic disturbances has already been made by King (1961), and later Briggs (1965) published a correlation function showing a delay of 1 day between the onsets of magnetic activity and spread-F and determined that the delay varied between ½ and 2 days depending on the phase of the sunspot cycle. If Briggs' results for the last solar cycle remain true for the present one, a near maximum lag of from 1½ to 2 days would be expected for the years 1964 and 1965 when the present observations took place, in very approximate agreement with the time lags evident in the 1964 correlation functions between scintillation amplitude and magnetic activity. The remaining correlation functions, as has already been pointed out, do not support the existence of a time lag.

An attempt was made to reproduce Briggs' result for the correlation between magnetic activity and spread-F utilizing the 1964 and 1965 indices used for the scintillation - spread-F correlations described in Section 6.6 -

these indices referring to a local time 2 hours after the Cygnus A source transit for a range of local times from 2100 to 0300 hours.

Data from the years 1964 and 1965 were treated separately and the 2 correlation functions thus obtained are shown in Figure 6.18. Even without determining the statistical significance of individual correlation coefficients, it is evident that the correlation functions do not show the desired time lag in association between magnetic activity and spread-F, nor do they show any other possible association between the two parameters.

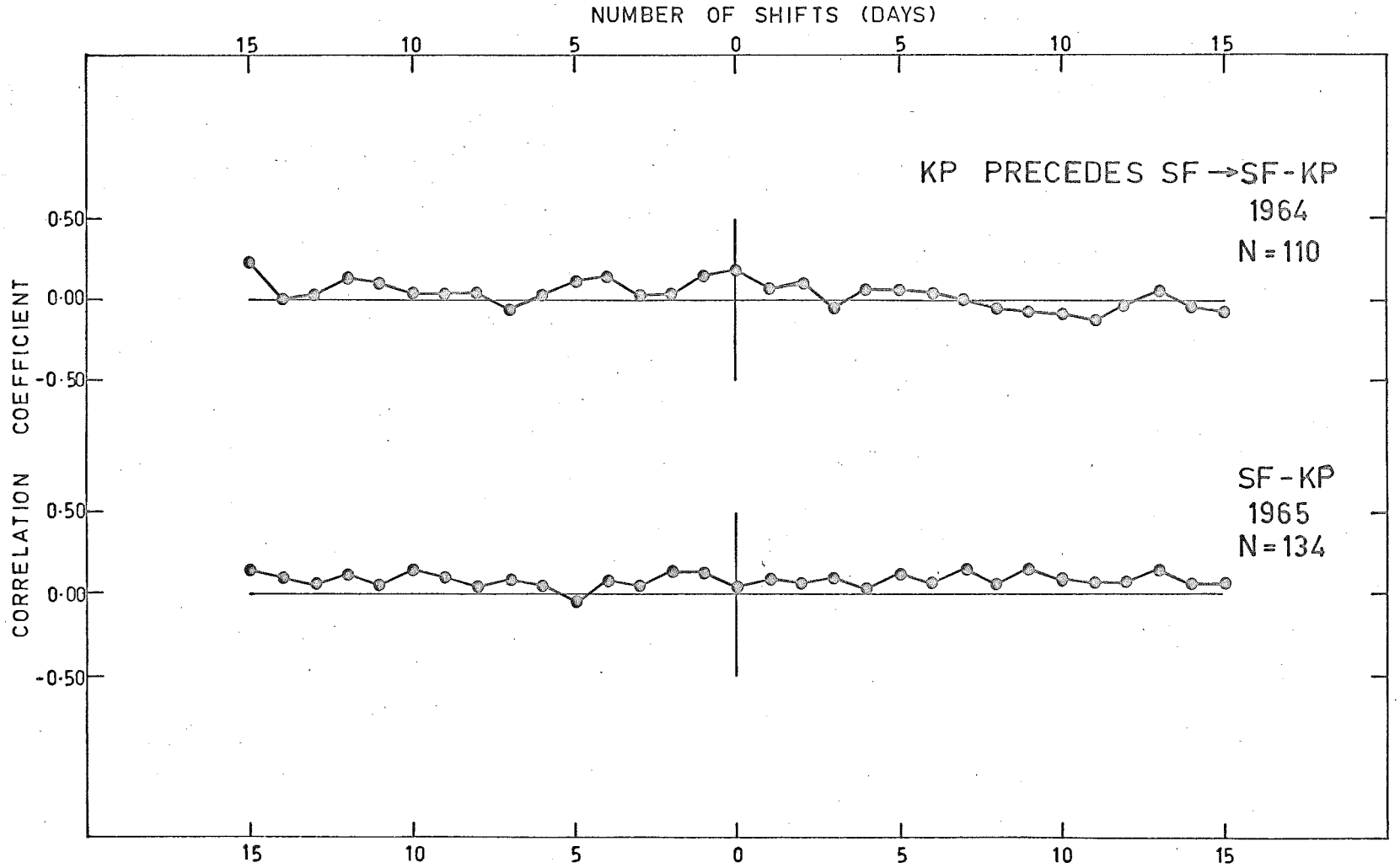

Figure 6.18 Correlation functions between spread-F and planetary K_p indices.

CHAPTER 7. SOME DETAILED EXAMINATIONS OF RELATIONSHIPS BETWEEN SCINTILLATION AND OTHER PARAMETERS

7.1 The Association of Scintillation Amplitude with Sporadic-E and Spread-F

In addition to the correlations evaluated on a purely statistical basis in Chapter 6, it is desirable to investigate the associations between scintillation and other parameters in more detail. Limited quantities of the scintillation amplitude data from the smaller interferometer records were compared directly with the sporadic-E and spread-F data from the Woomera ionograms.

(i) The Association with Sporadic-E. The amplitude scintillation indices from the day time (summer) transits of the Cygnus A source were compared for each transit with the maximum reflection frequencies of the sporadic-E layer - the few transits for which spread-F was observed being excluded from the comparison. Figure 7.1 shows the number of times each scintillation index was observed when the sporadic-E critical frequency was within a given range and, as in Chapter 6, the figure includes no distinction between the types of sporadic-E recorded at Woomera.

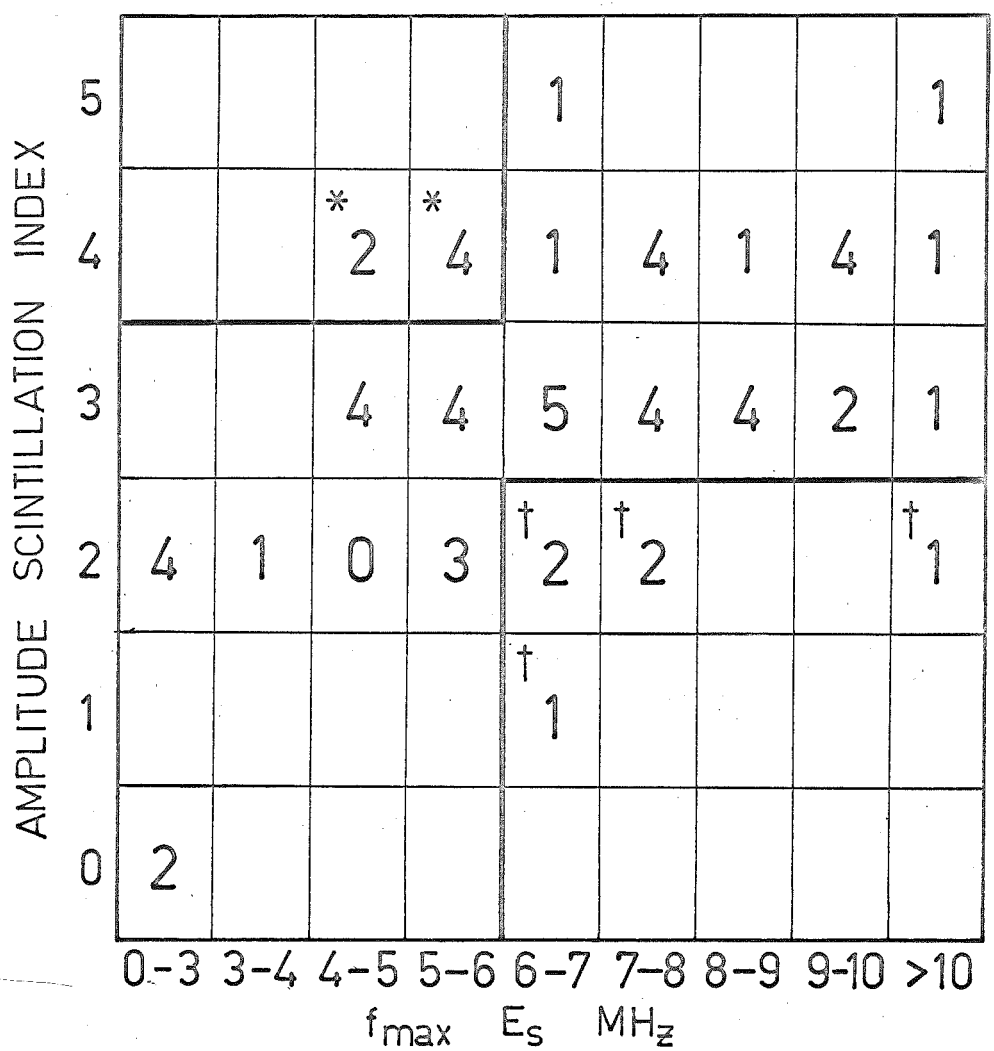

Figure 7.1 The number of associations of daytime (summer) scintillation index with sporadic-E maximum frequency.

It is evident from the Figure that generally the observed scintillation will be weak (index ≤ 2) if the critical frequency is less than 6 MHz and that it will be moderate to strong (index ≥ 3) if the critical frequency exceeds this value. However, even in the limited data presented in the Figure there are 6 occasions for which strong scintillation was observed when the sporadic-E critical frequency was less than 6 MHz and a further 6 occasions for which little scintillation was observed when the sporadic-E critical frequency was greater than 6 MHz. It was thought possible on those occasions when little scintillation was observed in association with a high critical frequency, that the appropriate ionogram might indicate that the sporadic-E layer was very thin or very smooth compared to other occasions when the critical frequency had a similar value and the observed scintillation was stronger. However this proved not to be the case.

Although Figure 7.1 indicates that there is a general increase of scintillation activity with increasing sporadic-E critical frequency, exceptions to this exist and this relationship between the parameters is not clear cut.

(ii) <u>The Association with Spread-F</u>. The amplitude scintillation indices from the night time (winter) transits of the Cygnus A source were compared for each transit with

the spread-F indices - the few transits for which sporadic-E was observed being excluded from the comparison. Figure 7.2 shows the number of times each scintillation index was observed for a given spread-F index.

It is evident that this Figure shows the same general increase of scintillation activity with increasing spread-F as Figure 7.1 showed for increasing sporadic-E, however there are again exceptions to this simple relationship. Specifically, there are 5 occasions for which little scintillation was observed in association with strong spread-F and 14 occasions for which moderate to strong scintillation was observed in the complete absence of spread-F. In fact, in the absence of spread-F, scintillation was as likely to be moderate to strong as it was to be weak.

Those occasions when scintillation indices of 3 and 4 were observed in the absence of spread-F (or sporadic-E) can be readily explained if the ionospheric irregularities responsible for the scintillation are at a height greater than the F region maximum electron density in which case they will be invisible to ground based sounders. The work of previous authors justifying this interpretation has already been reviewed in Section 1.4(iv). The observations of weak scintillation (index ≤ 2) in association with strong spread-F could be interpreted as evidence of inversion

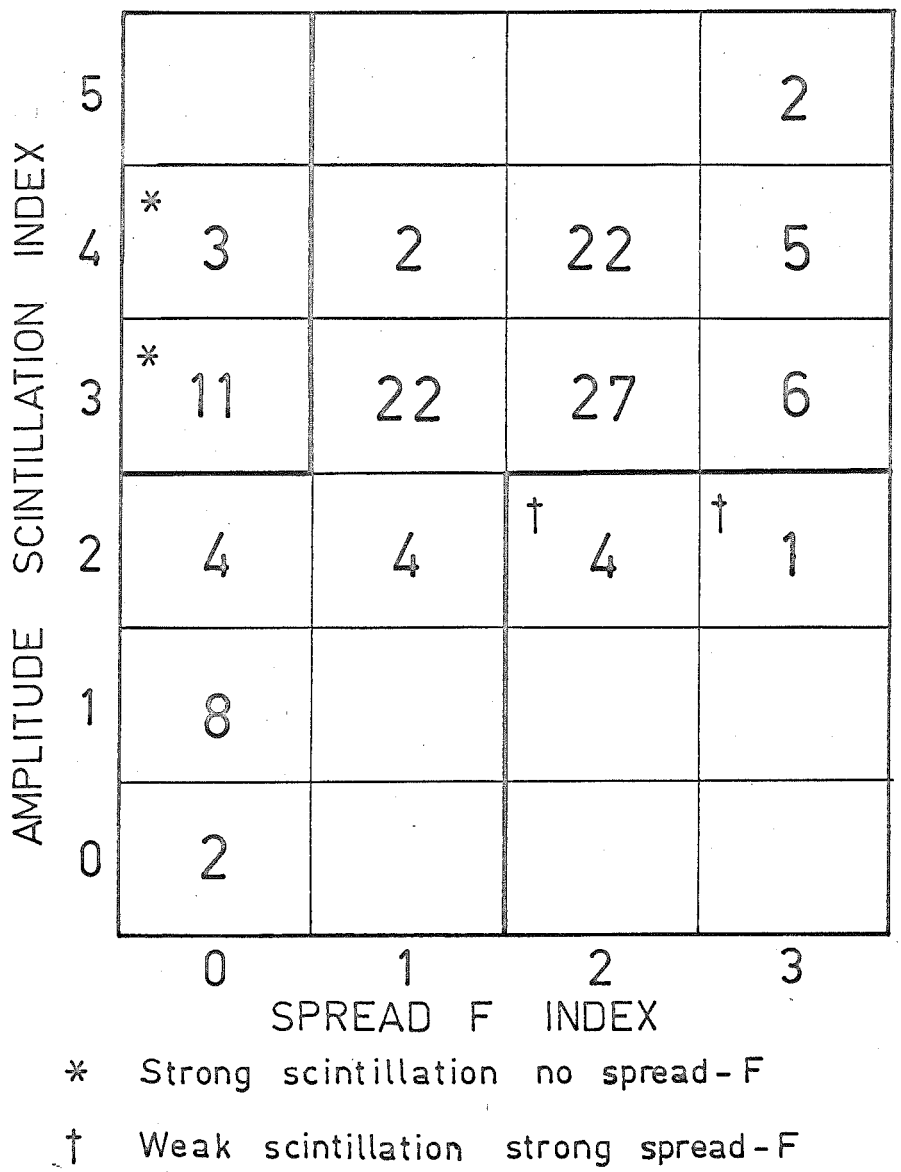

Figure 7.2 The number of associations of night-time (winter) scintillation index with a given spread-F index.

i.e. stronger scintillation might have been recorded if a higher observing frequency had been available, but the observations can also be explained from the patchy nature of spread-F: the phenomenon may not have been observed had the ionosonde been under the intersection point of the line of sight from the interferometer to the Cygnus A source with the F region.

The results show that inversion probably occurs during a small number of the transits of the Cygnus A source at night, but this number is not large enough to support the suggestion advanced in Chapter 5 that inversion might be responsible for the anomalous decrease in scintillation depth near the horizon.

7.2 On the Rate of Scintillation

Generally, the rate of radio star scintillation is determined by the scale size of the diffracting screen ($L = 2\pi r_o$) from which the scintillation originates and also by its drift velocity where, as Hewish (1952) concluded, the time varying electron density at a given point in the ionosphere is interpreted as arising from horizontal movements of unchanging irregularities rather than from rapid changes in a static ionosphere. It should be pointed out that neither the drift velocity nor the scale size of the diffracting screen can be determined from the observations of radio

star scintillation with a single interferometer since a value for one of these must be assumed before a value can be obtained for the other. A similar restriction applied to the satellite scintillation observations of Yeh and Swenson (1964) where they were forced to assume a height for the scintillation origin in order to obtain an estimate of the irregularity scale size. The inaccuracy of their size estimates has already been stressed in Section 1.4(iii).

Even in the absence of real drifts of the ionospheric irregularities, from the ground they will have an apparent drift towards the east (towards the west at the lower culmination of a circumpolar source), due to the earth's rotation. Hewish (1952) stated that this apparent drift is given by the expression $\omega z \cos \delta$ where ω is the angular velocity of the earth's rotation, z is the distance from the irregularities to the ground, and δ is the declination of the radio source. Tuominen et al. (1962) have since published the derivation of the above expression although their result was not reduced to this simple form. The apparent velocities of E and F region irregularities appropriate to the transit observations of the Cygnus A source from St. Kilda, South Australia are respectively 7 m/sec and 17 m/sec: both these velocities are much less than the actual drift velocities generally observed in these regions.

In particular, Reid (1957) and Tuominen et al. (1962) observed the different scintillation rates of the signals from the Cassiopeia A source at upper and lower transits and determined that the rate of scintillations originating in the F region was determined by a real rather than apparent drift. These authors did not consider variations in magnetic activity which, as discussed in Section 1.4(v) and below, could introduce additional variations in the scintillation rate: this should not have been important for their observations which spanned a full year since any effects of magnetic activity should have averaged out over this time.

Day to day (or shorter period) changes in the scintillation rate have been observed by many authors and can arise due to changes in the scale size of the diffracting screen or due to changes in its drift velocity. As noted in Sections 1.4(iii) and 1.4(v), the scale size of the diffracting screen is reduced and the drift velocities are increased during periods of enhanced magnetic activity. Dagg (1957a) observed a particularly close relationship between scintillation rate and magnetic activity.

The rate of the scintillations observed in the signals from the Cygnus A source may be influenced by magnetic activity but in this experiment there is an additional influence to be considered which probably was not present

in the northern hemisphere observations directed predominantly away from the equator.

In Chapter 6 it was shown that scintillations in the signals from the Cygnus A source were associated with sporadic-E irregularities during the day and with both sporadic-E and spread-F irregularities during the night. It is suggested that the rates of scintillation originating from the two regions would be different if the scale sizes and/or drift velocities in the E and F regions were not the same. Since most of the northern hemisphere observations were concerned with sources at higher elevation angles and no association was established between scintillation and sporadic-E, this possible cause of variations in the scintillation rate was excluded.

7.3 The Origin of the Day to Day Variations in the Scintillation Rate

The indices S, M, and F indicating slow, moderate and fast scintillation rates have already been discussed in Section 3.4(iii) and illustrated in Figure 3.5. They refer only to marked differences in rate from one day to the next - one of the indices being assigned to each recorded transit of the Cygnus A source by visual inspection. The records of Cygnus A showing no scintillation were excluded from the analysis.

In Table 7.1 the scintillation rates are compared in 4 contingency tables with the occurrence and non-occurrence of sporadic-E and spread-F to check on possible associations with these parameters. Since the assignment of the rate indices was not confined to transits showing strong scintillation, sporadic-E was deemed to occur if the maximum frequency of reflection exceeded 4.0 MHz. All the available data are included in the tables but the occasions when spread-F and sporadic-E were both present have not been excluded. Since it was intimated in Section 7.1 that such occasions were few, their inclusion should have little bearing on the results. On those occasions when slow scintillation was not present, fast scintillation may have been and vice-versa.

		SPORADIC-E OCCURRED		SPREAD-F OCCURRED	
		YES	NO	YES	NO
SLOW SCINTILLATION OCCURRED	YES	82	23	54	51
	NO	229	100	205	124
		$\chi^2 = 2.43$		$\chi^2 = 3.48$	
FAST SCINTILLATION OCCURRED		YES	NO	YES	NO
	YES	27	34	47	14
	NO	284	89	212	161
		$\chi^2 = 12.24$		$\chi^2 = 8.08$	

TABLE 7.1 Contingency tables between fast and slow scintillation, sporadic-E and spread-F.

The statistical significance of the distributions presented in Table 7.1 may be conveniently established with the aid of the χ^2 test as published in standard statistical texts and the value of χ^2 for each contingency table is included in Table 7.1. The standard texts indicate that the 2 x 2 contingency tables presented have only 1 degree of freedom and the values of χ^2 which indicate confidence levels of 95%, 99.0% and 99.9% that a distribution does not differ from the expected one by chance are respectively 3.9, 7.0 and 12.0.

The contingency tables show that fast scintillation is observed less often than expected when sporadic-E is present and more often than expected when spread-F is present. Both values of χ^2 exceed the 99% confidence level.

The situation is not quite so clear cut when slow scintillation is observed but there is a small tendency for slow scintillation to be observed more often than expected when sporadic-E is present and less often than expected when spread-F is present. Neither of the values of χ^2 reach even the 95% confidence level. However, the two contingency tables describing the occurrence of slow scintillation show their small departures from the expected distributions in opposite senses and Table 7.2 shows the number of observations of occurrence or non-occurrence of slow scintillation when spread-F occurred compared with

the same observations when sporadic-E occurred.

		Total	Slow Scintillation	
			Observed	Not Observed
Sporadic-E	Present	311	82	229
Spread-F	Present	259	54	205
Normalized		311	65	246

TABLE 7.2

If it is assumed that the expected distribution is that observed in the presence of sporadic-E then the value of χ^2 appropriate to the distribution in the presence of spread-F can be evaluated after normalizing the number of spread-F observations to allow for the fact that it was different from the number of sporadic-E observations. The value of χ^2 appropriate to Table 7.2 is 4.81 - in excess of the 95% confidence level. It is concluded that although neither distribution is significantly different on its own from the distribution expected if slow scintillation is completely unassociated with either sporadic-E or spread-F, the difference between the distributions in the presence of sporadic-E and spread-F is significant.

It should be realized that although the above associations of fast and slow scintillations with sporadic-E and spread-F appear conclusive, a cause and effect relationship

is not definitely established, Another influence, not considered, could be controlling the variations of the scintillation rate and ionospheric indices in such a way that the associations could be due to a common temporal variation in the parameters. To completely remove this possibility the analysis should be limited to a restricted range of local times when sporadic-E and spread-F have similar probabilities of occurring or not occurring. Unfortunately this limitation is a difficult one to overcome since during the day spread-F rarely occurs and sporadic-E almost always occurs and during the night spread-F almost always occurs. The complete occurrence or non-occurrence of one of the ionospheric indices within a restricted range of local times tends to reduce the significance of the analysis.

The scintillation rate indices may also be compared with magnetic activity indices. Due to the limited time resolution of the rate indices, the magnetic activity was considered strong or weak according to the published tables of 5 disturbed days (D) and 10 quiet days (Q and q) per month and was considered moderate on other days.

In the past, the objection has been raised that disturbed days in a magnetically quiet month might not have been listed as disturbed in a magnetically active month; however, this objection is thought not to apply here due

to the similar levels of solar activity in the years 1964 and 1965.

Table 7.3 shows a contingency table between the magnetic activity and scintillation rate on the same day and another between magnetic activity and scintillation rate on the following day. It includes the normalized numbers of quiet and disturbed day observations which take into account the fact that the numbers of these days were not the same as the number of days of moderate magnetic activity, and also includes the values of χ^2 calculated for the quiet and disturbed day distributions of scintillation rate - these values being calculated on the assumption that the expected distribution was observed on moderately active days. Unlike the previous contingency tables, those in Table 7.3 have 2 degrees of freedom and the values of χ^2 which indicate confidence levels of 95%, 99.0% and 99.9% that a distribution does not differ from the expected one by chance are respectively 5.9, 9.0 and 13.0.

The contingency tables show that there is no significant difference between the distributions of the scintillation rates during or following moderate or quiet magnetic conditions. On the other hand, the values of χ^2 for the distributions of the scintillation rates during or following disturbed magnetic conditions exceed the 99.9% signi-

SCINTILLATION AND MAGNETIC ACTIVITY ON THE SAME DAY

Magnetic Activity	Scintillation Rate				χ^2
	Slow	Mod.	Fast	Total	
Moderate	61	193	38	292	
Quiet	40	128	18	186	
	63	201	28	292	3.03
Disturbed	13	77	9	99	
	38	227	27	292	17.85

MAGNETIC ACTIVITY PRECEDES SCINTILLATION BY 1 DAY

Magnetic Activity	Scintillation Rate				χ^2
	Slow	Mod.	Fast	Total	
Moderate	57	198	35	290	
Quiet	43	124	23	190	
	65	190	35	290	1.50
Disturbed	14	76	7	97	
	42	227	21	290	13.79

TABLE 7.3

Contingency tables between the scintillation rate and magnetic activity.

cance level, but if the tables are examined closely, it is evident that the observations of fast scintillation are not enhanced under these conditions as would have been expected from past experiments; rather, the numbers of observations of fast and slow scintillation are both reduced in favour of an increased amount of moderate rate scintillation. This is an unexpected result with no physical basis for support.

It is probable that the indices of scintillation rate and magnetic activity have not been assigned sufficiently rigorously to show that the usual association between these indices is present here. However it does seem that in the present experiment, the rate of the scintillation is related more closely to the ionospheric region in which the scintillation originates than to the magnetic activity.

CHAPTER 8. FOCUSSED SCINTILLATIONS AND SOURCE VISIBILITY FADES

8.1 Focussed Scintillations

The focussing of radio star signals by ionospheric irregularities has already been discussed briefly in Section 1.1 where it was indicated that some scintillation observations from swept frequency interferometers were better interpreted from a ray optics approach than from a random diffraction approach. As Briggs (1966) pointed out, the two theories are not in any way in conflict, but the ray optics approach has advantages over the random diffraction approach when extended irregularities with large values of ϕ_0 are considered.

In particular, Warwick (1964) and Singleton (1964a and b) in the northern hemisphere and Wild and Roberts (1956) in the southern hemisphere observed fluctuations in signals from radio stars which they interpreted as originating from large irregularities in the electron density which behaved like converging lenses: they also observed fluctuations of a different character which they considered originated in large irregularities acting as prisms. Singleton (1964a) established an F region origin for the fluctuations introduced by the lens like irregularities.

Dagg (1957e) used a total power receiving system on a fixed frequency and also observed signal fluctuations on some occasions which he could not explain using diffraction theory. He explained these on the basis that they were produced by large ionospheric irregularities behaving like diverging lenses and established that their origin was associated with sporadic-E.

It should be noted that because the radio frequency refractive index decreases with increasing electron density, a converging lens-like irregularity is deficient in electrons compared with the electron concentration away from the irregularity.

In the present experiments, there were about 8 occasions when signal fluctuations appeared more likely to have originated from single irregularities than from a diffracting screen. Figure 8.1 shows 2 records of the Cygnus A source detected by the smaller interferometer. Two of these records are similar in appearance to the diffraction pattern calculated by Gagnon (1964) for signals which have been focussed by a converging lens, and the other shows similarity to the observations of Dagg (1957e) and therefore might be due to the passage overhead of an irregularity behaving like a diverging lens.

Figure 8.2 shows 2 records of the Virgo A source detected by the larger interferometer; one of them has

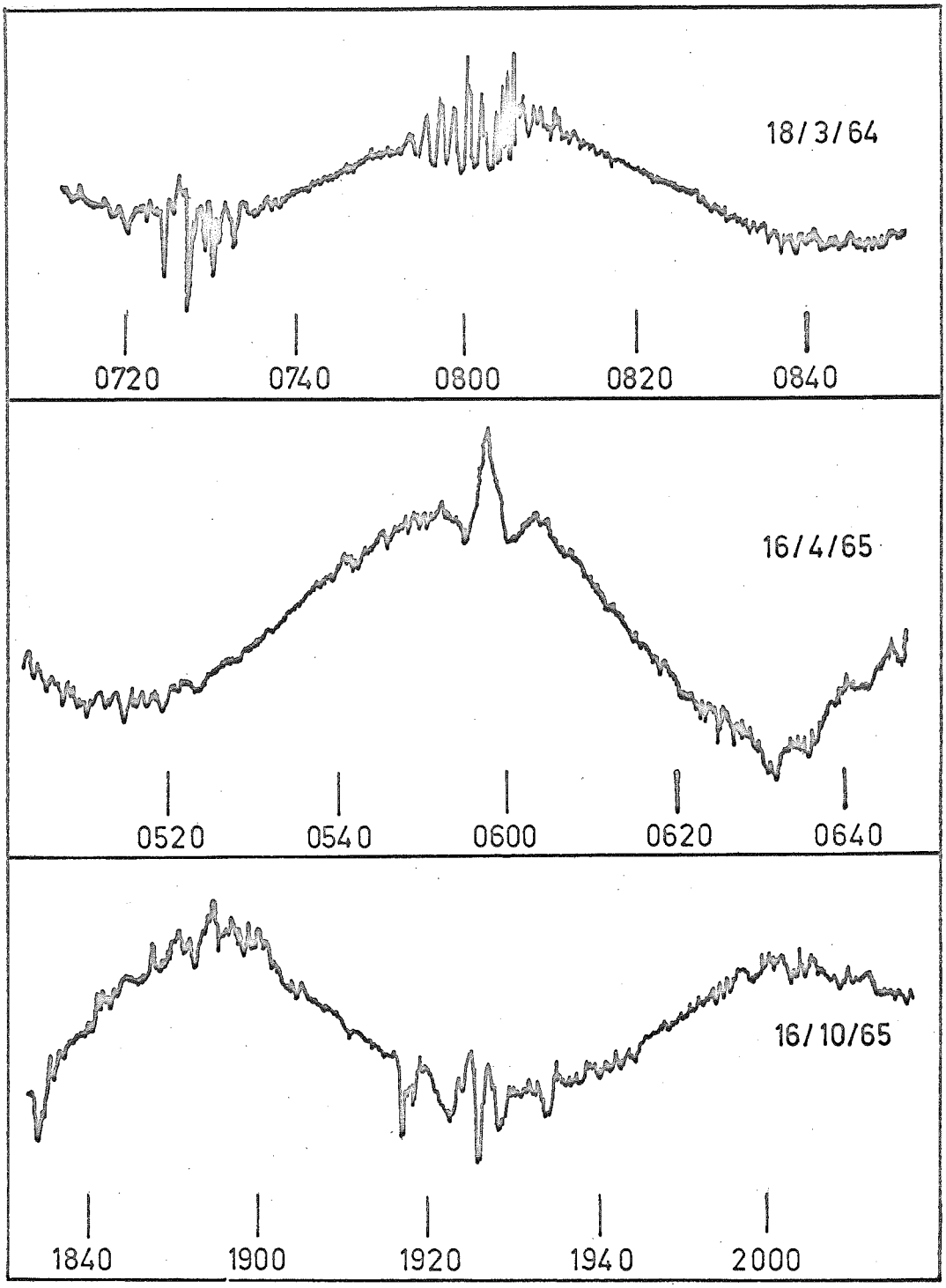

Figure 8.1 Evidence of focussing irregularities in the signals from the Cygnus A source.

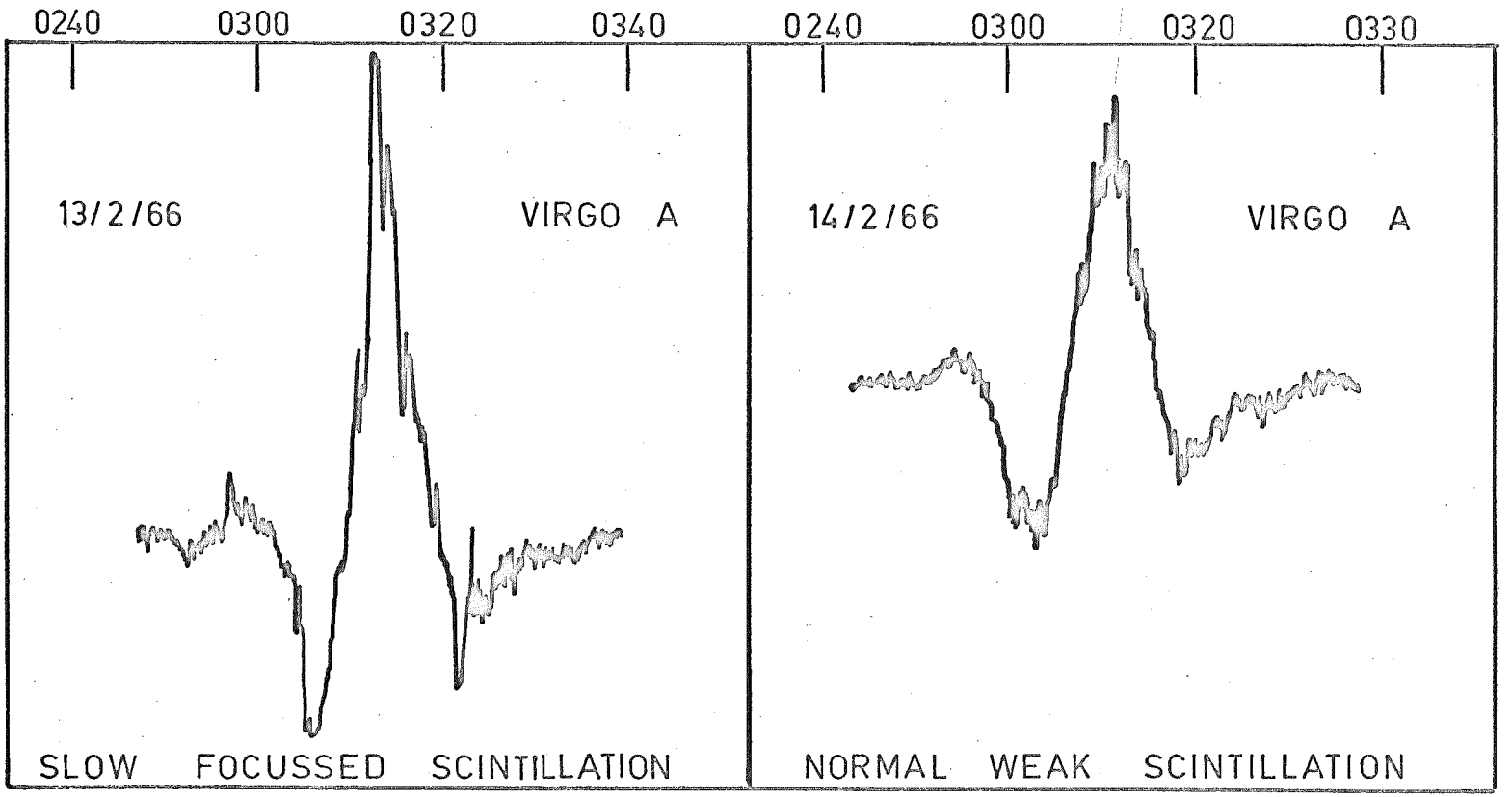

Figure 8.2 Possible evidence of a focussing irregularity in the signals from the Virgo A source.
The transits of the Centaurus A source on the same days (1 hour after Virgo A) indicated that the gain of the receiver was the same for the two Virgo A passes.

weak scintillation with the usual appearance (Figure 3.6), and the other (for the preceding day) shows a single amplitude fluctuation superimposed on the fringe envelope which appears likely to have originated from a focussing type irregularity.

The signals recorded at St. Kilda of the beacon satellites often indicated the presence of discrete focussing irregularities in the ionosphere but satellite passes within an hour of the radio source transits shown in Figures 8.1 and 8.2 did not indicate the presence of any such irregularities. The only possible vindication of the radio star observations came from a record of the satellite Be-B on February 13, 1966 which showed a single focussing irregularity low in the north-west, but this record was taken some 7 hours after the Virgo A transit occurred.

There were no unusual or consistent features of the Woomera ionograms which were recorded during the source transits shown in Figures 8.1 and 8.2. They showed variable amounts of sporadic-E and spread-F.

Due to the rare occurrence of the apparently focussed signal fluctuations, it was not possible to investigate the possibility of a diurnal variation in their occurrence. However, the St. Kilda beacon satellite observations

suggest that they are usually detected during the day and it is true that of the few occasions on which they were detected in radio star signals, only one occurred during the night.

The possibility of the shape of the fringe pattern of the smaller interferometer output being altered due to the influence of large irregularities in the ionization has already been discussed in Section 4.10 under the heading of irregular wedge refraction. The difference between the observations shown in Figures 4.5 and 8.1 is explained when it is realized that if the signals are influenced by a large irregularity during a zero-crossing in the receiver output, the position of the source appears to change, whereas if the influence occurs when the output is a maximum or minimum, the signal amplitude appears to change.

A focussing mechanism is also thought to explain the observation that especially during the transits of the Cygnus A source recorded by the smaller interferometer, there was a tendency for fluctuations to reach peaks of amplitude that could take values of several times the undisturbed signal strength from the radio star. These large fluctuations are probably similar to those observed by Dueno (1956) who did not offer an explanation for their occurrence.

Focussing is suggested as a possible explanation for these fluctuations because, even though they were of shorter duration than those of Figures 8.1 and 8.2 and were usually detected on the same records as were scintillations of normal appearance, there were often indications that their profile was similar to that calculated by Gagnon (1964) for the diffraction pattern on the ground for signals which have passed through a focussing irregularity. The shorter period of the fluctuations can possibly be explained in terms of the size, intensity, and height of the irregularities producing these fluctuations being different from the same parameters appropriate to the irregularities producing the longer period fluctuations.

Figure 8.3 shows parts of 2 records of the large amplitude fluctuations in scintillations of the signals from the Cygnus A source. Both are records of night time transits and the appropriate Woomera ionograms show that spread-F of moderate intensity was recorded throughout both transits, but there was no sporadic-E. There were no satellite scintillation records available for comparison with these passes - the beacon satellites not having been launched until later dates.

The transits of Cygnus A in Figure 8.3 were not isolated examples of the large amplitudes fluctuations

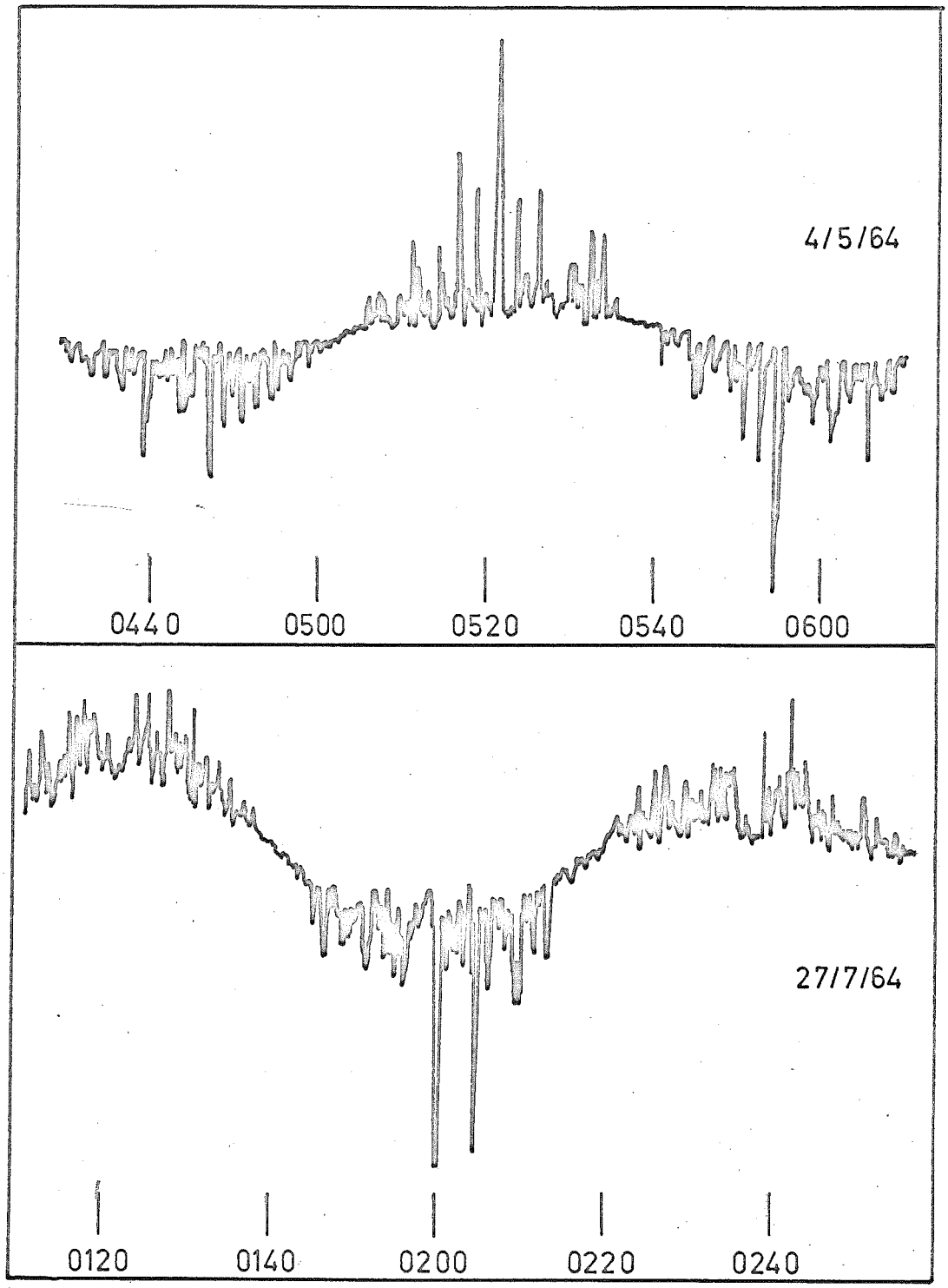

Figure 8.3 Night-time focussed scintillations in the signals from the Cygnus A source.

being detected: in fact there were 75 occasions throughout the 2 year period of operation of the smaller interferometer when they were thought to occur. However, when the normal scintillation was very strong there was some difficulty in recognizing the presence of focussing so that no serious attempt was made to determine whether the occurrence of focussing followed a diurnal variation although it did seem that occurrence was more likely at night (when scintillation was strongest).

Figure 8.4 shows a day time transit of the Cygnus A source where the large amplitude fluctuations supposedly due to single irregularities are difficult to distinguish from normal, strong scintillations. The ionograms recorded during the transit showed blanketing sporadic-E traces to 8.0 MHz but a record of the Be-B satellite made 4 hours later in the day showed no scintillation.

Hewish (1952) found that the intensity of moderate scintillations followed a displaced Gaussian distribution and that the intensity of very strong scintillations followed a Raleigh distribution. Thus, a record of strong scintillation (index = 5) is expected to show some large amplitude peaks similar to the those illustrated. However, particularly in the record for August 27th 1964 shown in Figure 8.3, the scintillation generally is only moderate

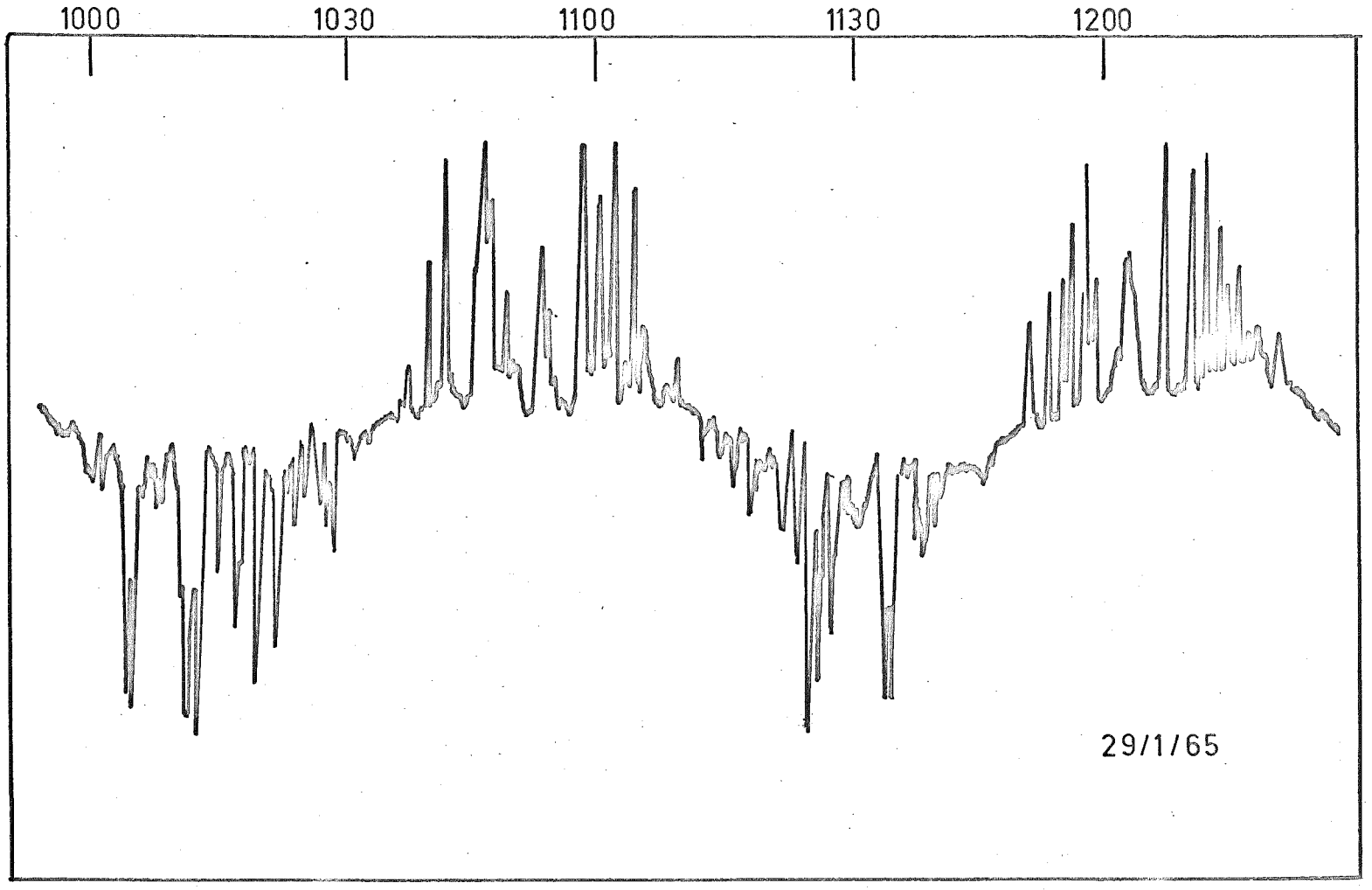

Figure 8.4 Daytime focussed scintillations in the signals from the Cygnus A source.

(index = 3), . . there are no instances where the signal level falls to zero due to the scintillation, and the displaced Gaussian distribution does not predict that the very large amplitude peaks should be observed. The scintillations on the other records shown are much stronger but they are included as examples of focussing since some of the large amplitude peaks show evidence of the profile expected from a focussing irregularity.

The origin of the focussed fluctuations has not been definitely established in this experiment but from the ionograms describing the day time pass of Figure 8.4 and from the possible maximum occurrence at night, it appears that focussing of radio star signals can be associated with either sporadic-E or spread-F irregularities. Some more definite association will probably be established when the St. Kilda Beacon satellite records are analysed in detail.

8.2 Source Visibility Fades

Source visibility fades on interferometer records have already been discussed briefly in Section 1.2 where it was specially noted that observations to date have been restricted to the equatorial and auroral regions. Visibility fades are thought to be observed when the angular

scintillation of the source is sufficiently large that the apparent position of the source varies rapidly through an angle larger than the interferometer lobe size. It is of interest to decide the likelihood that they be observed with either of the St. Kilda interferometers.

From Booker (1958) the root-mean-square angular scintillation in the far zone when ϕ_o is greater than 1 radian is given by:

$$\theta_o = \frac{\lambda}{2\pi r_o} \cdot \phi_o \qquad (8.1)$$

It depends not only on ϕ_o but also on r_o - the size of an irregularity.

It has already been pointed out in Section 2.5 that the output of an interferometer from a uniform extended source is reduced by a factor sin x/x where :

$$x = \frac{\pi d \Delta\theta}{\lambda} \qquad (8.2)$$

and $\Delta\theta$ is the angular diameter of the source in radians.

The root-mean-square angular deviation in position of a point source required to reduce the visibility by an equivalent amount is given by :

$$\theta_o = \frac{\Delta\theta}{2\sqrt{2}} \qquad (8.3)$$

and if the factor is to be one half, $x = 1.875$.

If the above 3 expressions are combined, the minimum value of the ratio ϕ_o/r_o associated with a given observation of a visibility fade may be determined, but the minimum ϕ_o alone cannot be determined unless a value is assumed for r_o. Further, from Briggs and Parkin (1963), $\phi_o \approx \lambda$ and so the value of the ratio ϕ_o/r_o for 39.5 MHz when the visibility fades were observed on a higher frequency may be determined.

The values of this ratio for the observations of Koster (1958) near the magnetic equator, and for Benson (1960) and Little et al. (1962) in the auroral zone are listed in Table 8.1 together with the minimum values required if a fadeout is to be observed on either of the St. Kilda interferometers.

Observer	Frequency MHz f	Wavelength M	Angle Degrees $\Delta\theta$	θ_o	Interferometer Baseline Wavelengths	ϕ_o/r_o f	ϕ_o/r_o 39.5 MHz
Koster	45	6.66	1.14	0.40	30	6.60×10^{-3}	7.50×10^{-3}
			6.82	2.41	5	3.98×10^{-2}	4.53×10^{-2}
Little et al. Benson	223	1.345	0.50	0.81	68	1.47×10^{-2}	8.30×10^{-2}
St. Kilda	39.5	7.60	8.55	3.02	4		4.37×10^{-2}
			2.85	1.00	12		1.44×10^{-2}

TABLE 8.1

It should be especially noted from the Table that Koster observed fadeouts on an interferometer with a baseline intermediate between the two St. Kilda interferometer baselines and he used a similar frequency.

Table 8.2 shows the minimum phase deviations corresponding to the above observations calculated on the assumption that r_o = 300 metres: this value is less than those used in Section 5.4 in the discussion of the zenith angles variations of scintillation depth but was suggested by Little et al. (1962) as the value likely to be appropriate to their fadeout observations which were made during magnetically disturbed periods.

Observer	Frequency	Interferometer Baseline	r_o = 300m	
			ϕ_o f	ϕ_o 39.5
Koster	45	30	1.98	2.25
		5	11.9	13.6
Little et al. Benson	223	68	4.41	24.9
St. Kilda	39.5	4		13.1
		12		4.3

TABLE 8.2

At first sight, the value of ϕ_o for the auroral zone appears anomalous since as this interferometer has the largest baseline and therefore requires the smallest angular

deviation, it might be though that the minimum value of ϕ_o corresponding to the observation for a given r_o would have been less than all the other values of ϕ_o. The apparent anomaly is resolved by expression 8.1 where the wavelength dependence of θ_o shows that for a given θ_o, ϕ_o must be larger at a smaller wavelength. Since the difference in frequency between Koster's observations and the St. Kilda observations is small, the wavelength dependence of θ_o is not as evident in these calculations as are the different θ_o values arising from the different interferometer baselines.

If r_o = 1 km, the root-mean-square phase deviations required to produce fadeouts on the records of the smaller and larger St. Kilda interferometers are respectively 43.7 and 14.4 radians. Although the values for the smaller interferometer are as large or larger (depending on r_o) than the values required in Section 5.6 for inversion to be observed due to the source size or scintillation bandwidth, (this observation was in any case not definitely established), it is just possible that if r_o is sufficiently small, a fadeout could be observed, the value of ϕ_o required being similar to that observed by Koster. For the larger interferometer the value of ϕ_o required to produce a fadeout is less than for the smaller interferometer and the probability of detecting one is enhanced.

A detailed inspection of the records showed that no visibility fades were detected by the smaller interferometer.

One disadvantage compared with other observers in seeking evidence of visibility fades in the records of the larger St. Kilda interferometer comes from the fact that the other observers recorded a series of maxima and minima in the output from a radio star source and usually detected a fade in only one or two of these: they were able to establish the presence of the fade by comparison with the other maxima and minima in the output from the same source during the same transit. As was illustrated in Figure 2.6, in the case of the larger St. Kilda interferometer, only a single maxima is observed in the output from each source and as well as making amplitude comparisons difficult, the period of time for which the ionospheric irregularities are under surveilance is reduced. In fact the nine sources received represent a total observing time of only two hours per day. On the question of determining whether or not the output from a source is reduced, the amplitude of the record from a given transit of one source must be compared with the amplitudes for the preceding and following transits of the same source and with the amplitudes of the output from other sources on all three days.

Since the receiver is operated with automatic gain control which is based on the signal level from the galactic background radiation, then variations in the amplitude of the records from the discrete sources arising from day to day changes in ionospheric absorption, should be minimised. In any case, ionospheric absorption (especially D region) is not expected to be important at night.

There was just one record from the larger interferometer which could possibly be interpreted in terms of a visibility fade. Figure 8.5 shows transits of the source Fornax A for 1900 hours local time and of the source Pictor A for 2100 hours local time for the 28th, 29th and 30th December, 1965. It is evident that the amplitudes of all the Pictor A records are very similar but that the amplitude of the Fornax A record for the 29th December is considerably reduced in amplitude although some indication of scintillation is still present. The Pictor A record two hours later also shows evidence of scintillation but has the expected amplitude for the output from this source.

There were no Woomera ionograms available for any of the three days in question but a pass of the Be-B satellite two hours before the Fornax A transit on the 29th December showed strong scintillation which was probably due to diffraction from the edge of intense sporadic-E clouds. In

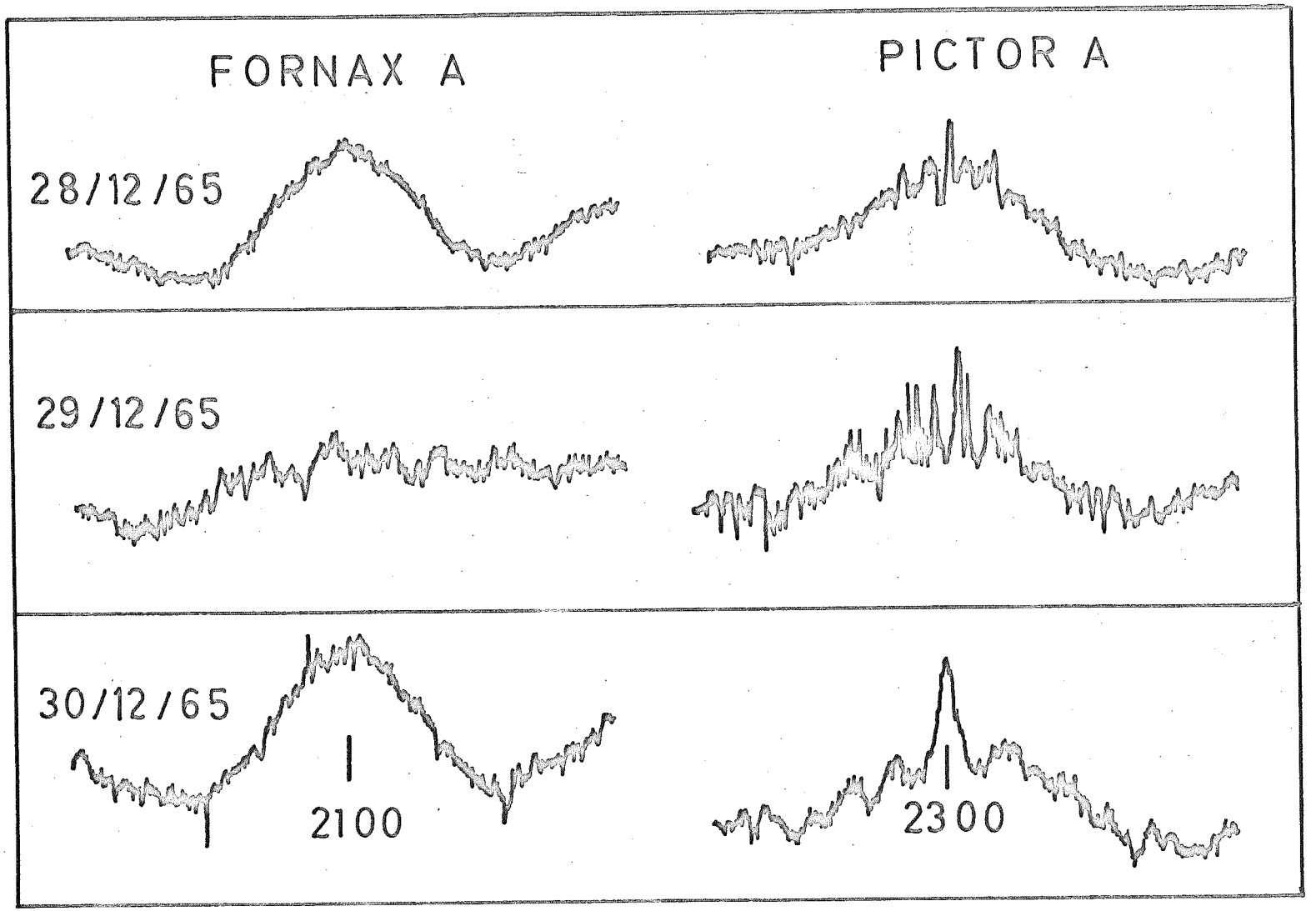

Figure 8.5 Evidence of a possible visibility fade in the signals from Fornax A on 29/12/65. Time scale 6" hour.

mid-latitudes, it is easier to visualize the small values of r_o and large values of ϕ_o required for a visibility fade as occurring in the E region rather than the F or a higher region.

CHAPTER 9. THE CONJUGACY OF F REGION PERTURBATIONS

9.1 Introduction

During the author's first year of candidature, a correlation analysis was carried out to investigate the possible relationship between the critical frequencies of the F region at magnetically conjugate points.

Singleton (1962a) correlated spread-F indices from three southern ionospheric stations with those from northern ionospheric stations - the indices from each southern station being correlated with those from the conjugate northern station and also with others recorded at some distance from the conjugate northern station. His spread-F indices were based on the daily total of hours for which spread-F was observed: thus he had one data point per day from each observing point. He found a significant positive correlation only between ionospheric stations in opposite hemispheres which were conjugate to each other and produced further results which suggested that the association of spread-F at conjugate points might be an indirect consequence of a more direct association of the critical frequencies at the same points.

Cummack (1967) used 2400 hourly values of $f_o F_2$ recorded over 100 days and, having removed the diurnal variation from

the data, found a significantly positive association between data from the conjugate ionospheric stations Rarotonga and Maui. The same association was not observed in data from stations with similar geophysical positions but which were not magnetically conjugate. Cummack also realized the importance of calculating more coefficients than just that for zero time shift between the sets of data although his cross correlation function was used for a different purpose than is the case here and in Chapter 6.

Other investigations have shown that many geophysical phenomena such as auroras, whistling atmospherics, and magnetic disturbances are related at geomagnetically conjugate points.

In the present analysis, the investigation was limited to data from Campbell Island in the southern hemisphere and from Anchorage, Fairbanks and Adak in the northern hemisphere. Table 9.1 shows, from Vestine and Sibley (1960), the geographic co-ordinates of the four ionospheric stations and also of the point near Anchorage which is conjugate to Campbell Island.

If the great circle distances between the various points in Table 9.1 are evaluated, Anchorage is found to be 280 km from the point conjugate to Campbell Island, Fairbanks and Adak are respectively 890 and 1940 km from Anchorage, and Fairbanks is 2165 km from Adak. The magnetic

Ionospheric Station	Geographic Latitude	Geographic Longitude
Campbell Island	52° 32'S	168° 59'E
Campbell Island Conjugate point	61° 58'N	154° 38'W
Anchorage	61° 10'N	149° 59'W
Fairbanks	64° 51'N	147° 50'W
Adak	51° 53'N	176° 39'W

TABLE 9.1

field line between Campbell Island and its conjugate point reaches a maximum distance from the earth's surface of 3 earth radii.

9.2 The Results of the Correlation Analysis

Using the correlation function program described in Section 6.4, cross-correlation functions were calculated between all possible pairs of ionospheric stations such that any association found between Campbell Island and Anchorage could be compared with associations found between Campbell Island and Fairbanks or Adak and also, the association of $f_o F_2$ between the three northern hemisphere locations could be determined. Hourly values of the F region critical frequency $f_o F_2$ were obtained for each of the observing sites from the CRPL data bulletins, values from

all the sites at times corresponding to 0000, 0600, 1200, and 1800 hours Campbell Island local time being selected. If the presence of the International Dateline is taken into account, Adak is 23 hours behind Campbell Island; the other northern stations are 21 hours behind. The data was for the year 1959 - the same as used by Singleton (1962d) - and was divided so that each length corresponded with a three month period centred on an equinox or solstice.

There were a number of missing values in the data, especially in that from Fairbanks, the most common cause of the missing values being polar blackout.

The above method of analysis is adequate for removing spurious correlations due to common diurnal variations in the sets of data and the shapes of the correlation functions indicate (as in Sections 6.7 and 6.8) whether the correlations observed for zero time shift are due to instantaneous associations between the data or due to common or opposite seasonal variations.

No distinction has been made between magnetically disturbed and quiet conditions.

With the data from 4 observing sites, 4 times of the day and 4 periods of the year, a total of 96 cross-correlation functions were evaluated. Some of these are illustrated in Figures 9.1 - 9.4. Since none of the Figures illustrate anything but instantaneous correlations, the

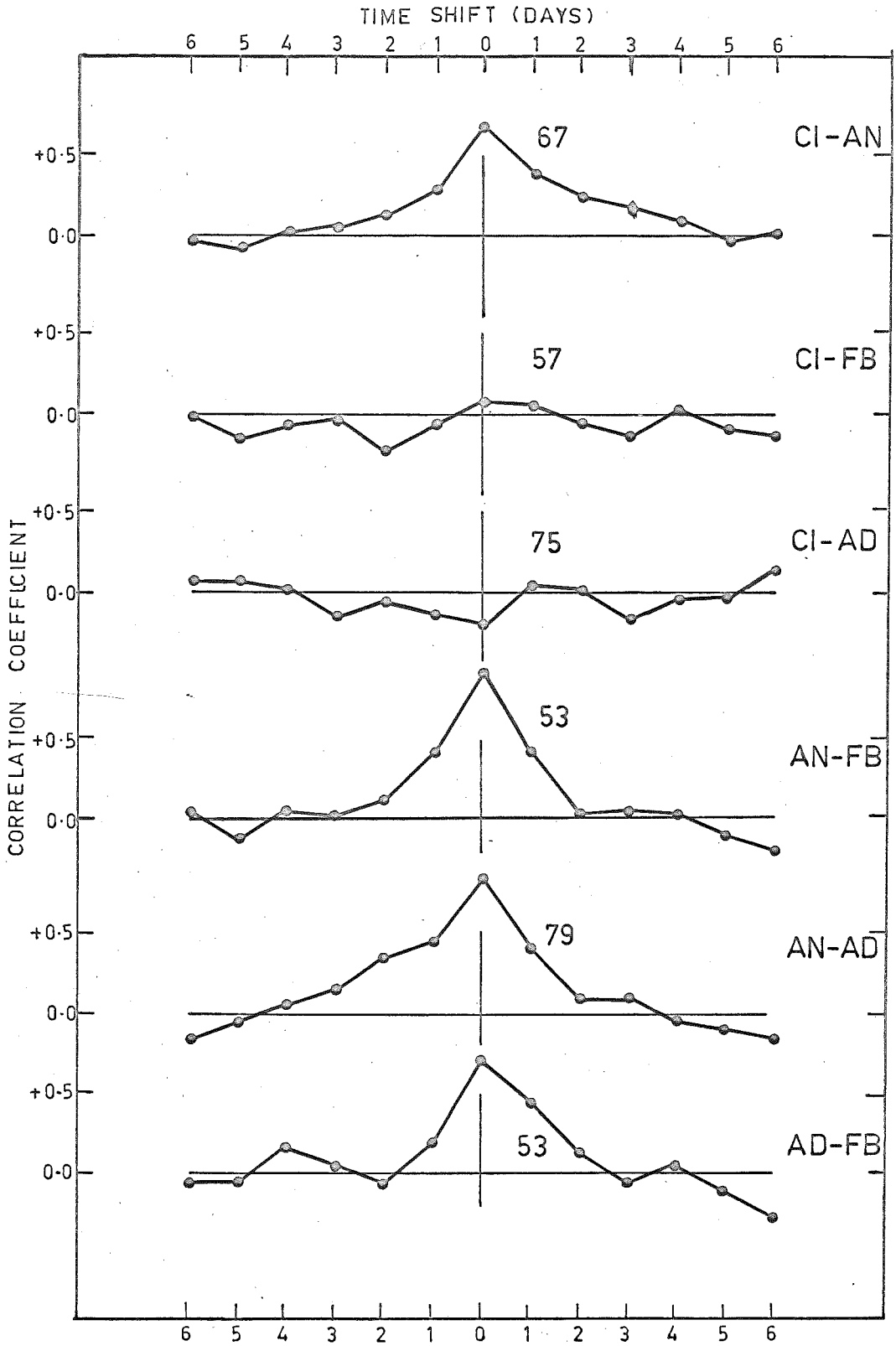

Figure 9.1 Cross-correlation functions of f_0F_2 at Campbell Island and three northern hemisphere locations for June, 1200 hours.

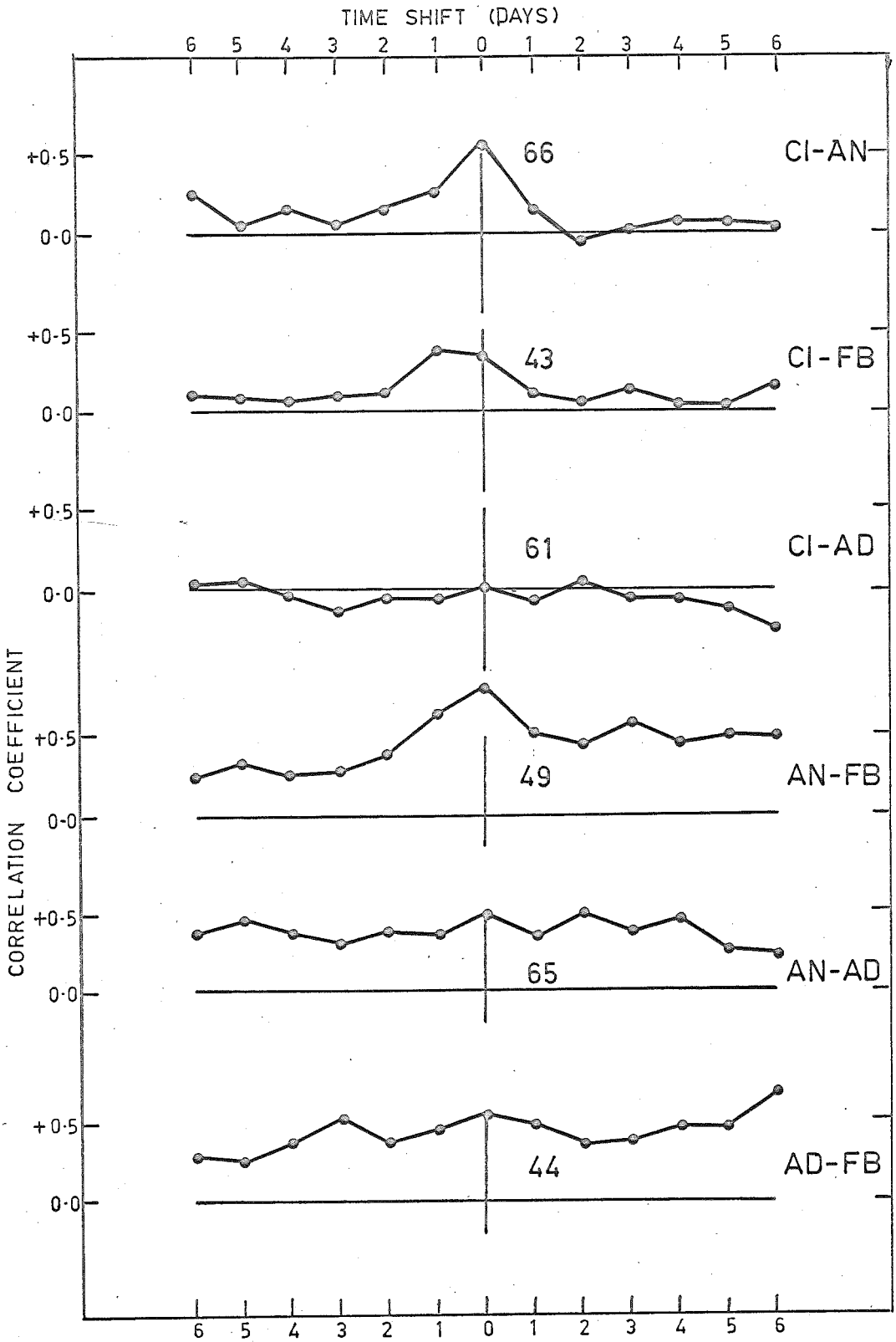

Figure 9.2 Cross-correlation functions of f_oF_2 at Campbell Island and three northern hemisphere locations for December, 0600 hours.

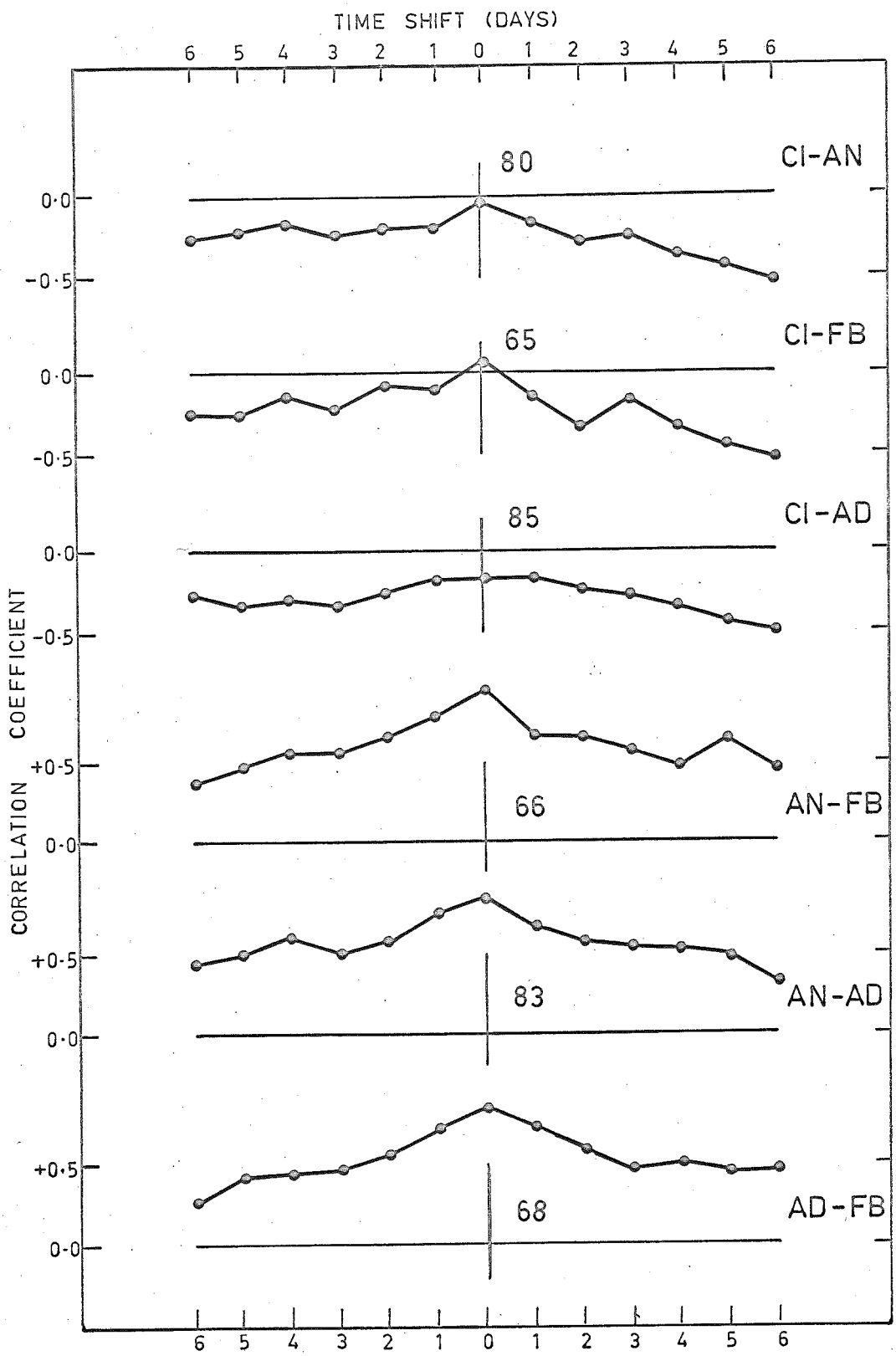

Figure 9.3 Cross-correlation functions of f_0F_2 at Campbell Island and three northern hemisphere locations for September, 1200 hours.

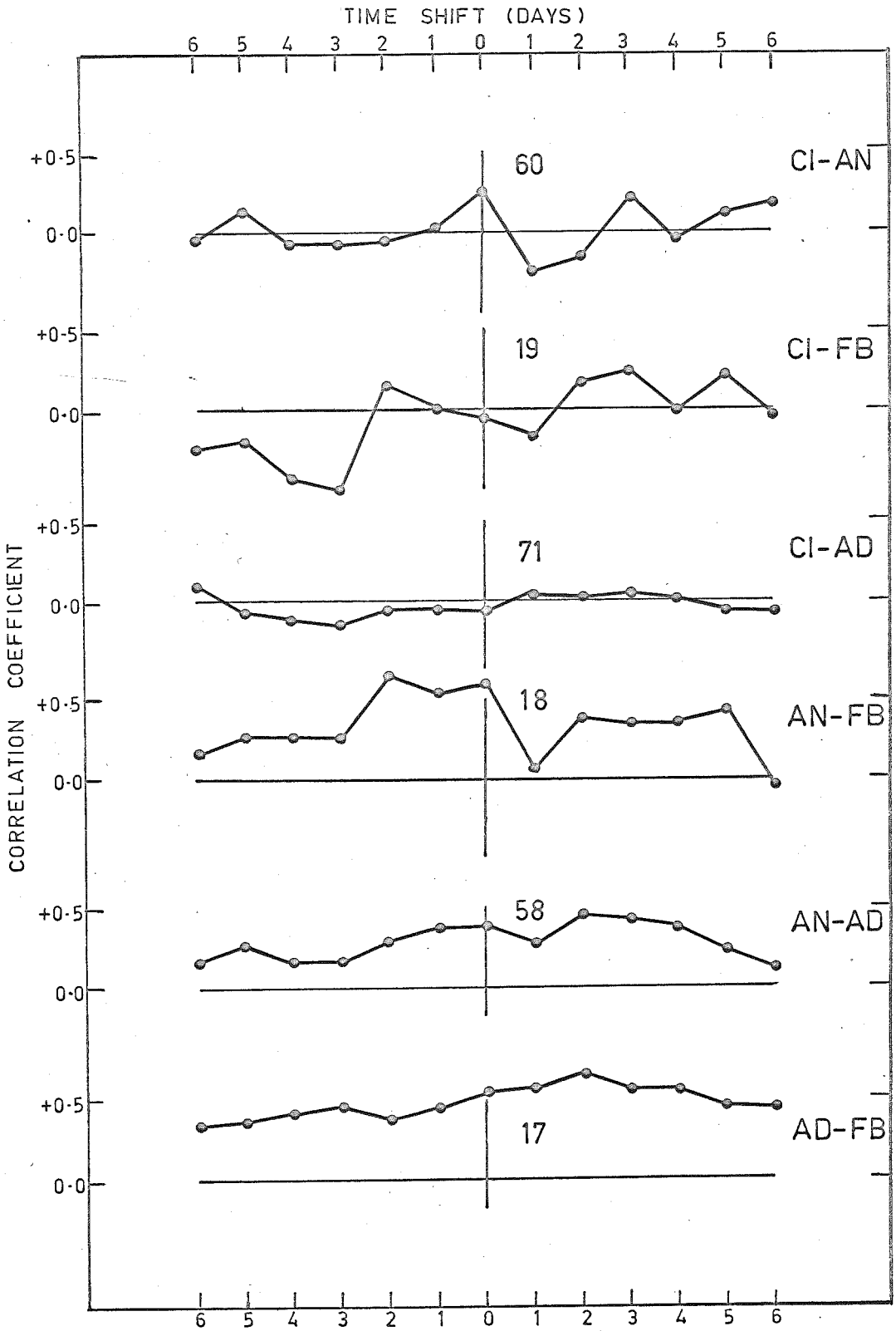

Figure 9.4 Cross-correlation functions of f_0F_2 at Campbell Island and three northern hemisphere locations for September, 0000 hours.

sense of the time shift in the correlation functions is not important but for consistency, it is the same as was defined in Section 6.6 and adhered to in the following chapters.

Figure 9.1 shows, for 1200 hours in June, a unique positive correlation between opposite hemispheres for the two conjugate stations at Campbell Island and Anchorage and also shows positive correlations between all three pairs of northern stations.

Figures 9.2 and 9.3 show, for 0600 hours in December and for 1200 hours in September, a positive correlation between Campbell Island and both Anchorage and Fairbanks and also show positive correlation between the northern pairs of stations - the correlation decreasing as the station separation increases more noticeably than in Figure 9.1.

Figure 9.4 shows, for 0000 hours in September, a positive correlation only between the two conjugate stations. This was the only evidence for any positive correlation between the two hemispheres at night.

Of the 16 cross-correlation functions between the data from Campbell Island and that from each of the northern stations, half of those with the Anchorage and Fairbanks data and 3 of those with the Adak data showed positive correlations.

It should be especially noted that all the Figures except 9.1 include examples of correlation coefficients for zero time shift which would have been misinterpreted if coefficients had not also been evaluated including the time shifts of several days. The correlation functions between the three northern pairs of stations are typically positive since these three stations share a common seasonal variation and those between Campbell Island and the northern stations in September in Figure 9.3 are basically negative due to the opposite seasonal variations in the two hemispheres. A similar result (not illustrated) is found for March.

9.3 Discussion

Generally, rather than a unique association between Campbell Island and the northern hemisphere ionospheric station nearest its conjugate point, the results suggest that the associations between Campbell Island and both Anchorage and Fairbanks are similar but that there is only occasional association between Campbell Island and Adak - the northern hemisphere station most distant from the Campbell Island conjugate point. Thus, from the present results, there seems to be an extended area conjugate to Campbell Island rather than a discrete location. Since

Fairbanks is 637 km from the conjugate point of Campbell Island, this figure may be taken as a lower limit for the extent of the conjugate area. This result is similar to that of Wescott (1961) who found an area to area correlation in his investigation of the association of magnetic variations recorded at Macquarie Island with those recorded at nine Alaskan stations.

As pointed out by Thomas (private communication 1964), the fact that F region critical frequencies are positively correlated between the northern pairs of stations means that the associations between Campbell Island and the three northern stations are not independent. He attempted to resolve this difficulty using partial correlation coefficients similar to those used in Section 6.7 in the interpretation of the correlation coefficients between scintillation, sporadic-E and spread-F. Strictly, the results presented in the previous section should also be subject to a partial correlation analysis.

It was also indicated by Thomas that magnetically quiet and disturbed days should be distinguished, previous authors having found different associations between conjugate points under different magnetic conditions. One point which does not appear to have been considered in the conjugate point investigations of any authors is the observation of King (1961) and later Briggs (1965) that if a given day was

magnetically quiet, a following day was more likely to represent the best selection of an ionospherically quiet day than was the same day.

The use of correlation functions in the present analysis of the conjugate point data should overcome the difficulty pointed out by King (private communication 1964) that, because of the opposite relationships between $f_o F_2$ in opposite hemispheres when one of the stations is experiencing a month near mid-winter, it can then be a waste of time to look for correlations between the two hemispheres.

CHAPTER 10. CONCLUDING REMARKS

The conclusions arising out of the work submitted in this thesis have already been presented in the summary and also in the relevant sections of the text. Therefore they are not reproduced here, the text of this Chapter being confined to the discussion of those points which require further explanation or emphasis and to suggestions for future experiments arising out of the work of the present experiments.

10.1 Points for Discussion Arising from the Text

(i) On the $f_o F_2$ Seasonal Anomaly. In Section 4.4, it was stated without amplification that inspection of the Woomera ionograms showed that if any effect due to ionospheric refraction was present, it would be at a maximum for a source which in summer transits during the day and in winter transits during the night. The author realizes that this statement is not in agreement with the generally observed seasonal anomaly in $f_o F_2$, but nevertheless, the relevant ionograms did indicate that there was a bigger difference between summer day time and winter night time critical frequencies than there was between those for summer night time and winter day time.

(ii) On the Nature of Spread-F at Woomera. In Section 6.3 it was pointed out that during the years 1964 and 1965, spread-F at Woomera was invariably of the frequency spreading type. Although this is a usual observation except in equatorial latitudes, the present observations from the Woomera ionograms appear to disagree with those of Singleton (1957) at Brisbane. The different observations should be suited to comparison since they were made during the same phase of (different) solar cycles but whereas range spreading was almost never observed from Woomera, it was often observed from Brisbane. It would be of interest to determine why the characteristics of spread-F are different at the two locations since Woomera is only 3^{o} further from the equator than Brisbane.

10.2 Suggested Further Work on Problems Arising from the Text

It is evident from several of the foregoing Chapters that further information would be desirable to clarify the interpretation of some of the results.

In Section 4.9, it was found that there was no detectable advance or retardation of the transit time of the Cygnus A source due to regular wedge refraction in the evening, but that in the morning the transit time appeared to be advanced by 1 minute - a result in the opposite sense

to that expected. It is possible, due to the amplitude of the output from the Cygnus A source being adjusted for optimum reading of amplitude scintillation indices, that the zero cross over times of the pen recorder trace could not be read as accurately as desired. Further data on this subject is required, preferably based on a larger amplitude pen recorder trace and a more accurately timed chart.

As was indicated in Section 5.1(ii) on the occurrence of scintillation and in Section 5.3 on the zenith angle variation of the scintillation depth, it is most desirable that data from the larger interferometer be available for a full year or better still, for several full years. It would then be possible to improve the reliability of the zenith angle results and it would also be possible to use a more accurate method - such as that used by Smerd and Slee (1966) - to determine the relative importance of the diurnal and seasonal variations.

In Section 6.9, it was concluded that correlations between scintillation activity and both sporadic-E and spread-F were strongest using those radio sources which had their daily transit at zenith angles such that the distance between the regions of the ionosphere responsible for the scintillation and for the spread-F or sporadic-E

was least. While it was suspected that despite the above result, scintillation in the signals from sources at low elevation angles might be primarily associated with sporadic-E, and scintillation in the signals from sources at high elevation angles might be primarily associated with spread-F, it was not possible to show this from the present arrangement of the scintillation and ionosonde observing sites due to the localized patchy nature of both sporadic-E and spread-F.

In Chapter 7, there is scope for a more detailed analysis of the associations of scintillation rate with spread-F, sporadic-E and magnetic indices - a faster chart speed would give an improved resolution of scintillation rate, and a local magnetic K index would probably be preferable to the planetary Kp index. Magnetic K indices from the observatory at Toolangi, Victoria could be used to advantage both in the correlation of magnetic activity with scintillation rate discussed in Chapter 7 and in the correlation of magnetic activity with scintillation amplitude in Chapter 6.

The author feels that generally throughout the later chapters, there is room for a more detailed comparison between records of radio star and satellite scintillations, and also feels that the better understanding of associations between phenomena through the use of correlation

functions rather than a single correlation coefficient should be emphasised. It should be noted that in the present text, otherwise misleading correlations, between scintillation and other parameters and between values of $f_o F_2$ in opposite hemispheres, have been resolved with the aid of correlation functions incorporating time shifts of at least several days.

10.3 Future Work

Several future projects at St. Kilda are based on interferometers, the design of which is related to the two described here.

The smaller interferometer has already been duplicated and now measures the east-west component of the drift velocity of the ionospheric irregularities responsible for the scintillation. These drift measurements will be compared with those of the meteor radar and of the fixed frequency sounder - both of these other experiments having their receiving antennas at or near the same site: additional information should be forthcoming regarding the height of origin of the scintillations.

The author has been associated with some of the initial plans for another new interferometer which will consist of four antenna arrays similar to that of the present larger interferometer: the baseline will still be

east-west and the four lines of antennas will be uniformly spaced in a north-south line. Providing that the north-south spacing is suitably adjusted, the interferometer should be insensitive to the signals from the strong Virgo A source and should detect scintillations of interplanetary origin in the much weaker signals from the small diameter source 3C 273. The two sources have a similar right ascension co-ordinate but differ in declination by 10°. The difference in the signal strength from the two sources is large but it is felt that with the above antenna array, this can be overcome by having a null in the polar diagram at the elevation angle of the Virgo A source transit.

It is recommended that the experiment described in Section 1.2(iii) be carried out to resolve the apparent uncertainty in the cause of the inversion of the usual dependence of scintillation depth on frequency - the recording of scintillations over a range of frequencies at the same site with antennas of different aperture being sufficient to distinguish between the antenna aperture and other effects as the cause of the inversion. It is also recommended that the analysis of Smerd and Slee (1966) to distinguish between a diurnal variation of scintillation activity and a dependence on the position of the sun (and anti-solar point) be carried out bearing in mind the discussion of Section 1.4(i). It was there pointed out that

the difference in declination between a radio star source and the sun was not a suitable measure of the angular distance between them. At present there are no plans for carrying out either of these recommendations at Adelaide.

BIBLIOGRAPHY

Aarons, J., Castelli, J.P., and Kidd, W., 1962, Proc. of the International Conference on the Ionosphere (London), July, 1962, p252.

Aarons, J., and Guidice, D.A., 1966, J. Geophys. Res., 71, 3277.

A.R.R.L. Antenna Book.

Axford, W.J., and Hines, C.O., 1961, Can. J. Phys., 39, 1433.

Basu, S., Allen, R.S., and Aarons, J., 1964, J. Atmos. Terr. Phys. 26, 811.

Bennett, A.S., 1962, Memoirs Roy. Ast. Soc. 68, 163.

Benson, R.F., 1960, J. Geophys. Res., 65, 1981.

Bolton, J.G., Slee, O.B., and Stanley, G.J., 1953, Aust. J. Phys. 6, 434.

Booker, H.G., Ratcliffe, J.A., and Shinn, D.H., 1950, Phil. Trans. Roy. Soc. A., 242, 579.

Booker, H.G., 1958, Proc. Inst. Radio Engrs., 46, 298.

Bowhill, S.A., 1964, AGARD-NATO Conference, Copenhagen, August 1964.

Bramley, E.N., 1954, Proc. Roy. Soc. A., 225, 515.

Bramley, E.N., 1967, J. Atmos. Terr. Phys., 29, 1.

Briggs, B.H., 1958, J. Atmos. Terr. Phys., 12, 34.

Briggs, B.H., 1961, Geophys. J. Roy. Ast. Soc., 5, 306.

Briggs, B.H., and Parkin, I.A., 1963, J. Atmos. Terr. Phys., 25, 339.

Briggs, B.H., 1964, J. Atmos. Terr. Phys., 26, 1.

Briggs, B.H., 1965, J. Atmos. Terr. Phys., 27, 991.

Briggs, B.H., 1966, Radio Science, 1, 1163.

Budden, K.G., 1965a, J. Atmos. Terr. Phys., 27, 155.

Budden, K.G., 1965b, J. Atmos. Terr. Phys., 27, 883.

Calvert, W., 1963, J. Geophys. Res., 68, 2591.

Calvert, W. Vanzandt, T.E., Knecht, R.W., and Goe, G.B., 1962, Proc. of the International Conference on the Ionosphere (London), July 1962, p324.

Calvert, W., and Schmid, C.W., 1964, J. Geophys. Res., 69, 1839.

Castelli, J.P., Aarons, J., and Silverman, H.M., 1964, J. Atmos. Terr. Phys., 26, 1197.

Chivers, H.J.A., 1960, J. Atmos. Terr. Phys., 19, 54.

Chivers, H.J.A., 1962, Proc. of the International Conference on the Ionosphere (London), July, 1962, p258.

Chivers, H.J.A., and Davies, R.D., 1962, J. Atmos. Terr. Phys., 24, 573.

Chivers, H.J.A., 1963, J. Atmos. Terr. Phys., 25, 468.

Clemesha, B.R., 1964, J. Atmos. Terr. Phys., 26, 91.

Cohen, M.H., Gunderman, E.J., Hardebeck, H.E., and Sharp, L.E., 1967, Astrophys. J., 147, 449.

Cummack, C.H., 1967, J. Atmos. Terr. Phys. 29, 811.

Dagg, M., 1957a, J. Atmos. Phys., 10, 194.

Dagg, M., 1957b, J. Atmos. Terr. Phys., 10, 204.

Dagg, M., 1957c, J. Atmos. Terr. Phys., 11, 133.

Dagg, M., 1957d, J. Atmos. Terr. Phys., 11, 139.

Dagg, M., 1957e, J. Atmos. Terr. Phys., 11, 118.

Dennison, P.A., and Hewish, A., 1967, Nature, 213, 343.

Dessler, A.J., 1958, J. Geophys. Res., 63, 1958.

Dueno, B., 1956, J. Geophys. Res., 61, 535.

Dyson, P.L., 1967, J. Atmos. Terr. Phys., 29, 857.

Gagnon, G., 1964, Radio Science J. of Res. NBS/USNC-URSI, 68D, 737.

Fejer, J.A., 1953, Proc. Roy. Soc., A. 220, 455.

Frihagen, J., 1962, Radio Astronomical and Satellite Studies of the Ionosphere (North Holland - Amsterdam), 1963.

Goodwin, G.L., 1965, J. Atmos. Terr. Phys., 27, 211.

Herman, J.R., 1966, Rev. Geophys., 4, 255.

Hewish, A., 1951, Proc. Roy. Soc. A., 209, 81.

Hewish, A., 1952, Proc. Roy. Soc. A., 214, 494.

Hewish, A., Scott, P.F., and Wills, D., 1964, Nature, 203, 1214.

Hewish, A., and Okoye, S.E., 1965, Nature, 207, 59.

Hey, J.S., Parsons, S.J., and Phillips, J.W., 1946, Nature, 158, 234.

Hines, C.O., 1960, Can. J. Phys., 38, 1441.

Hines, C.O., Paghis, I., Hartz, T.R., and Fejer, J.A., 1965, "Physics of the Earth's Upper Atmosphere" (London: Prentice Hall).

Howard, W.E., and Maran, S.P., 1965, Astrophys. J. Supplement Series, 10, 1.

Jesperson, J.L., and Kamas, G., 1964, J. Atmos. Terr. Phys., 26, 457.

Jones, I.L., 1960, J. Atmos. Terr. Phys., 19, 26.

Kent, G.S., 1961, J. Atmos. Terr. Phys., 22, 255.

Kidd, W., Silverman, H., Whitney, H., and Aarons, J., 1962, Nature, 193, 1246.

King, J.W., 1961, J. Atmos. Terr. Phys., 21, 26.

King, J.W., 1962, Proc. of the International Conference on the Ionosphere (London), July, 1962, p116.

King, J.W., and Graham, C., 1962, J. Atmos. Terr. Phys., 24, 107.

King, J.W., and Scott, J.L., 1962, J. Atmos. Terr. Phys., 24, 569.

Komesaroff, M.M., 1960, Aust. J. Phys., 13, 153.

Koster, J.R., 1958, J. Atmos. Terr. Phys., 12, 100.

Koster, J.R., and Wright, R.W., 1960, J. Geophys. Res., 65, 2303.

Koster, J.R., 1963, J. Geophys. Res., 68, 2579.

Krishnamurthy, B.V., 1966, J. Geophys. Res., 71, 4527.

Lawrence, R.S., and Jesperson, J.L., 1961, Proc. of the Second International Space Science Symposium 1961, p277.

Lawrence, R.S., Jesperson, J.L., and Lamb, R.C., 1961, Radio Science J. of Res. NBS/USNC-URSI, 65D, 333.

Lawrence, R.S., Little, C.G., and Chivers, H.J.A., 1964, Proc. Inst. Radio. Engrs., 52, 4.

Little, C.G., and Lovell, A.C.B., 1950, Nature, 165, 423.

Little, C.G., and Maxwell, A., 1951, Phil. Mag., 42, 267.

Little, C.G., Reid, G.C., Stiltner, E., and Merritt, R.P., 1962, J. Geophys. Res., 67, 1763.

Martyn, D.F., 1959, Proc. Inst. Radio Engrs., 47, 147.

McClure, J.P., 1964, J. Geophys. Res., 69, 2775.

McGee, C.R., 1966, J. Atmos. Terr. Phys., 28, 861.

Mercier, R.P., 1962, Proc. Camb. Phil. Soc., 58, 382.

Mitra, A.P., et al., 1964-65, Progress Report of the Radio Propagation Unit of the National Physical Laboratory, New Delhi, India.

Moorcroft, D.R., 1963, J. Geophys. Res., 68, 111.

Munro, G.H., 1958, Aust. J. Phys., 11, 91.

Parkin, I.A., 1967, Ph.D. Thesis, University of Adelaide.

Piddington, J.H., 1964, Planet. Space Sci., 12, 127.

R.S.G.B. Amateur Radio Handbook.

Rao, C.V.S., and Mitra, S.N., 1962, J. Geophys. Res., 67, 127.

Rao, N.N., 1967, J. Geophys. Res., 72, 2929.

Ratcliffe, J.A., and Pawsey, J.L., 1933, Proc. Camb. Phil. Soc., 29, 301.

Reid, G.C., 1957, Can. J. Phys., 35, 1004.

Roberts, J.A., 1963, Planet. Space Sci., 11, 221.

Rothwell, P., 1961, J. Phys. Soc. Japan, Supplement A1., 17, 263.

Rothwell, P., 1962, Proc. of the International Conference on the Ionosphere (London), July, 1962, p217.

Ryle, M., and Smith, F.G., 1948, Nature, 162, 462.

Ryle, M., and Hewish, A., 1950, Monthly Notices Roy. Ast. Soc., 110, 384.

Ryle, M., 1952, Proc. Roy. Soc. A., 211, 351.

Saltpeter, E.E., 1967, Astrophys. J., 147, 433.

Schrader, D.H., and Kan, J.R., 1966, J. Geophys. Res., 71, 5617.

Sharp, L.E., and Harris, D.E., 1967, Nature, 213, 377.

Shimazaki, T., 1959 I and II, J. Rad. Res. Lab. Japan, 6, 669.

Singleton, D.G., 1957, Aust. J. Phys., 10, 60.

Singleton, D.G., 1962a, J. Atmos. Terr. Phys., 24, 871.

Singleton, D.G., 1962b, J. Atmos. Terr. Phys., 24, 885.

Singleton, D.G., 1962c, J. Atmos. Terr. Phys., 24, 909.

Singleton, D.G., 1962d, Nature, 195, 4845.

Singleton, D.G., 1964a, Radio Science J. of Res. NBS/USNC-URSI, 68D, 867.

Singleton, D.G., 1964b, Radio Science J. of Res. NBS/USNC-URSI, 68D, 1095.

Slee, O.B., 1962, Aust. J. Phys., 15, 568.

Smerd, S.F., and Slee, O.B., 1966, Aust. J. Phys., 19, 427.

Smith, E.K., and Weintraub, S., 1953, Proc. Inst. Rad. Engrs., 41, 1035.

Smith, F.G., 1950, Nature, 165, 422.

Smith, F.G., 1952, J. Atmos. Terr. Phys., 2, 350.

Spencer, M., 1955, Proc. Phys. Soc. B, 68, 493.

Titheridge, J.E., 1964a, J. Atmos. Terr. Phys., 26, 159.

Titheridge, J.E., 1964b, J. Atmos. Terr. Phys., 26, 177.

Tiuri, M.E., 1964, Inst. Electrical and Electronic Engrs., MIL-8, 264.

Tuominen, J., Kataja, E., and Riihimaa, J., 1962, Physica A, 6, 3.

Unwin, R.S., 1966, J. Geophys. Res., 71, 3677.

Warwick, J.W., 1964, Radio Science J. of Res., 68D, 179.

Wescott, E.M., 1961, J. Geophys. Res., 66, 1789.

Wild, J.P., and Roberts, J.A., 1956, J. Atmos. Terr. Phys., 8, 55.

Vestine, E.H., and Sibley, W.L., 1960, Project Rand, Geomagnetic Field Lines in Space.

Yeh, K.D., and Swenson, G.W. Jr., 1964, Radio Science J. of Res., NBS/USNC-URSI, 68D, 881.

Yule, G.U., and Kendall, M.G., 1949, "An Introduction to the Theory of Statistics," (London: C. Griffin).

APPENDIX A.1 THE POLAR DIAGRAM OF AN ARRAY OF EIGHT ANTENNAS

The polar diagram of an array of eight antennas in a line with a uniform spacing of 3/2 wavelengths may be readily calculated using a vector addition technique. Initially, each antenna is assumed to have isotropic radiating properties; the effect of the departure from this in the present case of directional antennas is taken into account later.

If a unit amplitude signal is assumed to be incident on each antenna and a phase difference ϕ exists between the signals incident on adjacent antennas, then, if the centre of the array is taken as the phase reference point, the total signal S incident on the array is given by:

$$S = e^{i\frac{\phi}{2}} + e^{-i\frac{\phi}{2}} + e^{i\frac{3\phi}{2}} + e^{-i\frac{3\phi}{2}} + e^{i\frac{5\phi}{2}} + e^{-i\frac{5\phi}{2}} + e^{i\frac{7\phi}{2}} + e^{-i\frac{7\phi}{2}}$$

$$= 2\left(\cos\frac{\phi}{2} + \cos\frac{3\phi}{2} + \cos\frac{5\phi}{2} + \cos\frac{7\phi}{2}\right)$$

$$= \sin 4\phi / \sin\frac{\phi}{2} \qquad \text{(A1)}$$

where $\phi = \frac{2\pi d}{\lambda}(\cos\theta)$ radians, and $d = 3/2\ \lambda$.

θ is the angle between the line joining the antennas

and the direction of arrival of the signal.

For an east-west baseline interferometer such as the present one, the angle θ may be determined from either of the relations:

$$\begin{aligned} &\text{Cos } \theta = \text{Cos (declination)} \times \text{Sin (hour angle)} \\ \text{or} \quad &\text{Cos } \theta = \text{Cos (altitude)} \times \text{Sin (azimuth)} \end{aligned} \qquad \text{(A2)}$$

where the azimuth angle is measured east or west from the geographic north.

The derivation of expression (A1) is quite straightforward using standard trigonometric relationships and is not described here.

The equation (A1) is convenient for computing purposes except that the signal S is undefined if ϕ equals a multiple of 2π. These singularities can be allowed for when it is realized that for these values of ϕ , S tends to a limit of $\pm$ 8.

A.2 The Effects of the Directional Antenna Radiation Pattern and the Ground for the Eight Yagi Antenna Array.

This method for calculating the polar diagram has so far assumed that each antenna in the array is an isotropic radiator. This assumption is invalid in the first place

because the Yagi antennas used here have a directional radiation pattern, and in the second place because the antennas are mounted near the ground. Since the effects introduced by constructing the array from directional antennas and from mounting it near the ground are not mutually exclusive (the relative importance of these effects depending on the direction to which the array is pointing), a detailed calculation of the modifications necessary in the polar diagram was not attempted.

Those calculations that were made assumed that when the Yagi antennas were directed vertically, their high front-to-back ratio (measured to equal 17 db) would exclude any effects due to ground reflection or losses, and that the envelope of the array polar diagram could be considered as being modified only by the directional properties of Yagi antennas. Purely for computing convenience, the functions cos Z_{NS} and cos Z_{EW} were chosen to represent the polar diagram of the Yagi where Z_{NS} and Z_{EW} are respectively the projections of the zenith angle into the north-south and east-west planes.

Thus, the signal response of the array consisting of eight Yagi antennas in a line, with a uniform spacing between them of 3/2 wavelengths, is given by:

$$S = (\sin 4\phi / \sin \tfrac{\phi}{2}) \cdot \cos(Z_{NS}) \cdot \cos(Z_{EW}) \qquad (A3)$$

where $\cot(Z_{NS}) = \tan(\text{altitude}) / \cos(\text{azimuth})$

and $\cot(Z_{EW}) = \tan(\text{altitude} / \sin(\text{azimuth})$

A.3 The Effects of the Directional Antenna Pattern and the Ground for the Cygnus A Array

In the case of the Cygnus A array, where the source is detected from low elevation angles and the array is directed to the northern horizon, it seems sufficient (for computing purposes) to assume that the polar diagram of the Yagi antennas affects only the signal response as a function of azimuth and that the response as a function of altitude is due purely to reflection and loss from the ground. The variation in the signal response with azimuth was assumed to vary as the cosine of the azimuth and, from Figures 2.70 and 2.73 of the A.R.R.L. Antenna Book, the ground was deemed not to affect signals from angles of elevations greater than 10°; but for angles less than 10°, the signals were deemed to be effectively reduced by the factor sine (9xAltitude) which equals 1 for an altitude of 10° and equals 0 for altitude equal to zero.

Thus, for computing convenience, the signal response of each of the Yagi antennas constituting the interferometer is given by:

S = cos(azimuth for altitude $<10^{o}$

S = cos(azimuth) • sin(9xAltitude) for altitude $>10^{o}$

(A4)

APPENDIX B. THE SATELLITE METHOD OF MEASURING THE POLAR DIAGRAM

Soon after the period of routine running had commenced, it was noted that signals from the beacon satllite Be-C were often detected, although when the chart was run at its usual speed of 3 inches per hour, the interference to the radio star signals was not serious.

To measure the interferometer polar diagram, some eight passes of the satellite were recorded with a chart speed of 6 inches per minute and it was then possible to record the times for which the satellite's radio transmissions gave maximum output from the interferometer, correct to the nearest second. The only shortcoming of this method is the fact that the satellite's transmission frequency of 40.0 MHz was different from the design frequency of the array (39.5 MHz). This meant that for the satellite, the Yagi antennas were not 3/2 wavelengths apart but rather they were 40.0/39.4 x 3/2 wavelengths apart, and that the first order diffraction grating lobes were in fact a little nearer the main lobe at the satellite frequency. Assuming the main lobe was along the overhead meridian, its position was unaffected.

A satellite orbit program developed by I.A. Parkin which incorporated an interpolated form of the epoch

information supplied by the Goddard Space Flight Center in monthly bulletins, conveniently reduced the measured pass times to local altitude - azimuth co-ordinates. Errors from this calculation were less than 2^{o} in altitude - azimuth co-ordinates (less than $\frac{1}{4}^{o}$ in geocentric co-ordinates), and could be checked by calculating with the program the satellite position in geocentric co-ordinates at the time predicted for the previous equatorial crossing and comparing the calculated with the predicted position.

The accompanying Figure B.1 shows the results obtained with this method compared with the side lobe positions calculated from the array geometry as in Section 2.4. During the satellite experiment, the array was directed vertically upwards and the antenna elements aligned north-south as shown in the frontispiece.

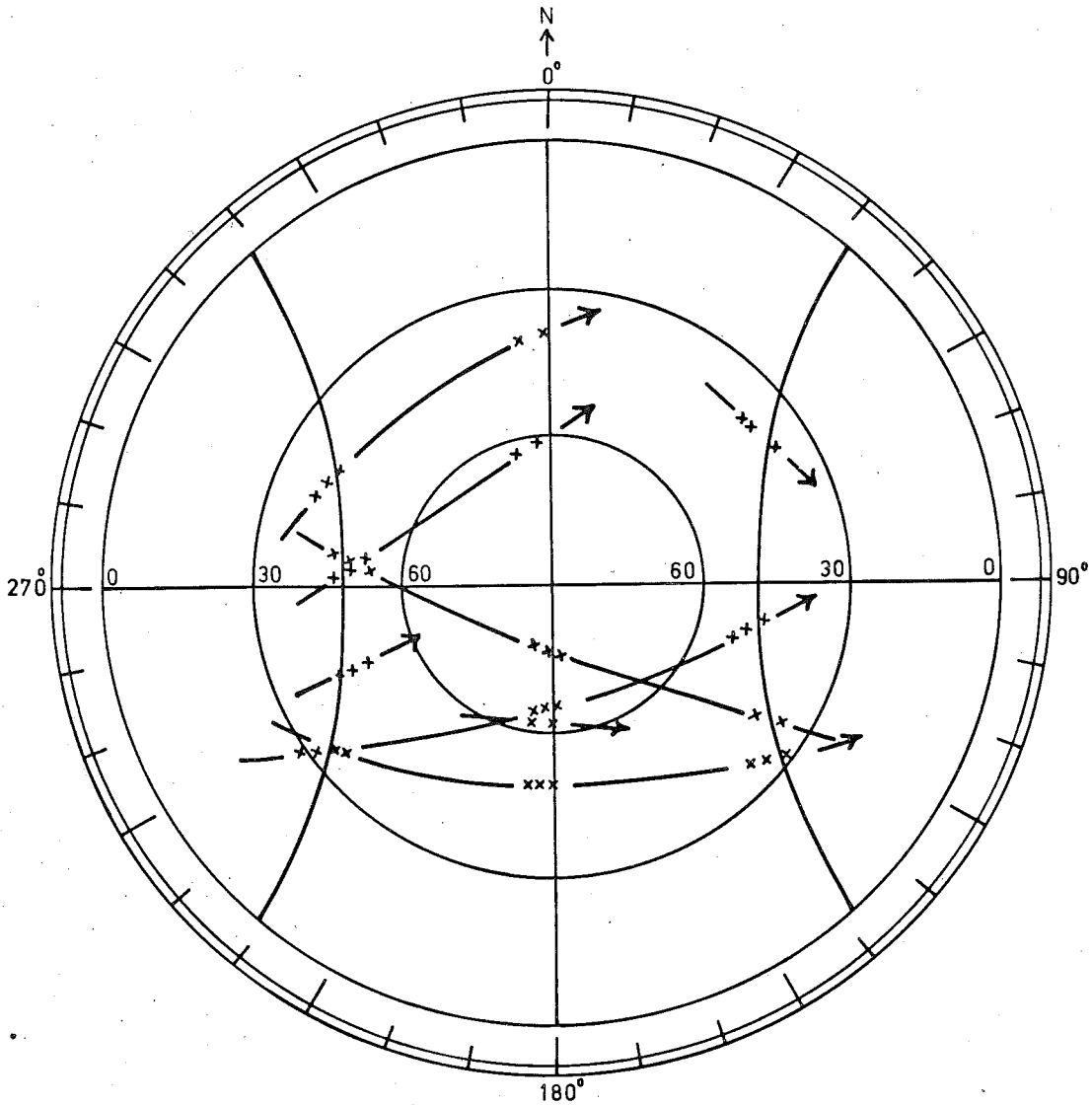

Figure B.1 The results obtained using passes of satellite Be-C to estimate the polar-diagram of the array.